

UNIVERSITY OF NOTTINGHAM
DEPARTMENT OF MANUFACTURING ENGINEERING
AND OPERATIONS MANAGEMENT.

COMPUTER SIMULATION OF ROTARY FORGING.

by

DAVID G. GRIEVE. B.Sc.

Thesis submitted to the University of Nottingham
for the degree of Doctor of Philosophy.

April 1991.

BEST COPY

AVAILABLE

Variable print quality

CONTENTS.

	Page
<u>LIST OF TABLES</u>	viii
<u>LIST OF FIGURES</u>	ix
<u>NOMENCLATURE</u>	xv
<u>ABBREVIATIONS</u>	xvi
<u>ACKNOWLEDGEMENTS</u>	xvii
<u>ABSTRACT</u>	xviii
1. <u>INTRODUCTION</u>	
1.1. Introduction	1.
1.2. A brief history of rotary forging	2.
1.3. Development of a package to simulate rotary forging	4.
2. <u>LITERATURE REVIEW</u>	
2.1. Introduction	8.
2.2. Use of special materials to investigate rotary forging	8.
2.3. Physical modelling	10.
2.4. Mathematical modelling	11.
2.5. Computer simulation and CAD - CAM	12.
3. <u>CLASSIFICATION OF ROTARY FORGING MOTIONS</u>	
3.1. Introduction	15.
3.2. Definition of rotary forging machines and their movements.	15.
3.2.1. Rotary forging tool and workpiece arrangement.	15.
3.2.2. Definition of rotary forging machines in terms of their movement	16.
3.3. Mathematical definition of the Eulerian motions	17.
3.4. Conclusions	18.

	Page
4. <u>APPLICATION OF EULERIAN MOTION TO ROTARY FORGING.</u>	
4.1. Introduction.....	20.
4.2. Application of the model to a computer programme.....	20.
4.3. Verification of the mathematical model and computer package.....	21.
4.3.1. Results for the path of a rotary forging die.....	21.
4.3.2. Results for a point lying on the edge of a rotary forging die.....	23.
4.4. Conclusions.....	23.
5. <u>RESULTS FROM PATH.</u>	
5.1. Introduction.....	26.
5.2. Results for rotary forging tool movement.....	26.
5.3. Application of PATH to determine the locus of a point on the surface of a tool.....	29.
5.3.1. Precession motion - the effects of altering the initial Nutation (θ_i).....	30.
5.3.2. Non - monotonic nutation - precession.....	31.
5.3.3. The effect of different angled tools under precession motion.....	31.
5.3.4. The locus produced for a point on a flat plate.....	32.
5.4. Results for the path of a point on a point on the surface of the base cone α during precession motion.....	33.
5.5. Conclusions.....	34.
6. <u>PREDICTION OF ROTARY FORGED SURFACES.</u>	
6.1. Introduction.....	37.
6.2. Specifications.....	37.
6.2.1 The preprocessor.....	37.
6.2.2. The processor.....	38.

	Page
6.2.3. The postprocessor.	39.
6.3. Modelling of the tool.....	39.
6.3.1. Generation of the profiled tool.....	40.
6.3.2. Tool material properties.....	40.
6.3.3. Tool movement.	41.
6.4. Modelling of the workpiece.	41.
6.4.1. Non - constant volume workpiece model.....	42.
6.4.2. The constant volume workpiece model.	42.
6.4.2.1. Limitations and approximations of the constant volume model.	45.
6.5. Contact detection between the tool and the workpiece.	45.
6.5.1. Reducing the search time.	46.
6.6. Calculation of the contact area.	46.
6.6.1. Limitations of the contact area calculation.	47.
6.7. Calculation of the displaced volume of material	47.
6.7.1. Limitations of the displaced volume calculations.	48.
6.8. Conclusions.....	48.
 7. <u>RESULTS FROM THE NON CONSTANT VOLUME MODEL</u>	
7.1. Introduction.	52.
7.2. The family of rotary forging machine motions.....	52.
7.2.1. Nutation motion.	53.
7.2.2. Precession motion.....	53.
7.2.3. Spin motion.	54.
7.2.4. Nutation - precession motion.	55.
7.2.5. Non - monotonic nutation - precession.	56.
7.2.6. Nutation - spin motion.....	57.
7.2.7. Nutation - spin - precession.....	58.
7.2.8. Precession - spin.	59.
7.3. Contoured tools.....	59.
7.3.1. Simulation using radially profiled tools.....	59.

	Page
7.3.2. Simulation using circumferentially profiled tools.....	60.
7.4. Application of PROFS to investigate a real rotary forging situation.....	61.
7.4.1. Simulation using a 37.8 mm diameter workpiece. (Stage i).....	62.
7.4.2. Simulation using a 46.0 mm diameter workpiece. (Stage ii).....	63.
7.4.3. Simulation using The 54.2 mm diameter workpiece. (Stage iii).	63.
7.5. Conclusions.....	64.
 8. <u>THE CONSTANT VOLUME MODEL.</u>	
8.1. Introduction.....	67.
8.2. Experiments using the precession motion on the 200 tonne Schmid machine.....	68.
8.2.1. The physical experiments.....	68.
8.2.2. The simulated experiments.....	68.
8.2.3. Results.....	69.
8.2.4. The initial contact.....	69.
8.2.5. The intermediate contact geometries.....	70.
8.2.6. The final revolutions.....	71.
8.3. Experiments using the spin motion on the 50 tonne machine.	72.
8.3.1. The physical experiments.....	72.
8.3.2. The simulated experiments.....	73.
8.3.3. Results.....	73.
8.4. Conclusions.....	74.
 9. <u>EXPERIMENTS TO VERIFY THE NON - CONSTANT VOLUME MODEL</u>	
9.1. Introduction	77.
9.2. Experimental equipment.....	78.

	Page
9.3. Experimental procedure.....	78.
9.3.1. Short lead milling.....	78.
9.3.2. Simulated experiments.....	80.
9.4. Results.....	80.
9.4.1. The contact areas.	80.
9.4.2. Volumes of displaced material.....	82.
9.4.3. The contact profiles.	83.
9.5. Comparison of PROFS with previous researchers.....	84.
9.5. Conclusions.....	84.
10. <u>CONCLUSIONS.</u>	
10.1. Introduction	87.
10.2. The package Path and its use in the study of rotary forging motions.....	88.
10.3. The development and evaluation of a package to simulate rotary forging.....	91.
10.4. Confirmation of the non - constant volume model workpiece.	93.
10.5. Experiments using the constant volume model workpiece.	94.
<u>SUGGESTIONS FOR FURTHER WORK.</u>	98.
<u>APPENDIX A.</u>	101.
<u>APPENDIX B.</u>	105.
<u>REFERENCES.</u>	
<u>TABLES.</u>	
<u>FIGURES.</u>	

LIST OF TABLES.

- Table 3.1.** Some rotary forging machine designs around the World in terms of their Eulerian motions.
- Table 5.1.** This table shows the number of petals in a rosette or the number of symmetries of a spiral during rocking die nutation - precession motion.

LIST OF FIGURES.

- Figure 1.1. Showing the general rotary forging machine setup.
- Figure 1.2. A typical Partial contact region formed on a workpiece during rotary forging with an inclined conic die.
- Figure 3.1. Showing the typical rotary forging tool and workpiece arrangement.
- Figure 3.2. Showing the three Eulerian motions of nutation, precession, and spin.
- Figure 3.3. Eulerian tool motion relationship presented in terms of nutation, precession, and spin.
- Figure 4.1. The four motions used by the Marciniak / Schmid type of rotary forging machines.
- Figure 4.2. Showing a typical die arrangement in rotary forging.
- Figure 4.3. Showing the non monotonic nutation movement.
- Figure 4.4. Showing the movement of a point on a die axis whilst undergoing non - monotonic nutation.
- Figure 4.5. Showing a nutation motion plotted by the package PATH.
- Figure 4.6. Showing a precession motion plotted by the package PATH.
- Figure 4.7. Showing a spin motion plotted by the package PATH.
- Figure 4.8. Showing the four motions of a Marciniak type rotary forging machine generated by PATH, by a point on the tool axis.
- Figure 4.9. Showing the nutation motion for a point on the periphery of a 30° conic rotary forging die produced by PATH.
- Figure 4.10. Showing the precession motion for a point on the periphery of a 30° conic rotary forging die produced by PATH.
- Figure 4.11. Showing the spin motion for a point on the periphery of a 30° conic rotary forging die produced by PATH.
- Figure 5.1. The asymmetric type of machine motion produced during the non - monotonic nutation, precession motion when the nutation rate equals the precession rate, as produced by the package PATH.
- Figure 5.2. The rosette type of machine motion produced during the non - monotonic nutation, precession motion, by the package PATH.
- Figure 5.3. The rosette motion produced during the non - monotonic nutation - precession motion, by the package PATH. The six petals are overlapping due to the precession rate being greater than half the nutation rate.

- Figure 5.4. The spiral type of machine motion produced during the non - monotonic nutation - precession motion, by the package PATH.
- Figure 5.5. Showing the nine different types of machine motion produced by a point on the surface of a conic 30° rotary forging tool during precession motion using different initial nutations, (θ).
- Figure 5.6. Showing the point P' lying below the surface of the conic die.
- Figure 5.7. The spiral motion for a point on the surface of a conic tool during the non - monotonic nutation - precession motion, by the package PATH.
- Figure 5.8. The rosette motion for a point on the surface of a conic tool during the non - monotonic nutation - precession motion, by the package PATH.
- Figure 5.9. Showing how different angled conic tools influence the type of path that a point on that tool will undergo during precession motion.
- Figure 5.10. Showing the locus for a point on a flat die during the precession motion.
- Figure 5.11. Showing a point P' below the surface of a conic rotary forging die.
- Figure 5.12. Showing the locus of a point P' lying the surface of a conic rotary forging die. Where point P' lies between points a and b on Figure 5.11.
- Figure 5.13. Showing the locus of a point P' lying the surface of a conic rotary forging die. Where point P' lies below b or the Y axis on Figure 5.11.
- Figure 5.14. Showing how point P' below the surface of die A, is an equivalent to point P' on die B.
- Figure 5.15. The cross section of a radially profiled tool showing how it is effectively made up from parts of different angled tools, α_1 , α_2 , α_3 .
- Figure 6.1. The generalised tool and workpiece layout as generated by the preprocessor PROFS.
- Figure 6.2. A 20° conic tool drawn by the preprocessor PROFS, with the nodal points of the surface joined by circumferential and radial lines.
- Figure 6.3. The menu of radial profiles available in PROFS which can be incorporated into the surface of any conic rotary forging tool.
- Figure 6.4. A 20° conic tool with the 4th. radial profile from the menu shown in Figure 6.3 incorporated into it, as generated and drawn by the preprocessor PROFS.
- Figure 6.5. The menu of circumferential profiles available in PROFS which can be incorporated into the surface of any conic rotary forging tool.
- Figure 6.6. A 20° conic tool with the 3rd. circumferential profile from the menu shown in Figure 6.5 incorporated into it, as generated and drawn by the preprocessor PROFS.

- Figure 6.7. A hexahedral element as used in the generation of a workpiece.
- Figure 6.8. A typical workpiece modelled by the preprocessor PROFS, constructed from a circular arrangement of hexahedral elements.
- Figure 6.9. Showing how a rotary forging tool surface intersects with a workpiece surface.
- Figure 6.10. The progression of a typical contact geometry calculated by the preprocessor COSIMORF. Only the non - constant volume workpiece is shown for clarity.
- Figure 6.11. Showing how the tool surface intersects with one of the workpiece elements in the constant volume model.
- Figure 6.12. Showing how the volume change for each step of the simulation is calculated for an element in the workpiece and added onto its length as a first approximation in the constant volume workpiece model.
- Figure 6.13. Showing how the elements of a workpiece are moved every alternate row which in effect causes every element in the whole workpiece to be effected, and causes an even radial expansion of the workpiece.
- Figure 6.14. Showing how the radii of the intersection cylinders on the workpiece surface are found from the radial expansion of the points in the mesh, and how these cylinders overlap to completely cover the area of the whole workpiece.
- Figure 6.15. Showing how a squared meshed workpiece would enable the radii of the intersection cylinders to be all the same size and smaller than for the radially meshed workpiece shown in figure 6.14, but still comprehensively cover the workpiece surface.
- Figure 6.16. Showing how a large radius of intersection cylinder will cause the point on the workpiece to be considered as an in contact point, when in fact it is not.
- Figure 7.1. A typical result from VIDEO, the post - processor, showing a workpiece with its contact geometry represented in green. The corner picture shows the orientation of the tool at this point in the simulation.
- Figure 7.2. Showing nutation motion using the non - constant volume model workpiece.
- Figure 7.3. The precession motion using the non - constant volume model workpiece.
- Figure 7.4. Showing the helical surface developed on a workpiece after the first revolution of the precession motion.
- Figure 7.5. The Spin motion developed on a non - constant volume model workpiece.
- Figure 7.6. Showing the similarity between the contact areas produced by the precession and spin motions during the first initial revolution of contact.

- Figure 7.7. Shows the contact geometry on the surface of a workpiece during the first revolution of a nutation - precession motion.
- Figure 7.8. Shows the contact geometry on the surface of a workpiece during the first revolution of a non - monotonic nutation - precession motion. The nutation rate = 300 c.p.m. and the precession rate = 100 c.p.m. producing a three petal rosette pattern of tool axis movement as shown in figure 7.9.
- Figure 7.9. Shows a three petal rosette pattern of tool axis movement produced by the non - monotonic nutation - precession motion. The nutation rate = 300 c.p.m. and the precession rate = 100 c.p.m.
- Figure 7.10. Shows the contact geometry on the surface of a workpiece during the first revolution of a non - monotonic nutation - precession motion. The nutation rate = 100 c.p.m. and the precession rate = 300 c.p.m. producing a spiral pattern of tool axis movement as shown in figure 7.11.
- Figure 7.11. Shows a spiral pattern of tool axis movement produced by the non - monotonic nutation - precession motion. The nutation rate = 100 c.p.m. and the precession rate = 300 c.p.m.
- Figure 7.12. Shows the contact geometry on the surface of a workpiece during the first cycle of a non - monotonic nutation - precession motion. The nutation rate = 33 c.p.m., producing a straight line pattern of tool axis movement.
- Figure 7.13. The contact geometries produced during the nutation - spin motion. The upper conic die speed = 100 c.p.m., and the lower die speed = 86.6 c.p.m.
- Figure 7.14. A radially profiled tool generated from profile 4 of Figure 6.3, incorporated into a plan 30° degree cone.
- Figure 7.15. The contact geometries produced by the precessing radially profiled tool, shown in figure 7.14.
- Figure 7.16. A circumferentially profiled tool generated from profile 2 of Figure 6.5, incorporated into a plan 30° degree cone.
- Figure 7.17. The contact geometries produced by the precessing circumferentially profiled tool, shown in figure 7.16.
- Figure 7.18. The production part produced by a 200 tonne Schmid rotary forging machine.
- Figure 7.19. The custom made upper die generated by the pre - processor PROFS, for the simulation of the 200 tonne Schmid machine.
- Figure 7.20. The contact geometries produced on a 37.8 mm diameter workpiece during the stage i. of the simulation of a real rotary forging process.
- Figure 7.21. The contact geometries produced on a 46.0 mm diameter workpiece during the stage ii. of the simulation of a real rotary forging process.
- Figure 7.22. The contact geometries produced on a 54.2 mm diameter workpiece during the stage iii. of the simulation of a real rotary forging process.

- Figure 7.23. Showing the development of the contact geometries throughout a typical rotary forging operation, using a simulated non - constant volume volume model workpiece.
- Figure 8.1. Results for the 200 tonne precession machine simulations showing the progression of the contact geometry throughout the whole simulation.
- Figure 8.2. The 50 tonne Nottingham University rotary forging machine.
- Figure 8.3. The billet used for the 50 tonne machine experiments.
- Figure 8.4. The results from the simulation of the 50 tonne spin machine experiments showing the radial expansion of the workpiece.
- Figure 8.5. The workpieces produced during the 50 tonne machine experiments.
- Figure 8.6. Showing the radial growth and development of the simulated constant volume workpieces during the 50 tonne machine experiments.
- Figure 8.7. Showing the workpiece diameters vs. the workpiece heights.
- Figure 8.8. Showing the experimentally and simulated displaced volumes of material vs. the height of the workpiece at five stages of the forging.
- Figure 8.9. Showing the simulated displaced volumes of material vs. the experimentally determined values.
- Figure 9.1. The short lead milling machine setup for the physical simulation of the rotary forging process.
- Figure 9.2. The short lead milling machine with protractor, handle and pointer attached to the main drive.
- Figure 9.3. Showing the simulated contact ares vs. the milled contact areas.
- Figure 9.4. Showing the simulated contact areas vs. the milled contact area in aluminium.
- Figure 9.5. Showing the contact areas for both the simulated and the milled experiments plotted against the degrees of motion of the tool.
- Figure 9.6. Showing the simulated volume of displaced material vs. the milled volume in perspex
- Figure 9.7. Showing the simulated volume of displaced material vs. the milled volume in aluminium.
- Figure 9.8. Showing the displaced volumes of material for both the simulated and the milled experiments, plotted against the degrees of motion of the tool.
- Figure 9.9. A perspex workpiece after 360 degrees of milling.
- Figure 9.10. The simulation using the non - constant volume model workpiece of the perspex specimens milled on the short lead milling machine.

- Figure 9.11. Showing the simulation of the perspex workpiece after 360 degrees of rotary milling / forging.
- Figure 9.12. Showing the comparison between the contact / cutting profiles produced by the milled and simulated experiments in perspex at 360° of motion.
- Figure 9.13. The graph of the coefficient λ vs. spiral feed (S) from Kubo and PROFS.
- Figure 9.14. The graph of the coefficient λ vs. $2rt \tan \alpha / S$ from Marciniak and PROFS.

NOMENCLATURE.

θ	Nutation.
ϕ	Precession.
ψ	Spin.
θ_i	Initial Nutation.
θ_a	Nutation Amplitude.
$\dot{\theta}$	Nutation Rate.
$\dot{\phi}$	Precession Rate.
T	Time.
α	Cone Angle.
ω	Angular Velocity.

ABBREVIATIONS.

c.p.s.	Cycles Per Second.
C.P.U.	Central Processing Unit.
C.V.M.	Constant Volume Model.
E.D.M.	Electrode Discharge Machining. (Spark Erosion).
F.E.	Finite Element.
I.C.A.	Instantaneous Contact Area.
I.C.G.	Instantaneous Contact Geometry.
N.C.V.M.	Non - Constant Volume Model.
N.M.N.	Non - Monotonic Nutation.
P.D.Z.	Plastically Deforming Zone.
Revs.	Revolutions.
S.D.	Standard Deviation.

ACKNOWLEDGEMENTS.

I would like to thank my supervisor Dr. Peter Standing for his invaluable help and support throughout this research work which has enabled this Thesis to be written. His advice has kept me inspired especially when the next hurdle of my research seemed to be daunting.

I would also like to thank Dr. Richard Barson, the system manager of the Department of Manufacturing Engineering and Operations Management for his invaluable help and advice over the years.

ABSTRACT.

This thesis presents two computer packages to simulate the rotary forging process, by means of a mathematical model. The results are displayed in a graphical and numerical manner, showing the tool movement and the tool / workpiece interaction.

The first package, PATH, is shown to be capable of simulating the motions of all known rotary forging systems. Its results show the rotary forging tool path throughout a chosen process. The motions of any rotary forging system can be programed by a simple set of instructions displayed on the screen, and the results displayed quickly and graphically. The widely used motions of rocking - die rotary forging machines were investigated. From these investigations, formulae were put forward, which were shown to be capable of predicting the tool motion of any rocking - die rotary forging situation.

The second package, PROFS, presents a meshed representation of the tools and workpieces used in rotary forging systems. The rotary forging tool is represented as a conic wire frame mesh, on which no forces or loads are considered to act. The workpiece is represented as a cylinder constructed from a number of hexahedral elements. The elements are treated in either a non - constant volume or a constant volume manner.

The non - constant volume model workpiece is one which is simply cut away by the action of the tool on it. This model is similar to a process of 'rotary cutting'.

Using the model, a technique of investigation into the progression of the contact geometries created during a real rotary forging, was developed. It enabled the progression and size of the contact geometry to be followed from start to finish of the forging cycle. No consideration of the loads or forces occurring during the process was taken into account.

The constant model workpiece requires that its volume remains fixed during the simulation. This is achieved by a radial expansion of the elements of the

workpiece as it is being 'deformed' by the tool. Again no consideration of the loads or forces occurring in rotary forging was taken into account. Investigations, using the model, enabled the instantaneous contact geometries, contact areas, and displaced volumes of material to be predicted during two real rotary forging processes. Results revealed the potential of PROFS, to determine areas of workpiece instability in the early stages of forging, and reveal areas of insufficient die fill. The potential of data from the simulations, to control a rotary forging machine, is discussed, and is seen as the first step towards the design and manufacture of rotary forging parts and dies by a C.A.D. - C.A.M. route.

Contact areas produced during the rotary forging process are essential for any calculations of the forces and stresses occurring in the die and workpiece. The possibility of PROFS to be used as a die / design tool and in pre production trials for new parts is discussed.

A physical simulation of a non - constant volume model workpiece was carried out using a 'short lead milling' technique to cut away a solid workpiece. This revealed the instantaneous contact geometries and areas of the workpiece, which were shown to be accurately predicted by PROFS using the non - constant volume. The results confirmed the accuracy and validity of the simulated instantaneous geometries, allowing a large degree of confidence to be assumed in the accuracy of the package.

A data base of radial, circumferential , and custom die profiles has been built up and incorporated into PROFS. From the data base a chosen profile can be used to generate a conic meshed representation of a rotary forging die. Investigations, using a die generated from a custom profile, revealed areas of possible workpiece instability.

The two packages put forward in this thesis have been shown to be capable of simulating the motions and contact geometries of the rotary forging process, and confirmed using physical and real rotary forging comparisons.

CHAPTER 1.

INTRODUCTION.

1.1 INTRODUCTION.

Rotary Forging, Orbital Forging, and Wobble Die Forging, are all terms used to describe the same process. Rotary forging is the most widely used and accepted of these names and shall be used throughout this thesis.

Rotary forging is a metal forming process which is dedicated mainly to the forming of circular parts such as bevel gears, synchro rings, bearing housings, clutch hubs, chain sprockets, couplings, ratchets and differential gears. Many of these parts are used in the construction of motor vehicles. It is estimated that nearly 80% of all forged parts produced in the World are circular in section. This shows the potential for expansion of rotary forging since, less than 1% of forged parts are currently made by a rotary forging route.

At present most of the industrial ^{metal} forging companies are geared towards the production of parts by conventional bulk forming techniques. Conventional forging is a well established route for the production of many parts. This factor coupled with the knowledge and expertise gained in conventional bulk forming has created a reluctance to change to new processes. The incremental nature of rotary forging offers a possible alternative to conventional bulk forming processes. Parts can be rotary forged using a fraction of the force needed by conventional bulk forming processes. On some rotary forging machines, parts can be rotary forged using up to 10 times less force, than by bulk forging techniques, [1].

Recent interest, by some of the largest motor vehicle manufactures, is seen as an indication of the processes acceptance as a viable cold forging alternative to hot bulk forming techniques. An international club has recently been set up to cater for industrial interest in rotary forging, and to provide information, and undertake research and development programmes.

In general, rotary forging machines can be described as having a central axis of rotation, along which are positioned two dies, one of which is inclined at an angle of several degrees, figure 1.1. The inclined die is usually of conic section. The dies can be rotated in several different ways. These are described in more detail in Chapter 2. For the time, it will suffice to the describe motions of rotary forging in terms of the two motions, 'rotation', and orbital. 'Rotational' movement simply involves the rotation of the die about its own axis. Orbital motion is where the die is rotated so that it describes a circle, causing the tool to be rolled around the surface of

a workpiece. Dies are usually moved either by a hydraulic system or by gears. Machines using the orbital motion usually have only one rotating die. On 'rotational' type machine systems both the upper and lower dies are 'rotated'. At the same time as the 'rotational' or orbital motion of the dies, they are brought together under the action of a hydraulic ram. The workpiece is located between the two dies and as a result of the inclined conic die, a partial contact region is formed. The partial contact, region shown in figure 1.2, produces a partial plastically deforming zone (P.D.Z.) extending below the surface of the workpiece. The P.D.Z. is swept about the workpiece by rotation of the inclined die axis, so, effectively, forming the whole workpiece into the upper and lower dies.

Rotary forging offers advantages over conventional processes. These can be identified by : lower capital input and smaller quieter machines. In addition, parts can be forged to size cold with improved surface finish, higher tolerances, and less machining of the finished part. Some cold rotary forged parts need little or no machining, since the tolerances and surface finish are considered superior to parts produced by conventional bulk forging techniques. In this way, rotary forging can reduce the number of machining and finishing operations needed to produce the final part.

1.2. A BRIEF HISTORY OF ROTARY FORGING.

Rotary forging was first recorded in a patent by E.E. Slick at the beginning of this century, [2]. His mill was designed for the production of wheel type forgings for trains and large vehicles. The mill consisted of two rotating circular, contoured dies mounted horizontally, between which the workpiece was forged. In operation, both the dies were rotated, with only one of these inclined to the horizontal axis by $10\frac{2}{3}^{\circ}$. In practice, the Slick the mill was capable of using hot billets of up to 50 cm in diameter, [3]. These were forged by compressing and simultaneously rolling them between the two rotating dies. A mill was still used by the Bethlehem Steel Corporation in the U.S.A. up to the early 1980s, and was believed to be very similar to Slick's original design.

A different type of rotary forging machine design was put forward by H.F. Massey in his patent of 1929. Unlike Slick, this design was never built, [4]. However, the patent pointed out certain characteristics which were peculiar to the

rotary forging process. One of these was a key slot constraint, to stop the upper die from turning, as it carried out its orbital motion. This is now a fundamental feature in many rotary forging machines. It was not until 1969 that B. and S. Massey Ltd. took out a further two patents regarding the design of a hemispherical, hydrostatic, multi - pad bearing, and a conical hydrodynamic rocking head bearing, [5], [6]. These were major steps forward for rotary forging machine design, since the bearings of rotary forging machines had always posed restrictions to machine development. (Slick's thrust bearings were believed to be the largest in the World at the time.) In trials, Massey was able to develop and test his machine design. In 1972, Massey produced the first production model of a rotary forging machine. This machine was a vertically mounted design with only the upper die rotating in an orbital manner. The machine was found to form parts best at 'warm' temperatures of 600 - 800°C. The upper die was inclined at an angle to the vertical of 3.5°. The lower die was hydraulically operated to impart the pressure to the workpiece between it and the rotating upper die. The machine's capacity was rated at 200 tonf, but it was estimated that this was equivalent to a conventional forging press of 2000 tonf.

A Polish designer, Marciniak, put forward a patent, in 1967, for a rotary forging machine, which had a single upper rotating die, [7]. The upper die was driven in an orbital fashion and incorporated a down stroking ram. The lower die was fixed with regards to both rotation and vertical movement. The machine was capable of forging components of up to 80 mm in diameter. The machine was specifically designed for cold forging so its upper die angle was kept to 2° in order to maximise die strength and support. Four types of rotary forging motions were possible with this machine, because of its unique gearing system, allowing the upper die to be rocked between -2° and 2° whilst undergoing an orbital motion. This machine design has been licensed to several machine manufacturers and is the basis for several commercially produced rotary forging machines.

In 1967, British interest in rotary forging appeared at UMIST with the design and construction of a prototype rotary forging machine, [8]. The machine was of a vertical construction and had an upper die inclination angle which could be set between 0 and 10°. In 1971 and 1972, further work was carried out resulting in the construction of a larger machine, this time with a capacity of 0.25 MN and a top die

inclination of 0 to 8°. The machine was used, mainly on a research basis, at the University. The machine was hydraulically operated and its design was very similar to that of the Rotaform machine.

In 1972, a paper from the the Government Research Institute, at Nagoya in Japan, put forward a machine design which was similar to that of the UMIST machine, [9]. The machine was vertically mounted with the top die rotating in an orbital manner. The upper die angle could be set between 0 and 10°. A larger machine of 1.2 MN capacity was built in 1973. This incorporated improvements in design and had a die inclination capable of being set between 0 - 5°.

Heinrich Schmid, a Swiss engineer, adopted the rocking head design of Marciniak, and took it through a design and manufacturing route to produce a commercial rotary forging press. Schmid has continued to produce presses, and now the Company is the leading manufacturer of rotary forging machines in the World. At present, Schmid produces a range of presses of 200, 400, and 630 tonne capacities. All the Schmid presses utilise the rocking head design of Marciniak and are capable of the four rocking die motions. The presses are all designed for cold forging and incorporate a die inclination angle variable between 0 and 2°. The largest of the presses is capable of forging solid cylindrical parts of up to 96 mm in diameter, and a synchro ring for a gearbox can be produced with an external diameter of 143 mm.

In 1986, at the University of Nottingham, H. Mwenda developed a new and unique rotary forging press, [10]. The press is microprocessor controlled, vertically mounted, and with an upper die range of inclinations of between 0 and 45°. Its two dies can be spun together, or individually, in a 'rotational' fashion, and has a main ram capacity of 50 tonne. The machine axis movement is infinitely variable and achieved under microprocessor control. This gives the machine a large range of applications and it has been used extensively for research and development of new product areas and applications.

1.3. DEVELOPMENT OF A PACKAGE TO SIMULATE ROTARY FORGING.

The development of F.E. and other bulk metal forming packages have been followed with interest by the forging industry. At present, there are several

commercially available packages capable of simulating conventional bulk forging processes. These packages took many years to develop, and only now, are becoming sophisticated enough to be important to the die design process. Finite Element (F.E.) packages have been shown to be capable of reducing the die design lead times by a significant amount. This is important since die lead times can be as long as 2 to 3 years for a production part and are a large proportion of the cost of producing the finished part.

The development of rotary forging, as a competitive and viable alternative to conventional bulk forging processes, would involve the development of software in the areas of simulation and machine control. Computer simulation also aids the understanding of the complex motions and actions of rotary forging machine tools. At present, commercial F.E. packages, available for bulk metal forming, are not sophisticated enough to accommodate the complex motions involved in rotary forging machines, and so cannot be applied to rotary forging situations. At present the area of die design in rotary forging is a costly one, since the methods used are carried out by 'a rule of thumb' and on a trial and error basis. In conventional forging, these methods work to a certain extent since the processes have been used and built upon over many years. However, since little or no history of die design techniques exists for the rotary forging process, simulation seems the obvious way forward. Simulation techniques should enable die lead times, costs, and design to be improved in rotary forging.

A first step, towards the goal of understanding rotary forging, would be the development of a computer package to simulate the motions of rotary forging machines. Such a package would enable the sometimes complex motions and actions of rotary forging machines to be seen and plotted so that their motion can be understood. The ability to 'see' what sort of incremental contact region is created on the surface of a workpiece during rotary forging has eluded researchers for some years now. The ability to be able to simulate the contact region, using any of the motions of rotary forging machines, would be a significant step forward in understanding of the process. Once the contact geometry can be predicted, during a rotary forging, the instantaneous contact area, and the volume of material displaced, could also be calculated. These values are needed as a starting point for any calculations of the forces and stresses involved in the rotary forging of a workpiece.

The development of a computer package, which is capable of simulating the contact geometries and hence the instantaneous contact area and displaced volume of material, is seen as an essential first step toward the goal of producing a C.A.D. - C.A.M. package specifically for rotary forging. These propositions are put forward as the aims of this research project.

CHAPTER 2.

LITERATURE REVIEW.

2.1. INTRODUCTION.

The simulation and modelling of rotary forging has been approached in many different ways. One of the earliest methods of investigation of the process was the use of modelling materials such as plasticine to model the workpiece, [11],[12]. Model materials were often used in conjunction with a physical model of a rotary forging machine. The low forces needed to deform material, provide an economical method of investigation, [13]. Rotary forging can be defined in terms of the geometrical shapes of cones and cylinders. The mathematical modelling of such shapes is easy to apply and has been used extensively by many researchers to simulate this process, [9],[14],[15],[16], [17]. Vector analysis has also been applied to rotary forging, but only for the modelling of the tooling motions taking place during the process, [18]. Computer simulation techniques, applicable to rotary forging, are few and far between. At present there is only one commercially available package, ASTRID , developed from the work of researchers Oudin et al., [19],[20].

2.2. USE OF SPECIAL MATERIALS TO INVESTIGATE ROTARY FORGING.

The use of plasticine, to investigate the movement of material and the strains which may occur during the rotary forging of hot steels, was used by Slater et al. , [11]. The plasticine was chosen as a workpiece because its rigid-perfectly-plastic properties are similar to the properties of hot steel workpieces during forging. Results, using multilayered specimens of plasticine, have been presented and claim to support evidence of velocity discontinuities in the workpiece during rotary forging. The paper put forward two mechanisms of deformation for radial flow in the workpiece.

Lead specimens have been used to investigate the size of the P.D.Z. produced in rotary forging. These studies showed the well known 'mushrooming' effect was due to insufficient axial forging force and hence only limited penetration of the P.D.Z. The work suggested a number of practical recommendations for the forging of circular workpieces, including the use of different initial H/D ratios, feed rate, and forging force to obtain desirable development of the P.D.Z. during the process. Further work produced a general expression involving experimentally

determined constants describing the relationship between the fractional reduction, R , and the number of revolutions of a conic die of angle α for cylindrical specimens of different H/D ratios, [12]. This was verified experimentally using lead workpieces. The contact area was found using 1 inch diameter lead specimens by simply indenting a 20° conic tool into the workpiece under different loads for a few seconds. No rotary forging took place. The specimen was then examined and the parabolic contact area was then measured and recorded. These contact areas were then used to determine the rotary forging die pressures. Results showed good agreement with an expression derived to predict the contact area, [21]. Using the plasticine and lead specimens, experiments again suggested that good die fill could be obtained with lower contoured dies for the forging of shallow flanged products.

Koch et al. used different colours of paraffin wax to construct multilayered workpieces, [13]. These were used in experiments to investigate the effect of the motions of rotary forging machines. The work showed the surprising result that the rosette and spiral motions of Marciniak / Schmid type rotary forging machines were less prone to produce the 'mushrooming' effect than the orbital or straight line motions. Further work involved the use of pressure pins placed on the bottom die beneath the workpiece. The pins were strain gauged to measure the pressure distribution across the base of the workpiece during forging. Results suggested that a central region of low pressure existed in the workpiece, and could be used to explain the centre thinning phenomenon. This work supported the results previously proposed by Hawkyard et al., [22].

Wanheim et al. developed the modelling technique using a mesh of multicoloured wax for the specimens, [23]. These were deformed and sliced at different sections. The revealed mesh was then photographed and mesh nodal points input into a computer programme. This then converted the points into coordinates from which the strain distribution, and distribution of maximum shear were obtained. The results were used to identify slip line fields and analyse deformation systems. This approach is particularly useful for workpieces deformed by processes such as rotary forging which are non - homogeneous, non-steady state, non-plane strain, and non-uniform. The rotary forging experiments using wax model material were carried out on a model Marciniak type rotary forging machine.

Hawkyard et al. used aluminium and lead as modelling materials on a 25 tonne capacity experimental rotary forging machine, [22] Of particular interest was an investigation of the pressure distribution across the workpiece using a pressure sensitive lower platen. The results suggested that the mechanism of deformation included a plastic hinge opposite to the tool contact region. This was confirmed using steel specimens which when specially heat treated and etched after forging showed yield zones, [16]. The incorporation of a plastic hinge mechanism into the deformation process assumes that the material not only deforms plastically in the contact region, but also as a hinge diametrically opposite. The relationship between the hinge and the workpiece is cyclic as the tool rotates over the surface.

More recently photoplastic materials have been used by Chou et al. to investigate the strains created in the workpiece during rotary forging, [24]. In this work a polycarbonate workpiece was forged, cut, sliced, ground, polished, treated, and photographed. The results produced isochromate streaks which when measured and substituted into six strain formulae, and entered into a computer program were then used to calculate the strain distribution across the workpiece. The results showed that compressive strains were lower in the centre region of the workpiece, again supporting the centre thinning phenomenon. The polycarbonate model material used was claimed to have a "similar stress-strain tensile curve as that of carbon steel". They also claimed that it had a Poisson's ratio of about 0.5, so providing an effective modelling material for plastic deformations.

2.3. PHYSICAL MODELLING.

Physical modelling is when a machine or test rig is used to simulate a rotary forging machine. Model machines can be said to be of a capacity not high enough to enable the rotary forging of real industrial parts. The building of small physical models or prototype machines has enabled researchers to successfully investigate many aspects of the rotary forging process.

Slater et al. published a paper on the development of an experimental rotary forging rig. The workpiece was loaded by means of a system of weights and levers, and was of low capacity, [8]. The rotary forging rig was used in experiments, with plasticine to investigate the deformation mechanisms in the workpiece, [11]. In 1973, Kubo et al. developed an experimental press at the Government Research

Institute at Nagoya, [9]. This was very close in design to that of the Rotaform machine. Hawkyard also designed and built a machine which was used for research in conjunction with model materials to investigate phenomena such as centre thinning, pressure distribution, mushrooming, yield zones and deformation mechanisms [16], [12], [25]. Koch et al. specifically built a machine based upon the Marciniak and Schmid type rotary forging presses to investigate rotary forging problems using wax materials, [13]. More recently Hayama used an experimental rotary forging machine to compare with his analysis of rotary forging. His machine included the use of pressure cells in the die and lower platen, [17].

Many more prototype machines are likely to exist, since reports are not always published by companies developing new rotary forging machines.

2.4. MATHEMATICAL MODELLING.

The tool and workpiece and the motions of the rotary forging process have been modelled mathematically. Rotary forging is suitable to this type of approach, since the tool is usually a conic section, and the workpiece of cylindrical form. In general these are both easily defined mathematically. The interaction between two geometrical shapes and an appreciation of the motion of rotary forging machines allow the process to be modelled.

Kubo et al. developed an empirical formula for the contact area generated during rotary forging based upon the geometry of a cone and a workpiece, [9]. Using this, they were able to derive further formulae to find the reduction in height of a workpiece after a number of revolutions of the die. The results of this showed fairly good agreement with experiments, [15]. Nakane et al. were able to calculate the forces necessary to deform the workpiece during forging and the power needed for the process, [26]. The combined use of mathematical modelling and computing techniques, enabled Su et al to predict the contact area, pressure distribution, circumferential strains, height reduction, and metal flow taking place in the workpiece, [17]. These results were confirmed by using specially prepared workpieces, and pressure sensitive pins and a computer to analyse the results and determine the loads. The material flow associated with the centre thinning phenomenon was discussed. Zhao also produced empirical formulae to predict the contact areas formed during rotary forging, but with little experimental confirmation,

[27]. Mansour was able to define the motions of rotary forging machines using a formulae based upon the Eulerian motions of nutation, precession, and spin. Computer software was written and used to simulate the motions of rotary forging machines [28]. Hu was also able to produce a simulation of the process by the use of vector analysis of the eccentric motions of the drive bushes of a Marciniak / Schmid type machine. [18].

2.5. COMPUTER SIMULATION AND CAD-CAM.

Researchers such as Carleone and Marciniak have suggested the use of computer simulation to develop and extend the rotary forging process, [29], [30]. Unfortunately, to date the high technology development of the rotary forging process has not existed. C.A.D. - C.A.M. systems have been developed for many forging processes, some of which have similarities to rotary forging. Mullineux developed a system for the design and the manufacture of rolling dies, where the desired finished product shape was input into the program, and a possible preform shape and tool design produced, [31]. The die could then be made on a numerically controlled E.D.M. using the data produced from the tool design package. The preform shape could then be tried out and modified with the help of the C.A.D. - C.A.M. system.

In 1985, Chou produced a computer package specifically designed to simulate rotary forging. This was called DEFEL (Dyna East Finite Element Lagrangian code.) [32]. The package was based upon a 2-D elasto-plastic finite element model. However, little is known whether there has been further progress to produce a 3-D version of DEFEL which would be needed to simulate real problems.

The upper bound approach has been used over a number of years by Oudin and Ravalard for the solution of metal forming problems, [19],[20]. Early work discussed in the papers was specifically targeted at the rotary forging of ring shaped components. Several assumptions were made in the empirical formulae concerning the mechanisms of deformation. It was assumed that a plastic hinge was associated with the deformation. From this the workpiece was subdivided into six individual regions for the purposes of calculation. Recently they have developed a general metal forming package called ASTRID based upon a finite element approach. It is thought that ASTRID is the first commercially available package claiming to be

capable of simulating rotary forging type problems.

A non - plastic approach was taken by Mansour using the Eulerian motions of nutation, precession, and spin, and formulae to describe these motions were applied to meshes representing a conic die and workpiece, [28]. The contact geometry between the die and the workpiece could then be found. The results could only show how the contact geometry developed during the first and last revolutions of the process.

There are many commercially available finite element packages for forging, but these are thought to be too generalised to be applicable to rotary forging. The reasons for this are: the difficulty in accommodating rotary forging type motions, and problems defining the boundary conditions for rotating dies, thus making the computing power requirements prohibitive.

CHAPTER 3.

CLASSIFICATION OF ROTARY FORGING MOTIONS.

3.1. INTRODUCTION.

Although rotary forging machines around the World vary considerably in their design and motion, they all share some basic common features. These are defined in this chapter, firstly in terms of the tool and workpiece arrangement, and then in terms of the movement of the dies. Over the years many terms have been put forward to group and classify machines in terms of their motions, such as the 'Type 1', 'Type 2' or 'Type 3', but these terms are easily confused, and do not divide the different types of machines into enough groups for clear and comprehensive classification, [1]. A simple approach is taken in this work, based upon Euler's representation of the motions of two rotating bodies in space, [33], [34]. This leads to a comprehensive classification of rotary forging machines, and a set of mathematical equations to define their motion.

3.2. DEFINITION OF ROTARY FORGING MACHINES AND THEIR MOVEMENTS

There is much confusion over the terms used to describe rotary forging machines. This chapter describes a different, but not yet fully recognised method of identifying different types of machines in terms of their motions. This method is comprehensive and more detailed than previous methods of classification, and is a prerequisite for describing the motions mathematically and providing the opportunity to simulate them.

3.2.1. Rotary Forging Tool and Workpiece Arrangement.

Analysis of the rotary forging machines has enabled an outline of the features to be drawn up which are common to every machine. These are listed below:

- i). There is an upper and lower die
- ii). One of the dies, normally the upper, is a conic or inverted conic shape.
Typically the cone angle (α) is between 1 and 10°.
The other die is not inclined and usually holds the workpiece.

- iii). The conic die is inclined to the centre line of the workpiece by an angle θ known as the nutation angle, described later in this chapter.
- iv). The upper die can be rotated or moved in any direction as long as its apex stays on the centre line of the workpiece. This point is very important in rotary forging, and is known as the pivot point about which all rotations of the conic die take place.

Figure 3.1 shows the basic conic die / workpiece arrangement in a conventional rotary forging setup.

3.2.2. Definition of Rotary Forging Machines in Terms of Their Tool Movement.

The basic tool and workpiece arrangement, shown in figure 3.1, is common to all rotary forging systems, their difference being determined by the movement and relationship of the tools, and in particular, the movement of the conic tool / workpiece.

In 1771 and 1776 the Swiss mathematician, Euler, analysed the motion of a body moving in space, [33], [34]. Using algebraic geometry he was able to define six independent parameters based on three simple rotations, namely, nutation, precession, and spin. Euler showed that these three motions could be used to define any rigid body rotation. Euler's formulae have proved useful in defining the motions of rotary forging machines. This idea was first applied by Standring and Appleton in 1979, when the terms Nutation, Precession, and Spin were adopted to describe the varied motions of rotary forging, [1]. The three motions are shown in terms of the basic conic tool and workpiece arrangement of rotary forging in figure 3.2.

In terms of rotary forging the Eulerian motions of figure 3.2 are defined as :

- a). Nutation: when the axis of a conic tool is rotated so that it rocks about the pivot point whilst moving in a plane.
- b). Precession: when a conic tool, inclined at the pivot point to the central axis of the workpiece, moves so that its axis rotates about the central axis.

- c). Spin: when a conic tool rotates about its own axis. The conic tool axis is usually inclined to the axis of the workpiece and both the tool and the workpiece are rotated during the deformation process. Rotational speeds are maintained to keep the the frictional forces between the die and the workpiece to a minimum.

The three simple motions can be combined to create seven different motions as shown schematically by the clover leaf in figure 3.3. Each area of the clover represents a motion and class or type of rotary forging machine. Physical evidence of rotary forging machine design in terms of their use of the Eulerian motions, is presented in table 3.1. Considering one example, that of the Marciniak / Schmid design, these are identified by the use of nutation, precession and / or nutation - precession motions. It would appear that only one of the areas of the clover leaf is not represented by existing rotary forging machines.

3.3. MATHEMATICAL DEFINITION OF THE EULERIAN MOTIONS.

Euler's mathematical description of the rotation of a rigid body involves the use of three equations. These can be combined to produce three more expressions in terms of the X,Y, and Z which are the coordinates of a point on a rigid body. They define the position of a point after any amount of nutation, precession, or spin. The equations were first used to describe Rotary Forging tool movement by Mansour and are shown below, [28].

$$\begin{aligned} X &= x_i(-\sin(\phi) * \sin(\psi) + \cos(\theta) * \cos(\phi) * \sin(\psi)) \\ &+ y_i(-\sin(\phi) * \cos(\psi) - \cos(\theta) * \sin(\phi) * \sin(\psi)) \\ &+ z_i(\sin(\theta) * \cos(\phi)). \dots\dots\dots\{3.1\}. \end{aligned}$$

$$\begin{aligned}
Y &= x_i(\cos(\phi) * \sin(\psi) + \cos(\theta) * \sin(\phi) * \cos(\psi)) \\
&+ y_i(\cos(\phi) * \cos(\psi) - \cos(\theta) * \sin(\phi) * \sin(\psi)) \\
&+ z_i(\sin(\theta) * \sin(\phi)).....\{3.2\}.
\end{aligned}$$

$$Z = x_i(-\sin(\theta) * \cos(\psi)) + y_i(\sin(\theta) * \sin(\psi)) + z_i(\cos(\theta))....\{3.3\}.$$

where: θ = Nutation, ϕ = Precession, and ψ = Spin.

where: x_i , y_i , and z_i are the original coordinates of a point on a rigid body.

The precession motion is somewhat complex in that using Euler's equations, a single simulated 2π precession rotation would also include a simultaneous 2π rotation of spin. In many rotary forging operations, simultaneous spin, whilst accompanying a precession motion, is physically prevented by the use of a 'constraining' mechanism. (A ring gear or key - way.). Mathematically this situation is simulated by incorporation of a negative 'spin' motion.

3.4. CONCLUSIONS.

A general tool and workpiece arrangement has been identified which is unique to rotary forging machines. A conic tool is said to be inclined to the workpieces axis, with its apex on that axis.

The movements of rotary forging machines have been shown to be capable of being represented by the Euler motions of Nutation, Precession, and Spin. The combination of these motions enabled more complex motions to be created. The motions, nutation, precession, and spin, were shown to be capable of identifying many of the rotary forging machine designs which have been produced.

Rotary forging machine tool motion was shown to be defined mathematically by a set of three equations. These equations were found by combining the three Eulerian equations for rigid body rotation, of nutation, precession and spin.

CHAPTER 4.

APPLICATION OF EULERIAN MOTION TO ROTARY FORGING.

4.1. INTRODUCTION.

As put forward in the previous chapter, rotary forging tool motions can be described mathematically by equations {3.1},{3.2},{3.3}. These equations were incorporated into the author's rotary forging computer simulation package. This enabled both the path of a point on an upper die, and the path of a point on the upper die axis to be determined at any instant during a rotary forging cycle. The computer package produced results which supported the results from other researchers such as Standring, Hu, Nakane, Marciniak, and Oudin, [1], [18], [26], [30], [35].

Marciniak / Schmid type machines are capable of producing a non - monotonic nutation motion of the axis of the die. This is where the nutation is not only in one direction, but in the two directions of +ve and -ve motion, in a single cycle of motion. When nutation is combined with precession, it produces the well known rosette and spiral shaped patterns of motion of figure 4.1, [30].

The simulation package was then used as a machine motion design tool and interesting new motions were discovered for different ratios of spiral and rosette actions. From these results an equation was derived to predict the axes of symmetry of a spiral motion and the number of petals of a rosette motion. The package has been used to gain an appreciation of the various patterns which result from a combination of individual rotary forging machine motions.

4.2. APPLICATION OF THE MODEL TO A COMPUTER PROGRAM.

The equations {3.1},{3.2},{3.3}, were incorporated into a computer program called 'PATH' which can calculate the position of any point on a conic die of a rotary forging machine. The program plots the position of a point incrementally for a number of steps so that its path could be traced and the displayed orthogonally as a plot on the screen. The program was written in 'C' and ran on a Prime mini computer. The computing time for 100 plotted points was 2 seconds and the drawing time was 6 seconds.

Figure (4.2) shows a typical conic die arrangement for a rotary forging machine with an angle α of 30 degrees. Point A represents a point on the tool axis and point B represents a point on the tool surface/edge. The locii of both these points can be plotted and are important, since point A will show what the die is

doing or the motion it is undergoing, and point B will show what the workpiece will 'see' when it is being deformed.

On Marciniak / Schmid, nutation - precession, type rotary forging machines, the motion is achieved by the use of eccentric gearing. This means that the nutation is, in effect, an oscillating Simple Harmonic Motion (S.H.M.), as shown in figure (4.3). This motion is often known as, "Rocking Die Nutation", but since the nutation is in both the +ve and -ve directions, it will be called "non - monotonic" Nutation for the rest of this thesis.

Described mathematically, the motion of a point on the die or the axis of the die will be given as shown in figure 4.4 by :

$$\theta = \theta_i + \theta_a * \sin(\dot{\theta} * T) \dots\dots\dots(4.1).$$

where: θ = Instantaneous Angle of Nutation. θ_i = Initial Nutation.
 θ_a = Amplitude of Nutation.

$\dot{\theta}$ = Nutation Rate. T = Time.

When non - monotonic nutation is chosen in the program, equation 4.1 is implemented for each of the steps of the dies movement to find the resulting instantaneous value of nutation which is then input into equations {3.1}, {3.2}, {3.3}.

4.3. VERIFICATION OF THE MATHEMATICAL MODEL AND
COMPUTER PACKAGE.

4.3.1. Results for the Path of a Rotary Forging Die.

Results plotted by the computer program for the motions of a point on the axis of a conic die of $\alpha = 30^\circ$ during nutation, precession, and spin motions are shown in Figures 4.5, 4.6, and 4.7. These results correspond to the motion of point A in figure 4.2. Figure 4.5 shows straight line nutation which is simply an arc in the Y - Z plane and a straight line in the X - Y plane. Figure 4.6 shows in plan view a circular motion for precession. (It should be appreciated that the plotting device

produced a slightly elliptical figure which in fact is circular.) It is this motion which gives rise to the often used term 'orbital forging'. and this is what would be expected to be seen. Figure 4.7 shows no apparent motion at all. This is because the motion is defined by a single point which can just be seen as a red spot on the Y axis in plan view.

More revealing results are produced when simulations are carried out for non-monotonic nutation and precession similar to that of a Marciniak type rotary forging machine. The machines are capable of producing the four types of motions as shown in figure 4.1. Figure 4.8 - a,b,c,d shows the enhanced motions of non-monotonic nutation produced using the 'PATH' simulation package. The figure shows the path of a 30° conic die oscillating about the vertical axis with a nutational amplitude (θ_a) of 30°.

- a.). straight line motion, or non monotonic nutation
- b). circular motion, or precession.
- c). rosette / planetary motion, or non - monotonic nutation - precession.
- d). spiral motion, or non -monotonic nutation - precession.

Figure 4.8 - a clearly shows that a point representing a point on a workpiece axis describes an arc of motion in the Z - Y plane, and this agrees with predictions from researchers such as Hu, Oudin and Ravalard for the motion of a Marciniak type machine, [18], [35].

Figure 4.8 - b shows the circular motion of a point on a precessing conic die axis, and this again agrees with the results of the above researchers.

Figure 4.8 - c shows the rosette / petal / planetary motion or non - monotonic nutation - precession which occurs when the nutation rate is greater than the precession rate. The figure shows clearly the pattern and number of petals produced, for example by a nutation rate of 3 c.p.s to a precession rate of 2 c.p.s.

Figure 4.8 - d shows the spiral motion or non - monotonic nutation - precession motion when the nutation rate is less than the precession rate. The figure shows a pattern which is similar to the spirals predicted by Hu and Oudin and Ravalard, [18], [35]. Hu obtained his results by vector analysis of the motion of the

bushes used to drive the PXWP-100C Marciniak machine. His locus of the spiral movement mirrors that modelled by the computer program 'PATH'. Oudin and Ravalard's results for a new flexible rotary forging machine design, again based on a Marciniak type of machine, show that it would be capable of producing spiral shaped tool paths, [35].

4.3.2. Results for a Point Lying on the Periphery of a Conic Rotary Forging Die.

The simulation of a point on a rotary forging die, ($\alpha = 30^\circ$), point B, shown in figure 4.2, during nutation, precession, and spin, produces some interesting results as shown in figures 4.9, 4.10, and 4.11.

Figure 4.9 shows the nutation motion for a simple monotonic nutation of 30° . The motion is a simple arc in the Y - Z plane, and a straight line in the X - Y plane (plan view).

Figure 4.10 for a precession motion, shows the commonly found teardrop shape in side elevation and a circle offset from the centre in plan view. This pattern shows good correlation with previous work carried out by Standring, and Appleton, and Nakane [1], [26], by both physical simulation methods and numerical analysis. The teardrop shape is effectively what the workpiece will 'see', or experience from a point on the die when it is moving in a precession motion with no feed rate, or die / workpiece penetration.

Figure 4.11 for a spin motion, shows an ellipse in plan and side elevation. Again the reader is cautioned about the validity of the plan view diagram due to plotting errors in the computing facilities

4.4. CONCLUSIONS.

A mathematical model for the Eulerian motions of spin, precession, and nutation, has been put forward and shown to be capable of simulating rotary forging machine movements in a computer package 'PATH'.

A formula for the simulation of non - monotonic nutation has been shown to be capable of producing the rotary forging patterns of spiral and rosette shapes when combined with the motion of precession.

Results from the non - monotonic nutation - precession simulations were shown to agree with those of the Marciniak type machine motions as predicted by Hu, Oudin and Ravalard [18], [35].

Spiral motions were found to be created during non - monotonic nutation - precession motion when the precession rate was larger than the nutation rate.

Rosette motions were found to be created during non - monotonic nutation - precession motion when the precession rate was less than the nutation rate.

Results for a point lying on the periphery of a conic rotary forging die were shown, for the precession motion, to agree with the results of previous researchers.

The Eulerian motions of nutation, precession, and spin have been shown to be capable of identifying many of every rotary forging machine designs which have been produced. Mathematically these motions have been modelled, and incorporated into a computer package. The combination of the motions has been demonstrated and shown to agree with previous researchers. The package 'PATH' has been shown to be capable of simulating many of the movements that are utilised in rotary forging machines.

CHAPTER 5.

RESULTS FROM PATH.

5.1. INTRODUCTION.

'PATH' is a computer package described in Chapter 4, capable of simulating the rotary forging motions of spin, nutation, precession and non - monotonic nutation, or any combination of these. In this chapter the motions of non - monotonic nutation - precession are discussed at length, and a formula proposed to predict the symmetry of a spiral or the number of petals in a rosette pattern.

As shown in Chapter 4, the locus of a point on the surface of a rotary forging tool produced different shapes to those of the motions of the tool axis. These results are explained in detail. In addition, because of their current importance in commercial rotary forging, the non - monotonic nutation - precession motions, used in Marciniak type machines are selected for investigation. The effects of varying the cone angle between 0 and 90 degrees have been investigated and results show the locus of a point on the conic tool surface to continuously change from a teardrop shape to a circle. The effect of varying the initial nutation for precession motion was also investigated. These results show a range of patterns from a point, to a figure of eight, supporting the predictions made by Nakane et al., [26].

5.2. RESULTS FOR ROTARY FORGING TOOL MOVEMENT.

When the instantaneous angle of nutation, obtained from equation 4.1, is combined with precession in equations 3.1, 3.2, 3.3, the locus of any nutation - precession motion can be found. When either the nutation rate or the precession rate is equal to zero then a simple nutation or precession will be produced. A chart was plotted showing the number of petals in a rosette or the symmetry of a spiral, against the nutation rate ($\dot{\theta}$) and precession rate ($\dot{\phi}$)

It can be seen, in table 5.1, that spiral motions are produced when the nutation rate is less than the precession rate, and visa versa. From table 5.1, a clear pattern can be seen, and from this an expression was derived to predict the number of petals of a rosette or the number of symmetries of a spiral. Only discrete values of the nutation rate and the precession rate are considered since the motions of present rotary forging machines are governed by gears with a whole number of teeth. This means that only integer values of the nutation rate and the precession can be used in

the following equations.

If $\dot{\theta} / \dot{\phi} = \alpha / \beta$

If the α / β ratio is found in its lowest common form then:

if α , and β are both odd, then :

$N = \alpha \dots\dots\dots\{5.2\}.$

if either α , or β are even then :

$N = 2 * \beta \dots\dots\dots\{5.1\}$

N = the number of petals in a rosette or the number of symmetries of a spiral.

Mathematically, equations 5.1, and 5.2 can be represented by the formula shown below :

$$N = \frac{\alpha ((-1)^{(\alpha + 1)} + 1) * ((-1)^{(\beta + 1)} + 1)}{4}$$

$$+ \alpha ((-1)^{(\alpha + \beta + 1)} + 1) \dots\dots\dots\{5.3\}$$

where α , and β are integer values in their lowest common form as a fraction.

Similar results were predicted by Baert et al. for the motions proposed for a new type of rotary forging machine, [35]. They produced a formula to predict the number of petals of a rosette based upon factor identified as Z .

where :

$$Z = \dot{\theta}_2 / \dot{\theta}_1 \dots\dots\dots\{5.5\}.$$

$\dot{\theta}_2$ rate = the rate of the main spindle, (equivalent to the precession rate).

$\dot{\theta}_1$ rate = the rate of rotation of the shaft which controls the nutational adjustment of the upper die. This is not the same as nutation rate, since the motion imparts precession motions as well as nutation.

Therefore, the number of petals produced in a rosette is given by:

$$N = \text{Numerator } |2(1 - Z)| \dots\dots\dots\{5.6\}.$$

where :

$2(1 - Z)$ is a fraction in its lowest form and

N = the number of petals in a rosette.

Interpreting Z in terms of the Eulerian motions is shown below.:

If the α/β ratio is found in its lowest common form, and α , and β are both odd, then :

$$Z = \frac{\beta}{\beta + \alpha} \dots\dots\dots\{5.7\}.$$

If the α/β ratio is found in its lowest common form, and if either α , or β are even then :

$$Z = \frac{\beta}{\beta - \alpha} \dots\dots\dots\{5.8\}.$$

Graphically, the results of Baert et al showed total agreement with those in figures (5.1),(5.2),(5.3),(5.4), [35]. This fact suggests further confirmation of the validity of the mathematical model and the computer package as a form of rotary forging simulation.

Figure (5.1) shows an asymmetric type of machine motion which is produced when the nutation rate equals the precession rate. This is neither a spiral nor a rosette motion and is produced because the precession motion reverses the direction of nutation after half a revolution so that the motion is always on the same side of the workpiece. Because of this, one whole cycle takes place in 180 degrees of precession. Figures 5.2, and 5.3, show the rosette motion with six petals, but the width of the petals are different, and in figure 5.3, they overlap.

Petals were found to overlap if the precession rate / nutation rate ratio $(\dot{\phi} / \dot{\theta}) > 0.5$.

Figure 5.4 shows that a spiral motion is produced at a nutation rate = 1 c.p.s., and a precession rate of 4 c.p.s., showing further evidence that this motion occurs when the precession rate is greater than the nutation rate.

5.3. APPLICATION OF 'PATH' TO DETERMINE THE LOCUS OF A POINT ON THE SURFACE OF A TOOL.

For this part of the work, the program 'PATH' was used to investigate the locus of a point on the tool edge of a conic rotary forging die as shown by point B in figure 4.2.

5.3.1. Precession Motion - The Effects of Altering The Initial Nutation (θ_i).

For the precession only case, the path of a point on the working surface of a conic tool describes a teardrop when the initial nutation angle θ_i , equals the cone angle α . If the initial nutation does not equal α , then other patterns of motion are produced. These are relevant to rotary forging tool design, since a contoured surface will deviate from the mean cone angle and will in effect undergo the same motion as for a point on the surface of the tool, when $\theta_i \neq \alpha$. Figure (5.5) shows the locii of nine different conic tool motions produced during precession given initial nutations between 0 and 180 degrees.

When the initial nutation, θ_i , equals zero, then nothing can be seen (figure (5.5) a). In fact a dot is produced, since the precession motion has no amplitude.

As values of θ_i are changed between 0 and the cone angle α , the motion gains amplitude and the familiar teardrop shape is developed, figure (5.5) a,b,c. However, for values of θ_i between α and 2α , the teardrop shape becomes larger and its motion extends below the horizontal line, figure (5.5) d,e.

For $\theta_i > 2\alpha$, then the motion produces a figure of eight shape where the crossover point lies on a line at $-\alpha^*$, from the horizontal X axis, side view (y - z plane), figure (5.5) f,g,h. Nakane et al. produced results for a conic tool with a point P' lying below the surface as shown in figure 5.6, [26]. The point P' can be considered to be a point lying on the periphery of a tool of a cone angle smaller than α^* , given as α_{ii}^* . If θ_i is $< 2\alpha_{ii}^*$ for P' the criteria for a figure of eight shape is satisfied. The results of Nakane et al. show that P' lies on a cone of $\alpha_{ii}^* < \alpha^*$ and that $\theta_i < 2\alpha_{ii}^*$. A figure of eight shape was produced for the locus of the point P' with a crossover point lying on the $-\alpha_{ii}$ line below the horizontal X axis.

When $\theta_i > (90 + \alpha)$, as in figure (5.5) g, the vertical component of the figure of eight reduces in height to simply movement in a plane, (figure 5.5 - i).

These movements could be generated by a tool with a profiled surface, especially, if, as many do, have a small cone angle. The motions shown in figure (5.5) b,c,d,e,f could all be generated instantaneously by different points on a single tool having a contoured surface. From this, it is important to understand what is happening to the tool, particularly since it must influence the way a workpiece would be deformed.

5.3.2. Non - Monotonic Nutation - Precession.

Figures (5.7), and (5.8), show the rosette motion and spiral motions during non - monotonic nutation precession motion. As can be seen, the spiral and rosette patterns are still produced, but they now have only one plane of symmetry. This is because they have taken up the teardrop pattern of the precession motion and become distorted. The spiral motion, figure (5.7), has become teardrop shaped, and the rosette motion, figure (5.8) has also developed a similar shape. This is important since it identifies the three dimensional movement of a tool as it is presented to the workpiece.

5.3.3. The Effect of Different Angled Tools under Precession Motion.

Figure 5.9 shows the effect of varying the cone angle α between 0 and 180° where α is always equal to θ_i during the precession motion. (i.e when the $\alpha / \theta_i = 1$). Four different situations of the locii are produced :

- i. For $0^\circ < \alpha < 45^\circ$ the locii increases in size from a point to the familiar teardrop shape, figures 5.9 - a and 5.9 - b.
- ii. For $45^\circ < \alpha < 90^\circ$ the teardrop shaped locus of a point on the tool surface becomes larger in diameter in plan view and reduces in height in the front and side elevation, figures 5.9 - b and 5.9 - c. At $\alpha = 90^\circ$ the locus is seen as a circle in the plan view and as a line in the front and side elevations, figure 5.9 - c.

- iii. For $90^\circ < \alpha < 135^\circ$ the cone angle is effectively negative and the cone convex in shape. The locus of a point on the cone is seen to change from a circle in plan view to an inverted teardrop shape in side elevation, figures 5.9 - c and 5.9 - d. The locus follows the same rules as for a positive cone of $0^\circ < \alpha < 90^\circ$.
- iv. For $135^\circ < \alpha < 180^\circ$ the inverted teardrop shape changes back again to a point of contact when $\alpha = 180^\circ$, not shown.

From these results it can be seen that the locii produced are continuous from $\alpha = 0^\circ$ through to $\alpha = 180^\circ$. For $180^\circ < \alpha < 360^\circ$ the cone shapes and hence the locii are the same as for $0^\circ < \alpha < 180^\circ$. The locii for α changing from 0 to 90° can be seen to be a mirror image in the X - Y plane of the concave conic situation, when α changes from 90° to 180° , figures 5.9 a, b, c, d,

5.3.4. The Locus Produced For a Point on a Flat Plate.

When the cone angle α equals 0° , i.e. a flat plate, then the locii produced are significantly different from those of a conic die. Although this shape of die would be unlikely, it is possible that a contoured die could have, as part of its surface, a point, or points, identical to those of a flat plate.

If a flat plate is given an initial nutation and undergoes precession motion, then a figure of eight shape is produced. Figure 5.10 shows the pattern produced and it is interesting to note that the shape is symmetrical about the Y axis, and that the crossover point is always on the Y axis for any initial nutation. As shown in figure 5.10 - a,b, the size of the path of a point on the tool surface is influenced by the initial angle of the tool axis nutation and its radius from the origin.

5.4. RESULTS FOR THE PATH OF A POINT NOT ON THE SURFACE OF THE BASE CONE α DURING PRECESSION MOTION.

Figure 5.11 shows a point P' below the surface of a conic rotary forging tool. Point P' could be said to represent a point on the profile of a conic tool which lies below the base cone angle α . The study of the locus of such a point during a rotary forging motion, would provide an insight into how such a profiled tool would move and affect the workpiece being deformed.

If point P' is between a and b as shown in figure 5.11 and the tool is inclined by an initial nutation $\theta_i = \text{the cone angle } \alpha$, then a figure of eight shape is produced as shown in figure 5.12. When P' is below the Y axis or below point b, and the tool is inclined by $\theta_i = \alpha$, then the pattern produced during precession is an inverted teardrop shape as shown in figure 5.13. What is effectively happening for point P' , is that it simply represents a point on a cone of a different angle from the one that it was extended from, the angle of this cone being the angle which the point P' subtends from the origin.

For example in figure 5.14 - a, Point P' lies at -10° below the horizontal axis Y, and is part of a 20° cone. Point P' could be assumed to be part of a -10° convex die, where point P' lies on the surface of the die as shown in figure 5.14 - b. If both these dies are inclined by 20° and undergo the same rotary forging motion, then the locii produced by both of these points will be the same as that shown in figure 5.13. This result shows that a profiled rotary forging tool can be considered to be effectively, a series of points on different angled cones with the same initial nutation θ_i each undergoing the same motion, as shown in figure 5.15. This implies that the movement of different points on the surface profile of a tool will not be the same. In fact, a point on one part of the tool could be undergoing a figure of eight type of movement, and one, on another part, may be undergoing an inverted teardrop movement. This will affect the material in these regions and the die life and wear.

5.5. CONCLUSIONS.

An expression was proposed to simulate the non - monotonic nutation motion of rotary forging machines based upon Simple Harmonic Motion. This type of motion is produced by eccentric gearing driving bushes and is found in most industrial rotary forging machines in the World This expression was shown to produce the recognised patterns of machine motion especially as in a Marciniak type rotary forging machine, when combined with the precession motion. The familiar motions of a spiral, rosette, circle and a straight line were able to be produced, confirming the validity of the work.

For non - monotonic nutation - precession motions an expression was presented to predict the number of petals and the number of symmetries for a Marciniak type rotary forging machine. The expression was shown to agree with predictions and results from the 'PATH' package, and also with results from other researchers such as Baert et al [35]. From this expression and the results from 'PATH', a table was drawn up for the number of petals produced in the rosette motion and the number of symmetries of a spiral motion. A mathematical expression was also put forward to predict this.

Rosette motions were shown to occur when the nutation rate was greater than the precession rate, and spiral motions when the nutation rate was less than the precession rate.

The ability to predict the number of petals in a rosette motion and the number of symmetries of a spiral motion, may be applicable in tailoring the tool motion to overcome areas of the die which are difficult to fill. This is seen as a major future possibility for the die designer.

Asymmetric tool patterns for machine motions of non - monotonic nutation - precession were found to take place in 180 degrees of precession because the non - monotonic nutation has the effect of reversing the direction of the precession motion.

Results predicting the path of a point on the surface of a rotary forging tool were shown to give insight into the motion of possible contoured tool surfaces.

The effect of the initial nutation θ_i , was investigated and shown to influence the patterns produced by the point on the surface of a rotary forging tool during precession motion. The patterns produced show nine different states, including the tear drop shape, the figure of eight shape and a circular motion.

A point on the surface of a rotary forging tool during non - monotonic nutation - precession was found to produce the same type of patterns as a point on the tool axis, but these motions were offset and tear drop shaped in outline.

The effect of changing the tool angle was shown to generate a continuous pattern of tool surface movements from a point where $\alpha = 0$ degrees through a teardrop to a circle when $\alpha = 90$ degrees.

During precession, flat plates were shown to produce locii having figure of eight type patterns with a crossover point on the Y axis. The effect of altering the initial nutation was shown to only change the size of the figure of eight.

When a point, not on the tool surface, was traced during various rotary forging motions, it was found to represent a point on the surface of another tool of cone angle α equal to that which the point subtended to the origin. The locii produced by both the points on the different tools was found to be the same as long as the initial nutation was the same.

CHAPTER 6.

PREDICTION OF ROTARY FORGED SURFACES.

6.1. INTRODUCTION.

The Prediction Of Rotary Forged Surfaces or 'PROFS', is a 3 part computer package, which is capable of generating and simulating the motions of tools and workpieces of all rotary forging machines. The package has a Preprocessor, a Processor, and a Postprocessor and is designed so that simulations can be set up and run over extended periods. The interaction of the tool and the workpiece is calculated in a step wise manner to determine the contact geometry, and hence the area of instantaneous contact. The results are written to a data file from which the Postprocessor 'VIDEO' can generate a 3 - D colour display of the tool and workpiece. Two models are proposed for the workpiece, based on constant or non - constant volume. An assessment of each model is given. The software allows various tool shapes and profiles to be generated. These are incorporated in a menu in the preprocessor for use in simulations.

6.2. SPECIFICATIONS.

'PROFS' was written and developed on a Prime 9650 mini computer with Ramtek 4015 and Tektronics 4001 colour graphics terminals. The software was written in the 'C' language. This was chosen for its portability and speed. Because of the large C.P.U. time needed to run the program, the package was split into three parts. This enabled jobs to be submitted and run over night and the results viewed the next day. The three parts of the package are described below :

6.2.1. The Preprocessor.

This is called 'PROFS' and enables the user to set out the simulation for batch processing at a later time or date. The basic layout of the simulation is tailored specifically to rotary forging. Figure 6.1 shows a generalised tool and workpiece arrangement as generated by the preprocessor PROFS. This consists of a rotating conic tool, and cylindrical billet. The apex of the tool lies on the workpiece axis, and is the point about which rotation of the tool takes place. The motions of movement are restricted to the Euler motions of a rotating body, namely those of nutation, precession, and spin. These have been shown, in Chapter 3, to adequately describe the motions of any type of rotary forging machine. The basic layout gives a flexible and usable approach to rotary forging simulation and in this is believed to be unique.

Before a simulation can be run the package requires a user to input the tool shape, tool angle and tooling motion together with, the workpiece diameter, height, and material model type, i.e constant or non - constant volume. Machine parameters to be specified include: the starting position of the tool in relation to the workpiece, the cycle time of the tool movement, the feed rate of the main ram, the number of cycles of the tool, the step size of the simulation in terms of degrees of rotation of the tool, and the number of steps which are to be stored in the output file. This information is then written to a control file and sent for batch processing by the processor.

6.2.2. The Processor.

This is called 'COSIMORF', and can be set into operation automatically from the preprocessor. It reads from the control file all the simulation details, then runs the simulation outputting the results at the specified intervals to an output or data file. It also calculates the instantaneous contact area and displaced volume of material. The typical running time for a simulation is around 4 to 6 hours.

The simulation is run as a series of discrete forging steps. As an incremental process, rotary forging lends itself well to this kind of approach. The step size is specified by the user in terms of the degrees of rotational movement of the tool over the workpiece and input into the control file. For example, if the step size were 15° , the toolspeed 240 c.p.m.

One step would take:

$$(15 / 360) / (240 / 60.0) = 0.01 \text{ seconds of simulated time.}$$

If a ramspeed of 24mm/sec were to be employed the new tool height would be obtained by subtracting the distance travelled, in this case:

$$0.01 * 24 = 0.24\text{mm.}$$

Thus, using this method, can give a 'time' dimension to the steps of the simulation.

This is essential because it is used to determine the bite size. During each iteration the instantaneous area of contact is calculated and depending on the material model used, a new workpiece shape, together with other information, is written to

the output file. The technique allows a sequence of 'deformation' stages to be stored in an output data file, for later processing and display by the Postprocessor.

6.2.3. The Postprocessor.

This is called 'VIDEO', and can read any of the output data files from the processor, 'COSIMORF'. 'VIDEO' can interpret the data and if desired, draw the workpiece and tool on the screen. Additional information includes: the instantaneous contact area, tool position, degrees of nutation and precession and / or spin. The software is also capable of outputting the information onto a colour graphics terminal in various formats. 'VIDEO's' features include:

- Solid or line representation of the workpiece and tool.

- Single picture viewing or multiple picture sequence viewing of the steps of the simulation.

- Colour choice to pick out the instantaneous contact area of the tool on the workpiece surface.

- Various views of the workpiece and tool, such as plan, elevation, and isometric.

- Ability to view the tool and the workpiece together, or separately, so that the workpiece is not obscured by the tool.

- The graphics are driven by a software package called 'T411X4', capable of 3 -D drawing and rotations.

A general overview of the PROFS package is given in Appendix A, in the form of flow diagrams.

6.3. MODELLING OF THE TOOL

A typical rotary forging tool is conic in shape and can be defined mathematically using a matrix of 3-D Cartesian coordinates, to represent the surface profile. Figure 6.2 shows a typical 20° conic tool drawn by the the preprocessor 'PROFS'. As can be seen the points of the surface have been joined by radial and circumferential lines to give the drawing depth, perspective, and orientation. The preprocessor allows the tool angle to be chosen, and, if desired, certain radial and circumferential profiles to be incorporated into the tool's surface.

A menu of the radial profiles is available as shown in figure 6.3. These are drawn on the screen so that the user can choose the desired profile. The profile is then incorporated into a tool with the chosen cone angle as indicated in figure 6.4. In the example, profile 4 of figure 6.3 has been incorporated into a tool having a cone angle of 20° . In a commercial environment, it would be sensible to have custom - made profiles input directly onto the tool by means of a mouse.

Circumferential profiles are also available and are represented as the deviation from the mean surface of the tool (or deviation from the slant height of the tool) around 360° of its circumference, see figure 6.5. Incorporation of profile 3 onto a 20° cone would generate a tool as shown in figure 6.6. The circumferentially profiled tools shown in figures 6.5, and 6.6 would typically be used in the manufacture of surfaces having extruded features, for example, face gears. The radially profiled tools shown in figures 6.3, and 6.4 would be used for the production of many different cylindrical parts such as a clutch hub.

6.3.1. Generation of the Profiled Tool.

The creation of a radially profiled tool is achieved by first constructing a lowest generator. This is a radial line of the required surface form. The line is then rotated (using the Eulerian equations of rigid body rotation), through 360° to generate the tool surface. Once this has been done, the coordinates of the tool are written to a file for the processor 'COSIMORF' to utilise in the simulation. Circumferential profiles are more complicated since the lowest generator must move vertically as it is rotated to form the tool surface. Special routines were written into the programme to produce the required profiles.

6.3.2. Tool Material Properties.

The package 'PROFS' does not include calculations of forces or loads. This is considered a next generation progression of the software leading to a possible finite element analysis of the process. For the present work the tool is assumed to be a 'Rigid' inelastic body. This simplified the representation of the tool, as described in section 6.2, and required only the surface to be generated as a mesh.

6.3.3. Tool Movement.

As shown in Chapter 5, the Eulerian motions can be used to describe the motions of rotary forging machines. Further, the formulae {3.1, 3.2, 3.3} can be directly applied to the matrix representing the conic tool, so enabling the motions of rotary forging to be imparted to the tool. The motion of spin requires both the conic tool and the workpiece to move with equal surface speeds so that no slip takes place between them. The rotational difference in speed, between the workpiece and the tool, necessary to achieve this, is calculated as follows:

$\omega_1 = \omega_2 / \cos \alpha$ {6.1}

where ω_1 = the angular velocity of the workpiece.

and ω_2 = the angular velocity of the tool.

and α = the cone angle.

Workpiece rotation is accomplished using the Eulerian equations defining spin motion. The feed is imparted to the conic tool by a simple height adjustment in the Z component to all surface coordinates.

6.4. MODELLING OF THE WORKPIECE.

The workpiece was represented by an array of Cartesian points arranged in elements. The elements were hexahedral in shape having eight corners / points / nodes, as shown in figure 6.7. The elements were arranged in a circular fashion from the centre of the workpiece, which meant they increased in size as their radial position increased. This is shown by the plan view of a modelled workpiece in figure 6.8. In all cases the rotary forging workpieces were assumed to be cylindrical. The dimensions of the workpiece can be chosen whilst using the preprocessor, enabling the height and diameter to be specified. The number of radial and circumferential points, and hence elements in a workpiece mesh, can also be specified. This directly effects the accuracy of the simulation and the length of time of computation. These values are then written to a file for the processor 'COSIMORF' to read, from which the workpiece is generated.

6.4.1. Non - Constant Volume Workpiece Model.

The non - constant volume model workpiece is perhaps the simpler of the two models. A meshed workpiece is interacted with the surface of a conic tool. The iterative process is capable of showing the instantaneous impression of the tool at any particular point during a forging cycle. The mesh is simply 'removed' by the contact between the tool and the workpiece. In figure 6.9, the points a to g, represent a vertical section through a workpiece surface. The corresponding tool surface is shown as the dark line. Collision between the points of the workpiece and those of the tool is detected by a routine in the processor called 'Intercept', described later in this chapter. The new position of a point on the workpiece is simply found by first identifying the closest 'intersecting' point on the tool. The Z coordinate of the point on the workpiece is then assigned to that of the point on the tool. As the conic tool progresses, the workpiece is effectively 'cut' away or removed by its motion. This means that the volume of the workpiece reduces as the 'deformation' continues. Although this not a realistic model, it does offer considerable insight into the movements and interactions of the tool on the workpiece during any type of rotary forging.

The instantaneous contact geometry can be found for a workpiece of a known diameter. This enables a researcher to 'see' how the contact geometry progresses during the process. Figure 6.10 shows how, in a typical precession motion, a 30° conic tool makes contact with and progresses over a workpiece. An amplified cone angle has been used in the simulation providing a clear effect of the interaction. In a real rotary forging situation a workpiece will increase in diameter as the tool moves into it. Using the 'Non Constant Volume Model' will mean that the diameter of the workpiece will stay the same for the whole of the simulation. It is possible to overcome this to some extent by running a short part of the simulation with different diameter workpieces. This can be used to build up a picture of the instantaneous contact geometry of the workpiece at different stages of the process. This is discussed in more detail in Chapter 7, and results are given for a physical experiment to validate this type of approach.

6.4.2. The Constant Volume Workpiece Model.

At the time of carrying out this research existing finite element packages which

have taken many years to develop, were not as yet capable of application to the rotary forging process. However, a real need does exist to develop some type of constant volume simulation model capable of being applied with both a reasonable input of research and C.P.U. time.

Such a model has been produced using the same mesh of elements and points as that of the non - constant volume workpiece. However, to keep the workpiece volume constant, it was necessary to allow the material / elements to move or 'flow' in some way. Several, rules for this movement were assumed and incorporated into the model. These are listed below :

1. each element of the workpiece has an original volume which will be kept constant for the whole of the simulation.
2. the workpiece is cylindrical, its axis remaining fixed and vertical during the whole simulation.
3. the model will allow displaced material to flow outward from the axis in a radial fashion only.
4. a step wise movement of the tool into the workpiece is followed by radial flow of an element until the zero volume change has been achieved.

Consider a single element of the workpiece during the simulation, as shown in figure 6.11. The tool surface is shown by the dark solid lines. Its intersection with the workpiece is found using the 'intercept' routine. Once this is known, the element can have a new height assigned to it; i.e. points 1,2,3,4, are moved so that their Z coordinates lie on the tool surface, 1a,2a,3a,4a. The new volume of the element is calculated and compared to its original volume, and hence the volume change is found for this step. The volume change is the volume of material which will have to be moved radially to accommodate the reduction in height.

If V_c = Volume Change of an element, then, as an approximation, this can be added to the outside edge of the element, (3,4,7,8), as an extra part in the shape of a hexahedral block. However, this volume is assumed to be rectilinear for the first step of an iterative process, as shown in figure 6.12. The clear region shown in the figure equals the volume change (V_c). This is not the true shape of the new element, since the element has radially converging sides. The clear region gives a good first

approximation of the new element shape. Since all the coordinates of the element are known, it is possible to find the height, h and width, w of the volume V_c . The length of the volume V_c can be found from the extended radius 'xrad', needed by that element to match its original volume V_o .

$$xrad = V_c - (h * w){6.2}$$

Points 3,4,7,8, can be expressed using the polar coordinate system (r,ϕ) so that they can be expressed in terms of the radii r_3,r_4,r_7,r_8 , and angles $\phi_3,\phi_4,\phi_7,\phi_8$.

A subroutine called 'newrad' is used to find the new position of the points after the length xrad has been added to the component r .

$$r_3 = r_3 + xrad, \quad r_4 = r_4 + xrad, \quad r_7 = r_7 + xrad, \quad r_8 = r_8 + xrad ..{6.3}$$

Using this routine the new Cartesian coordinates can be found and from these the new volume (V_o) can be calculated, using the subroutine 'Quadrl'.

The accuracy of this new volume (V_o) is tested by :

$$if \quad |V_n - V_o| < V_t{6.4}$$

where: V_n = the new volume of an element.

V_o = Original volume of the element. V_t = the tolerance.

If the difference between the new volume and the original volume is less than the specified tolerance then the new position of the coordinates has been found.

If not, the volume difference is used to find the next value of xrad using equation {6.2}. This is done until the volume is within the tolerance for each element of the workpiece, at which point the incremental step is complete.

Within each circumference of elements in the workpiece, on every alternate row, an element is moved radially so that its volume is maintained. The nodes of the adjacent elements are joined to the moving element, so their volumes and shape are affected by their neighbours 'movement'. The elements are moved from the centre

circumferences outwards, so that the effect of their expansion can be taken into account by the subsequent circumferences of elements. This movement causes every element in the workpiece to be moved radially and change in shape. In figure 6.13, the elements a1,c1,e1 are moved. On the next circumference, the 'opposite' rows of elements are moved, (b2,d2,f2). The moving of every alternate element and opposite row of elements also has the effect of stopping the radial movement from becoming distorted.

6.4.2.1. Limitations and Approximations of the Constant Volume Model.

- i) The element height is set to that of the closest point on the tool in contact with it. In cases of fast ram speed or a large deformation, this height would not be the true height of the point, when expanded to its new position, because of the curvature of the tool.
- ii) In rotary forging, a wave of material is caused to form ahead of the die - workpiece interface, and produces a circumferential movement of material. This is not taken into account by the model.

6.5. CONTACT DETECTION BETWEEN THE TOOL AND THE WORKPIECE.

This is carried out by a routine called 'intercept' in the processor for each step of the simulation. Each point on the workpiece surface can be said to have an intersection cylinder. All points of the tool are said to be in contact if they lie inside the cylinder and below the Z coordinate

The cylinder is assumed to have a radius equal to the radial distance between the point and its next radial point on the workpiece. Figure 6.14 shows the top mesh of the workpiece and the two points from which the cylinder radius is calculated.

$$\text{Intersection radius} = ((ix - jx)^2 + (iy - jy)^2)^{0.5}$$

The choice of this radius ensures that an overlap is obtained between all the radii of the points on the workpiece. Using this method, no dead zones are created, which would give rise to areas of zero deformation in the workpiece. If the chosen intersection were to be too big, then the points outside the area of contact would be seen to be in contact with the tool and give rise to a false contact geometry and area.

If a perfectly square mesh could be ensured throughout the the simulation then a smaller contact cylinder radius could be used, as shown in figure 6.15. However, this is never the case in a cylindrical billet, since the spacing of the mesh increases from the centre to the outside diameter, so creating a varying element size.

Each point on the workpiece may have several possible points of contact with the tool, so the closest intersecting point is taken as the contact point and the rest are ignored. The point on the workpiece is then moved to the same height as that of the intersecting point on the tool, by assigning the same Z coordinate as that of the one on the tool.

6.5.1. Reducing The Search Time.

A large part of the processing time during the early simulations was found to be taken up with the detection of the contact between the tool and the workpiece. This was due to the fact that every point on the workpiece must be compared with every point on the tool, so with a $70 * 10$ point workpiece and a $70 * 10$ point tool, 490,000 comparisons must be made for each step of the simulation. This was reduced by limiting the points searched for on the tool. Only points on the tool, which were lower than the highest point on the workpiece, were searched for as possible contact candidates, since points above this height cannot possibly be in contact. This is especially effective during the early stages of the 'deformation' since only a small proportion of the tool is in contact with the workpiece. This limited search technique reduces the C.P.U. time for the whole simulation by about a half.

6.6. CALCULATION OF THE CONTACT AREA.

The instantaneous area of contact between the tool and the workpiece can be found by finding the area of the elements in contact at each step of the simulation. When a point on the workpiece is found to intersect a point on the tool then it is said to be in contact for that step of the simulation. The point is then assigned the height of that point on the tool, as explained in section 6.5., and it is marked as an 'in-contact' point for that step of motion. Examination of the workpiece surface matrix later in the programme, by a routine called 'varea', enables the elements in the workpiece which are in contact to be identified.

Contact is said to occur when 3 or 4 of the element surface points are 'in-

contact', the reason for this being that 1 or 2 points would not give a positive area of contact. Three points of contact would mean that a triangular shape would be formed. The area of this could be found by a routine called 'triang'. Four points of contact would mean that the surface area would be a quadrilateral shape and this could be found using a routine called 'quadrl', which uses a numerical approach based on the Gaussian theorem, [36].

Each element on the surface of the workpiece is searched for in turn, seeking contact points, to enable the contact area to be calculated and summed. From this the total instantaneous contact area can be found, and recorded in the output file along with the workpiece shape, tool position and simulation conditions.

6.6.1. Limitations of the Contact Area Calculation.

- i) Since the workpiece is divided into a mesh, the calculated contact area can only be an approximation.
- ii) Elements with only one or two points in contact are ignored. This may mean that the contact area is a slight underestimate by about 7%.
- iii) The contact surface between the 3 or 4 points is assumed to be a flat one. This is not necessarily true, since if the tool is conic, it will produce a concave surface on the workpiece.
- iv) Given their contact radii, points on the edge of the contact zone may be said to be in contact with the tool. Figure 6.16 shows such a case where a point will be considered to be in contact when in fact it is not. This can be improved by decreasing the element size on the workpiece, but at the expense of increased C.P.U time.

6.7 CALCULATION OF THE DISPLACED VOLUME OF MATERIAL.

The displaced volume of material, is the volume of material moved or lost due to the action of the tool on the workpiece. The displaced volume is calculated in the package COSIMORF by the routine called 'varea' at the same time as the instantaneous contact area. When the simulated tool intercepts with the workpiece,

its contact is detected by the routine 'intercept', described in section 6.6. The points intercepting in each element are found and their coordinates stored in an array. The points, in the workpiece, are then assigned their new coordinates found from the intersection.

An 'in - contact' element will have either 3 or 4 points on its upper surface which are deemed to be in contact. These points will describe a pentahedron or hexahedron respectively. Using the old and the new values for these points either 6 or 8 coordinates will be found to enclose the volume of material moved. This volume is now calculated using the two routines called 'vpgaus' and 'vhgaus' which use a numerical approach based on Gaussian theorem, [36]. The calculated volumes are then added to the total displaced volume at each step of the simulation, so that the displaced volume is a cumulative value. The displaced volume is written to an output file along with the instantaneous contact area, the workpiece shape, tool position and the simulated coordinates

6.7.1. Limitations of the Displaced Volume Calculations.

- i) Since the workpiece is divided into a mesh, the calculated displaced volume can only be an approximation.
- ii) Elements with only one or two points in contact are ignored. This may mean that the displaced volume is an underestimate by about 19 %.
- iii) Given their contact radii, points on the edge of the contact zone may be said to be in contact with the tool. Figure 6.16 shows such a case where a point will be considered to be in contact when in fact it is not. This can be improved by decreasing the element size on the workpiece, but at the expense of increased C.P.U time.

6.8. CONCLUSIONS.

A three part computer package has been developed, which is capable of generating tools and workpieces for rotary forging machine simulation problems.

The package is capable of generating a number of radial and circumferential profiles on to conic shaped tools for use in the package and in rotary forging applications.

The package is capable of imparting the Eulerian motions of nutation, precession, and spin to a chosen tool and workpiece, therefore simulating the complex motions of any type of rotary forging machine.

A method of detecting the interaction between the tool and the workpiece has been put forward, revealing the complex contact geometries created during rotary forging.

Two material models have been proposed for the simulated deformation of a workpiece.

- i). The non - constant volume model, enables the instantaneous contact geometry to be seen for a certain diameter of workpiece, as the tool progresses. Since the workpiece does not deform as the tool advances the workpiece reduces in volume, making this process and model equivalent to one of 'rotary cutting'.
- ii). The constant volume model, keeps the volume of each element constant by allowing them to expand radially as the tool moves downward. This enables the user to identify and evaluate the instantaneous contact geometry between the tool and the workpiece throughout the whole simulation.

A post processor called 'VIDEO' has been developed which allows the results of the simulation to be displayed graphically, in various formats, on a colour monitor. It enables the user to see a selection of the stages of the simulation, or just one picture during the 'deformation' process. Solid or line representation of the tool and the workpiece can be chosen, along with a choice of colours to enable the instantaneous contact geometry to be picked out.

A contact area calculation routine has been developed, to enable the instantaneous contact area to be calculated at each step of the simulation. This is stored to an output file which can then be read and displayed on every picture of the simulation by the post - processor 'VIDEO'.

A routine has been developed which is capable of calculating the displaced or lost volume of material created, when the tool interacts with the workpiece, at each step of the simulation. This is output to a file which can then be read and displayed by the post - processor 'VIDEO'.

CHAPTER 7.

RESULTS FROM THE NON CONSTANT VOLUME MODEL.

7.1. INTRODUCTION.

The non - constant volume model workpiece discussed in Chapter 6 is a 3 dimensionally meshed representation which responds to contact between a tool and its surface by deforming to the shape of the tool. None of the material in the workpiece is deformed by this action but is simply 'cut away'. The workpiece volume is reduced throughout the simulation by the action of the tool upon it.

The seven distinct motions of rotary forging, described in Chapter 3, are investigated and run as simulations using the PROFS package with a non - constant volume model workpiece

The monotonic nutation - precession motion typical of the Marciniak / Schmid rotary forging systems is investigated using the petal, spiral, and line motions available to these machines.

PROFS is shown to be capable of generating radially and circumferentially configured dies. Results of simulations using the dies with a precession motion reveal the potential of PROFS as a possible die design tool.

A custom designed die profile was generated and used to simulate a real rotary forging process in several stages. The initial, mid, and final contact geometries are simulated, and reveal new and interesting results.

7.2. THE FAMILY OF ROTARY FORGING MACHINE MOTIONS.

Rotary forging motion can be defined from the Eulerian movements of Nutation, Precession and Spin by seven distinct motions. These seven motions have been simulated and the results are discussed in detail in this Chapter. The seven motions are, Nutation, Precession, Spin, Nutation - Precession, Nutation - Spin, Precession - Spin, and Nutation - Precession - Spin as shown and discussed in Chapter 3 section 3.2.2.

The simulations were all run using a 30° conic tool, since this amplified the effects of each of the motions, enabling the development of the contact geometry to be viewed and interpreted more easily. Real rotary forging situations often involve the use of cone angles of 2° or less. However, with no prior knowledge, simulations run with such a small angle, would not allow the difference in the

motions effects to be properly interpreted. The results, in this chapter (drawn by the postprocessor, 'VIDEO'), show the workpiece, in blue, and the contact geometry, in green. If the tool were also to be included, the contact geometry would be obscured and the figures become confusing. The postprocessor 'VIDEO' has a facility to allow the user to show a small picture of the tool and the workpiece in the corner of the screen, so that the orientation of the tool and workpiece can be understood. The main features can then be drawn unobscured by the tool, but with the information about the orientation being available, for example in figure 7.1 showing a workpiece geometry produced by a precessing 30° die.

7.2.1. Nutation Motion.

The simulation shown in figure 7.2 is a simple inclination of the conic tool axis from 0° to 32° with equal intervals of motion in steps of 8° with a constant ram feed rate of 30mm/sec. This gives a sequential insight into the development of the contact geometry as the tool makes initial contact with the workpiece. The workpiece is shown as blue lines and the contact between the tool and the workpiece as green lines.

As would be expected the contact geometry increases throughout the simulation, particularly in the last step, as the angle of inclination θ nears $\alpha = 32^\circ$. Since the model is of non - constant volume, the workpiece is seen to be effectively 'cut away' by the the action of the tool, and the total volume of the workpiece decreases throughout the simulation.

7.2.2. Precession Motion.

Figure 7.3 - a and b. shows how the initial contact geometry is produced on a workpiece during precession motion. For this simulation a constant feed / ram speed rate was used (15 mm/sec), coupled with a constant rotational speed of 100 c.p.m. of the tool. These details are given on the screen for each step of the simulation, together with the instantaneous contact area and the nutation, precession, or spin angle. The contact geometry is shown in green against a blue workpiece, for nine steps of the first revolution of the simulation, in 40° steps between 0 and 360° of precession movement. The simulation shows the development of the contact

geometry, from a near straight line contact at the beginning of the simulation at 30° precession movement, to a half parabolic shaped contact at 360°. If tool motions remain constant, then during the second and subsequent revolutions of the process, the instantaneous contact area will remain constant to within the accuracy of the simulation. This is because the non - constant volume model removes material and so no increase in workpiece diameter or deformation takes place. This means that under conditions of constant feed, and speed of the tool, the instantaneous contact area, once established, also remains constant.

As shown in figure 7.4., the surface of a helix is developed on the workpiece during the first revolution of the forming cycle. Assuming the workpiece speed and ramspeed are kept constant, the form of the surface will remain unchanged until the final cycle is started, when the ramfeed is stopped and the surface is flattened again.

The last revolution of a rotary forging will involve the tool reducing contact with the workpiece. This in effect is the same as the first revolution of the process, but in the reverse order. This means, that in the last revolution, the contact geometry will be seen to reduce in size until it eventually becomes a single line of contact at the final instant of the forging.

It should be noted that the precession motion, is, at the time of writing, the most widely used of all rotary forging machines motions. From the present work it is hoped that the ability to generate contact geometries for any size of workpiece will prove of particular use to machine and die designers.

7.2.3. Spin Motion.

Figure 7.5 - a,b. shows the spin motion under identical conditions of ramspeed, step size, mesh size and conic tool angle, as that of the precession motion, shown in figure 7.3. General views of figures 7.3 and 7.5 show a close similarity in the size and shape of the contact geometries.

Again, the contact can be seen to develop from an initial line to a half parabola after 360° of spin. The only difference is the position of the contact area during spin motion remains the same as seen by a stationary observer. The red line shown in the figures, indicates instantaneous position of the anti - clockwise rotation of the workpiece with respect to the initial starting position. During precession

motion, the contact geometry moves around a stationary workpiece. In fact, the contact geometries produced by the spin and precession motions are in the same relative positions on the workpiece at the same instant, but in the spin case the workpiece is moving. Examination of the instantaneous contact areas shown in Figure 7.6, indicates that a reasonable correlation exists between the two types of motion. The reason for some small discrepancy, approximately 3.8%, is that the discrete meshes of the tool and workpiece, will if slightly differently aligned, produce slightly different contact geometries. This confirms that the Spin and Precession motions produce, for the same kinematic conditions, similar tool / workpiece interactions.

The deviations seen in the graph, of figure 7.6., at 40, 120, 160 and 200 degrees of tool motion, are points of maximum misalignment of the meshes, between the two motions. These deviations could be reduced by decreasing the mesh size of both the tool and the workpiece. After 340° of tool motion, the instantaneous contact areas, for both the precession and spin motions, cease to increase. This is because the initial revolution has almost been completed, on a non - constant volume workpiece.

Spin motion involves both the tool and the workpiece moving at equal surface speeds, so that true spin motion will occur without slip between the tool and the workpiece. This motion is used in many machines, including the early Slick mill and the 50 tonne Nottingham University nutation - spin machine. The total amount of spin of the upper conic tool is shown in the legend of each diagram. It must be appreciated that the tool must spin $(360^\circ / \cos 30^\circ) = 415^\circ$ for each 360° of motion of the workpiece, since non - slip conditions of movement are required at the tool / workpiece lowest generator interface. This is automatically implemented by the program since it is not of any advantage to have slip occurring.

7.2.4. Nutation - Precession Motion.

Figure 7.7 shows the contact geometry on the surface of the workpiece during the first revolution of a nutation - precession motion. As can be appreciated the die starts in the vertical position with nutation = 0° and as the revolution progresses the nutation increases uniformly to $\theta = \alpha (30^\circ)$ at precession (ϕ) = 360°. The contact

area can be seen to increase from a near central circular area of contact at 10° nutation and 120° precession to the full half parabolic area of contact at 30° nutation and 360° of precession. This motion is similar to the spiral motion of the Marciniak / Schmid machines as described in Chapter 4. However, this only shows the first half of the motion. For a complete cycle it is necessary to use the non - monotonic nutation option in the simulation so that the nutation will vary between 0 and 30° , then 30 and 0° , then 0 and -30° , and then -30 and 0° .

If the simulation were to be extended for further revolutions then the nutation would become greater than the cone angle ($\theta < \alpha$) i.e. greater than 30° and the tool would cause the workpiece to be 'cut' almost completely away in only a few steps. The nutation - precession motion is not used in practice, but Schmid / Marciniak rotary forging machines use the non - monotonic nutation - precession motion. The rates of the two motions can be varied infinitely to produce an infinite number of different tool axis motions as discussed in Chapter 5.2. The effects of different nutation and precession rates upon the tool / workpiece interaction are discussed in section 7.2.5.

7.2.5. Non - Monotonic Nutation - Precession.

This motion is used by rotary forging machines of the Marciniak / Schmid type. As was shown in Chapter 5, the computer package, 'PATH', is capable of simulating all the motions of these type of machines, such as circular, line, rosette and spiral type motions. In this Chapter the contact geometries are examined for these motions using the package 'PROFS'. Figure 7.8 shows how the tool contact area varies throughout non - monotonic nutation - precession for a 30° conic tool with a nutation rate = 300 c.p.m. and a precession rate = 100 c.p.m. This produces a three petal rosette pattern of tool axis motion as shown in figure 7.9. From figure 7.8, each part of the movement of the tool can be seen, showing the contact geometry at the critical points of the motion. For example, in 7.8 - 2 the contact geometry is very small because the tool axis is at 0° nutation. In 7.8 - 3 following a nutation and precession of -30° and 90° respectively, the contact geometry is seen to be much larger and covers the workpiece from its centre to the edge.

Since the tool is undergoing a rosette motion, very large swings in the contact

geometry position and size, can be seen in figure 7.8. The simulation of figure 7.8 was produced under conditions of constant feed, precession and nutation rate of the tool. However, in a rotary forging machine, the feed rate is often a function of the pressure developed by the resistance of the workpiece to deformation. Under conditions of pressure control, the size of the contact area would stay almost the same for the whole of the cycle, whilst changing its position as in figure 7.8. The simulation method is considered to be most important in allowing the instantaneous area of contact to be defined. For example, with positional control, the tool tip would see a large change in force during a cycle and therefore could be identified as an area where tool wear might become excessive.

Spiral motions are produced when the non - monotonic nutation rate is less than the precession rate. Figure 7.10- a,b. shows the contact geometries produced between 0° and 540° at 60° intervals of precession for a 30° conic tool with a nutation rate = 100 c.p.m. and a precession rate = 300 c.p.m. The associated tool axis motion is shown in figure 7.11. The simulation shows a small contact geometry at 180° of precession motion which gradually increases until a half parabola of contact is achieved at 360° . The contact geometry is then seen to gradually reduce until it is a small central area of contact at 540° of precession motion. It is thought that this motion is particularly useful in deforming parts where radial flow is of significance, since this motion has a larger radial component of movement than either precession or spin motions. However, this motion is not used by the Schmid manufactures, since they have found it to be of no advantage. It is believed that, because the nutation and precession rates of Schmid machines are fixed, the full potential of this motion has not yet been realised.

Straight line motion occurs when the precession rate equals zero. This type of motion, shown in figure 7.12 - a, b, deforms the central area of the workpiece, and two parabolic regions across a diametral plane. The deformation does not occur over the whole surface of the workpiece, and is often used for making parts with non circular cross sections. Normally, a shaped upper and lower die would be used to produce a non circular part, for example, a watch case.

7.2.6. Nutation - Spin Motion.

The simulation of the contact conditions of this motion was again carried out

using a 30° plain conic tool and a cylindrical workpiece. Conditions of a constant feed rate of 15 mm/sec, a rotational upper die speed of 100 c.p.m., and workpiece rotational speed of 86.8 r.p.m. Figure 7.13 shows the development of the contact geometry for this motion. The contact geometry can be seen to form a small central contact at $\theta = 10^\circ$ to a half parabola at $\theta = 30^\circ$. Examination of figures 7.7 and 7.13 appears to show contact geometries of similar shape and size. Comparison of actual contact areas shows a maximum difference of 3.9%. As before, the differences are simply due to the coarseness of the elements in the mesh exaggerating the differential positioning between the tool and the workpiece elements. This discrepancy could be reduced by increasing the number of points in the mesh of both the tool and the workpiece.

The nutation - spin motion is known to only be used by the 50 tonne Nottingham press previously mentioned. All other machines of the spin motion type have a fixed angle of inclination, which cannot be altered during the forging cycle. The microprocessor control of the Nottingham machine gives it scope for movement that is infinite in its possibilities. At present, the simulation package 'PROFS' does not have a programmable motion option to enable several different combinations of motions to be used in one forging cycle. This limits the ability of PROFS to simulate combinations of motions used by the Nottingham machine. PROFS is capable of simulating all rotary forging motions, but requires further development to incorporate several different motions in one forging cycle. However, with a little further research time this could be easily encompassed into the existing program. Features such as, varying speeds of feed, varying rotational rate, and several tool motions, could input into PROFS, enabling a tailor made simulation of a whole forging cycle to be produced.

7.2.7. Nutation - Precession - Spin.

This is as yet a totally unused motion in rotary forging machines. Simulations were run using this motion, and produced results similar to those of the precession - spin motion. Since the precession and spin motions are kinematically the same, there seems to be no advantage over the simple nutation - precession motion. Moreover, the additional rotational slip which occurs between the tool and the workpiece, due

to the action of the spin motion would probably be undesirable, producing interfacial rubbing and wear. From the machine design point of view, it seems unlikely that a rotary forging machine having such a motion will ever be built unless the two motions of nutation - precession and nutation - spin are required from the same machine.

7.2.8. Precession - Spin.

This motion seems to have no advantage over the precession and spin motions. As pointed out in section 7.2.7. the extra wear and rubbing due to the combination of the two motions would probably make this motion undesirable. However two machines were designed which used the precession - spin motion. One of these machines was built at UMIST and used for early investigations of the rotary forging process, [8]. However, the machine was never used for any production of rotary forged parts, because of the problems associated with its motion. The spin motion occurred because the upper die was not restrained by a key and slot or gearing arrangement. Later machines incorporated an upper die restraint to stop the added spin motion.

7.3. CONTOURED TOOLS.

As was shown in chapter 6, PROFS, has a selection of radial, circumferential and custom profiles available to the user to enable profiled tools to be generated and used in simulations. Simulations have been run using the precession motion and tooling of both radial and circumferential profiles. Further simulations were carried out using a custom profile of an inverted conic tool with a radial profile, described in section 7.4.

7.3.1. Simulation using radially profiled tools.

The package 'PROFS' allows the user to choose from a menu of 6 radial profiles as shown in figure 6.3. Several of these profiles were used in simulations using spin or precession only motions. Figure 7.14 shows the radially profiled tool generated from profile 4 in figure 6.3., incorporated into a plain 30 degree conic tool. Figure 7.15. shows the contact geometry produced by this profile during the first revolution of a simulation, using a precession motion of 100 c.p.m., a non

constant volume workpiece and a ram speed of 15 mm/sec. As can be seen from the early stages of deformation, figure 7.15 - 1,2,3, the contact geometry starts to develop with two zones of contact, until after 360° (fig. 7.15 - 4.), when the full radial contact is established. The significance of this is important to the tool designers and manufacturers, since it identifies areas of possible folding and faulting which could be caused. This may result in the premature in service failure of the component due to crack propagation from these sites. PROFS has been shown to be able to predict problems which may occur during the forging cycle. This is seen as a possible die and process design tool.

7.3.2 Simulation using circumferentially profiled tools.

The preprocessor part of 'PROFS' could be used to select circumferentially profiled tools from a menu of profiles. To demonstrate a simulation, profile 2 was chosen from figure 6.5 and incorporated into a 30° conic tool as shown in figure 7.16. The simulation was run using a precession motion at 100 c.p.m. and a ram speed of 15 mm/sec. Figure 7.17, shows the contact geometries produced during the first revolution at 90° intervals. The second revolution is not shown, since it has the same contact geometry and area as the fourth part on figure 7.17. As was explained in section 7.2.2, the constant volume model workpiece will produce the same contact geometry, once the first revolution has been established, under conditions of constant feed and rotation.

It is interesting to note, however, that the profile is gradually incorporated into the workpieces surface as the first revolution proceeds. Contact is initially a small area (see fig. 7.17 - 1) and finally after 360°, the full radial contact area is established, (fig 7.17 - 4) with the profile extending around the full circumference of the workpiece. The ability to 'see' the development of a radial profile is useful to die and process designers since certain radial features may not be filled properly.

Rules have been put forward, by Mansour, for the basic design limits of profiles on rotary forging tools so as to avoid insufficient die fill, [28]. These could be incorporated into the package PROFS as a die profile design aid.

Since with precession the tool is constrained from rotation about its own axis, (see 3.3 of Chapter 3), this will cause the profiled tool to automatically re-mesh with the forming profile on the workpiece on each revolution of the tool. On real rotary

forging machines, such as the Marciniak / Schmid type, the tool is constrained mechanically, so that it cannot rotate. PROFS uses a mathematical method of constraint on the precessing tool, by incorporating a negative spin motion of the tool axis, into the precession motion. This has the same effect as the mechanical constraint. These constraints allow the profile to be forged onto workpieces, without any problem of re-meshing of the tool with the workpiece surface. This enables fine gears to be simulated using the precession motion.

7.4. APPLICATION OF PROFS TO INVESTIGATE A REAL ROTARY FORGING SITUATION.

A series of simulations were carried out on a real rotary forging process. The process used was a 200 tonne Schmid rotary forging machine, undergoing the precession motion. The forging process took place at an industrial forging company plant where the machine was housed. The process was videoed in action and the data collected from this, used as input for the simulated experiments. The simulations were carried out to see how capable the package is of predicting the contact conditions and how the contact area developed for a known rotary forging situation.

The required forging part is as shown in figure 7.18. The upper die designed to forge the part, consisted of a basic 15° inverted concave cone, having a profile of the top of the forging incorporated into it. It was decided to simulate only the profiled upper die of the real forging process, since this would reveal the instantaneous contact geometries. Figure 7.19 shows the upper die generated by the preprocessor 'PROFS'. This was specifically programed into the package since a mouse controlled tool design facility is not as yet available for users to design their own dies. The profile was entered into a menu of custom die profiles for subsequent users to select from, if the need arises.

The initial billet shape was a cylinder 100.7mm high and 37.8mm in diameter, and the forging was carried out cold. The full details of the forging conditions are given in appendix B. In order to simulate the whole process with this model, it was necessary to break down the simulation into stages. This is because, using a non - constant volume model, the workpiece diameter does not change. However, by increasing the diameter of the workpiece after each iteration, the approximate contact

conditions can be generated for the whole of the forging. It is important to note at this stage of the process, apart from the first and the last stages, the true contact geometry is found only after the tool has established its full contact surface on the workpiece. This is usually after several cycles, when the tool establishes full radial contact with the workpiece and after the helical surface has been established. The first stage, simulates the starting conditions and the development of the contact geometry during the first revolution of the process. The last stage simulates the last revolution of the process and the reduction of the contact geometry.

The simulation was split up into three parts according to the diameter of the starting billet. The diameter was chosen because it reflects the amount of radial growth of the workpiece and the size of the contact geometry. By considering the initial and final diameters, the forging could be equally divided into 3 parts as follows :

- i) the workpiece was 37.8mm in diameter, and 100.7mm in height.
- ii) the workpiece was 46.0mm in diameter, and 68.0mm in height.
- iii) the workpiece was 54.2.0mm in diameter, and 49.0mm in height.

From the above, a full picture of the development of the contact geometry could be built up for the three stages of the process. The need for this technique leads directly to the development of the constant volume model described in Chapter 8 of this work.

7.4.1. Simulation Using a 37.8mm Diameter Workpiece.(Stage i).

This part of the simulation shows how the tool develops its initial contact with the workpiece. The first revolutions are an important part of the forging since they show how quickly the tool imparts itself onto the workpiece and, and how quickly the full contact area is established. As can be seen from figure 7.20 - a,b. the contact at 840° precession soon becomes a very large fraction of the total cross sectional area of the workpiece surface. In fact after only 840° of motion the workpiece is almost completely in contact the tool. The first two revolutions of the process are important since they show how the tool develops its contact with the workpiece. With the third and subsequent revolutions of the simulation, the upper tool contact geometry does not change and the simulation past this stage is of little further

interest. At this point the second stage of the simulation must be examined.

7.4.2. Simulation Using a 46.0mm Diameter Workpiece. (Stage ii)

This assumes that the workpiece has deformed and increased uniformly in diameter to 46.0mm. The simulation is run until full contact is established, at which point the simulation is stopped. In the initial stages of the simulation, where the helical surface on the workpiece is being initiated, and the full radial contact between the tool and the workpiece is being established, the contact geometry is of little interest. Since, at this point in the real forging situation, the tool is already in full contact with the workpiece, figure 7.21 - a,b. Hence, the full contact geometry as shown in figure 7.21- b., view 9 at 1320° of motion, shows what contact area would be expected at this stage/diameter of workpiece during the forging. The ability to see these contact geometries is important, since no method is known to exist, which can reveal the instantaneous contact geometries of a real rotary forging process. This is because the rotary forging machine would have to be stopped dead, in mid - flow from a rotational speed of 340 r.p.m. to 0 r.p.m., so that the contact geometry could be 'captured'. This obviously is not physically possible. However, by physical simulation of the rotary forging process using machining techniques, it is possible to see predicted contact geometries machined from solid workpieces. This technique is described in Chapter 9.

7.4.3. Simulation Using The 54.2.0mm Diameter Workpiece. (Stage iii).

This simulation assumes that the workpiece has been deformed and expanded to its final diameter. From figure 7.22-4 it can be seen what the final contact geometry and contact area will be in the final stages of the forging. Figures 7.22 - 1,2,3,4, of the simulation show the last revolutions of the process and demonstrate how, in reverse order, the tool will reduce the degree of its contact with the workpiece.

The three stages of the simulation were put together to show how the contact area develops throughout the whole of the process. Figure 7.23 shows stages i), ii), iii), in the simulation with their relevant contact geometries and areas against the number of cycles in the process. This clearly shows the development, progression

and pattern of deformation, and the contact areas which could be expected throughout the whole process. This kind of approach is hoped to give die designers and manufacturers an insight into what is happening during the process. Die designers in particular will be able to identify areas of the die / workpiece interaction, which might cause problems in use.

The ability to see and predict the contact geometries during a rotary forging situation is of significant interest. Any calculation of the loads or forces occurring in the workpiece during a rotary forging would first require the size of the contact area to be calculated. Upper bound, slip line field and finite element analysis techniques would all require the contact geometry and contact areas as a starting point for the calculations. Such calculations could reveal problems of die fill, in service failure and predict possible weaknesses which could lead to catastrophic failure of the dies. The ability to predict upper and lower die fill problems is also a possibility using the technique of section 7.4.

7.5. CONCLUSIONS.

'PROFS' was shown to be capable of producing the contact geometries in a non - constant volume workpiece, along with calculations of the of the contact areas, for all the motions used by present rotary forging machines. The package has been used to investigate the effect of possible rotary forging machine motions which are not known to have been employed.

The rotary forging motions of precession and spin were shown to produce similar contact geometries, under the same conditions of ram speed, rotational rate, mesh size and conic tool angle. The contact geometries were were shown to be orientated in the same positions on the workpiece. Their contact areas at each stage of the process were shown to be very close.

'PROFS' was shown to be capable of simulating the contact geometries between radially or circumferentially profiled tools and workpieces.

A custom tool with a unique profile was input into the program and stored in a menu of custom profiles for further subsequent use. This way a data base of custom

tool shapes could be stored and built up.

A method of examining the progression of the contact geometry during a real rotary forging situation, was introduced, using the customised die from the database. A series of experiments were run with different diameter workpieces for each stage of the forging process. The contact areas and geometries produced using this method could be found 'mid-forging'.

A table of the contact geometries and areas at each stage of the simulation was built up from the results of the simulations, enabling the contact geometry development and progression to be 'seen' for the whole of the process. This was thought to be a useful tool to die and machine designers, since they would be able to identify possible problems such as insufficient die fill and areas of high wear on the die. Also, the instantaneous contact area produced would first be necessary for any stress analysis of the rotary forging process. Stress analysis could be used, for example, for the calculation of possible die weaknesses which may lead to catastrophic failure. This is seen as the way forward for the development of C.A.D. - C.A.M. for rotary forging processes.

CHAPTER 8.

THE CONSTANT VOLUME MODEL **WORKPIECE.**

8.1. INTRODUCTION.

This chapter examines the Constant Volume Model Workpiece and its interaction with the tools undergoing the motions used in real rotary forging situations. The Constant Volume Model workpiece was explained fully in Chapter 6.4.2. This model was used for all the simulations mentioned in this Chapter.

Two experiments were carried out using two different Rotary Forging processes. Each process was investigated by physical experimentation and by simulation using the constant volume model as part of the PROFS package. The first investigation was of a Schmid 200 Tonne Rotary Forging machine using a Precession type motion. The part produced was a demonstration piece used by an industrial forging company to assess the machine and the rotary forging processes capabilities. Results show the ability of the package to detect possible problems of instability in workpiece location during the early stages of the forging. Results reveal the progression and development of the contact geometry on the workpiece surface throughout the whole of the forging cycle.

The second experiment used cylindrical billets which were deformed on the Nottingham University 50 Tonne Rotary Forging machine by a spin type motion. The experiments were done in five stages to show the development of the finished part. This technique enabled direct comparison between the experimental and simulated results. The simulated results reveal the development and progression of the instantaneous contact area throughout the forging. The diameters of the experimental and simulated constant volume workpieces throughout the process, were found to be in good agreement. The displaced volume of material was compared between the simulated and forged experiments and found to have a correlation coefficient of 0.9. The average percentage error between the two sets of results was found to be 39%.

The results from the two simulations show that the PROFS package is a comprehensive research tool, versatile in its applications.

8.2. EXPERIMENTS USING THE PRECESSION MOTION ON THE 200T SCHMID MACHINE.

8.2.1. The Physical Experiments.

The physical experiments were run 'on site' at the premises of a company using an industrial rotary forging machine. The machine used was the 200 Tonne Schmid Rotary Forging machine, using with a Precession motion. The part was produced as part of a production run and the results were recorded and logged by videoing the machine in action. The part used is shown in figure 7.18, and is a test piece used by the manufacturers for an assessment of the rotary forging and machines capabilities. From figure 7.18, the part can be seen to incorporate several different types of profile, on both, above and below the flange. The part was forged cold using profiled upper and lower dies. It was decided to simulate the upper die only and monitor the progression of contact development on the surface of the workpiece. The upper contact area has a major influence on forming the part. This concerns the forging forces, friction conditions, suitability of the workpiece material, and resulting tool life. The forging conditions used are listed in Appendix B.

8.2.2. The Simulated Experiments.

The upper die was defined using the custom profile part of the PROFS package, initially set up for the experiments described in Chapter 7, shown in figure 7.19. The ram and rotational speeds were established using a video recording made of the forging carried out at the plant. The digital readout from the machine was used as input data into the PROFS package. The actual forging time was found to be 2.5 seconds, which at 340 r.p.m gave about 14 revolutions of the upper die. The simulation was run for only the same period so as to minimise the simulation time. Full details of the simulation conditions used are listed in Appendix B. The simulation was set up to run with output being generated at every 360°, (otherwise too much information would be generated and too much file space used.) The simulations were run and results displayed on a Prime mini - computer using the package 'VIDEO' running on a Ramtek colour graphics terminal. The results were screen dumped and show the workpiece in blue and the contact areas in green.

8.2.3 Results.

Figures 8.1 a - h. show the 14 stages in the development of the simulated contact zone throughout the forging in both isometric and plan views. The die is not shown in the figures since it would obscure the contact geometry. The simulation is of the top configured die interacting and 'forging' the top part of the workpiece. Examining the figures shows a steady progression and radial expansion of the workpiece and contact geometry. However, in figures 8.1 - c and g, view 12 has a smaller contact area than that of view 11. This can only be explained as a short fall in the packages discrete mesh size used. The contact geometries and contact areas found from the simulation are needed as a starting point for any calculation of the forces involved in the rotary forging of this part. This simulation shows excellently how the contact region develops as the workpiece expands and its height is reduced. This is believed to be the first time an instantaneous contact geometry of a real rotary forging operation has been simulated, throughout the whole of the forming cycle.

8.2.4. The Initial Contact

Pictures 1 and 2 of figures 8.1 -a and e show only a very slight, line contact, at the outside edge of the workpiece. This looks unusual, but is quite normal since the tool is an inverted conic shape, and its outer edge makes contact with the workpiece first. The instantaneous contact area value for the two figures is shown as zero, since a line contact area cannot be used to calculate positive contact area values as explained in Chapter 6.5. The figures show that the tool has an influence on the workpiece several revolutions before any major forming or contact can be seen to have taken place. The instantaneous contact area is assumed to have a centroid close to the edge of the workpiece which causes unstable loading of the workpiece and could cause the workpiece to 'wobble' as it is being formed. An unstable 'wobbling' workpiece is deformed in quite a different manner to that of a stable one. In an unstable workpiece a large amount of deformation takes place on the base of the workpiece and the base is formed into the lower die before the top is formed. Situations which may cause unstable workpiece / tool interactions could be revealed using the PROFS package and action could be taken to avoid it before production trials take place.

8.2.5. The Intermediate Contact Geometries.

In view 3 of figures 8.1 - a and e. at 1080° of precession, the tool has been driven far enough into the workpiece for its top inside face to make contact with the workpiece surface. Workpiece instability is not a problem in this forging, since after only three revolutions of the die, the instantaneous contact geometry is a significant proportion of the workpiece area. In view 3, the instantaneous contact geometry reveals a ring of non - contact (in blue), which can be explained by the top edge of the die where workpiece material has not reached / filled. A region of non - contact is seen to extend to the edge of the workpiece which would be expected from a die inclination of 2° . The assumed centroid of the instantaneous contact area is now much closer to the centre of the workpiece. In fact, the instantaneous contact area is nearly symmetrical so its centroid must be close to the centre. The assumed centroid of the contact area also indicates the centre of loading of the tool upon the workpiece. This suggests that a stable forging situation is achieved after only 3 revolutions of the upper die.

What is surprising is how large the contact area is, compared with the size of the workpiece. This is of interest since rotary forging is thought to gain its force advantage over conventional bulk forging processes due to its small contact area. The force advantage of rotary forging could also be accounted for by the shear forces created by the rotational movement of the die, causing material to be continuously 'worked' in cyclic manner. The simulation suggests that the above explanation may play a part in the force advantage seen in rotary forging processes.

After five revolutions (view 5, in figures 8.1 - b and f.) the instantaneous contact area on the workpiece can be seen to cover almost the whole of the cross section. This is because material has now reached / filled the top edges of the die. The area of non - contact due to the inclination of the die is still seen for the rest of the simulation, views 5 to 14, in figures 8.1 - b to d, and f to e. In the figures the area of non - contact can be seen to increase as a proportion of the total instantaneous contact area as the simulation and radial spread progresses. This is because the die is an inverted cone and in the final stages / revolutions., the workpiece, being almost at its final diameter, is formed by the outer shoulder of the die. As explained in Chapter 6, contoured dies can be considered to be made up

from a number of different angled dies. The change in the ratio of instantaneous contact area to non - contact area is seen because, different parts of the die are undergoing fundamentally different motions due to them effectively having different die angles.

8.2.6. The Final Revolutions.

In the final revolutions, views 13, and 14, of figures 8.1 - d and h. the workpiece is almost at its final diameter and completely formed. The workpiece has been simulated and 'forged' for the whole of the cycle. The final revolutions in the real forging would involve a reduction of contact between the tool and the workpiece. This would be similar to the initial development of the contact geometry as found in views 1 and 2 of figures 8.1- a and e. In Chapter 7 the same die was used for simulating the process using a non - constant volume model workpiece. The final 'run out' of the contact is seen in figure 7.22 but in reverse order.

The constant volume model has enabled the development of the top workpiece shape and contact geometry to be followed from start to finish. PROFS has been shown capable of providing a quick graphical / numerical result of contact geometries for a rotary forging operation, revealing the way in which the contact geometry is created and progressed throughout the forging cycle. This could not possibly be seen by conventional experimental techniques. The capability to predict contact geometries and output quick graphical results is likely to provide an invaluable tool to aid die and workpiece design and to assist in establishing the initial setting of machine forging parameters.

The final real forging shape is more complex than that of the simulation, since it has both upper and lower die contours. The present package does not attempt to simulate this part of the process; in fact it would have to be a very sophisticated finite element type of package which could match the complex boundary conditions created during the rotary forging process. At present no available commercial package is thought to be able to model this.

8.3. EXPERIMENTS USING THE SPIN MOTION ON THE 50T MACHINE.

8.3.1. The Physical Experiments.

Several experiments were run on the Nottingham University 50 Tonne rotary forging machine to show how a simple billet / workpiece is deformed during a forging cycle with a spin type motion. The machine shown in figure 8.2. is unique in its motions and capabilities, since it is micro - processor controlled and has a nutation angle which can be varied between 0 and 45°. The machine is a Nutation - Spin type, which coupled with its micro - processor control is capable of producing an infinitely wide and varied range of motions by controlling the nutation, nutation rate, spindle speeds and ramspeed during a forging. This makes it ideal for research investigations into the process.

Figure 8.3 shows the billet of 40mm diameter and 50mm high, used for the experiments, and chosen for its stable h/d ratio. It had a central spigot machined into its base so that it could be located in a recess in the lower die, so that it was centred prior to forging. The workpieces were machined from aluminium alloy H.E. 30 and annealed for 3 Hours at 500°C. The tooling used on the upper die was a plain conic 2° die. The nutation angle (θ) was fixed at 2° throughout the forging, so that $\alpha = \theta$ and a pure spin type of motion would be obtained. The upper and lower spindle speeds were set to 120.0 r.p.m. and 119.9 r.p.m. respectively and the forging force was set to a maximum of 45 Tonne. Five workpieces were forged to reveal the five different stages of the workpiece development. Each stage was forged to a different height calculated on the amount of material that was being displaced for each step. This enabled the progression of the final forming to be seen at various stages, heights and diameters. Data logging of the nutation, nutation rate, spindle speeds, ram position, and ram force was carried out throughout the experiments. This style of investigation was chosen to make the simulated experiments easy to set up and comparison between the experimental and simulated results possible.

8.3.2. The Simulated Experiments.

The simulation was run using the data logged from the physical experiments on the 50 tonne machine. Averages were calculated from the experiments for the ramspeed and the spindle speeds. The simulation was carried out on a Sun Spark workstation to reduce the C.P.U time. Results were transferred onto the Prime mini - computer and displayed graphically using the package VIDEO on a Tektronix colour graphics terminal. The results were screen dumped. The workpiece is shown in blue and the contact areas in green. The red line is a datum line originally lying on the Y axis, and used to indicate the amount of rotation of the workpiece.

8.3.3. Results.

Figures 8.4 a - g. show the full simulated sequence of the 50 Tonne experiments in 360 degree steps. Figures 8.5 - a and b. shows the actual billets deformed using the 50 tonne machine. In each view of figures 8.4 a - g. the tool is advanced a further 1.325 mm into the workpiece. Views 6,11,17,22, and 27, in figures 8.1 a - g, can be compared directly with the billets produced on the 50 tonne machine shown in figures 8.5.a and b. The first two experimental billets show clearly a slight 'mushrooming' effect of the top surface of the billet, due to localised deformation of the top region of the workpiece. By the time the third billet is reached, deformation at the base of the workpiece has started to influence the shape of the billet . More radial expansion was seen on the base of the workpiece from this point on, due to an instability of the workpiece. This instability was caused by the centre of the die force acting at a point away from the centre of the workpiece. This caused the workpiece to be tilted and a partial contact region was created on its base. Hence, a localised plastic zone was produced around the base region of the workpiece. The final workpiece shape can be seen to be clearly bigger in diameter at the base of the workpiece than at the top, and the classic orange peel effect can be seen to have been created on the sides of the workpiece. The effect was probably due the large grain size produced in the workpiece during the annealing operation.

The simulation of this process is obviously nowhere near as complex, but it does show that even a complicated forging scenario can be followed though by a simulation such as this. Figure 8.6 shows the simulated progression of the workpiece size from the start to the finish of the forging. This figure demonstrates

the constant volume models ability to simulate the contact geometry and radial growth of a workpiece. Figures 8.7 a and b, show the comparison of the simulated and experimental diameters. When the average diameters of the simulated and experimental workpieces were plotted against the workpiece height in figure 8.7 - a, they had an average percentage error of 0.4%. The two curves are produced because $\text{height} = \text{volume} / (\pi(D/2)^2)$ for a constant volume workpiece. In figure 8.7 - b, the simulated and experimental workpiece diameters were plotted against each other and show a good linear regression with a correlation coefficient of 0.999. These results show an excellent prediction by PROFS, using the constant volume model, of the experimental workpieces diameters throughout the whole of the simulation.

The displaced volumes for all these five steps were also compared with the simulated displaced volume of material as shown in figure 8.8. The average percentage error between the two results is 39%, (S.D. = 11). This is within the accuracy expected from the constant volume model with the discrete mesh size used, as explained in Chapter 7. In figure 8.9 the simulated displaced volumes of material were plotted against the experimental, and the correlation coefficient was found to be 0.973. This shows a good linear relationship between the simulated and experimental results confirming the constant volumes models ability to simulate the radial growth of a workpiece. It is expected that with a decrease the mesh sizes of the workpiece and the tool, the accuracy of displaced volumes of material could be improved, at the expense of increased C.P.U. time.

8.4. CONCLUSIONS.

The Constant Volume Model workpiece used in the PROFS package has been shown to be able to simulate the size of the contact geometry produced during a real rotary forging process for the whole of the forging cycle.

The Constant Volume Model workpiece has been shown to reveal areas of instability during the initial stages of the forging, which may lead to problems later in the forging cycle. It is hoped that PROFS could be used to to identify these areas of instability before forging tests or the tool design is carried out.

The contact areas simulated by PROFS in the 200 tonne machine experiments have been shown to be large in comparison to the total area of the workpiece. These results are not as would be expected because of the force advantage that rotary forging shows over other conventional bulk forging processes. This suggests that other forces and factors, such as the shear forces due to the motion of the die, influence the yield characteristics and plastic deformation of the workpiece.

The constant volume model workpiece has been shown to be able to predict accurately the size of the workpiece diameter during a rotary forging. This result allows great confidence to be afforded in the predicted workpieces shape and contact geometry.

PROFS has been shown to be able to calculate the displaced volume of material of the workpiece throughout a simple rotary forging situation. Good linear correlation has been shown between experimental and simulated values.

CHAPTER 9.

EXPERIMENTS TO VERIFY THE NON - CONSTANT VOLUME MODEL.

9.1 INTRODUCTION.

A series of experiments were carried out using a metal cutting process to investigate the type of contact areas created during the rotary forging of non - constant volume workpieces. The experiments were carried out using a Short Lead Milling Machine arrangement, which, by careful milling of the workpieces, could produce the instantaneous contact areas created during the rotary forging of non constant volume workpieces. This was achieved by using an inclined cutter blade mounted on a cylindrical rotating tool. The blade moved in such a way as to simulate a rotating conic die on a rotary forging machine undergoing the precession motion. The speed at which the blade advanced into the workpiece was geared to the rotation of the workpiece and was equivalent to the 'lead' of a helix. The 'lead' is similar to the 'bite' used in rotary forging and if combined with the cutter movement can be used to physically simulate the rotary forging process.

The results from experiments were compared with a set of simulation results, run under the same 'forging' conditions on the package PROFS. The resulting profiles milled on the workpieces were measured and compared to those created by the package PROFS. The instantaneous contact areas generated by PROFS were shown to be very close to those of the milled experiments. The results showed an average 8.5% difference between the milled and simulated values. The small discrepancy was attributed to the discrete mesh size used in the simulations and the method of calculation of the milled contact areas. Excellent correlation was shown between the two results, showing that a good linear relationship was achieved between the milled and simulated results.

The displaced volume of material, is the amount of material moved or removed (in this case) between each step of the experiment. The results for the simulated and milled experiments were compared and shown to have a good linear relationship. However, an average 57.5% error was found between the simulated and milled displaced volumes. This was attributed to the discrete mesh size used in the simulations, which although in the calculation of the contact areas gave a small error, in the displaced volumes results was large because of the third dimension used in the calculation of the displaced volumes. The error was shown to be decreased if the mesh of both the tool and the workpiece was increased.

A good agreement was also shown between the results of instantaneous

contact area obtained using PROFS compared to those of other researchers Marciniak and Kubo, [14], [9].

The work of this Chapter shows that a certain amount of confidence can be expected in the accuracy of the PROFS package, in predicting the size and geometry of instantaneous contact areas produced during the rotary forging of non - constant volume workpieces.

9.2 EXPERIMENTAL EQUIPMENT.

A Parkson milling machine was set up for Short Lead Milling using a 40:1 dividing head in a horizontal position, (Fig 9.1). A blank cylindrical workpiece was then placed in the jaws of the chuck of the dividing head. A handle was attached to the main drive of the head and a protractor and pointer fixed so that the angle the handle, and hence the workpiece, was turned through, could be recorded.(Fig 9.2). The gears for the desired 'lead' were placed on the dividing head so that when the handle was turned, the workpiece would advance into the moving cutter blade at that 'lead' / bite.size. (Fig 9.2).

A cutting blade was held in a circular tool at 10.5 degrees and this was placed in the chuck of the driven spindle of the Parkson milling machine as shown in Figure 9.1. The edge of the blade was then adjusted by moving the spindle of the machine so that it was both vertical and parallel to the face of the workpiece. When the machine was started, the cutter was rotated so that its leading edge described a cone of 10.5 degrees. When the workpiece was moved into the cutter it was effectively being cut away by a 10.5 degree conic tool, similar to that on a precession type rotary forging machine.

9.3 EXPERIMENTAL PROCEDURE.

9.3.1 Short Lead Milling.

Each blank cylindrical specimen was placed in the jaws of the dividing head chuck and the head moved until the workpiece was close to the edge of the cutter. The machine was then switched on and the lubricant started or applied. The specimen was then advanced slowly by turning the handle with the protractor attached (fig 9.2) until the cutter could be felt to just touch the surface of the

workpiece, and wisps of swarf were seen. This was taken as the 0 degree point and the protractor was moved to read 0 by the pointer. The handle was then turned steadily, so that the workpiece turned, and advanced into the tool so being cut away by the spinning blade. When the desired angle was reached on the protractor, the machine was simply switched off, so that the blade would stop spinning and the workpiece would not be cut away or the contact area disturbed in any way. This way the instantaneous cutting area / contact area on the surface of the workpiece could be found.

Two sets of experiments were carried out using seven specimens each, one set in aluminium and the other in perspex. The aluminium workpieces were 50mm diameter and 60mm in height. The perspex workpieces were 54mm diameter and 37mm in height.

The first set of experiments were carried out using aluminium alloy HE - 30, using a lead or 'bite' of 1.5258 mm/rev. The gears needed to obtain this were a driven gear of 24 and a driver of 100. The workpieces were machined through to 60, 120, 240, 300, 360, and 720 degrees. These angles were chosen to show the development of the cutting / contact area during the initial revolution. After the first revolution of the workpiece, the cutting / contact area should remain constant, hence the 720 degree machined workpiece was chosen to show this. Chroma Tap 2 was used as a lubricant to prevent burning and re-working of the metal swarf back into the surface of the aluminium workpieces.

The contact areas produced after the first experiment were small in comparison with the area of the workpiece, so a larger lead was chosen of 4.0688 mm/rev, using a driven gear of 64 and a driver of 100 as shown in fig 9.2. Perspex workpieces were used, because the larger leads would produce considerable wear on the tool tip if aluminium were used. The workpieces were again milled though to 60, 120, 180, 240, 300, 360, and 720 degrees, and the lubricant used was suds (an oil based lubricant), particularly important so that the workpiece did not melt or burn due to heat produced by the fast moving cutter.

Each specimen was weighed and measured prior to machining, so that its initial volume was known. The final workpieces were then weighed again so that the volume of the displaced material could be found. The cutting / contact areas produced on each workpiece, were projected onto a piece of paper by placing each

specimen on an epidiascope, and then the profile could be traced onto the paper. This profile was then measured using a planimeter (an area measuring device), and hence the cutting / contact area could be calculated.

9.3.2 Simulated Experiments.

Two experiments were carried out using exactly the same workpiece sizes and 'leads' / 'bite' as those in the short lead milling experiments. The package PROFS was used with a precession type of rotary forging motion, and the results recorded at 60 degree intervals up to 720 degrees of motion.

The computational part of the problem was carried out on a Sun Spark Workstation, because of its speed and reduced C.P.U. time compared to the Prime. It was however not possible to display the results on the Sun using the post - processing package Video, so the results were transferred back to the Prime and displayed and interpreted there. The results were displayed using a Ramtek colour graphics terminal, and screen dumped to produce the figures shown in this chapter. In the figures, the workpiece is represented by blue lines and the contact geometries by green lines.

9.4 RESULTS.

9.4.1. The Contact Areas

Figures 9.3 and 9.4 show graphs of the simulated contact areas versus the milled contact areas produced in perspex and aluminium respectively. These plots show clearly that a very good linear relationship was obtained between the two results. The correlation coefficients of these were 0.998, and 0.995 to 3.d.p. respectively, with linear regressions for the Perspex of:

$$Y = -38.213 + 0.99058X$$

and Aluminium of:

$$Y = 97.026 + 0.69047X$$

When the contact areas were plotted on the same axes against the degrees of motion as shown in figure 9.5, they showed the accuracy to which both sets of experiments agree with each other. The graph shows how the contact area develops throughout the experiments, and that the simulated values closely follow those of the

milled ones. However the short lead milling results were consistently higher than the simulated results in both the perspex and the aluminium experiments. This may be because of the finite number of elements used to describe the workpiece and the tool during the simulated experiments, which in effect would give an approximation of the contact occurring between the the tool and the workpiece surface. Also the contact area calculating routine ('intercept') in the package COSIMORF can only calculate the contact if 3 or 4 points/nodes in each element of the workpiece are deemed to be in contact. This is because 1 or 2 points/nodes will not allow a positive contact area to be calculated. The actual contact area between four points on an 'in contact' element is assumed to be flat, and is calculated thus, when in fact it would be concave, and therefore slightly larger. Chapter 6.6.1 gives a full explanation.

The methods used to determine the contact area during the short lead milling experiments may have some margin of error, due to the contact area of the workpiece only being measured as a projected area, not as a true area. (The simulated experiments will give some approximation of the true area since PROFS finds the area over the curvature that the elements cover.) Using the planometer to measure the projected areas was not easy, although repeatability was demonstrated in its results, the scale factor used influenced the final values significantly.

The first result produced from the aluminium milled experiment at 60°, is slightly smaller than that in the simulated one and does not follow the trend set up in the subsequent results. This was thought to be because of a slight imperfection in the milled workpiece surface, giving a false impression of when the first line of contact was achieved. This would cause a smaller contact area to be cut away than was desired.

The average error for the perspex was found to be 7% with a standard deviation of 1.6%, and for the aluminium the average error was 10% with a standard deviation of 9.9%. Clearly the perspex shows a much higher degree of accuracy and which could be attributed to the larger contact areas and area of the perspex specimen used, as compared to that of the aluminium. The aluminium contact areas were approximately 47% smaller than those of the perspex. This suggests that the accuracy of the results is influenced by the size of the contact areas created during the physical experiments. The perspex experiments produced a lower percentage error and used larger workpieces and a faster 'lead', so producing larger

contact areas. The accuracy of the results is better for larger contact areas, in both the physical and simulated experiments.

These results confirm PROFS ability to simulate the contact areas produced in real rotary forging situations and allows a significant amount of confidence to be assumed in subsequent simulations.

9.4.2. Volumes of Displaced Material.

Figures 9.6 and 9.7 show the volume of the displaced material produced in both sets experiments. Again an excellent linear relationship was shown with correlation coefficients of 1.000 to 3.d.p.d. and 0.999 for the perspex and aluminium experiments. The linear regressions were found to be:

$$Y = 21.399 + 0.45279X$$

and:

$$Y = 26.413 = 0.3518X \text{ respectively.}$$

However 55% (S.D = 3.4) and 60% (S.D. = 5.3) differences were found for the perspex and aluminium respectively between the simulated and milled results, when the all the results were plotted against the degrees of motion shown in figure 9.8. The simulated results show that the same changes take place in the simulated volumes as in the milled ones. These results show a consistent underestimate by the simulated values compared to the milled ones. The reason for this may be because of the extra dimension used in the volume calculations of the simulated experiments, so further exemplifying the differences created by the discrete mesh size of the elements used to calculate the contact areas and displaced volumes on the workpiece surface. The excellent correlation and linearity obtained between the simulated and milled results does seem to confirm the above explanation. The milled, displaced volumes are assumed to be accurate since these were measured by weighing each specimen, before and after the milling, and a minimum of error is present in this technique. Further experiments were carried out using a reduced mesh size for both the tool and the workpiece. The results from the simulations, only improved the error of the displaced volume by about 6%. It is thought that a further reduction in the mesh size would be necessary to produce the required accuracy, but this would be at the expense of the C.P.U. time.

9.4.3. The Contact Profiles.

A typical contact profile from the milled experiments can be clearly seen in figure 9.9, showing the perspex specimen at 360° of motion. The geometrical spiral shape of the profile can be clearly seen and is particularly of interest in the central region where the tool is cutting the material behind the centre point. This is the area where the tool will see the most wear, since it is constantly in contact with the workpiece and rotating at the same time. The development of the contact area can be clearly seen in figure 9.10 - a,b,c showing a simulation of the contact profiles for the perspex experiments. The definition in these simulations is not good enough to see the contact zone in its finest detail. A further experiment was run using more points / elements on the tool and the workpiece. Figure 9.11 shows the perspex simulation at 360°, it can now be seen to clearly show the geometrical spiral on the leading edge of the contact zone which is similar to that in the photograph of figure 9.9. The results for the contact areas and volumes have also improved by about 1.4%, confirming that the underestimates talked about in the previous section, (9.3.1.), are at least partly due the mesh size chosen.

A direct comparison between the profiles of the simulated and milled experiments is shown in figure 9.12 for the perspex experiments at 360°. From the figure it can be seen that the simulated profile is slightly smaller than the milled profile over the major region of the contact area. This as would be expected due to the size of the mesh used to to run these simulations. Around the central region of the workpiece the two profiles merge, which can be explained by the fact that the mesh size used in the workpiece and the tool decreases towards the centre due to the radial spacing of the lines (see figures 6.2 and 6.8.), so improving the accuracy of the simulated contact geometry. The simulated contact area can be seen to be very close to that of the milled one, again validating the ability of the package to simulate real rotary forging instantaneous contact areas. The instantaneous contact areas produced from such simulations could be used for the solving of rotary forging problems in the design and development stage of the production of a part. PROFS has been shown to be a valid tool for die and workpiece design.

9.5. COMPARISON OF PROFS WITH PREVIOUS RESEARCHERS.

Kubo investigated the relationship between the coefficient λ and the spiral feed S , for a die of angle $\alpha = 2^\circ$, [9]. Where $\lambda = \text{I.C.A.} / \pi R^2$ and R equals the radius of a workpiece. Figure 9.13 shows the results for Kubo compared with those produced by PROFS, using the non - constant volume workpiece model. PROFS results show a consistent close agreement with those of Kubo for several different diameter workpieces.

Marciniak undertook similar investigations using physical experimentation to investigate the relationship between $(2R \tan \alpha / S)$ and λ , [14]. Figure 9.14 shows the results of Marciniak plotted alongside those of PROFS. Where the angle of the die $= \alpha = \theta = 2^\circ$, and λ is the coefficient of the instantaneous contact area, i.e. the I.C.A. divided by the cross sectional area of the workpiece. S is described as the axial feed per revolution of the press (mm / rev), and R the radius of the workpiece. The results of PROFS show a good agreement with those of Marciniak.

These results show a good correlation with the work of other researchers, allowing confidence to be assumed in the accuracy of the PROFS simulations.

9.6. CONCLUSIONS.

These results show that PROFS is capable of producing accurate simulations of the instantaneous contact geometries of physical rotary forgings. This allows a confidence can be assumed in subsequent simulations of the contact areas produced by the package PROFS of physical rotary forging situations.

Comparison between the physical (milled) and simulated contact areas shows that the package PROFS is capable of simulating real rotary forging instantaneous contact areas to within a good degree of accuracy. The contact areas produced have been shown to follow the same trends in both the size and the shape as those of a physical (milled) rotary forging. This was done using the non - constant volume model workpiece.

The results show that PROFS is capable of producing reasonable estimates of the displaced volume of material for any step in a rotary forging process. The accuracy of this may be improved by the use of smaller mesh sizes for the tool and the workpiece.

The mathematical formulae put forward by Kubo and Marciniak have been shown to be in good agreement with simulations run on PROFS, again confirming the confidence which can be afforded to the accuracy of PROFS calculations of instantaneous the contact area.

CHAPTER 10.

CONCLUSIONS.

10.1. INTRODUCTION.

A computer package called PATH has been developed which has enabled detailed investigations into the motions of rotary forging machines to be carried out. These motions are of interest because of the complex nature of the process. The motions of rotary forging machines were described using the Eulerian motions of a spinning body, and incorporated in the package PATH. The package was shown to be capable of simulating all possible rotary forging machine motions. In particular, the widely used non - monotonic nutation motion employed by Marciniak / Schmid type machines was simulated and investigated. Results from these investigations led to the development of formulae to predict different motions, and displayed in a tabular form. Other areas of rotary forging tool motion investigated using the package were : the effect of the initial nutation on the tool motion, the effect of the tool angle on the tool motion, and the locus of a point not on the tool surface. For each of these investigations, graphical results were produced and trends revealed in the movement of the tool. PATH has been shown to be extremely useful in allowing an understanding of the complex motions of rotary forging machines to be obtained.

A computer package has been developed called PROFS which has been shown to be an accurate tool for the prediction of rotary forging die and workpiece interactions. PROFS has been written as a three part package consisting of a pre - processor, a processor, and a post - processor. This enabled a data base of the simulations carried out during the research programme to be built up. The data base can be quickly accessed by the post - processing part of the package, called VIDEO, and the results displayed graphically on the screen.

A package was developed with two types of workpiece available. These could be selected in the pre - processing part of the package called PROFS. The two models were, non - constant volume workpiece and the more sophisticated constant volume. All the motions of the rotary forging machines were simulated using the constant volume workpiece model and their contact geometries, contact areas, and displaced volume of material predicted. An experiment was carried out using a short lead milling process to investigate the validity of the non - constant volume model workpiece. Results of the physical and simulated experiments showed close agreement between the contact areas and geometries, and reasonable agreement between the displaced volumes of material.

Two real rotary forging processes were compared and investigated using the constant volume model workpiece simulations. The first experiment involved the use of a 200 tonne Schmid rotary forging machine operating with the precession type motion. This was used to forge a test workpiece produced in trials by an industrial forging company. Results from the simulations revealed the development of the contact geometry throughout the whole of the forging cycle. The second experiment involved a 50 tonne rotary forging machine using the spin type motion. This was used to forge a simple cylindrical billet. The diameters of the forged and simulated workpieces were compared and shown to be in close agreement. The displaced volumes of material were also compared between the experimental and simulated results and shown to produce good correlation.

The results of PROFS were also compared with those of the researchers Kubo, and Marciniak, and found to be in good agreement, [9], [14].

The results and investigations discussed in this thesis show the powerful capabilities of a simulation package in the application of rotary forging. It has shown its ability to : reveal trends, rationalise rotary forging machine motion by classification, aid the understanding of complex motions, and act as a die, workpiece and machine motion design tool.

10.2 THE PACKAGE PATH AND ITS USE IN THE STUDY OF ROTARY FORGING MOTIONS.

A general tool and workpiece arrangement was identified for all rotary forging machines. A mathematical model was put forward based on the Eulerian motions of nutation, precession and spin and was proved to be capable of simulating the motion of rotary forging machines. This was used as a basis for the development of a general rotary forging simulation package. The common factors are : a central axis for both the workpiece and the tool and a conic or inverted conic tool, which has its axis rotated about a point on the axis. It is important to note that, movement of the tool should always be about the point on the axis otherwise a true rotary forging motion will not occur.

The rocking die motion of Marciniak / Schmid type rotary forging machines, was modelled in the package PATH using the non - monotonic nutation -precession motion. The non - monotonic nutation movement was based upon S.H.M. motion,

reflecting the eccentric gearing used to drive rotary forging machines. PATH was shown to be capable of producing the same tool motion paths as those of known rotary forging machines. The orbital (precession) motion, the line (non - monotonic nutation) motion, the rosette and spiral (non - monotonic nutation - precession) motions were all simulated and PATH was shown to be able to produce the same paths of tool motion as those of Marciniak / Schmid type machines.

The results produced using PATH and the non - monotonic nutation - precession motion were also shown to agree with researchers Marciniak, and Baert et. al's. predictions of these motions, [28], [35]. Baert et. al. produced a formula, based on a factor Z, to predict the number of petals in a rosette motion that would be produced from different rates of axis rotation. This was shown to agree with the analysis produced from the results of PATH. The graphical output from PATH was shown to agree closely with the tool motion predictions of Baert et. al.

From the results using PATH a table of the different types of spiral and rosette motions was produced. The table revealed trends and discontinuities in the theory of rotary forging motion. Rosette motions were found to occur when the non - monotonic nutation rate was greater than the precession rate and spiral motions were found to occur when this situation was reversed. One interesting pattern revealed from the results of path was the non asymmetric circular tool motion. This is produced when the non - monotonic nutation rate is equal to the precession rate. The asymmetric pattern was classified as neither a rosette motion nor a spiral motion. The reason for this strange motion was explained by the fact that in 180 degrees of precession the non - monotonic nutation had the effect of reversing the direction of the precession motion so tool motion only took place in one half (180°) of the of the workpiece

The flexibility and comprehensive selection available using the package PATH shows its use in tailoring motions for dies with special profiles. For instance a circumferentially profiled die, such as bevel gear, with 28 teeth could be forged beneficially by the use of a rosette tool motion having 28 petals. This could cause more radial flow of workpiece material into the teeth of the lower die resulting in better die fill. Such a motion would require the development of a sophisticated micro - processor controlled rotary forging machine. At present, no such machine is known to exist.

The effect of the initial nutation θ_i was investigated and shown to influence the pattern produced by a point on the surface of a rotary forging tool during precession motions. The results show nine different states, including a tear drop, a figure of eight, and a circular motions. These states were shown to be continuous as the initial value of nutation was changed.

Results for the path of a point on the surface of a rotary forging tool were shown to give an insight into the motion of contoured tool surfaces. A point on the surface of a rotary forging tool during non - monotonic nutation - precession was found to produce the same type of patterns as a point on the tool axis. These motions were offset and had the outline of an inverted tear drop.

During the precession motion, flat plates were shown to produce locii having a figure of eight type motion with the crossover point on the Y axis. The effect of altering the initial nutation was shown only to change the amplitude of the figure of eight.

For a point on the surface of a tool the effect of changing the tool angle was shown to generate a continuous pattern of tool surface movements. The movements for $\alpha = 0$ degrees, produced a teardrop locus, through to a circle when $\alpha = 90$ degrees. When a point not on the base cone angle α , tool surface, i.e. below the tool, was traced during various rotary forging motions it was found to represent a point on the surface of another tool angle α equal to that which the point subtended to the origin. This has serious implications for the design of rotary forging tooling, since a feature on a tool will not subtend the same angle of a point on another part of the tool. Such a point will effectively lie on a cone of different base angle α and will hence undergo a different motion from other points. A workpiece will therefore 'see' many different motions from different parts of the tool surface. When designing tools with large deviations from the base cone angle α , the motion of different parts of the tool must be considered especially with respect to material flow, and die life.

10.3 THE DEVELOPMENT AND EVALUATION OF A PACKAGE TO SIMULATE ROTARY FORGING.

A three part computer package has been developed which is capable of simulating the instantaneous contact areas and the displaced volumes of material produced onto a workpiece by a rotary forging tool.

The PROFS pre - processor has been shown to be capable of generating a wire frame tool of a basic conic shape from a data base of circumferential and radial profiles. The chosen profile can be incorporated into the basic conic shape of the workpiece imposed onto the basic conic shape. The base cone angle α and the number of points on the tool can be selected in the pre - processor.

A custom tool facility was designed as part of the package and in the form of a data base of custom tool profiles. This enabled complex tool shapes to be accommodated into the basic conic shape. The facility was used in the simulation of the 200 tonne Schmid machine in Chapter 7 & 8.

A workpiece was generated using an elemental mesh of hexahedral elements arranged in a circular fashion. This enabled the elements to be moved and deformed as they interacted with the tool surface.

The pre - processor is capable of setting up any number of combinations of forging situations by the use of a comprehensive menu choice system for the user. This has enabled any rotary forging machine situation to be modelled and its effect simulated. The information for each simulation is written to a file for subsequent processing by the processor.

Within the processor part of the PROFS package, COSIMORF, one of two material models can be selected:

The non - constant volume model, enables the instantaneous contact geometry to be seen for a certain diameter of workpiece, as the tool progresses. Since the workpiece does not deform as the tool advances the workpiece reduces in volume, making the model equivalent to 'rotary cutting'.

The constant volume model, keeps the volume of each of its elements constant, by allowing them to expand radially, thereby causing the workpiece to

move and expand as the tool moves downward. This enables the user to 'see' the instantaneous contact geometry between the tool and the workpiece throughout the whole simulation.

The PROFS package was shown to be capable of incorporating the Eulerian motions of nutation, precession, and spin by means of a mathematical model. The chosen tool and workpiece, could therefore be moved in such a manner as to simulate the motion of any rotary forging machine.

A method of detecting the interaction between the tool and the workpiece has been put forward, so revealing the complex contact geometries created during the rotary forging.

A contact area calculation routine was developed to enable the instantaneous contact areas at each step of the simulation to be calculated. This was done by first finding the 'in contact' elements and then calculating the area of each element before summing them. The displaced volume of material in the workpiece was also calculated by this technique allowing the total volume of displaced material to be found at each stage of the rotary forging simulation.

A post processor called 'VIDEO' has been developed which allows the results of the simulation to be displayed graphically on a colour monitor in various formats. It enables the user to see a selection of the stages of the simulation, or just one iteration during the process. Solid or line representation of the tool and the workpiece can be chosen, along with a choice of colours to enable the instantaneous contact geometry to be identified.

The three parts of the package PROFS enables a database of results to be set up. This allows simulations to be run overnight. The results from the simulations can be viewed by the post - processor VIDEO and displayed on the screen as a tool and 'deformed' workpiece. This would allow a comprehensive data base of rotary forging simulations to be built up. These could then be selected by designers to investigate the interactions of similar tools and workpieces.

10.4 CONFIRMATION OF THE NON - CONSTANT VOLUME MODEL WORKPIECE.

'PROFS' was shown to be capable of predicting the contact geometries and instantaneous contact areas on a non - constant volume workpiece, for all the motions used by present day rotary forging machines, and also some, as yet, not produced.

The rotary forging motions of precession and spin were shown to give the same contact geometries, under the same conditions of ram speed, rotational rate etc., but with the workpiece orientated in different positions due to the different actions of the two motions. Their contact geometries and contact areas at each stage of the process were shown to be the same within the accuracy of the experiment.

'PROFS' was shown to be capable of simulating the contact geometries between radially or circumferentially profiled tools and workpieces. The constraint used in the model for giving the tool a precession motion was shown to be capable of allowing the tool to re-mesh with its previous circumferential profile on the workpiece, created from the previous revolution, so emulating the constraint used in rotary forging machines.

A custom tool with a unique profile was input into the programme and stored in a menu of custom profiles for further and subsequent use. This way a data base of custom tool shapes could be stored and built up, for further user.

A method of examining the progression of the contact geometry during a real rotary forging situation, was developed, using a customised die shape from the database. A series of experiments were run using different diameter workpieces for each stage of the forging process. From the results of the simulations, a table of the contact geometries and areas at each stage of the simulation was built up, enabling the contact geometry development and progression to be 'seen' for the whole of the process. This was thought to be a useful tool to die and machine designers, since they would be able to identify possible problems such as insufficient die fill and

areas of potentially high die wear.

Experiments were carried out using the short lead milling process to physically simulate the rotary forging process. The milling process was set up to simulate a precession type of rotary forging machine motion. Two sets of experiments were carried out using perspex and aluminium workpieces. The physical results revealed the development of the contact geometries throughout two rotations of the die. The simulations of this process gave results for the contact geometries and contact areas which were in good agreement with those of the physical process. The accuracy of the instantaneous contact areas were shown to be improved upon by increasing the mesh size of both the tool and the workpiece. This confirmed the ability of PROFS to accurately predict rotary forging contact geometries.

The displaced volumes of material were found to have an average 57.5% error compared to the physical values. This was thought to be due the discrete mesh size of the simulated workpiece and tool. This was confirmed during further experiments using a reduced the mesh size in the tool and the workpiece. The accuracy of the displaced volumes was not found to be greatly improved by an increase in mesh size of both the tool and the workpiece. The mesh size may need to be further reduced to obtain the required accuracy, but at the expense of increased C.P.U. time. This leads to the development of PROFS to calculate a recommended minimum mesh size that would produce results in a reasonable C.P.U. time.

Results from PROFS for the contact areas produced during rotary forging were found to be in good agreement with those of other researchers Marciniak and Kubo, [14], [9].

10.5 EXPERIMENTS USING THE CONSTANT VOLUME MODEL WORKPIECE.

Experiments using two different rotary forging machine processes were carried out to compare experimental and simulated results using the constant volume workpiece model. The first experiments used a 200 tonne Schmid rotary forging

machine The data for its simulation was collated from a video recording of a commercial rotary forging operation.

The results showed the development of the contact geometry throughout the forging cycle. The contact geometries revealed an instability in the location of the workpiece at the first contact of the tool with the forging. The simulated workpiece was seen to be stable for the rest of the forging cycle. The contact areas were found to be large in comparison with the size of the workpiece. This suggested that the force advantage seen by the rotary forging process over conventional bulk forging processes is not totally due to the reduced cross sectional area of contact between the tool and the workpiece. It is suggested that the the force advantage is partly due to the rotational shear forces created by the complex movements of the tool upon the workpiece These movements are further complicated by the profiled tooling used in many rotary forgings, causing different motions to be imparted to the workpiece by different parts of the die surface.

The possibility of a package such as PROFS to be used in pre - production trials has been demonstrated by this thesis. It would be possible to reveal potential workpiece instability at the initial tool - workpiece contact, together with other problems such as insufficient die fill. The contact areas calculated by PROFS are seen as a useful first step for any calculations involving the forces and loads occurring in the workpiece during the rotary forging cycle.

The second experiment involved the use of a 50 tonne micro - processor controlled spin type rotary forging machine. The experiment was carried out using a plain cylindrical workpiece and a plain conic upper die. The results were data logged and used as data to run the simulation of the process.

The simulated workpiece diameters were compared directly with those of the experiments and found to be in close agreement. This confirmed the ability of the constant volume model to simulate a constant volume workpiece. This also lends credibility to the predictions of the contact areas calculated using the constant volume model workpiece.

The displaced volumes of material in the workpiece were compared with those produced by the experimental and simulated trials and found to have good

correlation, but with an average 39 % error. Again this is put down to the discrete mesh size of the tool and the workpiece

The simulation of the 50 tonne machine is seen as an important step in the development of C.A.D - C.A.M. for the rotary forging process. This has been demonstrated by, the data logged from the 50 tonne machine, being used as input to control a computer simulation program. The reverse is true, if a compatible computer and micro - processor controlled rotary forging machine system is developed.

SUGGESTIONS FOR FURTHER WORK

To enable further flexibility of the package PROFS it is suggested that it be run from a table of instructions containing information about the forging conditions at each step of the forging. This would mean that conditions such as ramspeed, nutation rate, rotational speed etc. could be altered during a forging cycle, so modelling the more sophisticated rotary forging machines cycles of forging.

The implementation of a digital input tablet into the package PROFS would enable custom tool shapes to be input quickly and easily into the package.

Some further work to enable the package to become self explanatory would be necessary to aid inexperienced users. At present the package is fairly comprehensive in its questions and answers for setting up the machine control characteristics, but for special motions such as rosette and spiral motions the input process is not yet user friendly. Also an editing ability of these characteristics would be a useful and time saving facility.

The ability of PROFS to find the instantaneous displaced volume of material at each step of the simulation could be improved. This would involve the development of a more accurate volume finding routine for each element of the mesh. Also, an optimisation routine for the calculation of the mesh size required, for the tool and the workpiece, in order to give results of a desired accuracy, within a reasonable C.P.U. time.

A database of the toolings used in rotary forging could be set up to provide the die designer and researcher basic information.

The implementation of the whole of the package on a SUN or similar workstation would allow the package to be portable and compact. At present only the Processor part of the package has been implemented on a SUN workstation. The other two parts contain 'in house' graphics routines unique to the Prime, so would require some rewriting.

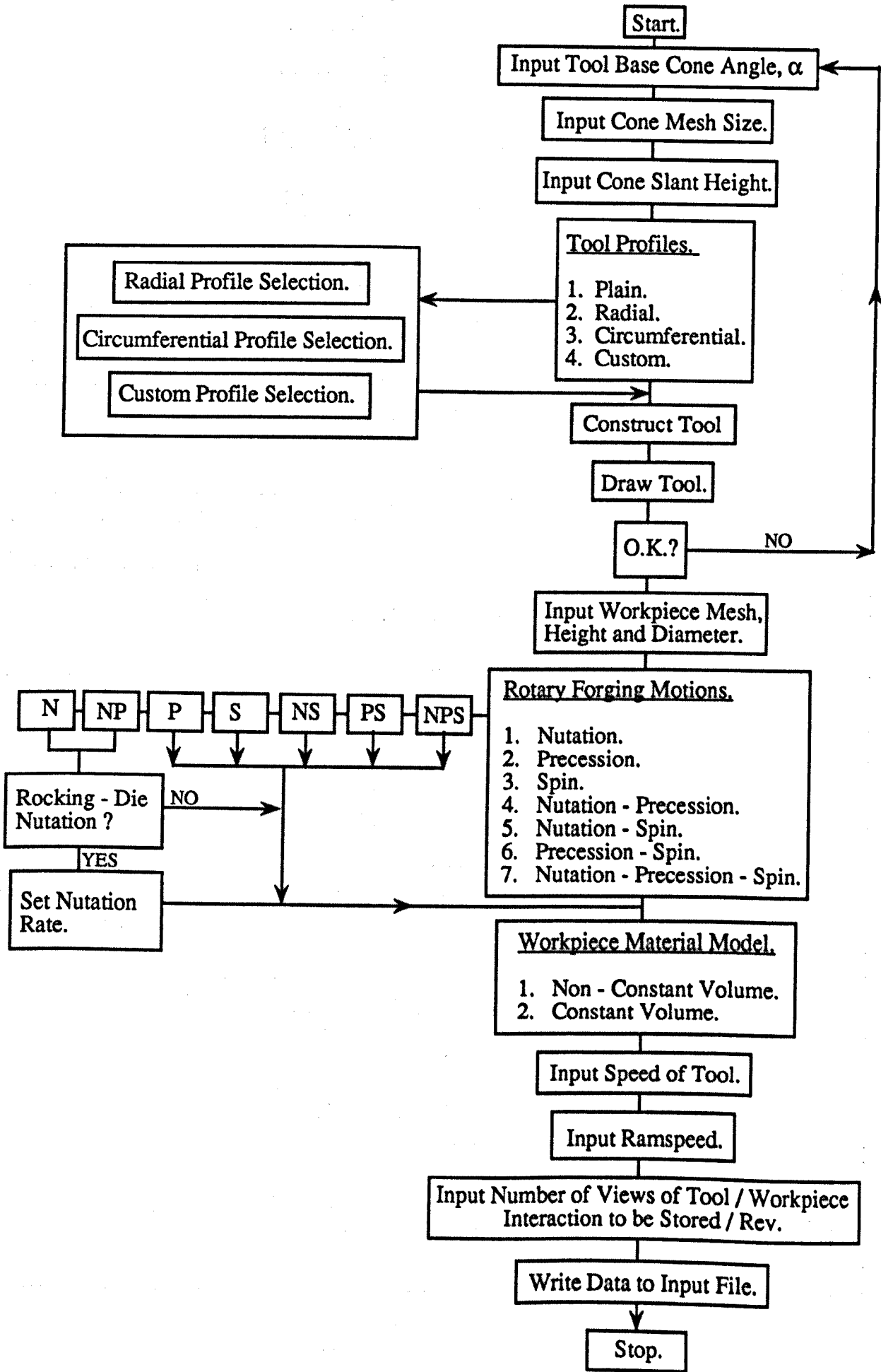
The post - processor VIDEO could be improved to give a more flexible arrangement of views of the workpiece. At present it can show single, 4,6,9,and 12 views of the results, and scale these to suit the user. It would be of further use if the user could section and rotate the workpiece and tool if necessary to see the contact region in more detail. This could allow the desired views to be produced for subsequent printing.

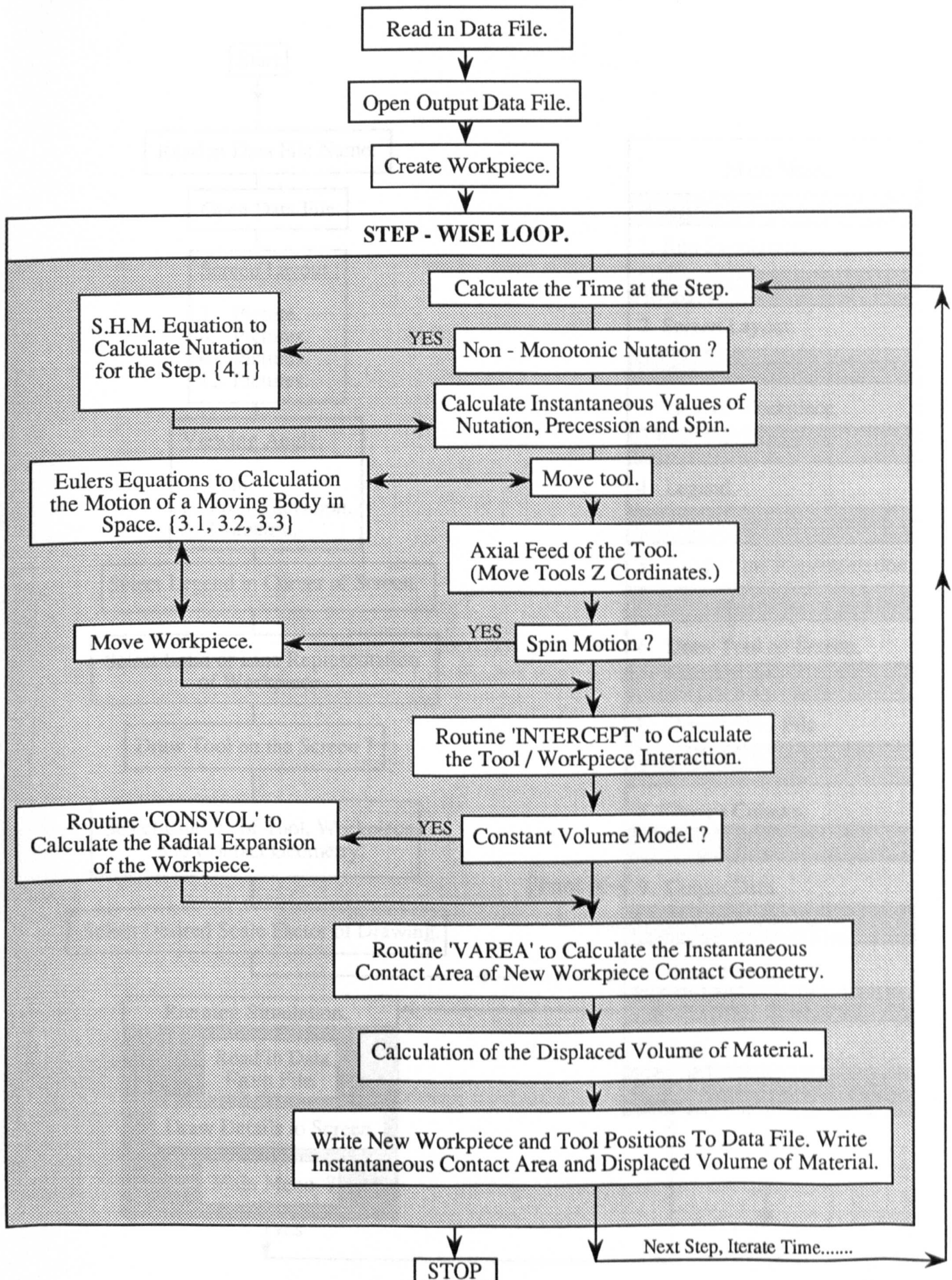
The implementation of upper and lower dies which could both be customised to suit a complex forging situation. This would greatly improve the investigative properties of the package. However, it would also need the implementation of a new type of material model to accommodate the deformations which would be produced by the use of these dies.

The package could be improved by the addition of an elasto - plastic or similar finite element type of approach to the material model. This is seen as a long term research aim, since the contact conditions created during rotary forging are constantly changing, and these have a major influence on the way a piece of material will deform. What is more, the present F.E. packages available for conventional forging have taken many man years to develop. It would seem foolish to start down this road now, when a commercially available conventional forging package may well be capable of simulating some of the simpler rotary forging type motions. Given further improvements in the years to come these may well be able to accommodate some of the more complex rotary forging motions. Such a package would inevitably use a large amount of C.P.U. time compared to PROFS.

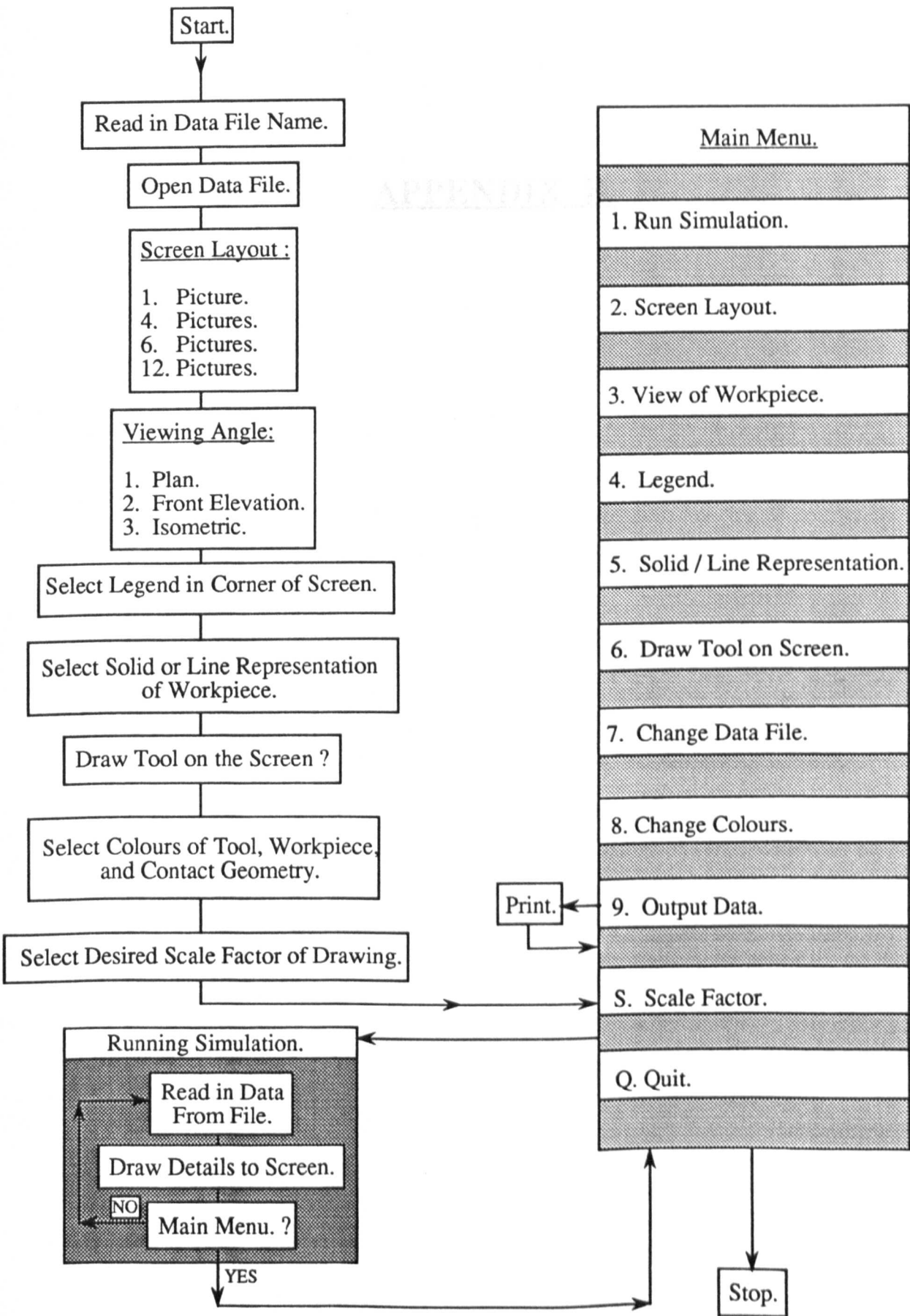
Further research work would be useful in the field of finite element analysis of the rotary forging motions, using an established package with the simple motions of rotary forging machines. For example these packages could be used to investigate the reasons for the force advantage that rotary forging has over other conventional forging processes.

APPENDIX A.





Flow Diagram of Postprocessor 'VIDEO'.



APPENDIX B.

**CONDITIONS USED IN THE 200 T SCHMID MACHINE EXPERIMENTS
AND SIMULATIONS.**

Tool Dimensions.

Tool diameter	80.00 mm
Tool height	13.5 mm

Workpiece Dimensions.

Workpiece height	100.7 mm
Workpiece diameter	37.8 mm
Workpiece material	Steel - E.N. 3A.

Rotary Forging Conditions.

Tool Motion	Precession.
Tool inclination	Fixed at 2°.
Cycle time for one forging.	9 secs.
Forming cycles of the tool	14
Tool start height	100.7 mm
Tool cycle rate	340 c.p.m.
Ramspeed	24 mm/sec.
Workpiece temperature.	Cold

Simulation Conditions.

Workpiece mesh	15 x 50 points
Tool mesh	16 x 70 points.
Workpiece model	Non - Constant Volume
Increment size	15°
No. of views. per rev.	1.
Tool start height	100.0 mm
Initial nutation of the tool	Fixed at 2°
Tool motion	Precession
Total amount of precession	5049°

REFERENCES.

- [1] Standring P.M. Appleton E. The Kinematic Relationship Between Angled Die and Workpiece in Rotary Forging. The 1st. Int. Conf. on Rotary Metal Working Processes. London U.K. pp. 275 - 288. November 1979.
- [2] Slick E.E. Manufacture of Wheels. Patent No. 965035. U.S.A. Filed June 1907.
- [3] Standring P.M. Appleton E. Rotary Forging Machine Design. Chartered Mechanical Engineer. Vol. 26. No. 4. pp 44 - 50. April 1979.
- [4] Massey Ltd. Improvement in Forging and Upsetting Machines. U.K. Patent Specification No. 319065. September 1929.
- [5] B. and S. Massey Ltd. U.K. Patent Specification. No. 1224259. Filed July 1969. Published March 1971.
- [6] B. and S. Massey Ltd. U.K. Patent Specification. No. 1224260. Filed July 1969. Published March 1971.
- [7] Marciniak Z. Patent Specification. No. 1205171. Filed Jan 1968. Published September 1970.
- [8] Slater R.A.C., Barooah N.K., Appleton E. and Johnson W. The Rotary Forging Concept and Initial Work with an Experimental Machine. Proc. Inst. Mechanical Engineers. Vol. 184. Part I. No. 32. pp. 577 - 586. 1969 - 1970.
- [9] Kubo K., Hirai Y., and Ito S. The Preliminary Work on Rotary Forging with an Experimental Press. J. Japan Soc. Tech. Plasticity. Vol. 14, 151. pp. 646-655. August 1973.

- [10] Mwenda H.M. Design, Construction and Evaluation of a Nutation - Spin Forging Press. Ph.D. Thesis. University of Nottingham 1986.
- [11] Slater R.A.C. and Appleton E. Some Experiments with Model Materials to Simulate the Rotary Forging of Hot Steels. 11th. Mach. Tool Des. Res. conf. pp. 1117-1136. 1970.
- [12] Appleton E. and Slater R.A.C. The Analysis of Rotary Forging Investigations as an Aid to Design. 12th. Mach. Tool Des. Res. Conf. pp. 557-566. 1970.
- [13] Koch L.T. and Wanheim T. Physical Simulation of Rotary Forging. Rotary Forming - Proc. of Int. Conf. pp. 165-176. Beijing 1989.
- [14] Marciniak Z. A Rocking - Die Technique For Cold - Forming Operations. Machinery and Production Engineering. Vol. 11. pp. 792 - 797. November 1970.
- [15] Kubo K., Hirai Y. Deformation Characteristics of Cylindrical Billet in Upsetting by Rotary Forging Machine. 1st. Int. Conf. on Rotary Metal - Working Processes. London U.k. pp. 99 - 110. November 20 - 22. 1979.
- [16] Dimitrov D. and Hawkyard J.B. Investigations of Yield in Rotary Forging by the Indentation of Thin Discs. Proc. 18th. Mach. Tool Des. Res. Conf. pp.133-136. 1977.
- [17] Su H., Kawai K. and Hayama m. An Analytical Study on Deformation Mechanism in Rotary Forging Process. Rotary Forming - Proc. of Int. Conf. pp. 171 - 176. Beijing 1989.

- [18] Hu Y. Four Motion Types of the Upper Die of PXWP-100c Rocking Die Press Represented by Rotating Vectors. Rotary Forming - Proc. of Int. Conf. pp. 192 - 196. Beijing 1989.
- [19] Oudin J. and Ravalard Y. An Upper Bound Method for Computing Loads and Flow Patterns in Plane Strain Forging Process. Int. J. Mach. Tool Des. Res. Conf. Vol. 21 No. 3/4. pp. 237-250. 1981.
- [20] Oudin J., Ravalard Y., Verwaerde G. and Gelin J.C. Force, Torque and Plastic Flow Analysis in Rotary Upsetting of Ring Shaped Billets. Int. J. Mech. Sci. Vol. 27. No. 11/12. pp 761-780. 1985.
- [21] Appleton E. and Slater R.A.C. Effects of Upper Platen Configuration in the Rotary Forging Process and Rotary Forging into a Contoured Lower Platen. Int. J. Mach. Tool Des. Res. Vol. 13 pp.43-62 1972.
- [22] Hawkyard J. B., Gurnani C. K. S., Johnson W. Pressure Distribution Measurements in Rotary Forging. J. of Mech. Eng.Sci. Vol. 19. No. 4. pp. 135-142. 1977.
- [23] Wanheim T. and Danckert J. Combined Physical and Numerical Modelling of Metal Forming Processes. Advanced Technology of Plasticity. Vol. 1. Stuttgart FRG. pp. 24 - 28. August 1987.
- [24] Chou D., Wang Z.R., Zhao J., Liu M., Hu Y., Hou H., and Sun J. Recent Development of the Theory and Experimental Research on Rotary Forging. Rotary Forming - Proc. of Int. Conf. pp. 149 - 159. Beijing 1989.
- [25] Hawkyard J. B. Recent Developments in Rotary Forging. Proc. 6th. Int. Cold Forging Congress. pp. 25. May 1980.

- [26] Nakane T., Nakamura K., and Kobayashi M. Accuracy of Rotary Forged Products. Proc. Spring Synoposium on Metal Forging. pp. 603. 1978.
- [27] Zhao J. On Contact Contour and the Relative Spiral Feed During Rotary Forging. Rotary Forming - Proc. of Int. Conf. pp. 181 - 184. Beijing 1989.
- [28] Mansour S. A Computer Package for Simulation and Analysis of Rotary Forging. Ph.D. Nottingham University England. 1988.
- [29] Carleone J., Chou P. C., and Muelleur M. Numerically Controlled Orbital Forging: Feasibility of High Precision. Proc of 2nd. Int. Conf. on Rotary Metalworking Processes. pp. 101-112. U.K. 1982.
- [30] Marciniak Z. The Influence of the Type of Motion of the Tools on the Cold or Warm Metal Forming Process. Proc. of the 4th. Conf. on Production Engineering. pp. 759-768. Tokyo 1980.
- [31] Mullineux G. and Knight W. A. Integrated CAD / CAM of Dies for Hot Forgings. Proc. of 21st. Mach. Tool Des. Res. Conf. pp. 593-602. Swansea U.K. 1980.
- [32] Chou A. and Labriola M. Rotary Forging - A Precession Process. Mech. Eng. pp. 73-77. March 1985.
- [33] Euler L. Problema algebricum. Novi Commentarii Academiae Petropolitanae. Vol. XV. pp. 137-138. 1771.

- [34] Euler L. *Formulae Generales Pro Translatione Quacunque Corporum Rigidorum. Novi Commentarii Academiae Petropolitanae. Vol. XX. pp. 137-273. 1776.*

- [35] Baert P., Meslem P., Oudin J., and Ravalard Y. *Design and Performances of a New Flexible Cell for Rotary Forging. Proc. of 20th. Int. Mach. Tool Des. Res. Conf. pp. 367-374. 1988.*

- [36] Barson R.J. *Computer - Aided Mesh Generation for Finite Element Analysis. Ph.D. Thesis. University of Leicester. 1982.*

TABLES.

Table 3.1 Some Rotary Forging Machines Designs Around the World in Terms of their Eulerian Motions.

DESIGNER	COUNTRY	DATE	TYPE OF MOTION						
			N	P	S	NS	NP	PS	NPS
Slick	U.S.A.	1906		P	S				
Slick	U.S.A.	1907			S				
Slick	U.S.A.	1907		P					
Slick	U.S.A.	1910			S				
Slick	U.S.A.	1911		P					
Brindley	U.K.	1914				(NS)			
Slick	U.S.A.	1918						PS	
Massey (H.F.)	U.K.	1928		P					
Silichev	U.S.S.R.	1962		P					
Silichev	U.S.S.R.	1962		P					
Silichev	U.S.S.R.	1964		P					
Sci. & Res. Institute of Automobile Ind. Tech.	U.S.S.R.	1964		S					
Marciniak	Poland	1967	N	P			NP		
Massey (B & S)	U.k.	1969		P					
UMIST	U.K.	1969		P				PS	
Ulrych	W. Germany	1971			S				
Silichev	U.S.S.R.	1971		P					
Silichev	U.S.S.R.	1972		P					
Kubo	Japan	1972		P					
Kubo	Japan	1972		P					
Silichev	U.S.S.R.	1973	N						
Silichev	U.S.S.R.	1974	N						

continued.....

Table 3.1 Continued.....

DESIGNER	COUNTRY	DATE	TYPE OF MOTION						
			N	P	S	NS	NP	PS	NPS
Silichev	U.S.S.R.	1974		P					
UMIST	U.K.	1975		P					
Silichev	U.S.S.R.	1976	N						
Wuhan Automobile Gear Factory	P.R. China	1978	N						
Schmid	Switzerland	1979	N	P			NP		
Nottingham Uni.	U.K.	1979		P					
Harbin Institute of Technology	P.R. China	1979		P					
Wagner Dortmund	W. Germany	1980			S				
Aisin Seiki	Japan	1980		P					
Nitto Seiko	Japan	1980		P					
Kyodo	Japan	1980		P					
Shanghai Inst. of Res.Mach. Tool Bldg. Tech.	P.R. China	1981			S				
City Uni.	U.K.	1981			S				
Grzeskowiak	Poland	1981	N						
Kiev Polytechnical Institute	U.S.S.R.	1982	N	P			NP		
Dyna East	U.S.A.	1983			S				
Nottingham Uni.	U.K.	1984	N		S	NS*			
University of Valenciennes	France	1988	N	P			NP		
Technical University of Denmark	Denmark	1989	N	P			NP		
Sumitomo Metal Ind.	Japan	1989			S				

N = Nutation, P = Precession, S = Spin.

* Micro processor controlled, so is infinitely variable over the whole range of nutation and spin motions.

Table 5.1 This Table Shows the Number of Petals in a Rosette or the Number of Symmetries of a Spiral During Rocking Die Nutation - Precession motion.

Precession Rate cps.	1	2	3	4	5	6	7	8	9	10	11
Nutation Rate cps.											
1	1	2	1	2	1	2	1	2	1	2	1
2	4	1	4	2	4	1	4	2	4	1	4
3	3	6	1	6	3	1	3	6	1	6	3
4	8	4	8	1	8	4	8	2	8	4	8
5	5	10	5	10	1	10	5	10	5	2	5
6	12	3	4	6	12	1	12	6	4	3	12
7	7	14	7	14	7	14	1	14	7	14	7
8	16	8	16	4	16	8	16	1	16	8	16
9	9	18	3	18	9	6	9	18	1	18	9
10	20	5	20	10	4	5	20	10	20	1	20
11	11	22	11	22	11	22	11	22	11	22	1

- Number of Petals .
- Symmetries of a Spiral.
- Marciniak / Schmid Machine Motions.

FIGURES.

Figure 1.1 Showing the General Rotary Forging Machine Setup.

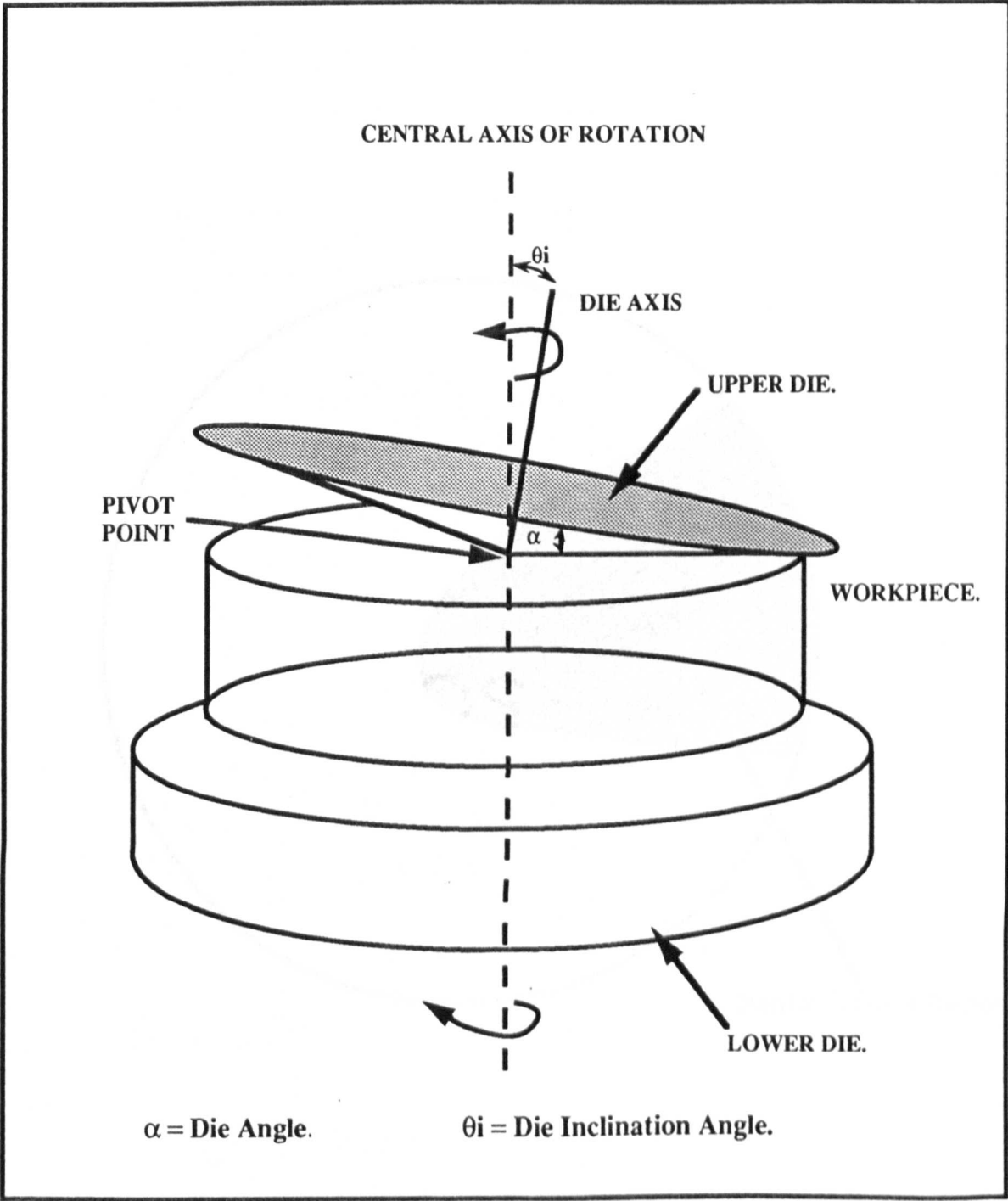


Figure 1.2 A Typical Partial Contact Region Formed on a Workpiece During Rotary Forging With an Inclined Conic Die.

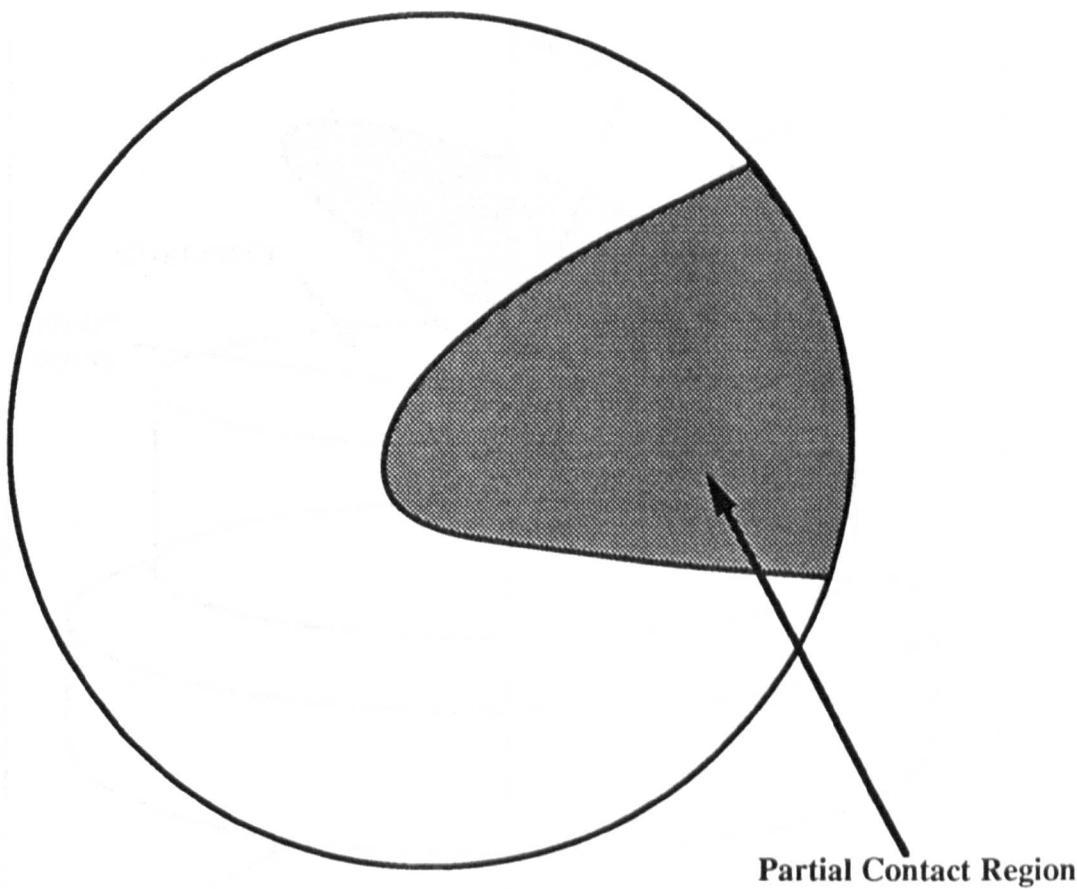


Figure 3.1 Showing the Typical Rotary Forging Tool and Workpiece Arrangement.

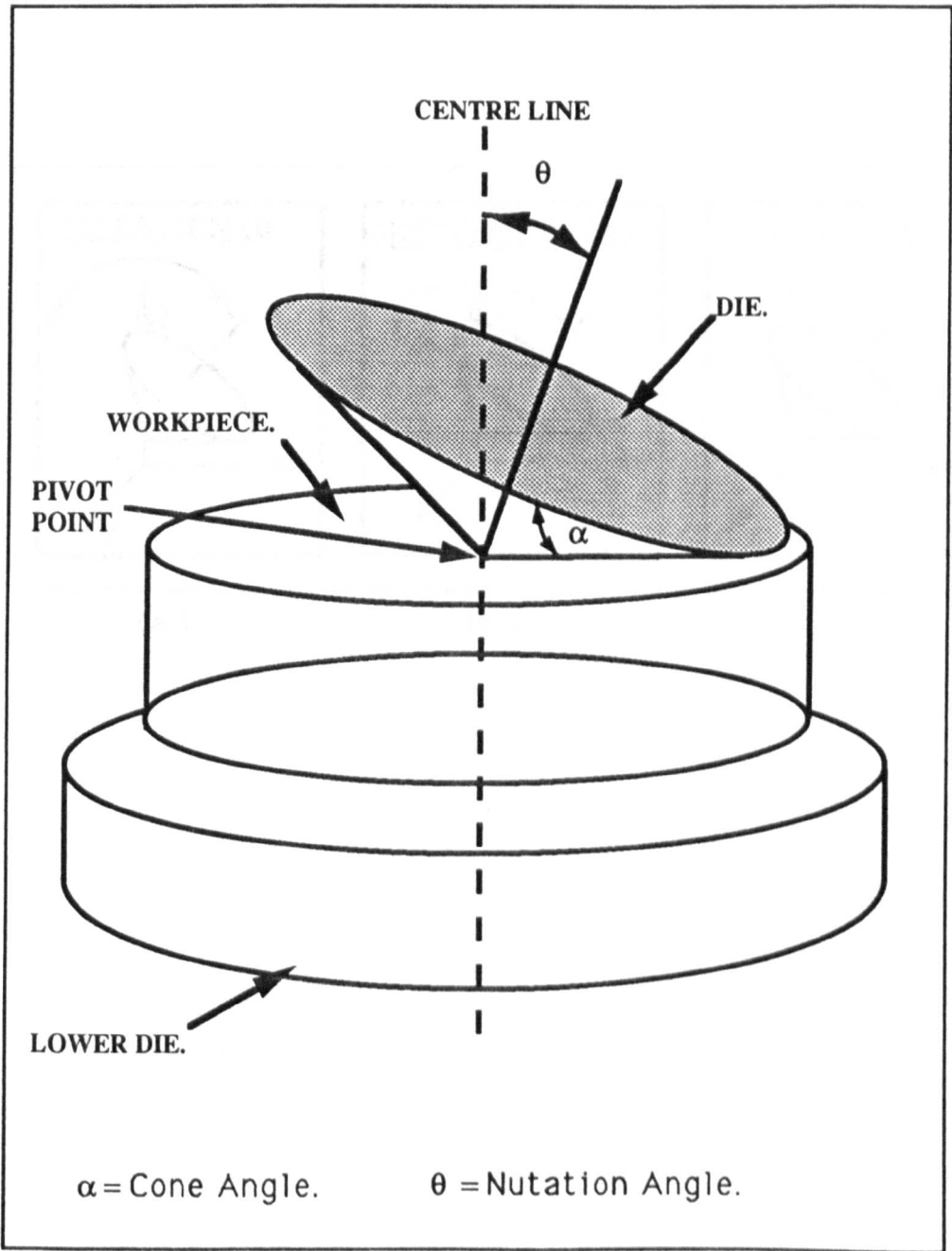


Figure 3.2 Showing the Three Eulerian Motions of Nutation, Precession, and Spin.

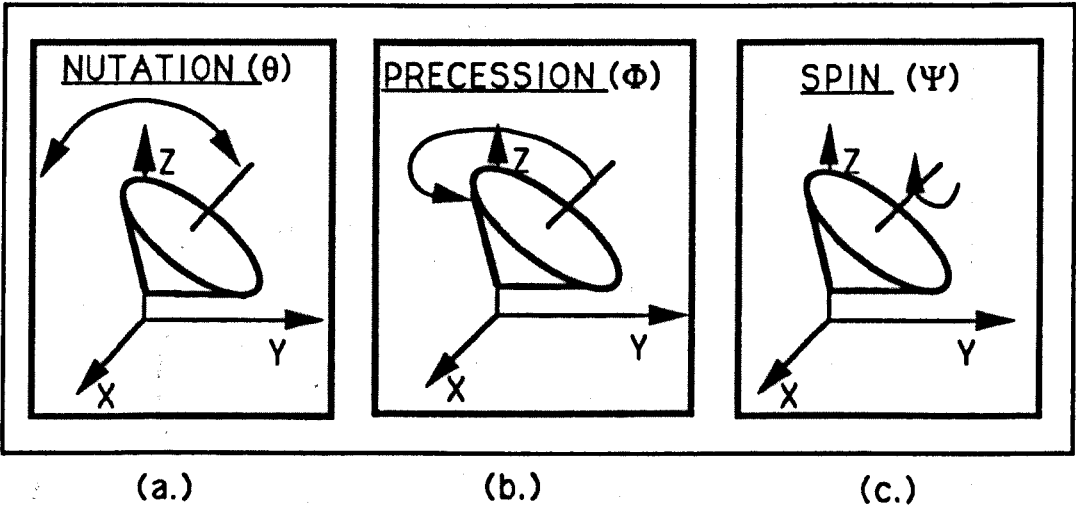


Figure 3.3 Eulerian Tool Motion Relationship Presented in Terms of:
Nutation Precession, and Spin.

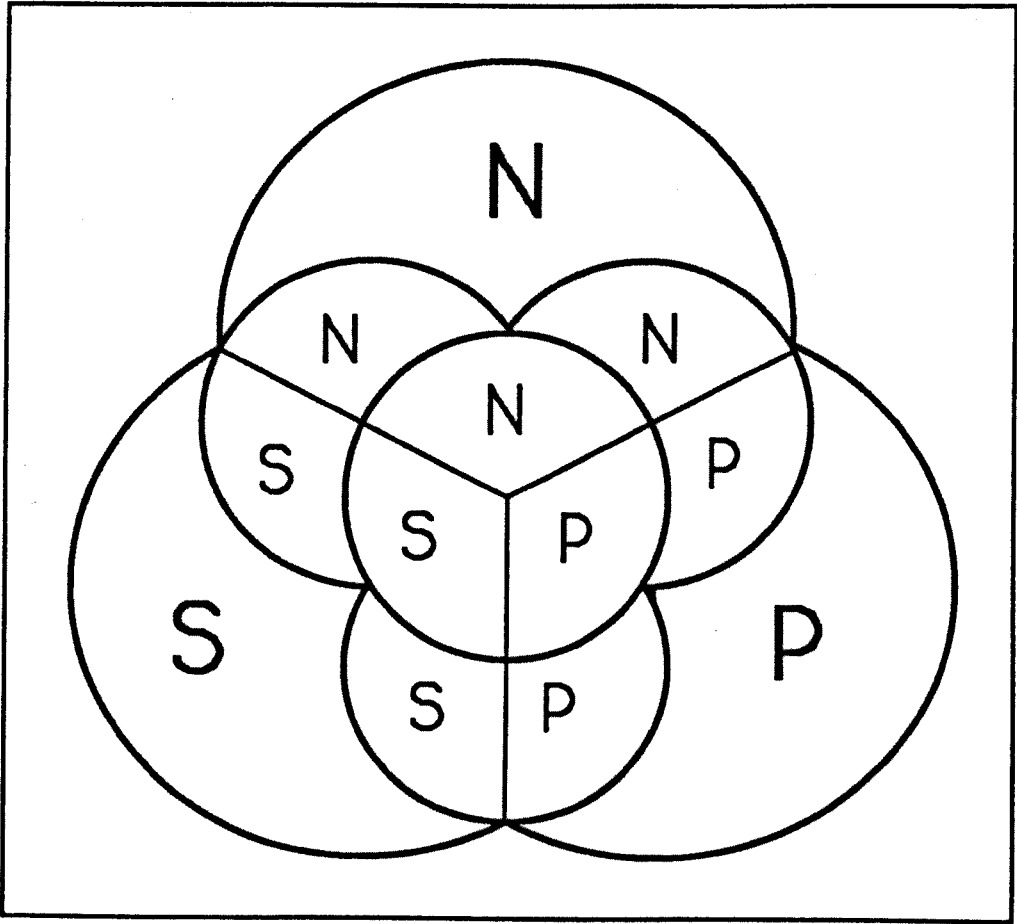


Figure 4.1 The Four Motions used by the Marciniak / Schmid Type of Rotary Forging Machines.

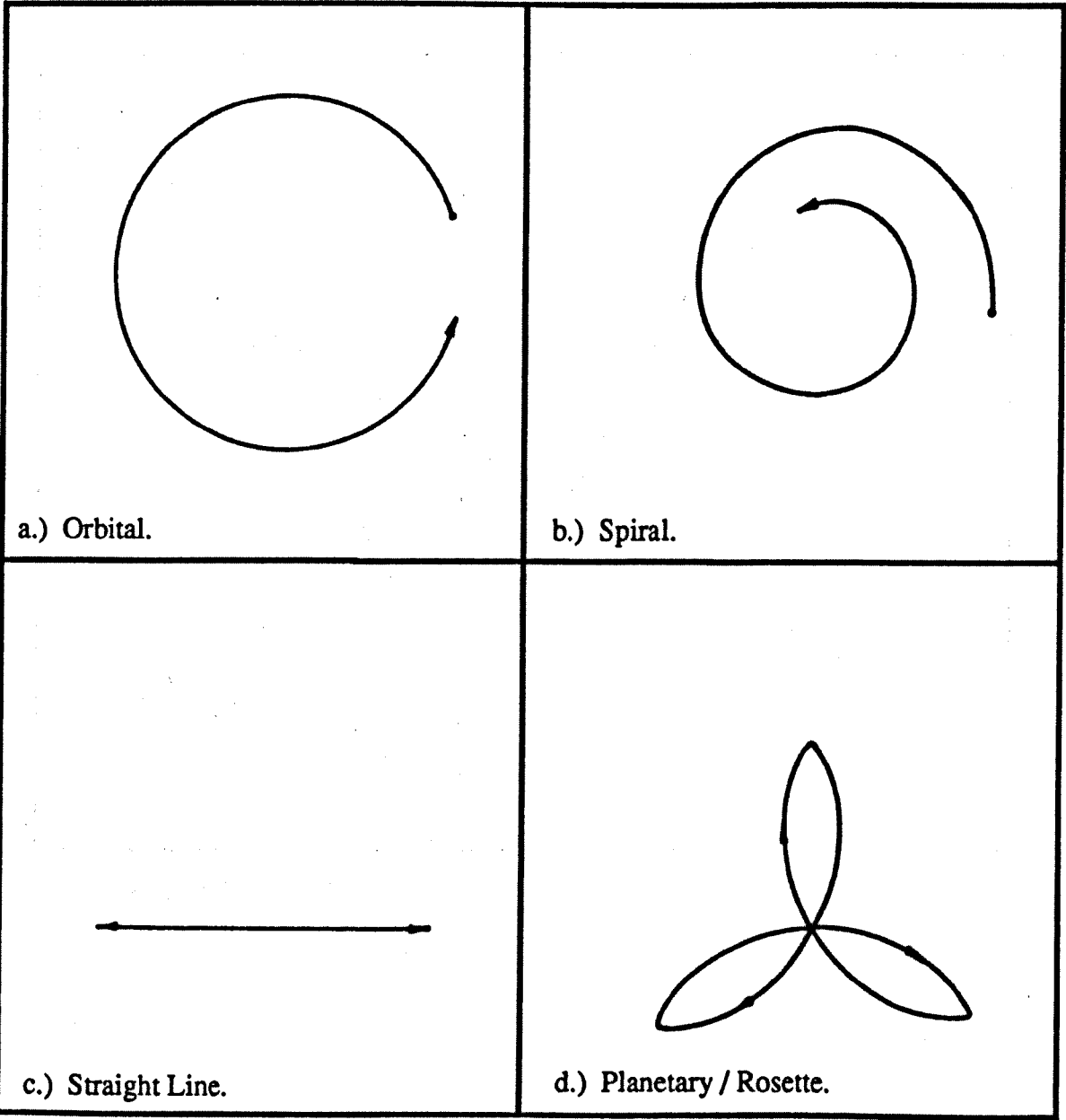
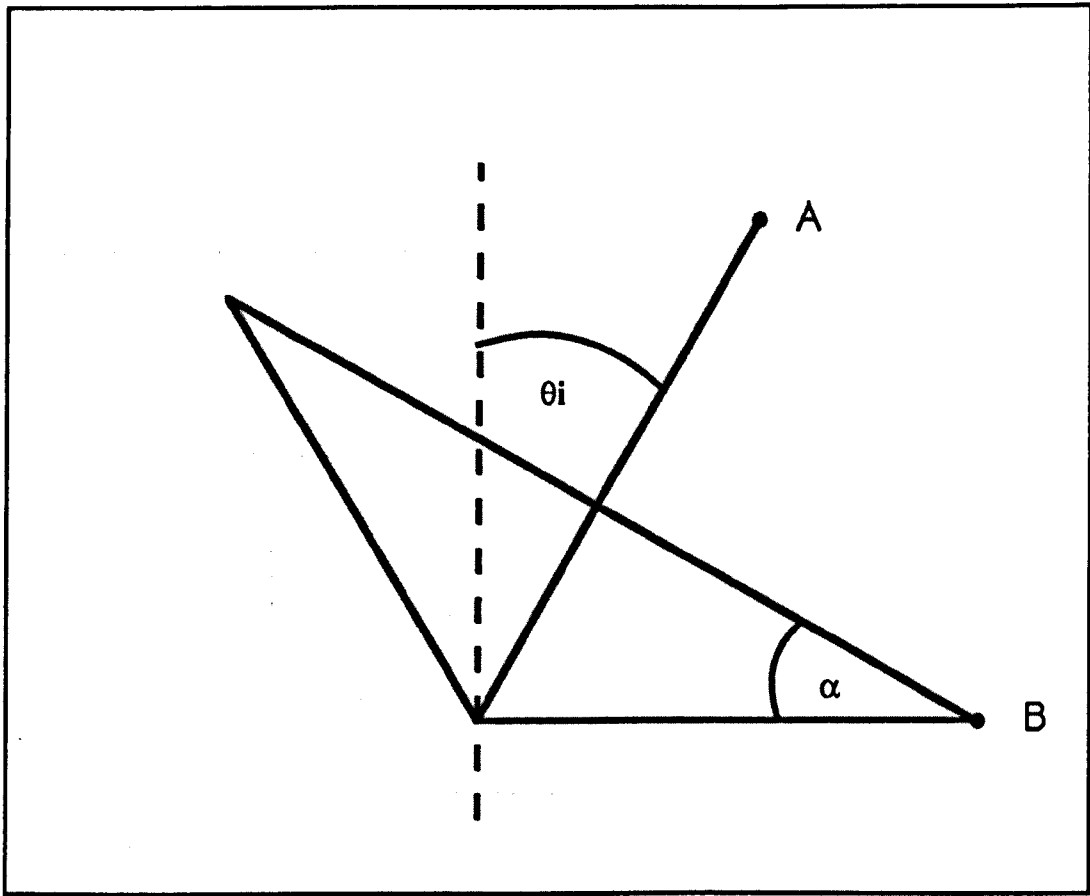


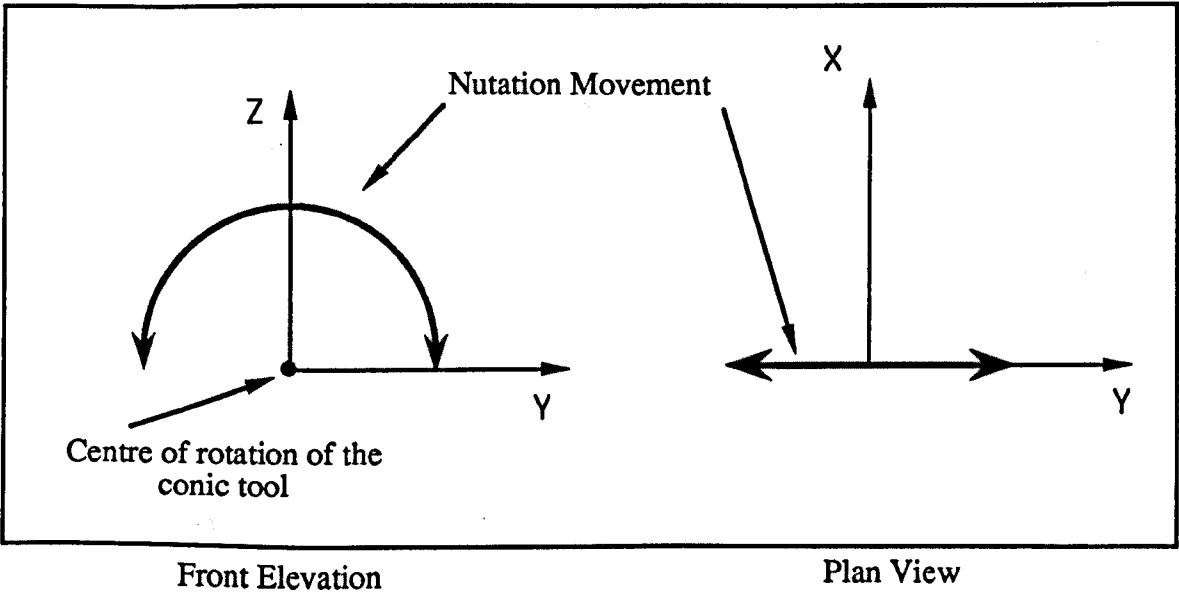
Figure 4.2 Showing a Typical Die Arrangement in Rotary Forging Machines.



Cone Angle (α) = 30°

The Initial Nutation = θ_i .

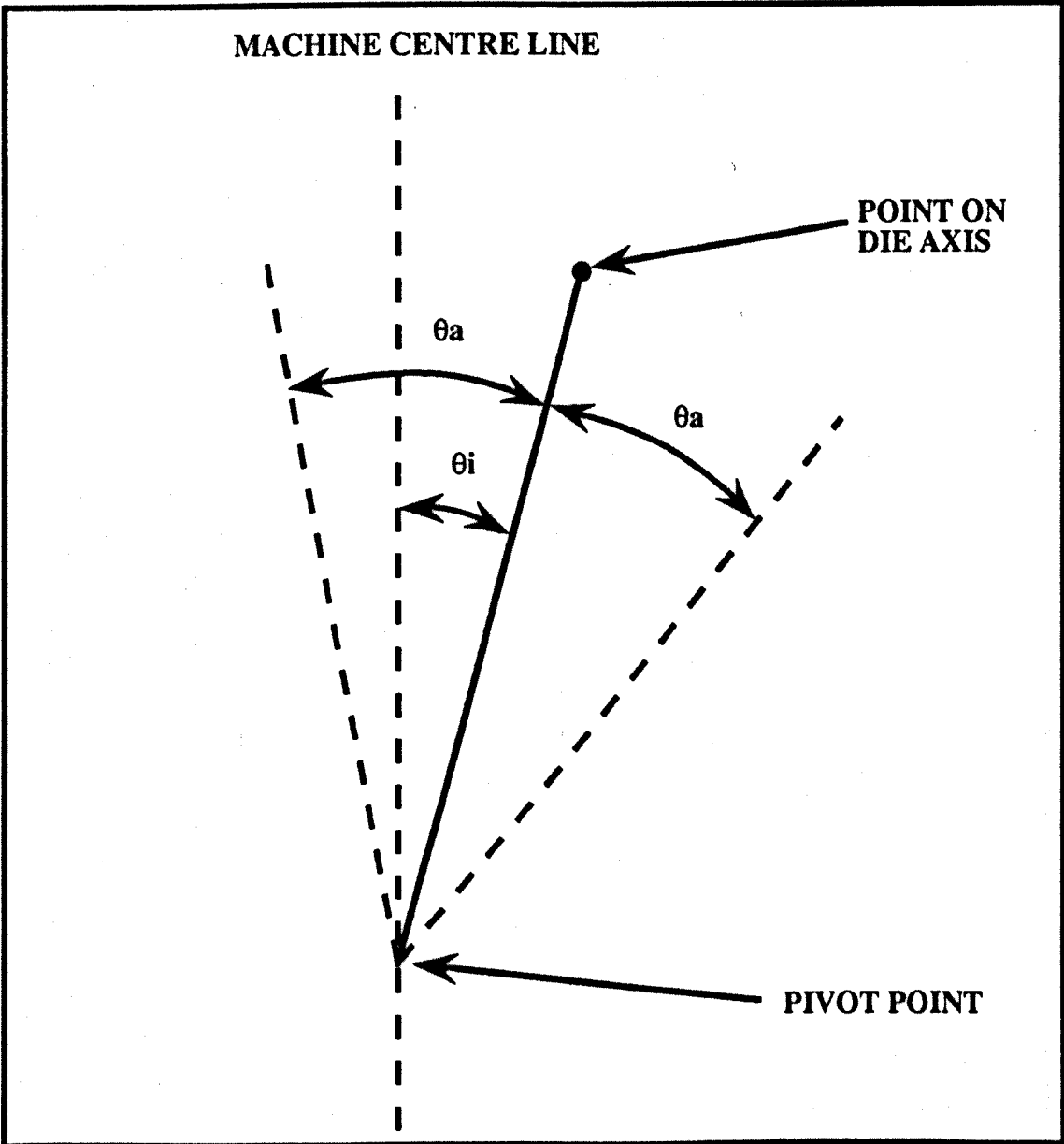
Figure 4.3 Showing the Non - Monotonic Nutation Movement.



Movement of a point on the axis of a conic rotary forging tool undergoing nutation movement.

The axes X,Y,Z are the Eulerian axes of rotation.

Figure 4.4 Showing the Movement of a Point on a Die Axis Whilst Undergoing Non - Monotonic Nutation.



θ_a = Amplitude of Nutation.

θ_i = Initial Nutation.

Figure 4.5 Showing a Nutation Motion Plotted by the Package 'PATH'.

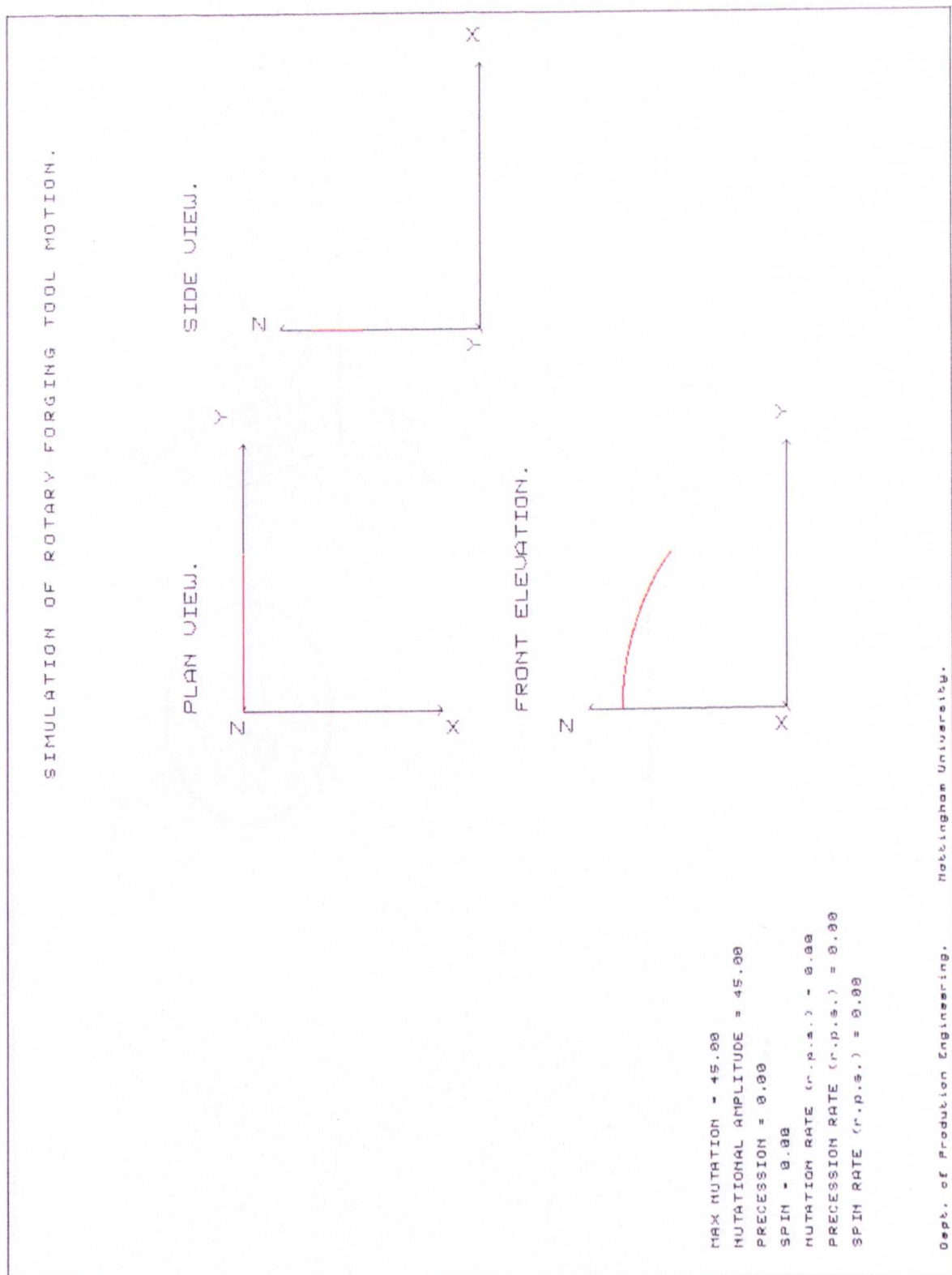


Figure 4.6 Showing a Precession Motion Plotted by the Package 'PATH'.

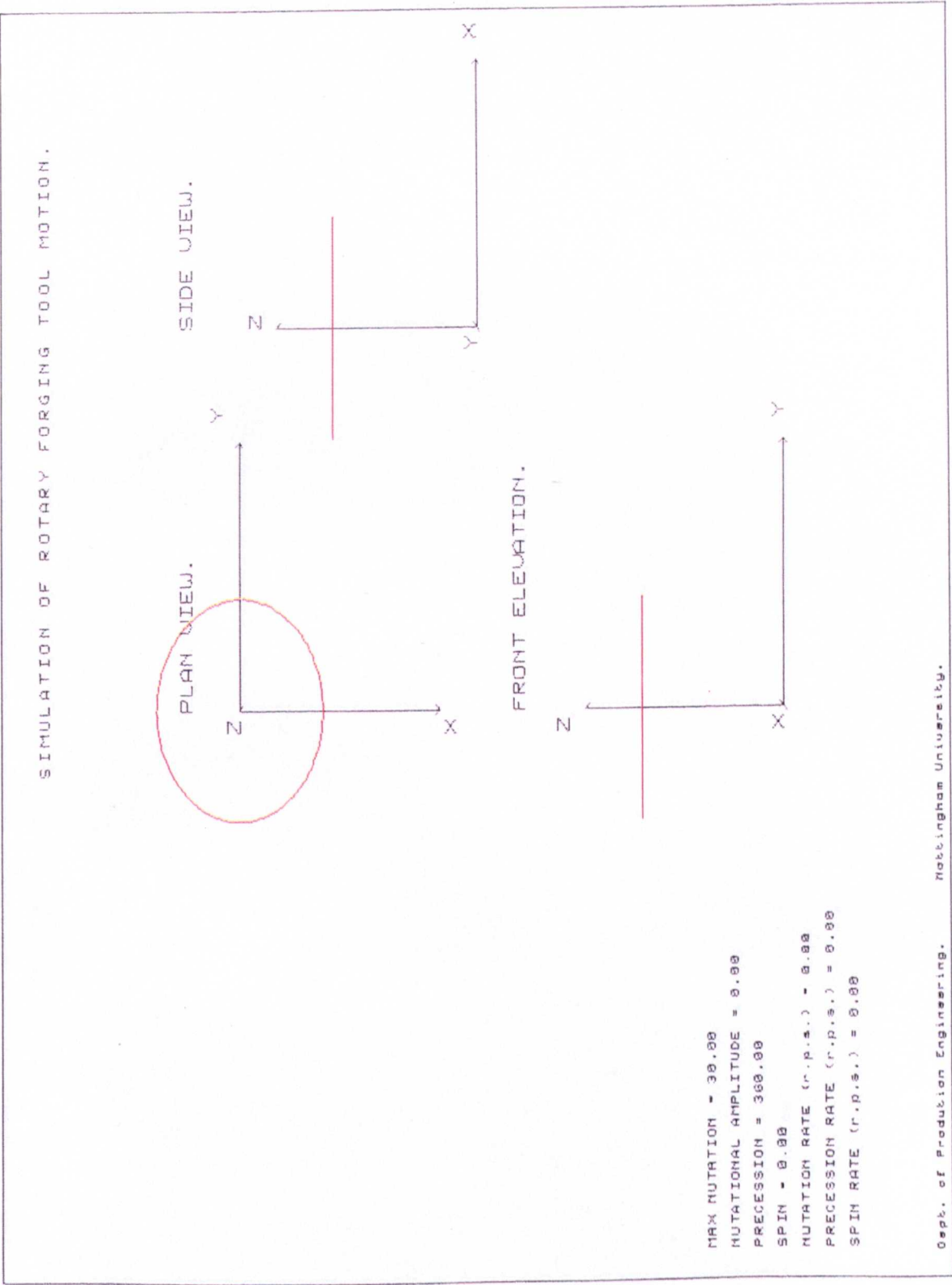


Figure 4.7 Showing a Spin Motion Plotted by the Package 'PATH'.

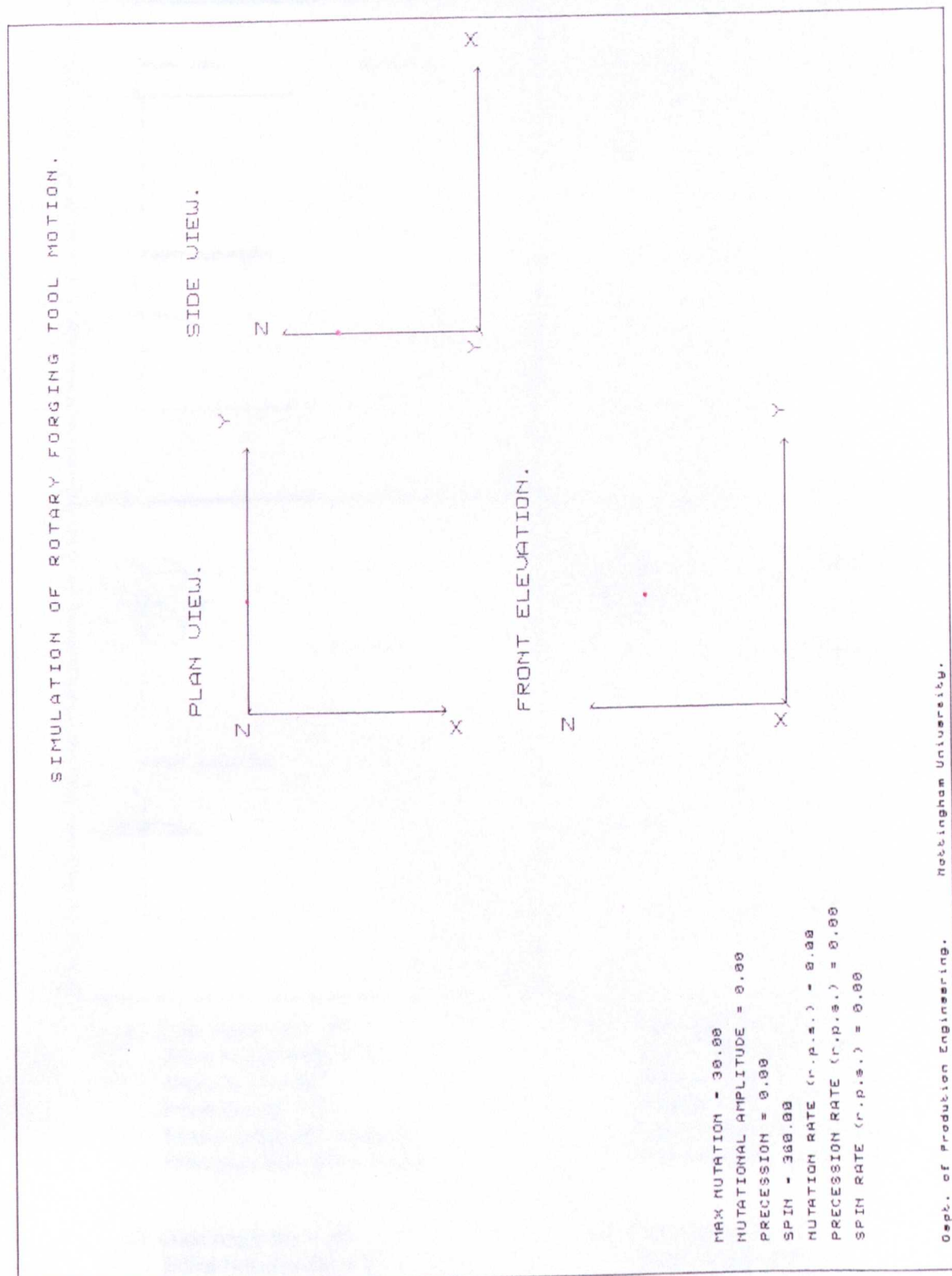
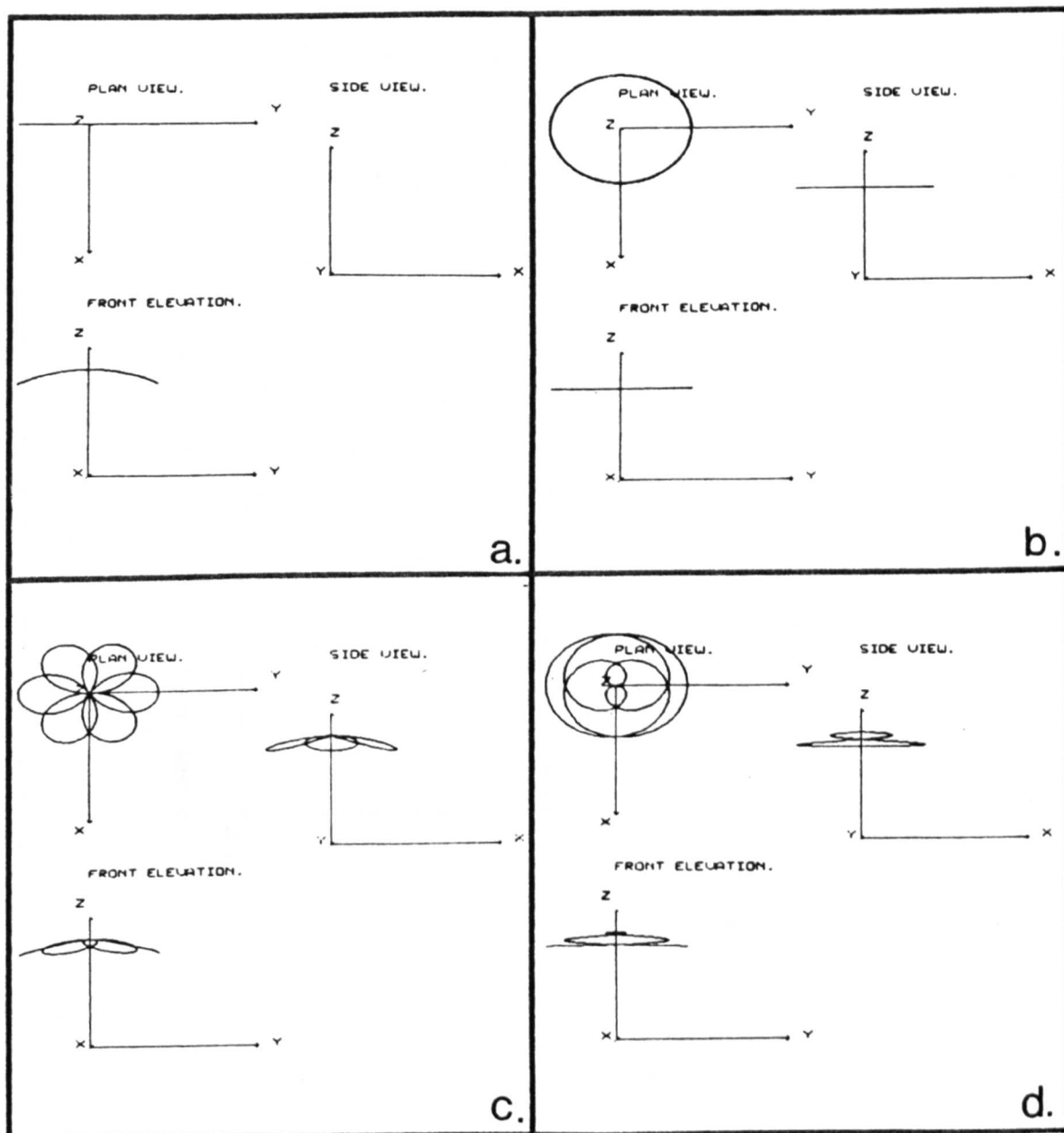


Figure 4.8 Showing the Four Motions of a Marciniak Type Rotary Forging Machine as Generated by 'PATH', by a Point on the Tool Axis



a.) Cone Angle (α) = 30° .
Initial Nutation (θ_i) = 0° .
Nutation (θ) = 30° .
Precession (ϕ) = 0° .
Nutation Rate (θ°) = 1 r.p.s.
Precession Rate (ϕ°) = 0 r.p.s.

b.) Cone Angle (α) = 30° .
Initial Nutation (θ_i) = 30° .
Nutation (θ) = 0° .
Precession (ϕ) = 360° .
Nutation Rate (θ°) = 0 r.p.s.
Precession Rate (ϕ°) = 1 r.p.s.

c.) Cone Angle (α) = 30° .
Initial Nutation (θ_i) = 0° .
Nutation (θ) = $0 - 30^\circ$.
Precession (ϕ) = 720° .
Nutation Rate (θ°) = 3 r.p.s.
Precession Rate (ϕ°) = 2 r.p.s.

d.) Cone Angle (α) = 30° .
Initial Nutation (θ_i) = 0° .
Nutation (θ) = $0 - 30^\circ$.
Precession (ϕ) = 1440° .
Nutation Rate (θ°) = 1 r.p.s.
Precession Rate (ϕ°) = 4 r.p.s.

Figure 4.9 Showing the Nutation Motion for a Point on the Periphery of a 30° Conic Rotary Forging Die Produced by 'PATH'.

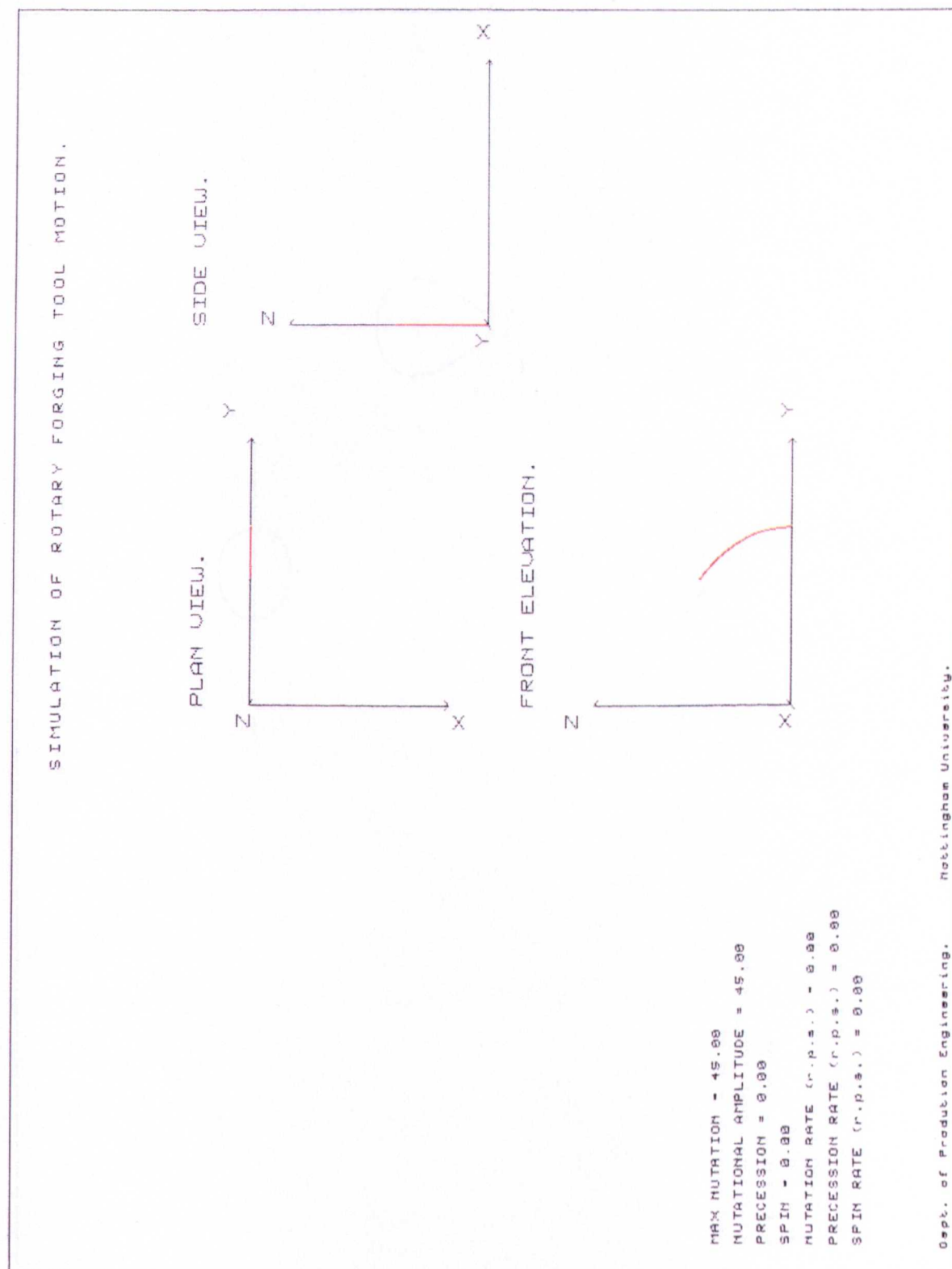
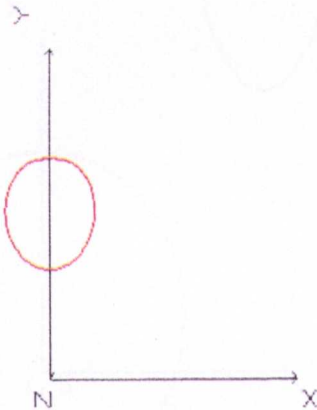


Figure 4.10 Showing the Precession Motion for a Point on the Periphery of a 30° Conic Rotary Forging Die Produced by 'PATH'.

SIMULATION OF ROTARY FORGING TOOL MOTION.

PLAN VIEW.



FRONT ELEVATION.



MAX NUTATION = 30.00
 NUTATIONAL AMPLITUDE = 0.00
 PRECESSION = 360.00
 SPIN = 0.00
 NUTATION RATE (r.p.s.) = 0.00
 PRECESSION RATE (r.p.s.) = 0.00
 SPIN RATE (r.p.s.) = 0.00

Figure 4.11 Showing the Spin Motion for a Point on the Periphery of a 30° Conic Rotary Forging Die Produced by 'PATH'.

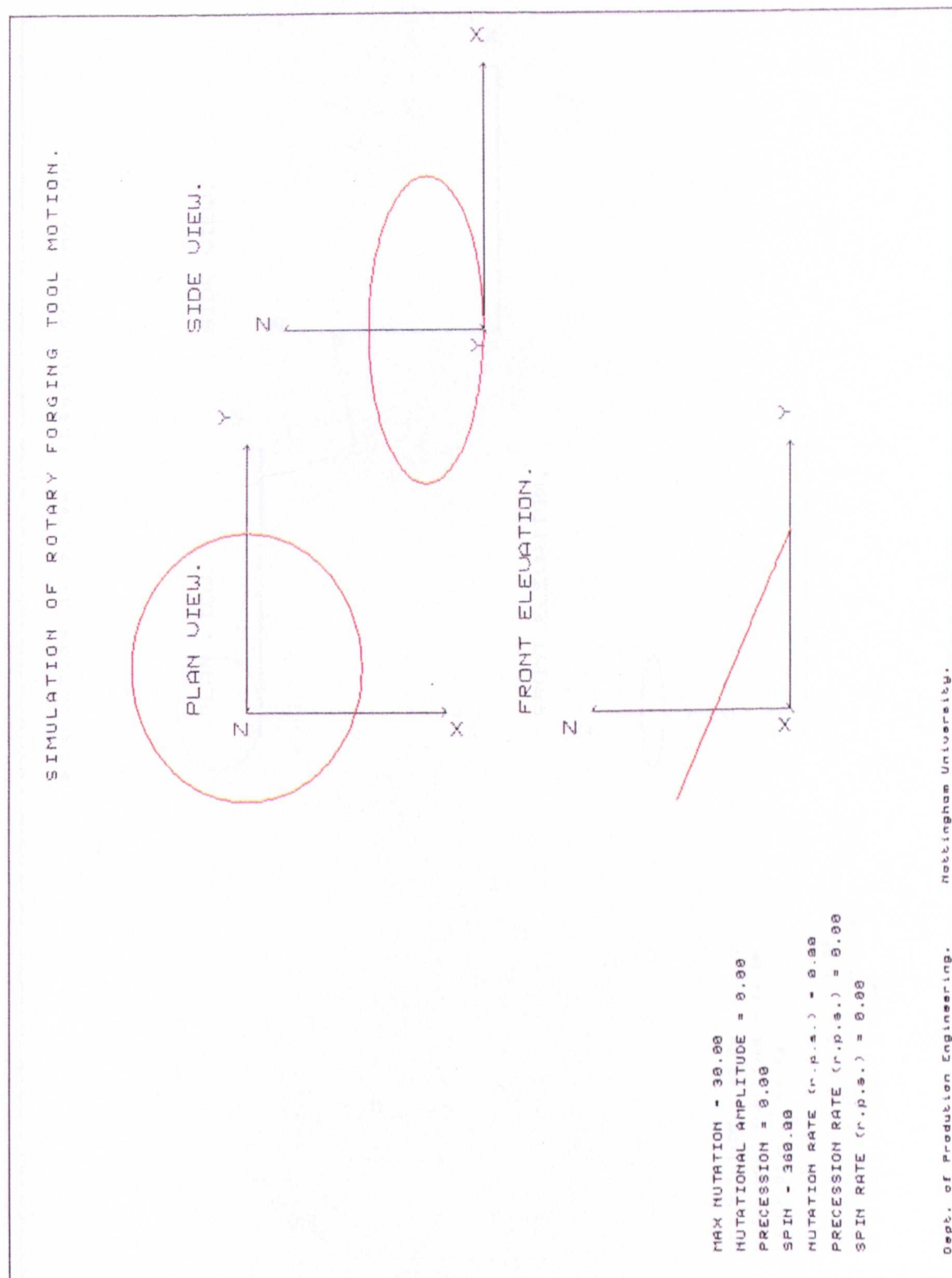


Figure 5.1 The Asymmetric Type of Machine Motion Produced During the Non - Monotonic Nutation, Precession Motion When the Nutation Rate Equals the Precession Rate, as Produced by the Package 'PATH'.

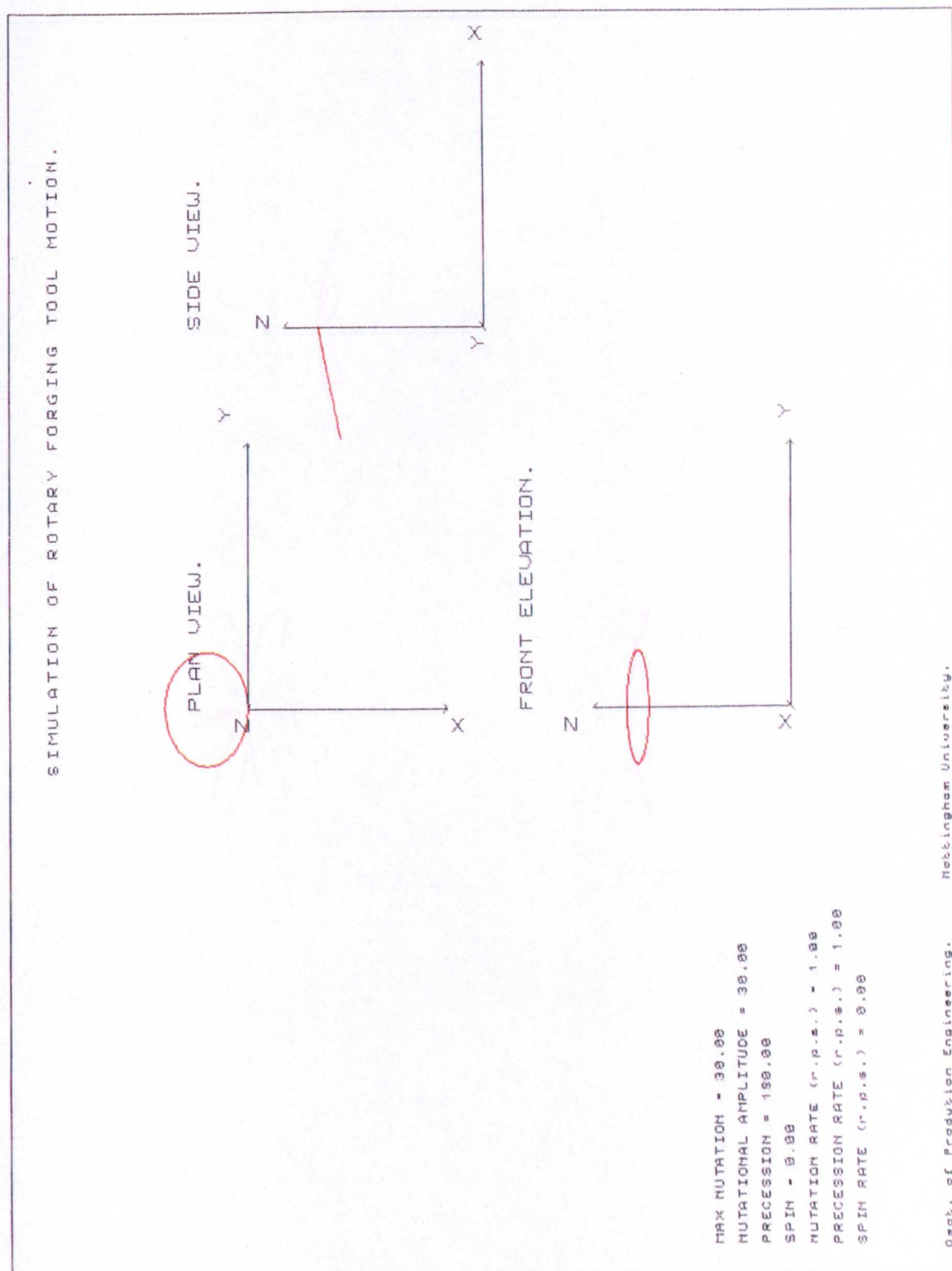


Figure 5.2 The Rosette Type of Machine Motion Produced During the Non - Monotonic Nutation, Precession Motion, by the Package 'PATH'.

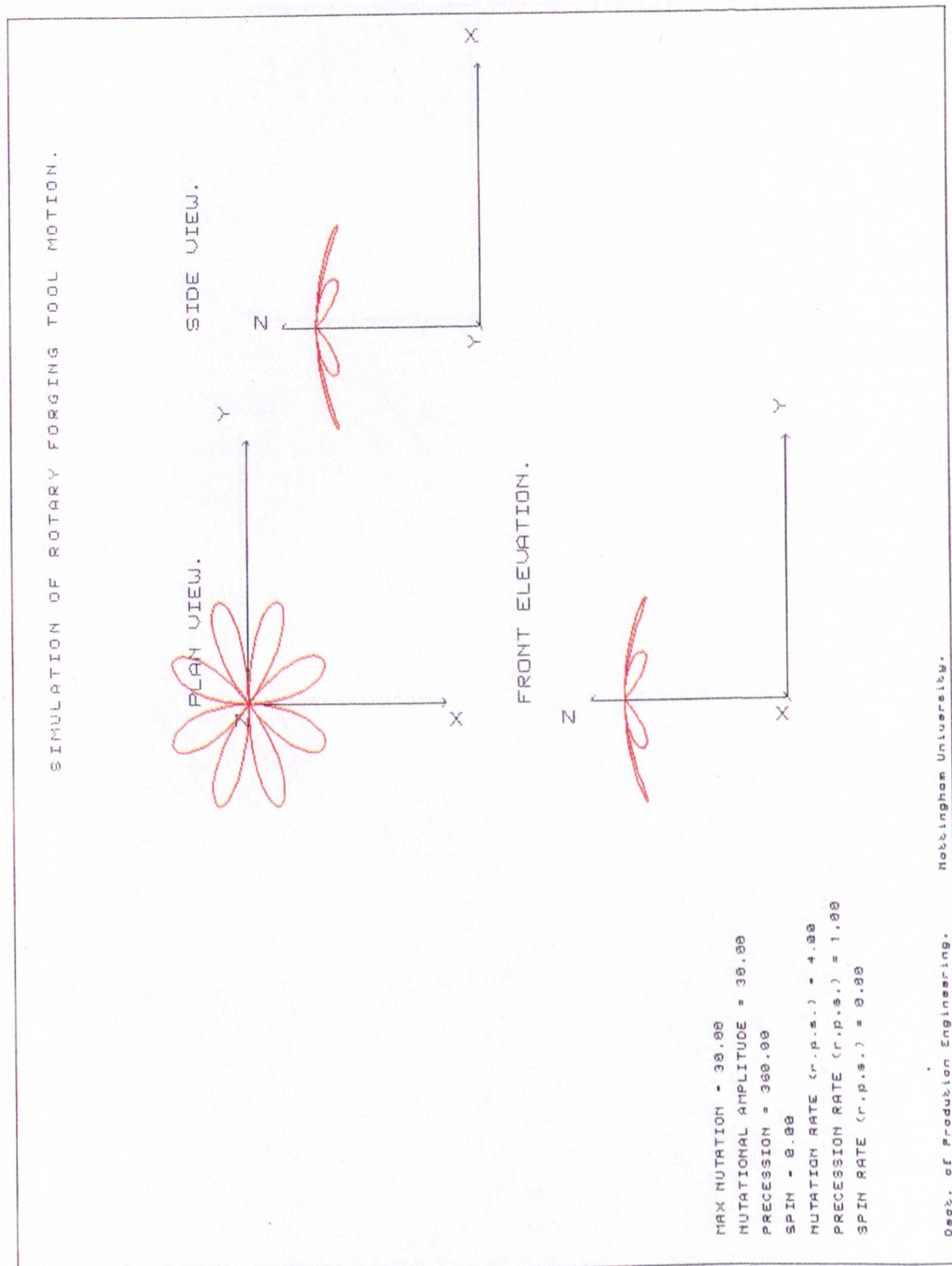


Figure 5.3 The Rosette Motion Produced During the Non - Monotonic Nutation, Precession Motion, by the Package 'PATH'. The Six Petals are Overlapping Due to the Precession Rate Being Greater Than Half the Nutation Rate.

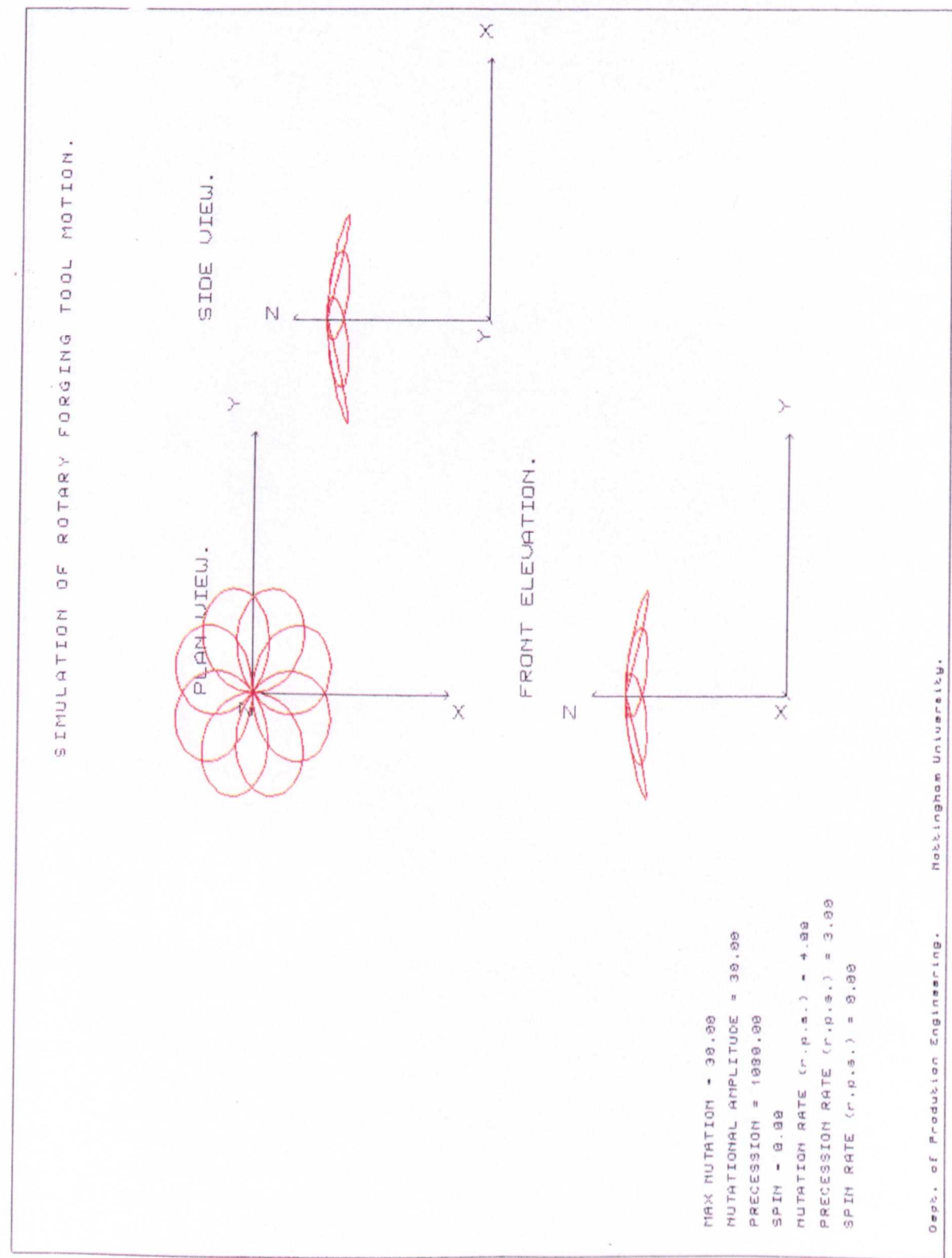


Figure 5.4 The Spiral Type of Machine Motion Produced During the Non - Monotonic Nutation, Precession Motion, by the Package 'PATH'.

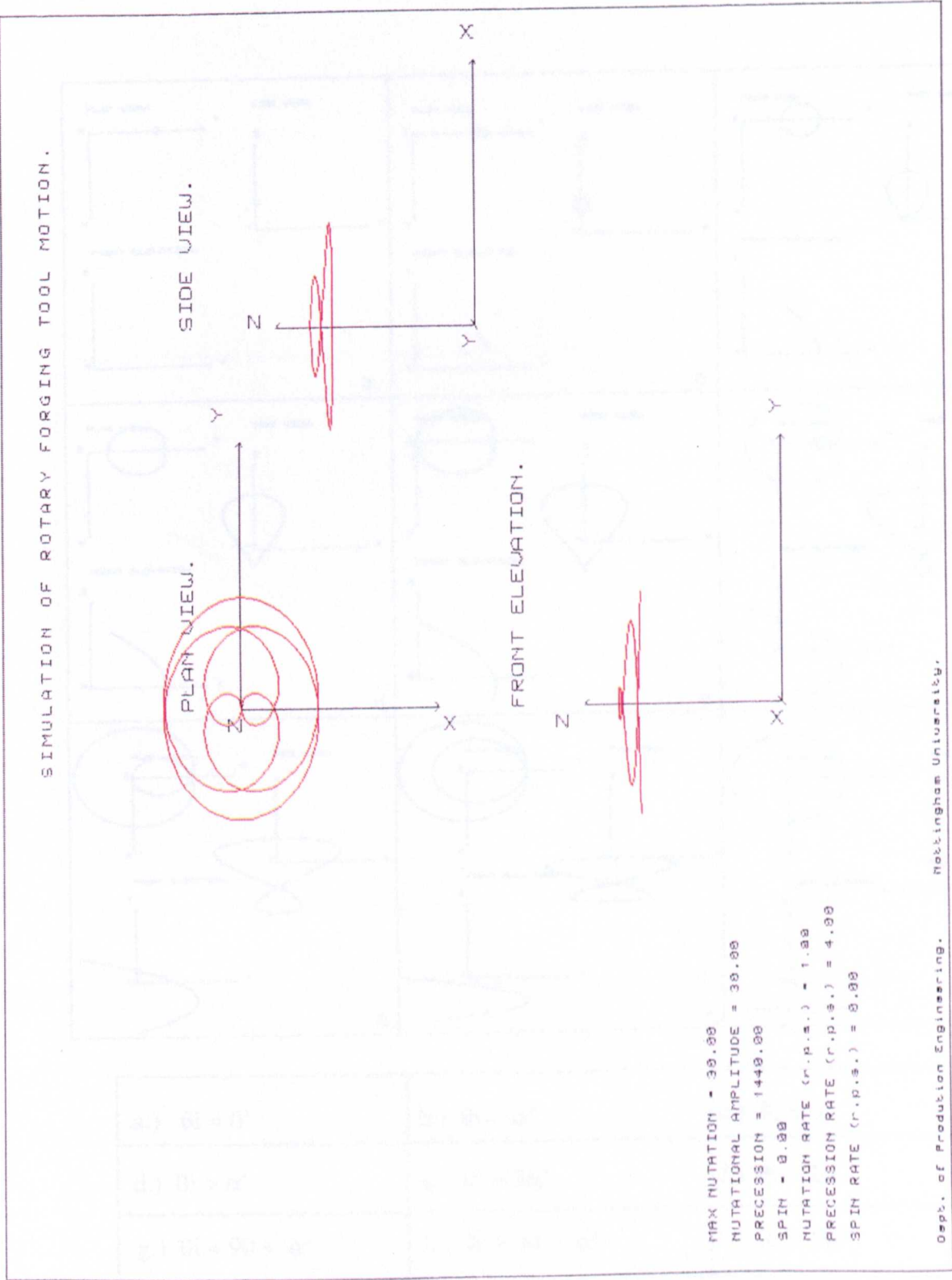
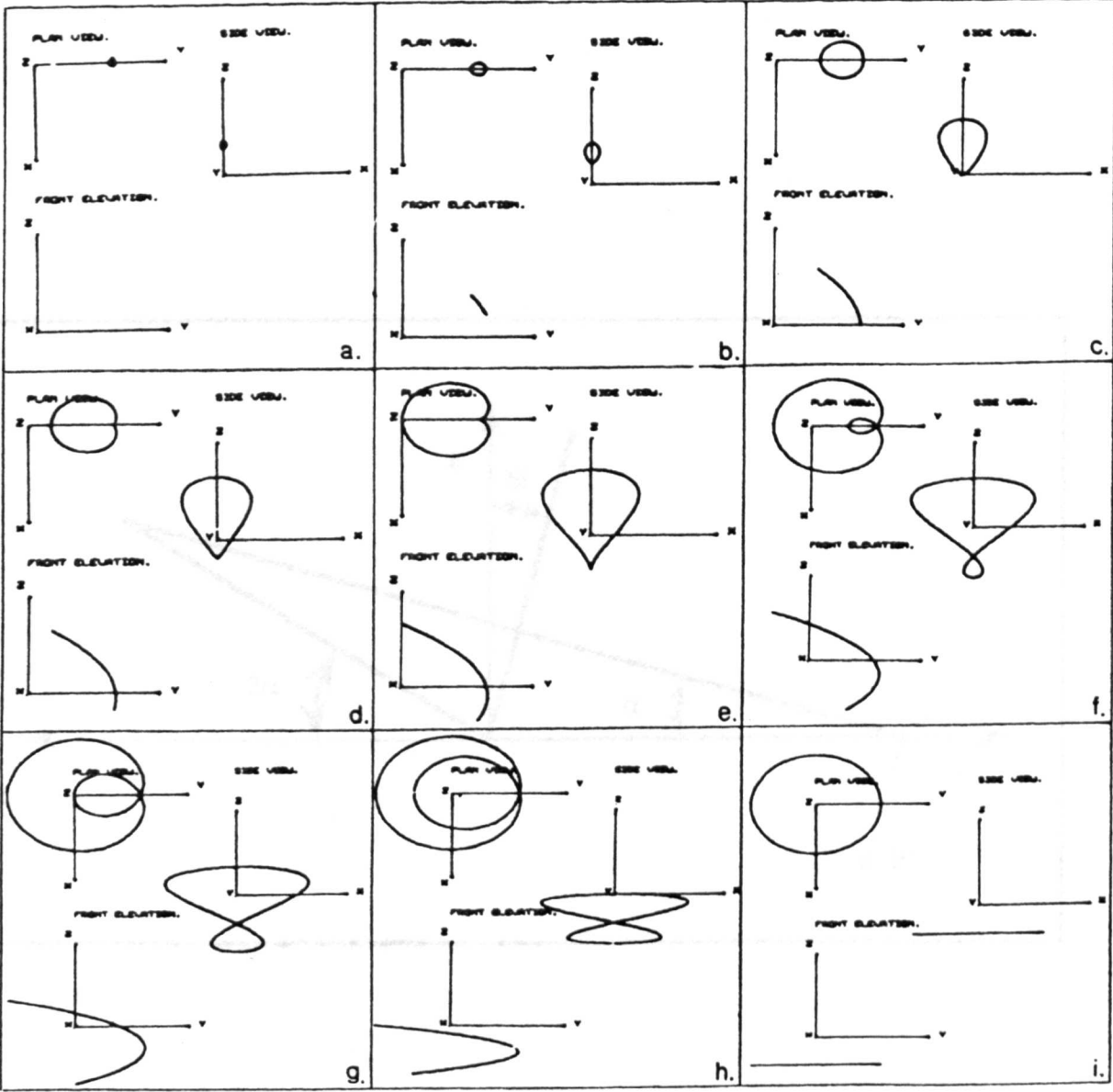


Figure 5.5 Showing the Nine Different Types of Machine Motion Produced by a Point on the Surface of a Conic 30° Rotary Forging Tool During Precession Motion Using Different Initial Nutations (θ_i).



a.) $\theta_i = 0^\circ$	b.) $\theta_i < \alpha^\circ$	c.) $\theta_i = \alpha^\circ$
d.) $\theta_i > \alpha^\circ$	e.) $\theta_i = 2\alpha^\circ$	f.) $\theta_i > 2\alpha^\circ$
g.) $\theta_i = 90 + \alpha^\circ$	h.) $\theta_i > 90 + \alpha^\circ$	i.) $\theta_i = 180^\circ$

α = Cone Angle. (30°).

θ_i = Initial Nutation

Figure 5.6 Showing the Point P' Lying Below the Surface of the Conic Die

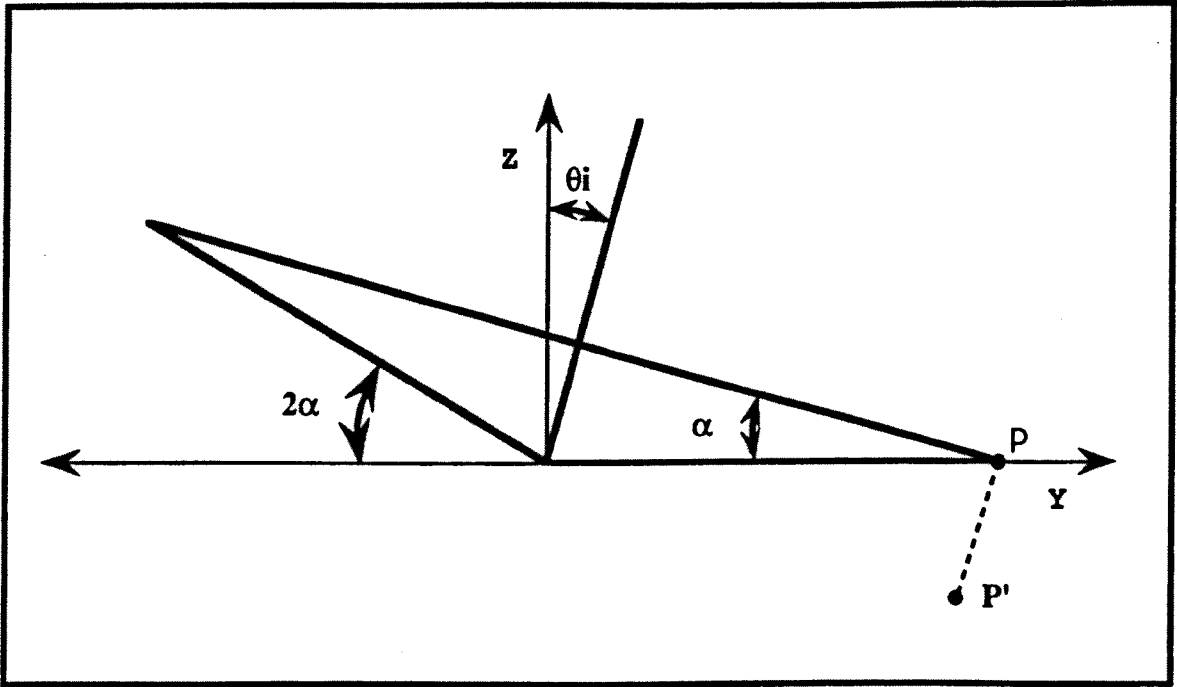


Figure 5.7 The Spiral Motion Produced for a Point on the Surface of a Conic Tool During the Non - Monotonic Nutation, Precession Motion, by the Package 'PATH'.

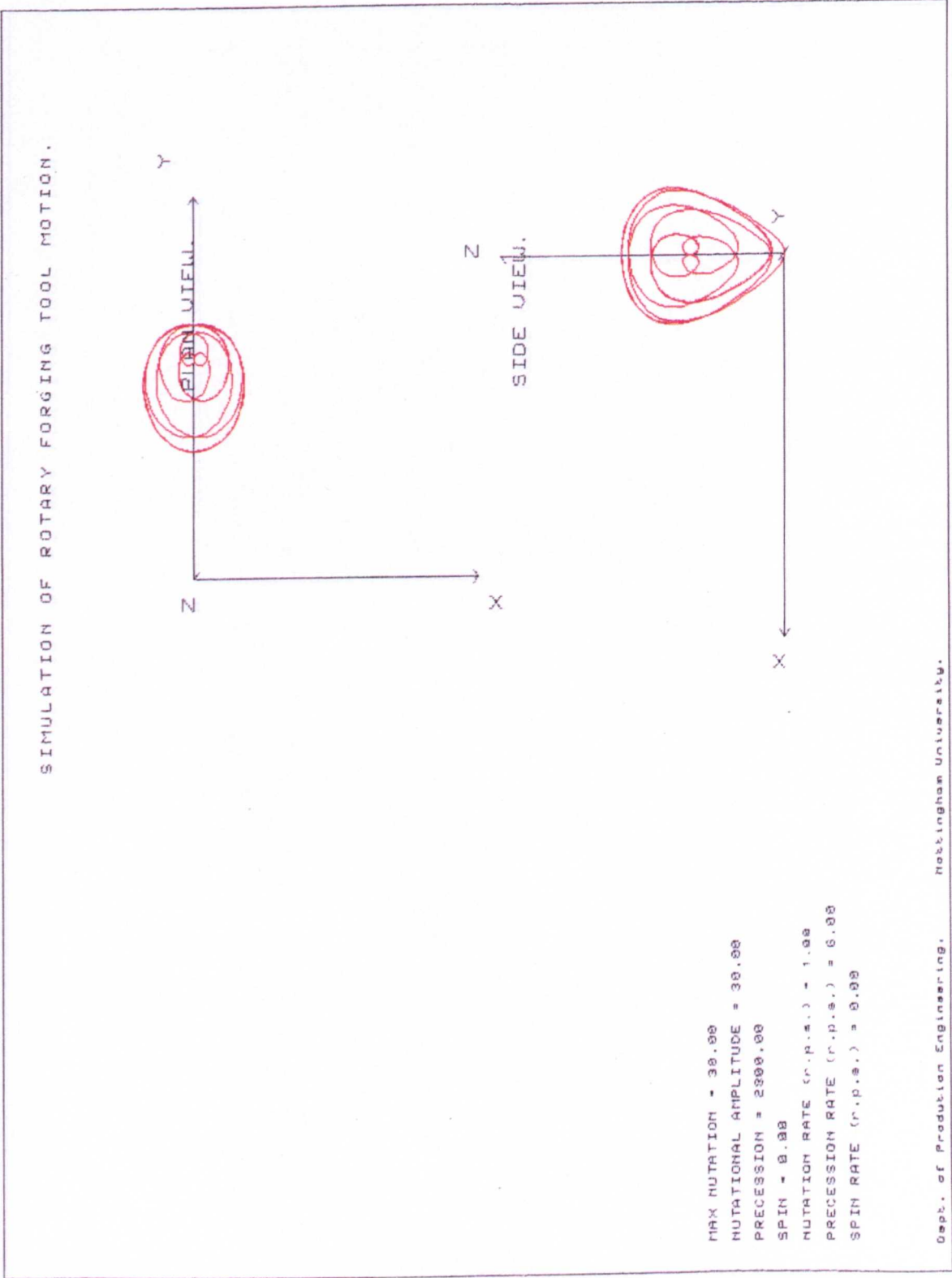


Figure 5.8 The Rosette Motion Produced for a Point on the Surface of a Conic Tool During the Non - Monotonic Nutation, Precession Motion, by the Package 'PATH'.

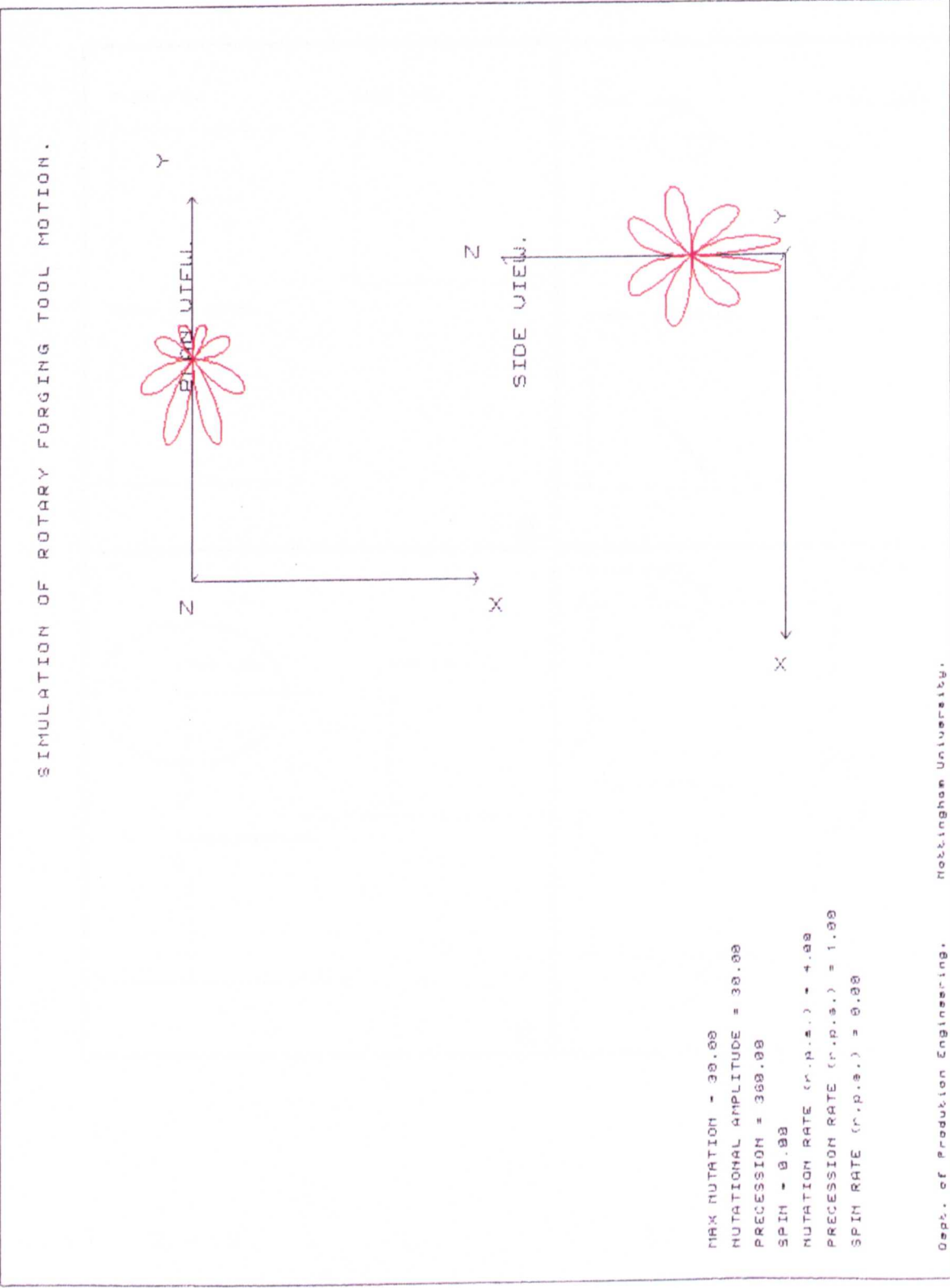
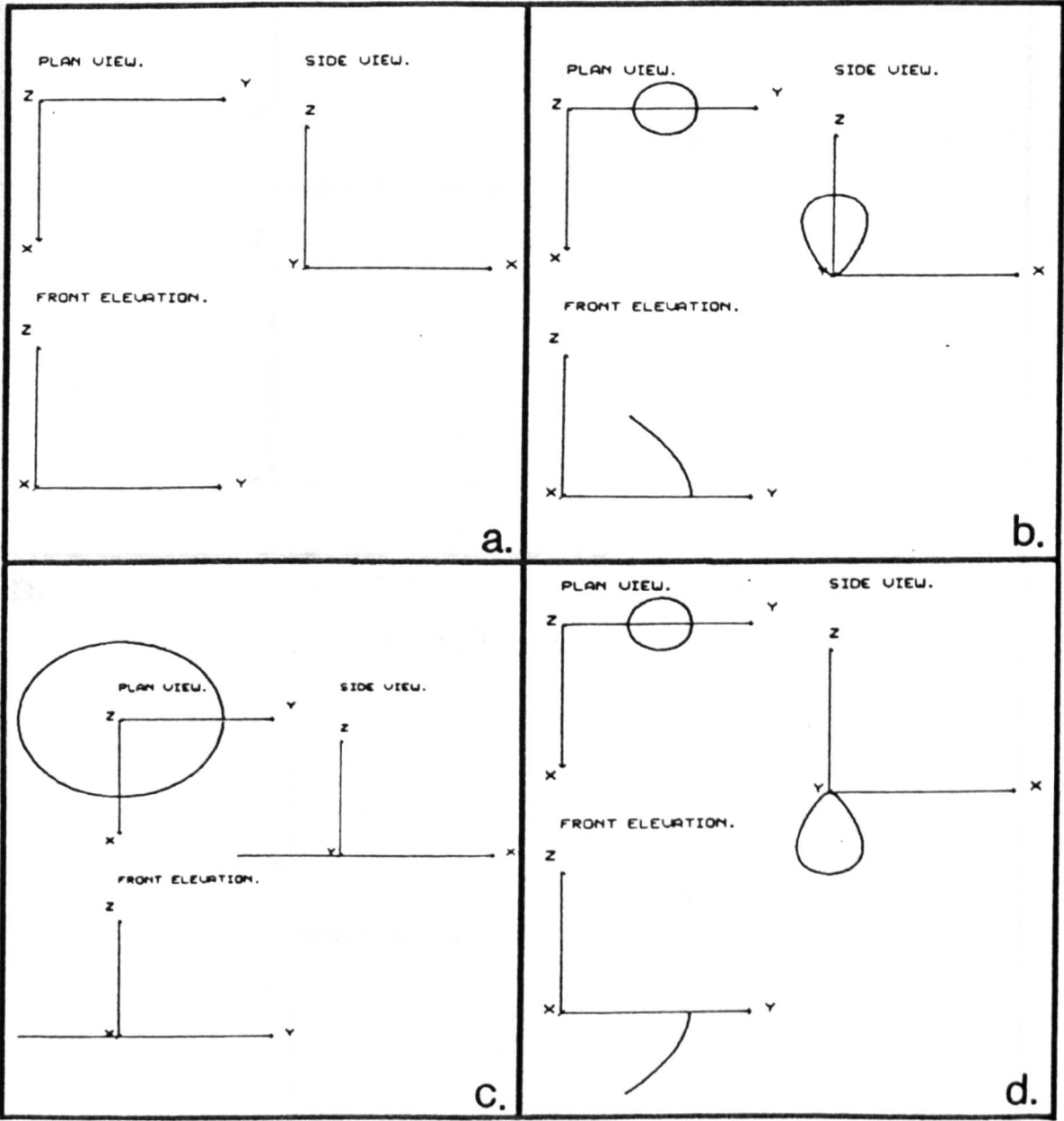


Figure 5.9 Showing how Different Angled Conic Tools Influence the Type of Path that a Point on that Tool will Undergo During Precession Motion.



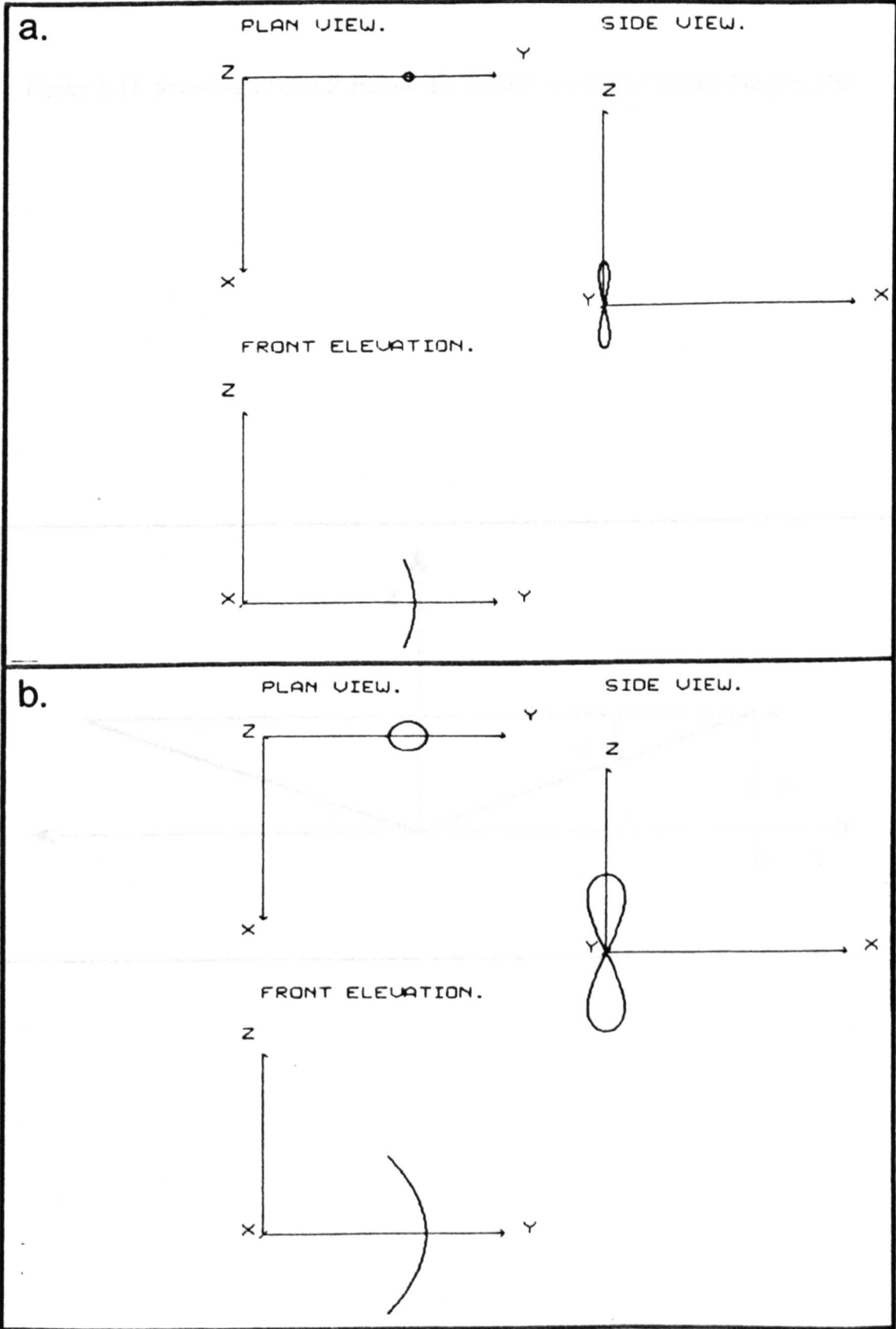
a.) $\alpha = 0^\circ$.

b.) $\alpha = 45^\circ$

c.) $\alpha = 90^\circ$.

d.) $\alpha = 135^\circ$.

Figure 5.10 Showing the Locus for a Point on a Flat Die During the Precession Motion.



a.) Initial Nutation (θ_i) = 10°

b.) Initial Nutation (θ_i) = 30°

Figure 5.11 Showing a Point P' Below the Surface of a Conic Rotary Forging Die.

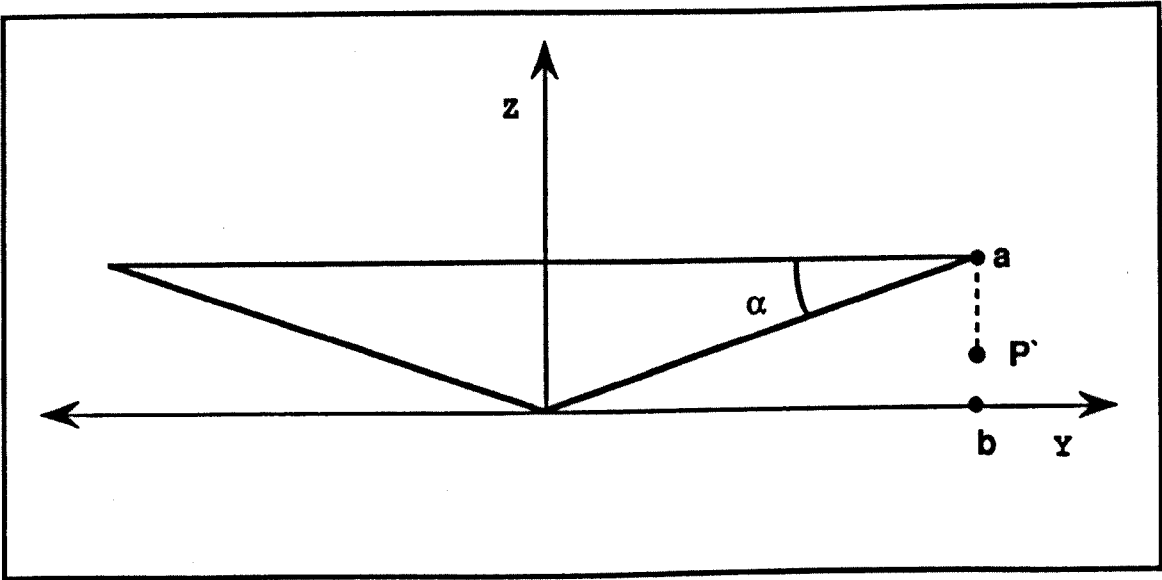


Figure 5.12 Showing the Locus of a Point P' Lying Below the Surface of a Conic Rotary Forging Die. Where Point P' Lies Between Points a and b on Figure 5.11.

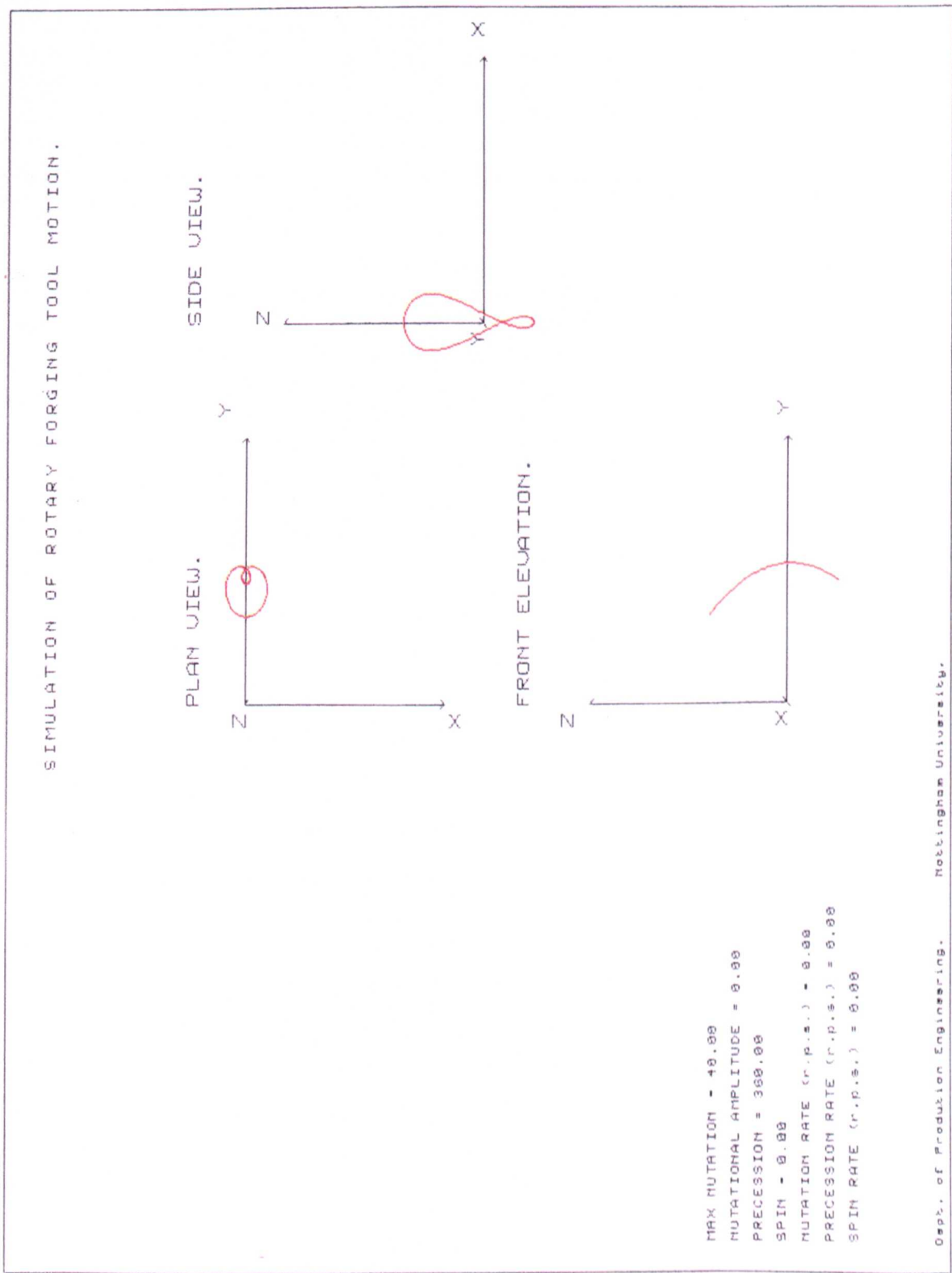


Figure 5.13 Showing the Locus of a Point P' Lying Below the Surface of a Conic Rotary Forging Die. Where Point P' Lies Below Point b or the Y Axis on Figure 5.11.

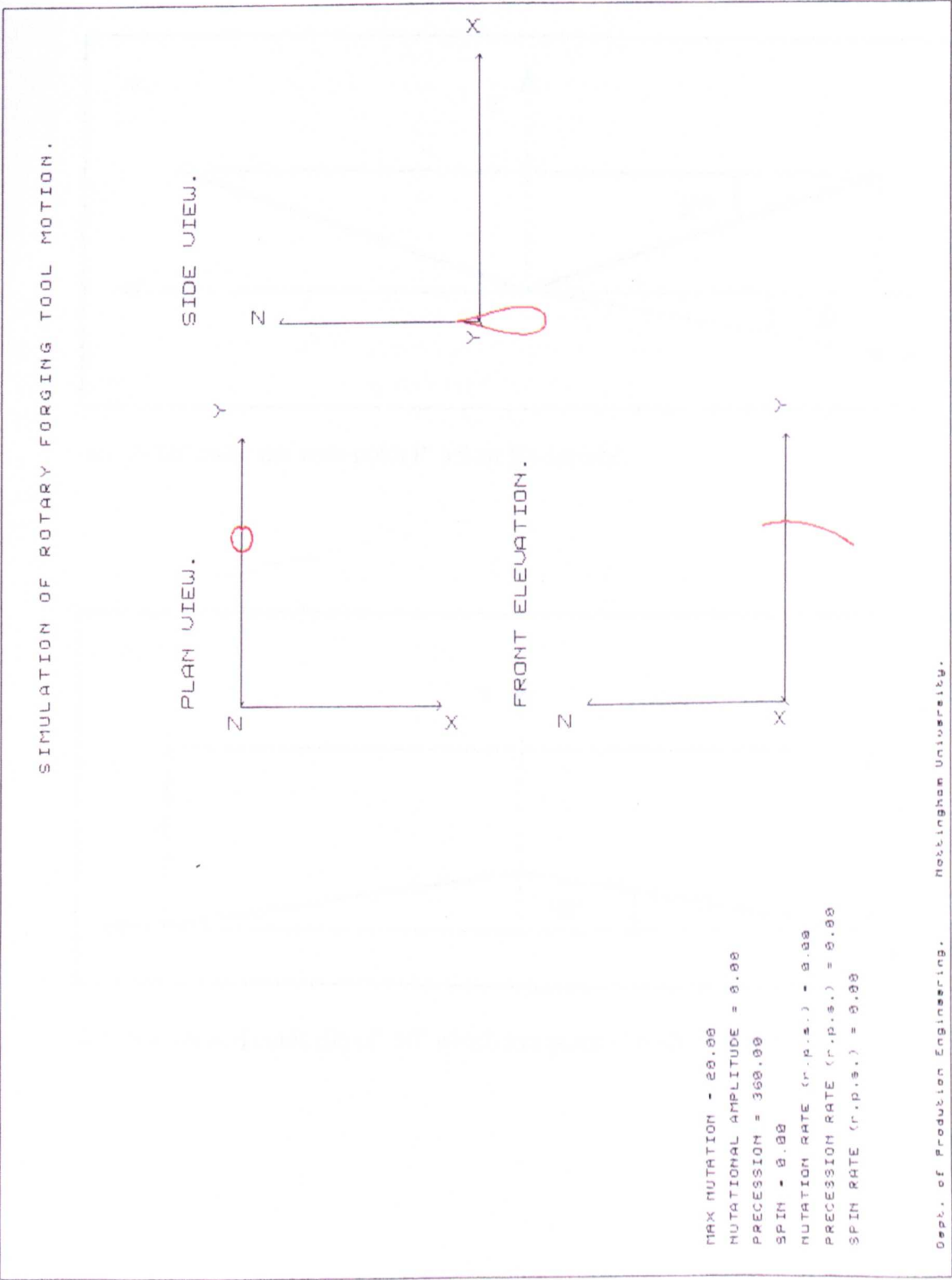
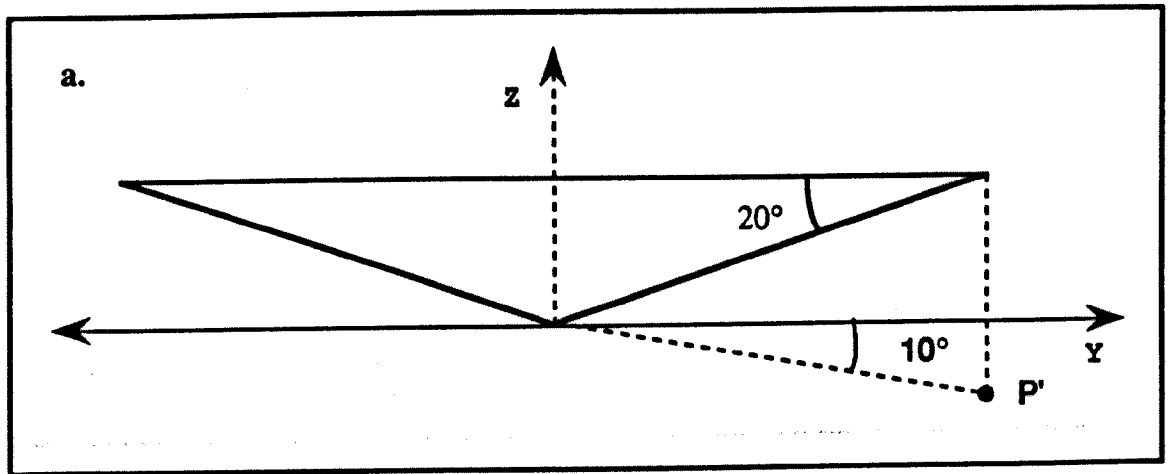
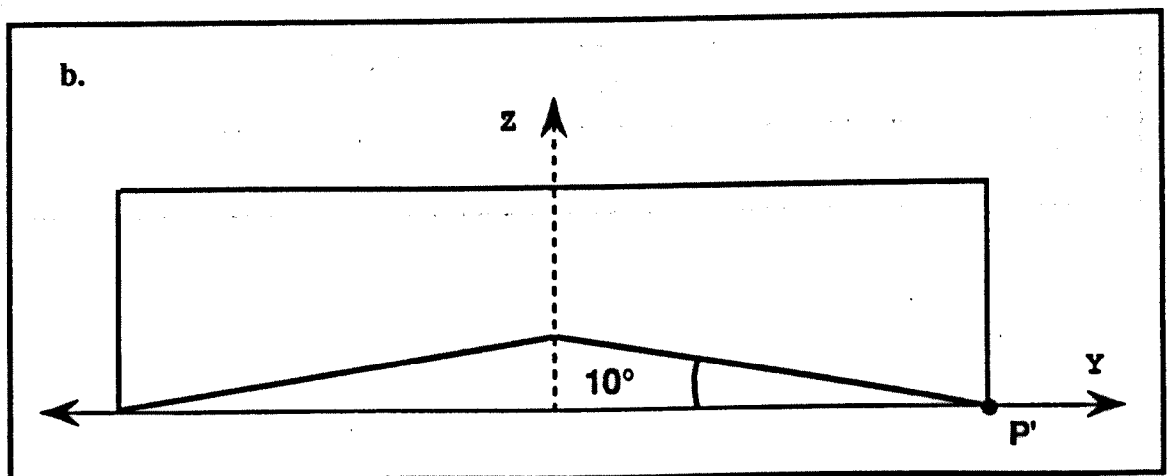


Figure 5.14 Showing How Point P' Below the Surface of Die A is an Equivalent to Point P' on Die B.



a.) A 20° conic die with point P' below it's surface.



b.) An inverted conic die of -10° which has point P' on it's surface.

Figure 5.15 The Cross Section of a Radially Profiled Tool Showing How it is Effectively Made up From Parts of Different Angled Tools, $\alpha_1, \alpha_2, \alpha_3$.

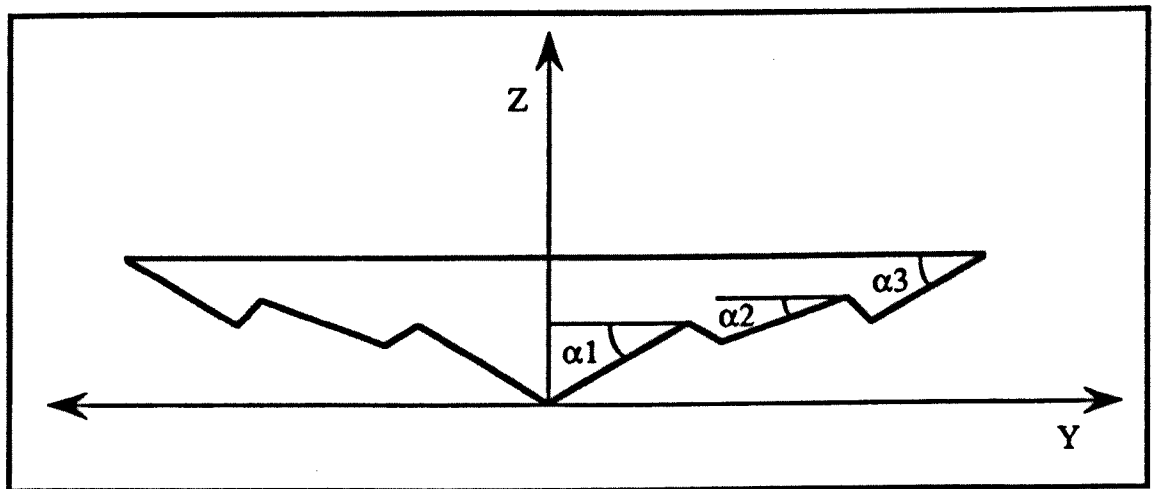


Figure 6.1 The Generalised Tool and Workpiece Layout as Generated by the Preprocessor 'PROFS'.

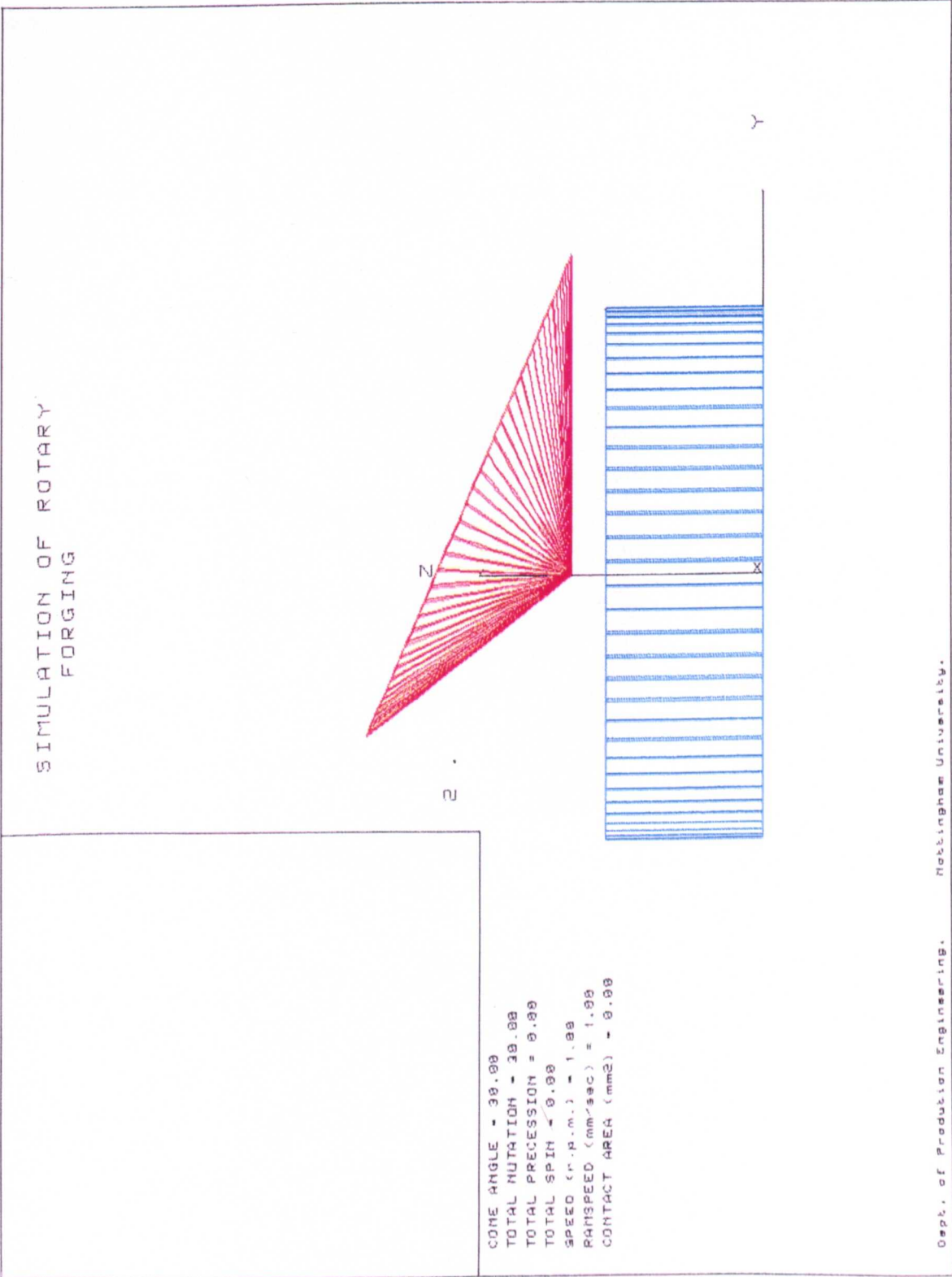


Figure 6.2 A 20° Conic Tool Drawn by the Preprocessor 'PROFS', with the Nodal Points of the Surface Joined by Circumferential and Radial Lines.

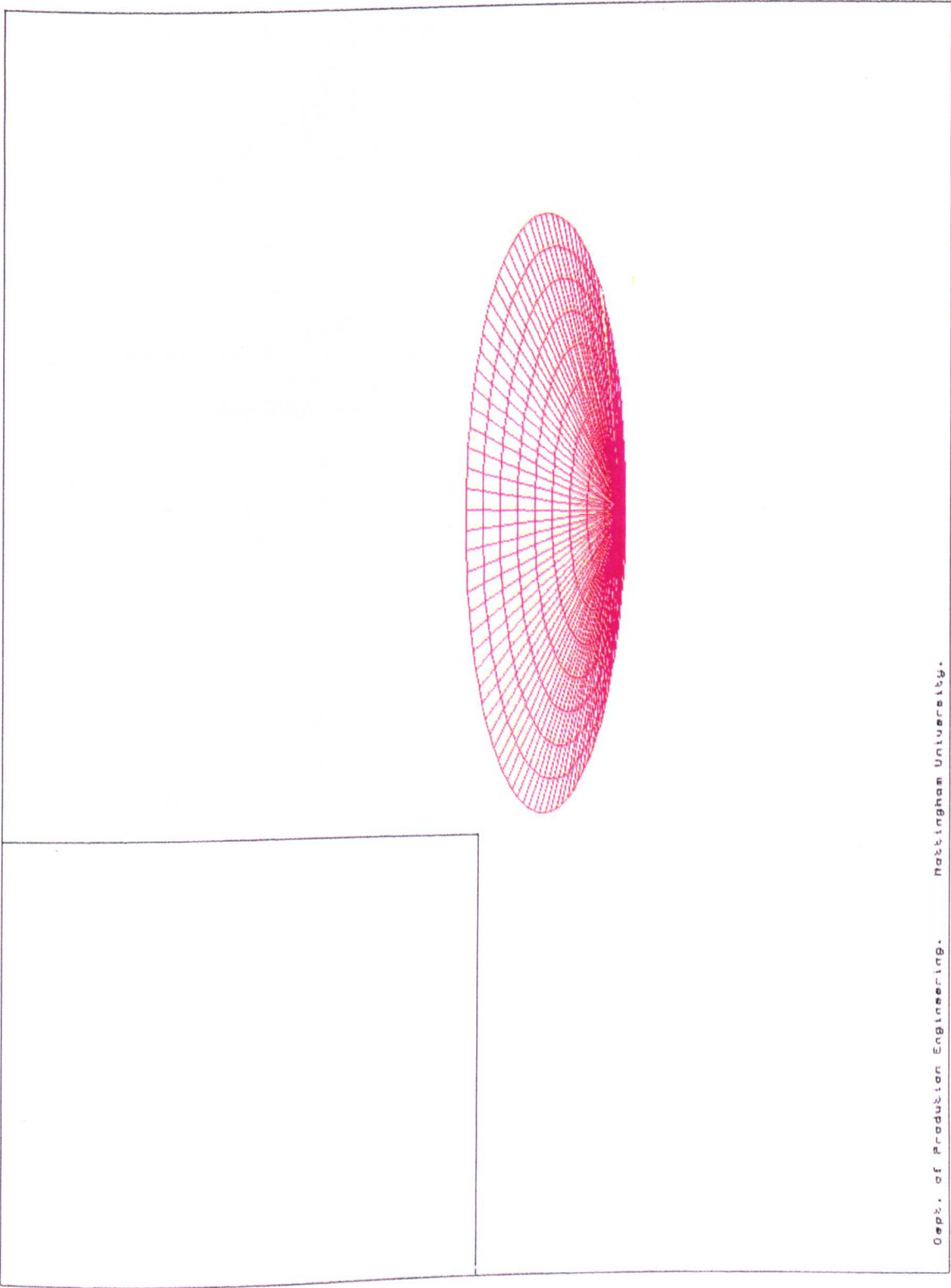


Figure 6.3 The Menu of Radial Profiles Available in 'PROFS' which can be Incorporated into the Surface of Any Conic Rotary Forging Tool.

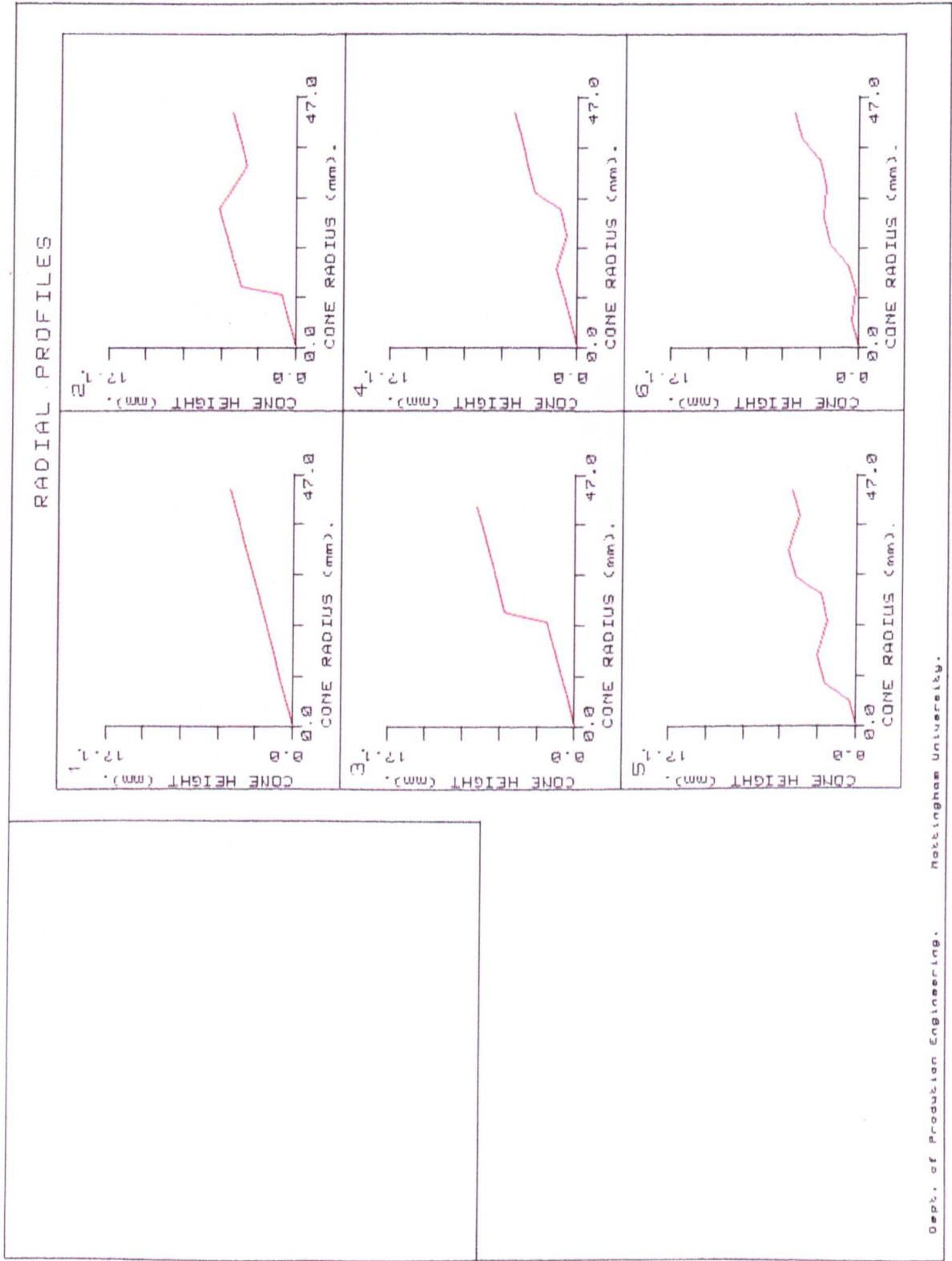


Figure 6.4 A 20° Conic Tool with the 4th. Radial Profile From the Menu Shown in Figure 6.3 Incorporated into it, as Generated and Drawn by the Preprocessor 'PROFS'.

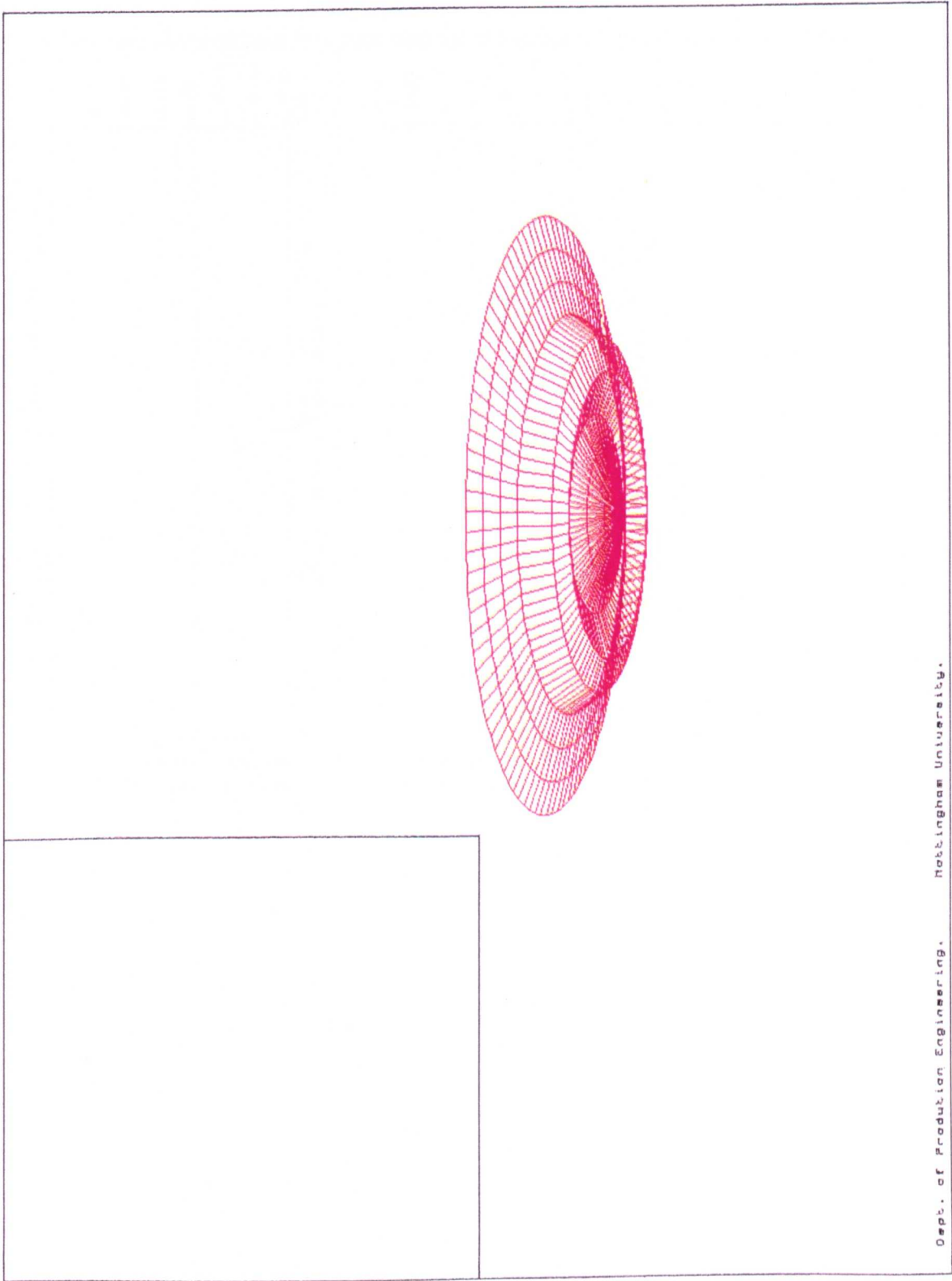


Figure 6.5 The Menu of Circumferential Profiles Available in 'PROFS' which can be Incorporated into the Surface of Any Conic Rotary Forging Tool.

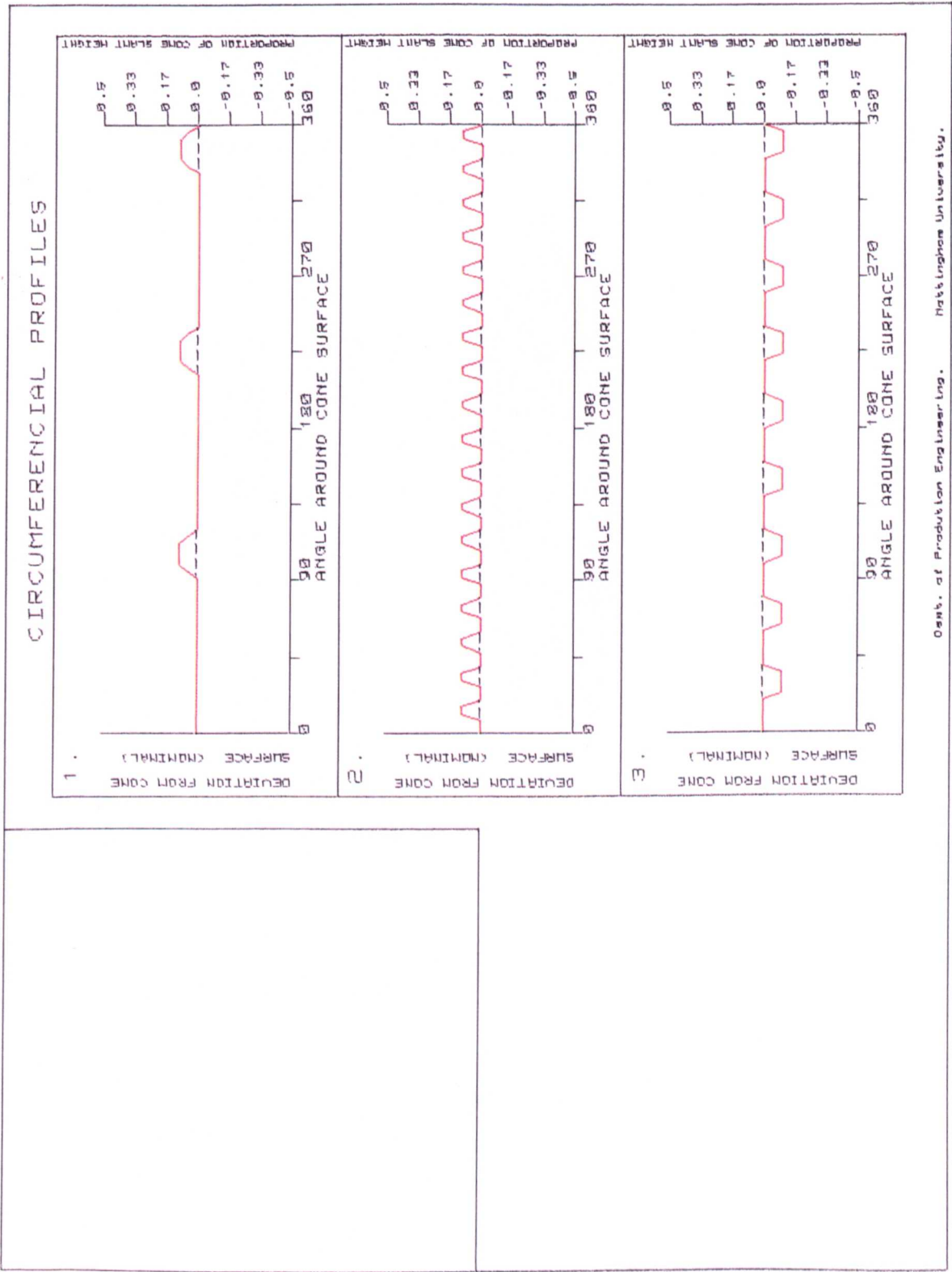


Figure 6.6 A 20° Conic Tool with the 3rd. Circumferential Profile From the Menu Shown in Figure 6.5 Incorporated into it, as Generated and Drawn by the Preprocessor 'PROFS'.

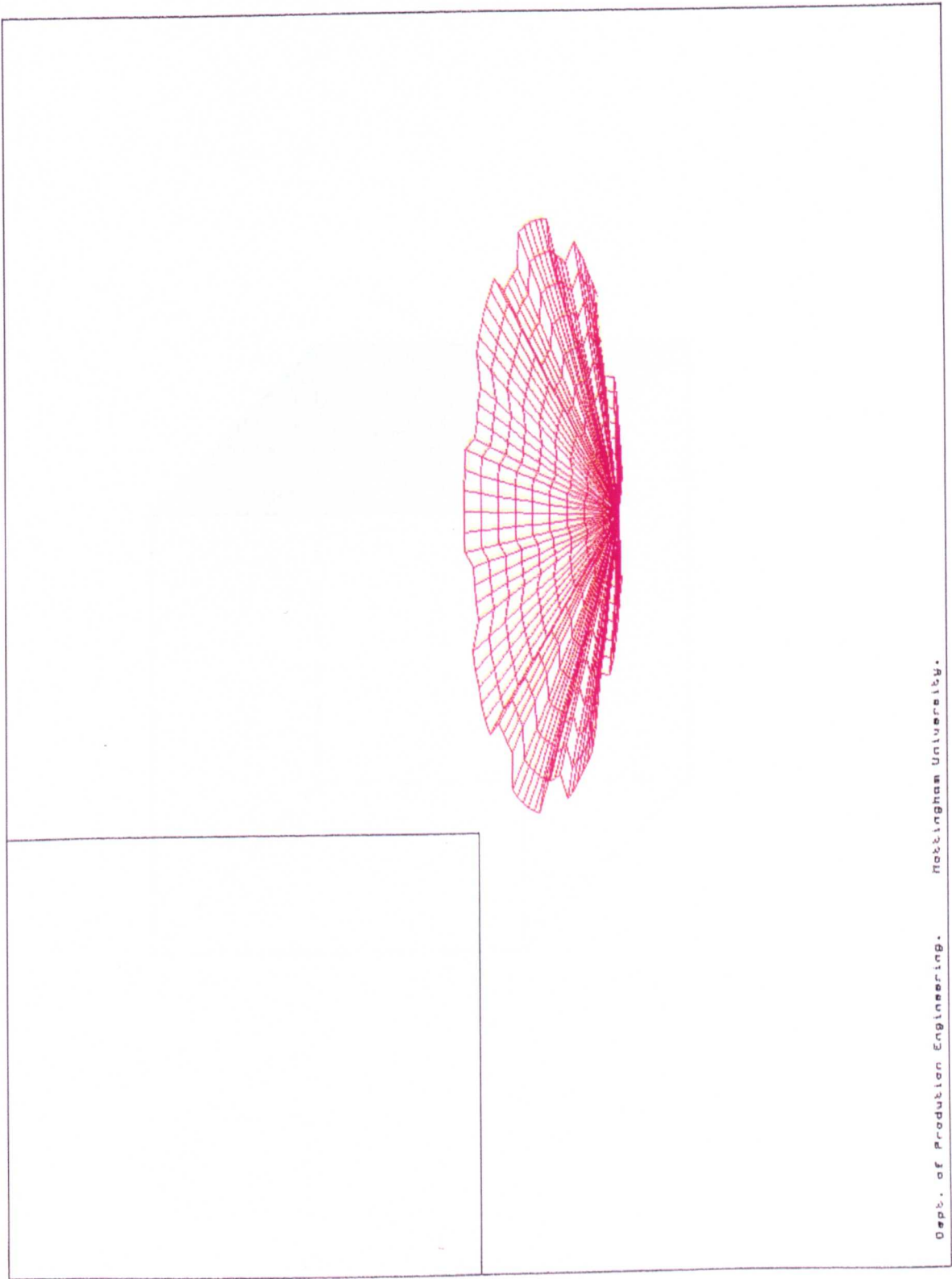


Figure 6.7 A Hexahedral Element as Used in the Generation of a Workpiece.

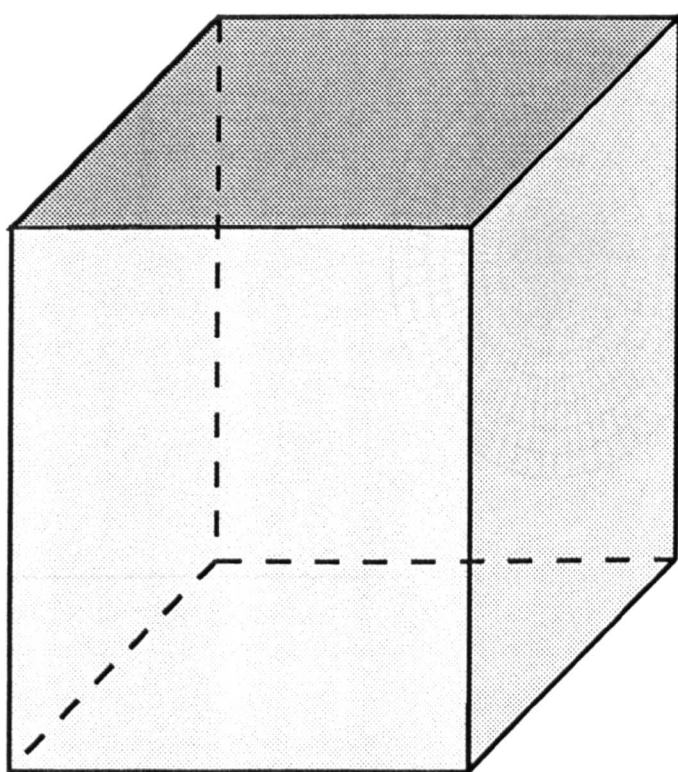


Figure 6.8 A Typical Workpiece Modelled by the Preprocessor PROFS, Constructed From a Circular Arrangement of Hexahedral Elements

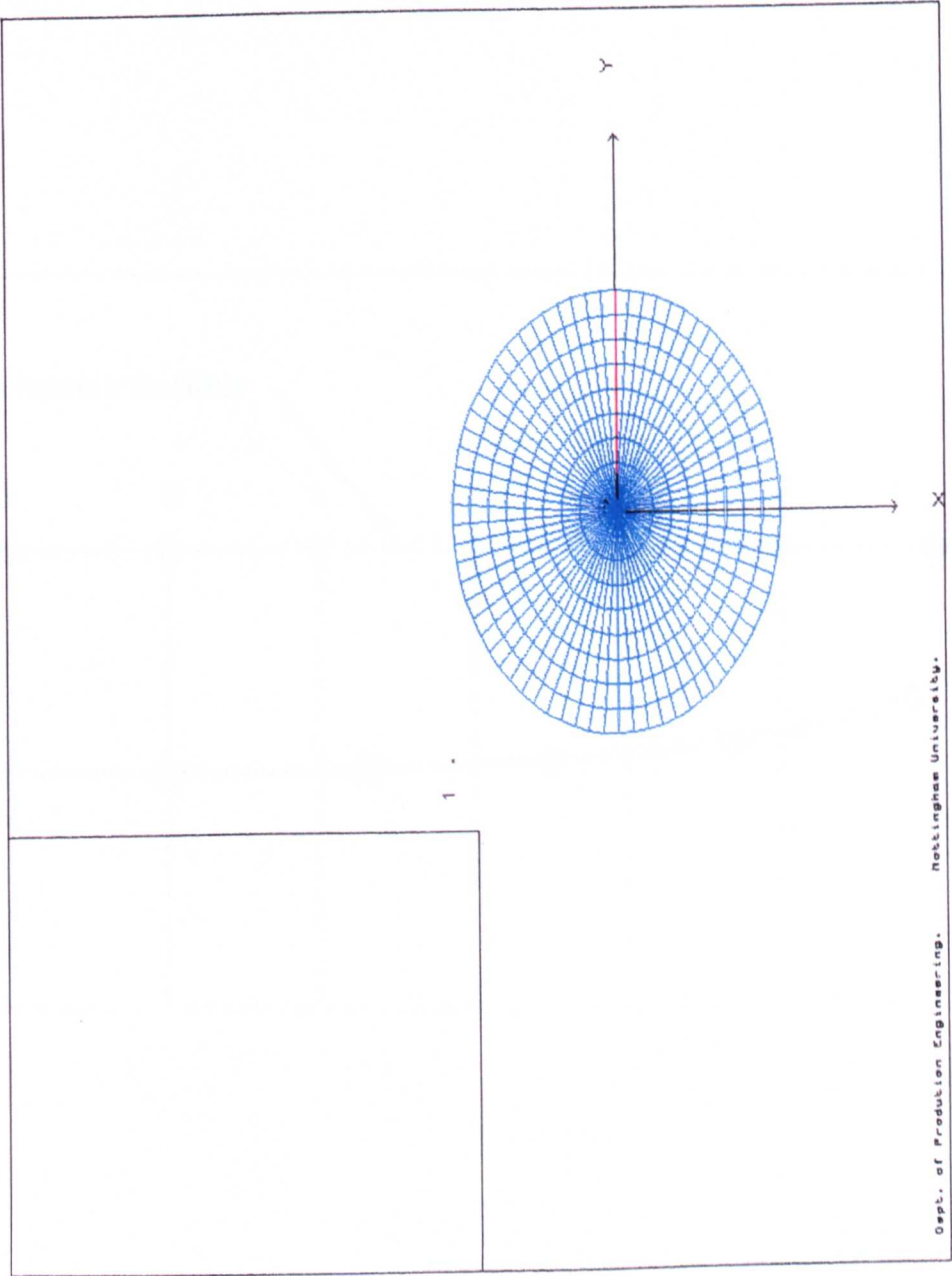


Figure 6.9 Showing how a Rotary Forging Tool Surface Intersects with a Workpiece Surface.

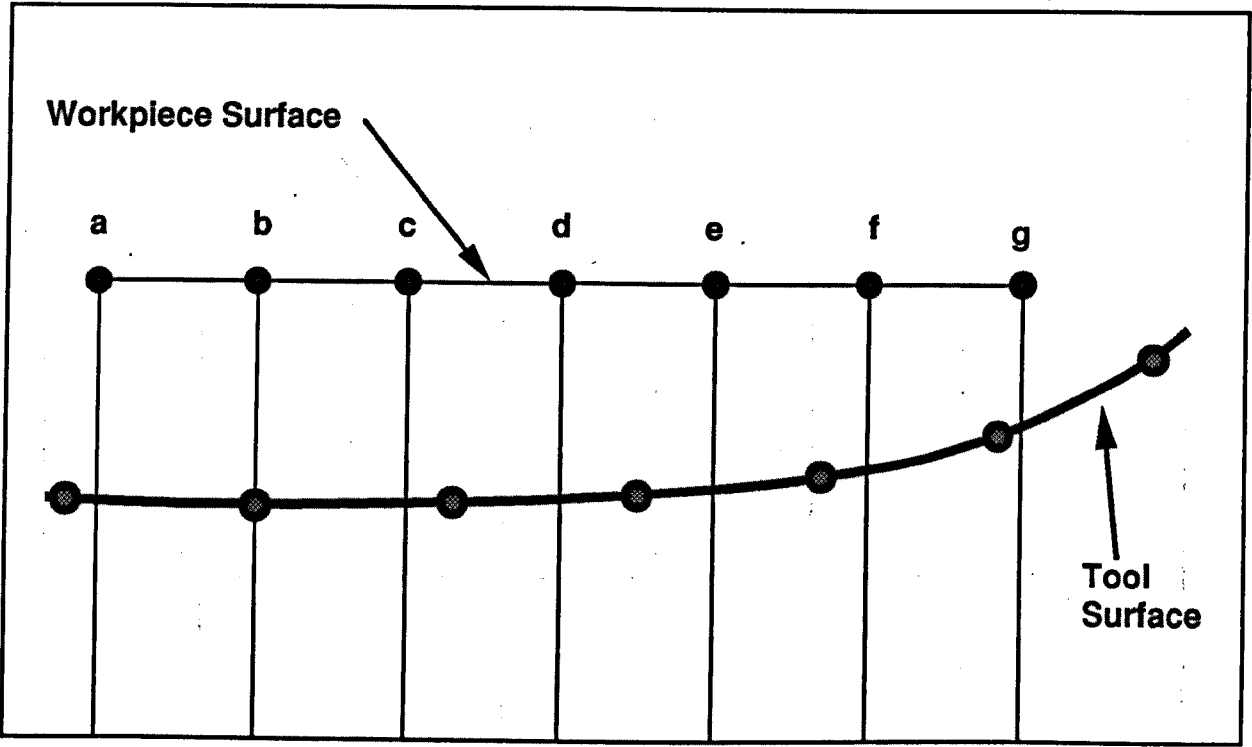


Figure 6.10 The Progression of a Typical Contact Geometry Calculated by the Processor COSIMORE. Only the Non - Constant Volume Workpiece is Shown For Clarity.

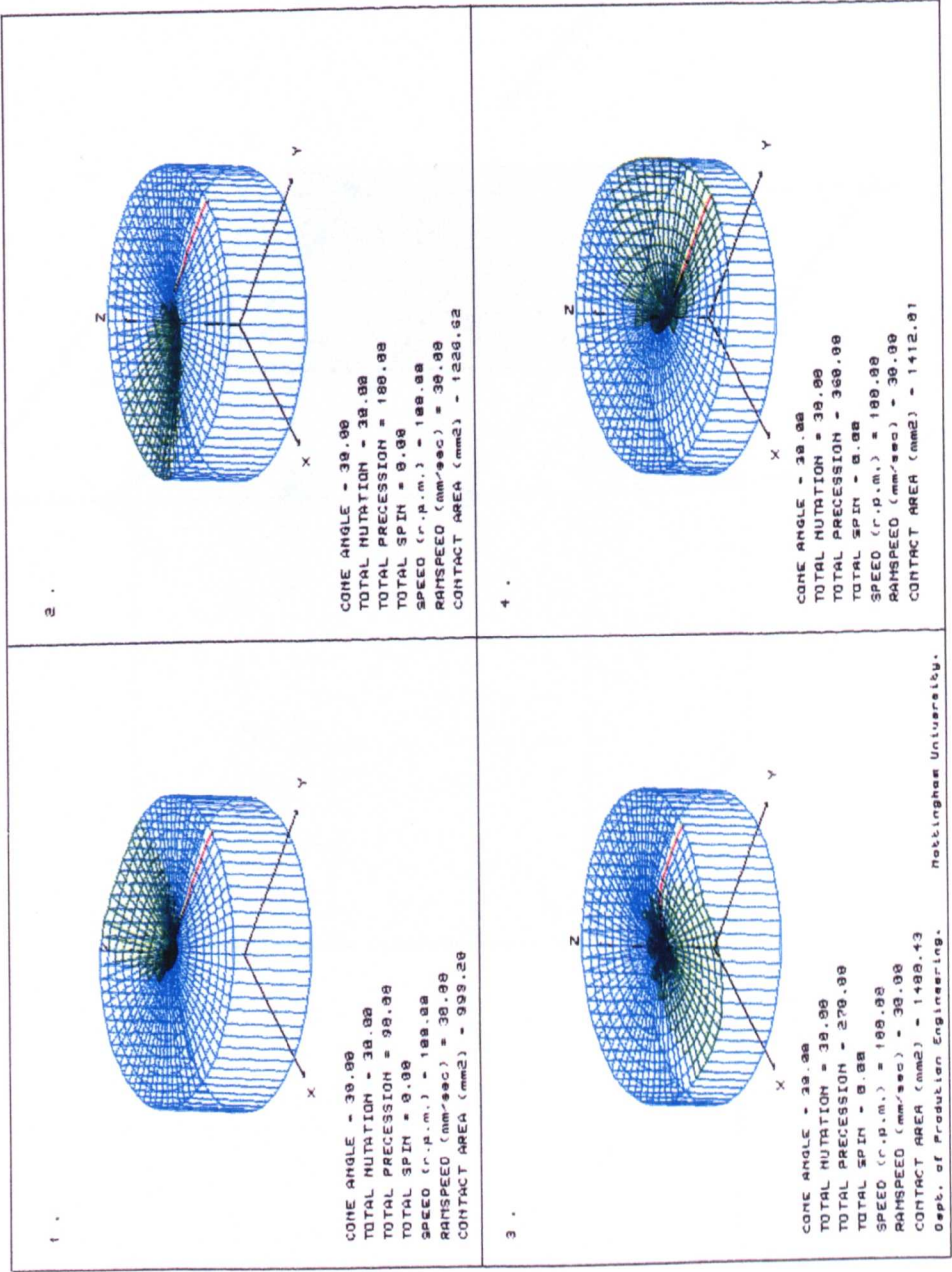


Figure 6.11 Showing How the Tool Surface Intersects With One of the Workpiece Elements in the Constant Volume Model.

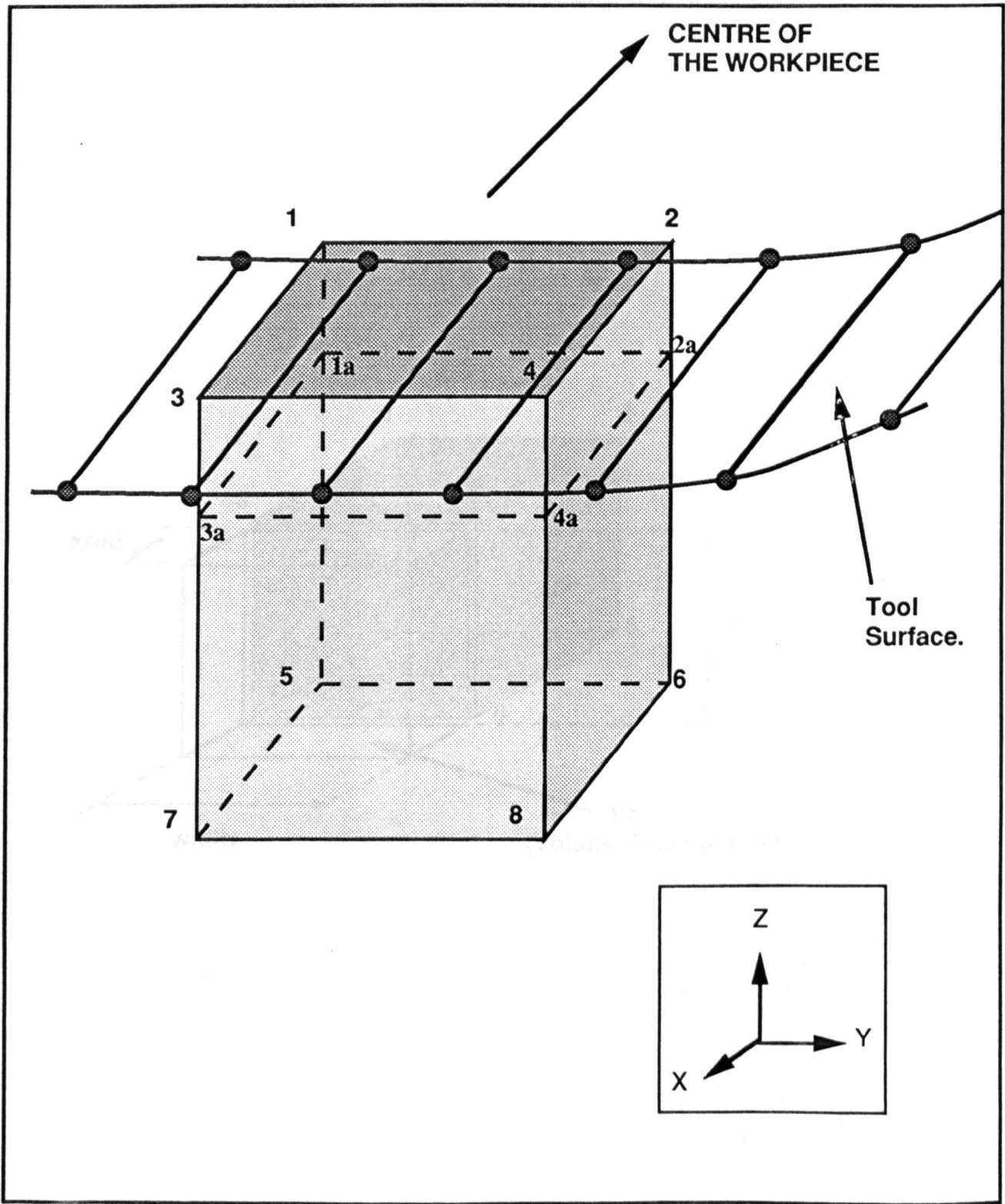


Figure 6.12 Showing How the Volume Change For Each Step of the Simulation is Calculated For an Element in the Workpiece and Added on to its Length as a First Approximation in the Constant Volume Workpiece Model.

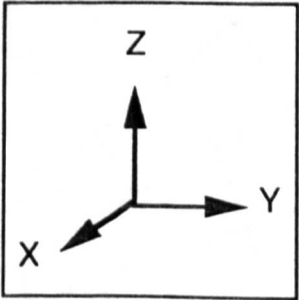
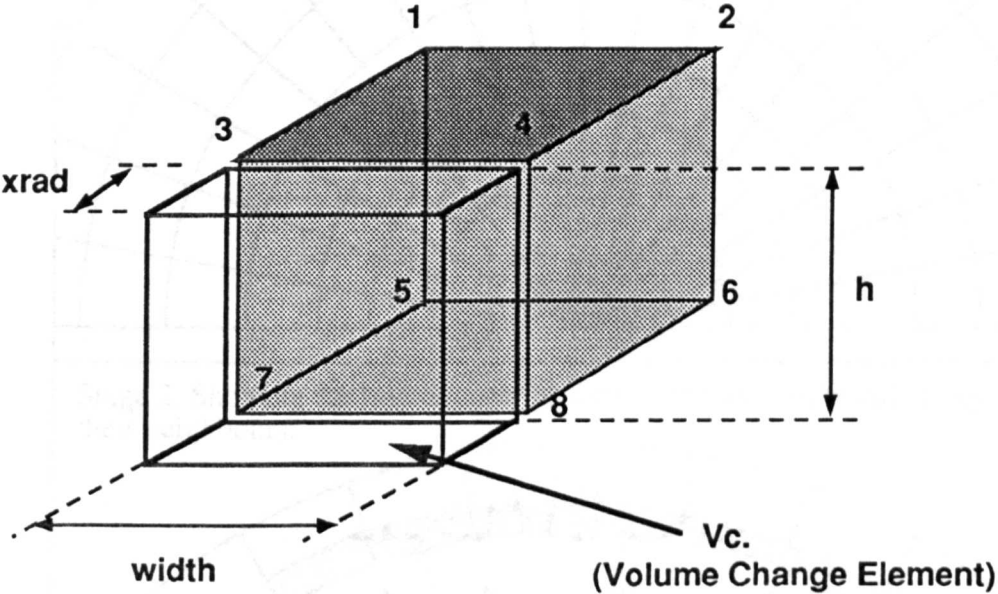


Figure 6.13 Showing how the elements of a workpiece are moved every alternate row which in affect causes every element in the whole workpiece to be effected, and causes an even radial expansion of the workpiece.

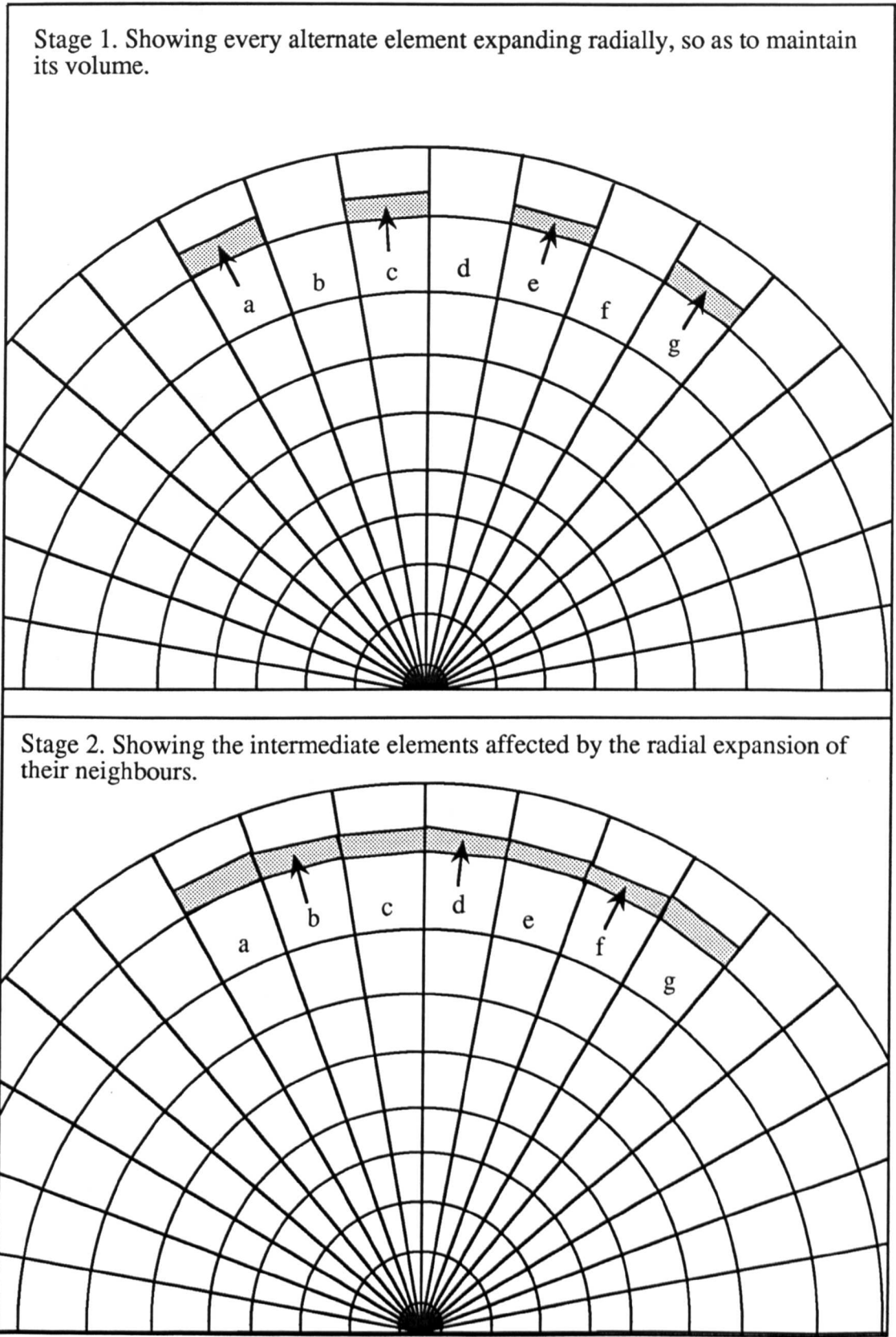
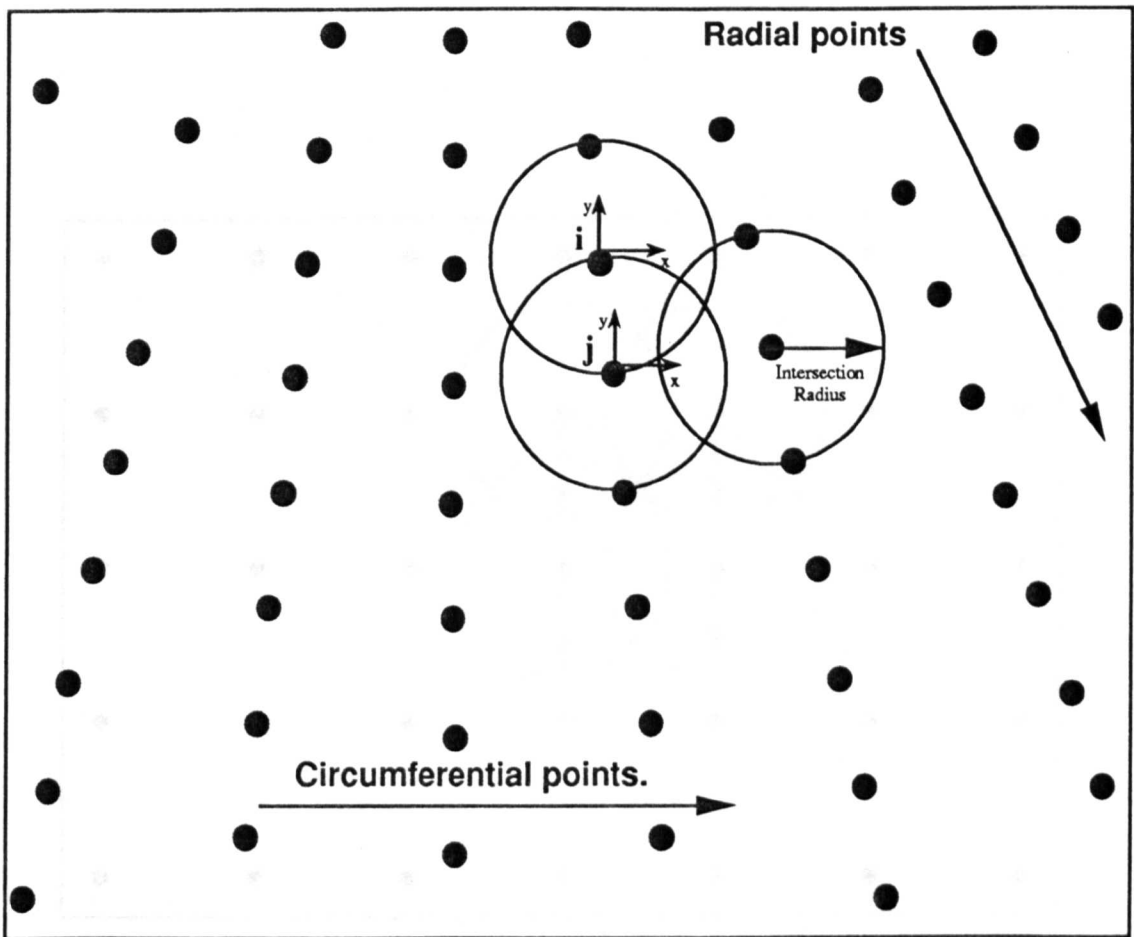


Figure 6.14 Showing how the radii of the intersection cylinders on the workpiece surface are found from the radial spacing of the points in the mesh, and how these cylinders overlap to completely cover the area of the whole workpiece.



Point j is the next radial point to point i. The radius of the intersection cylinder is found from the coordinates of the two points.

Figure 6.15 Showing how a squared meshed workpiece would enable the radii of the intersection cylinders to be all the same size, and smaller than for the radially meshed workpiece shown in figure 6.14, but still comprehensively cover the workpiece surface.

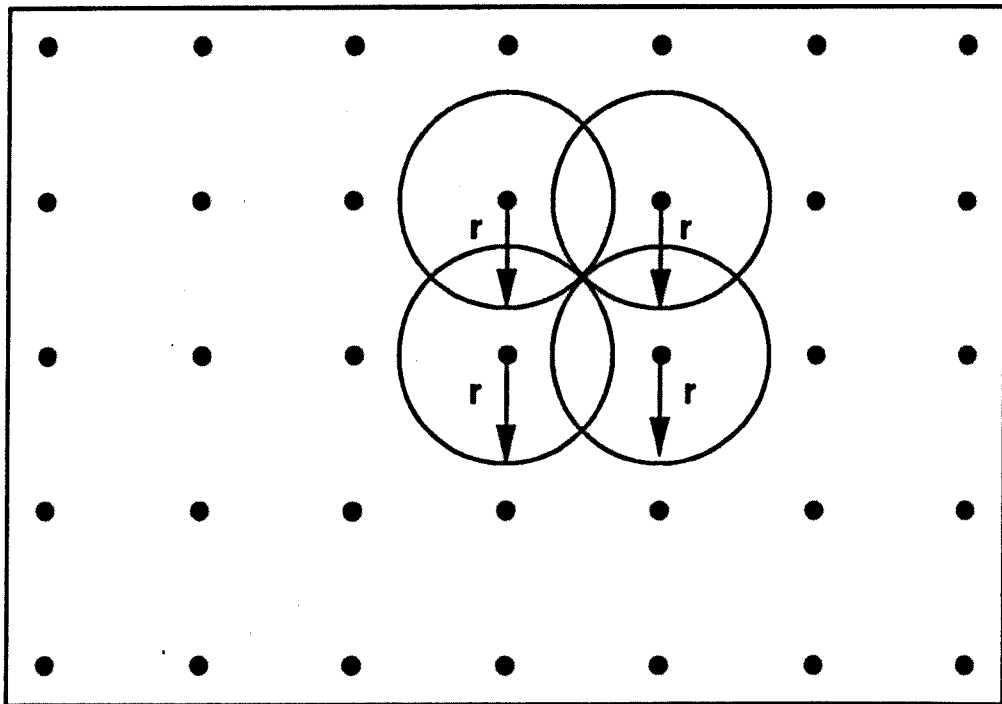
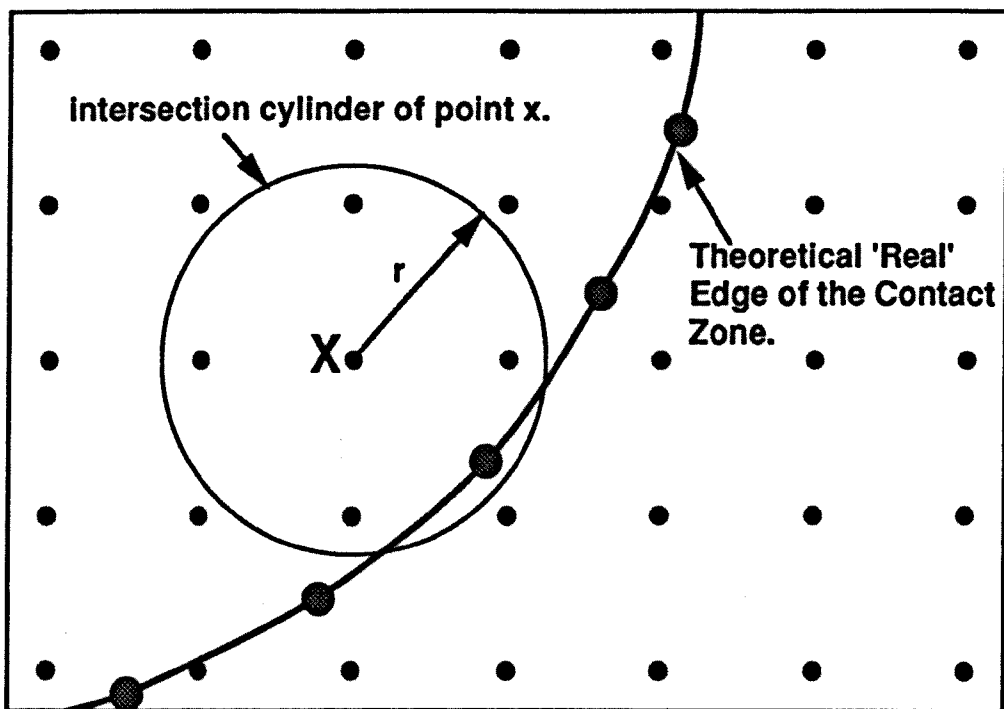


Figure 6.16 Showing how a large radius of intersection cylinder will cause the point on the workpiece to be considered as an in contact point, when in fact it is not.



Point x will be deemed to be in contact since it overlaps with a point on the edge of the tool, when in fact it is not. With a smaller radius 'r' of the intersection cylinder this could be avoided.

Figure 7.1 A Typical Result From VIDEO, the Post - Processor, Showing a Workpiece With its Contact Geometry Represented in Green. The Corner Picture Shows the Orientation of the Tool at This Point in The Simulation.

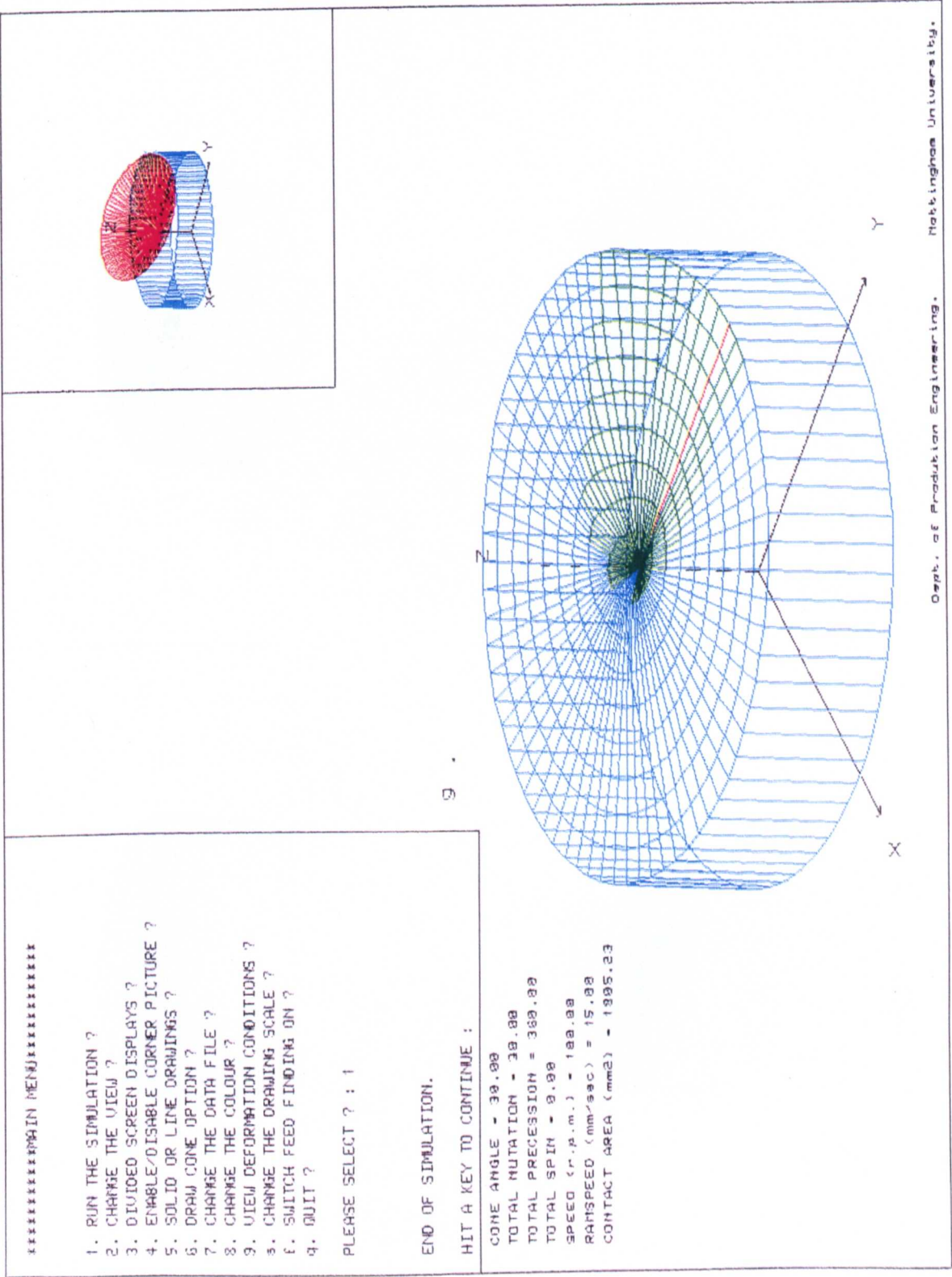


Figure 7.2 Showing Nutation Motion Using the Non - Constant Volume Model Workpiece.

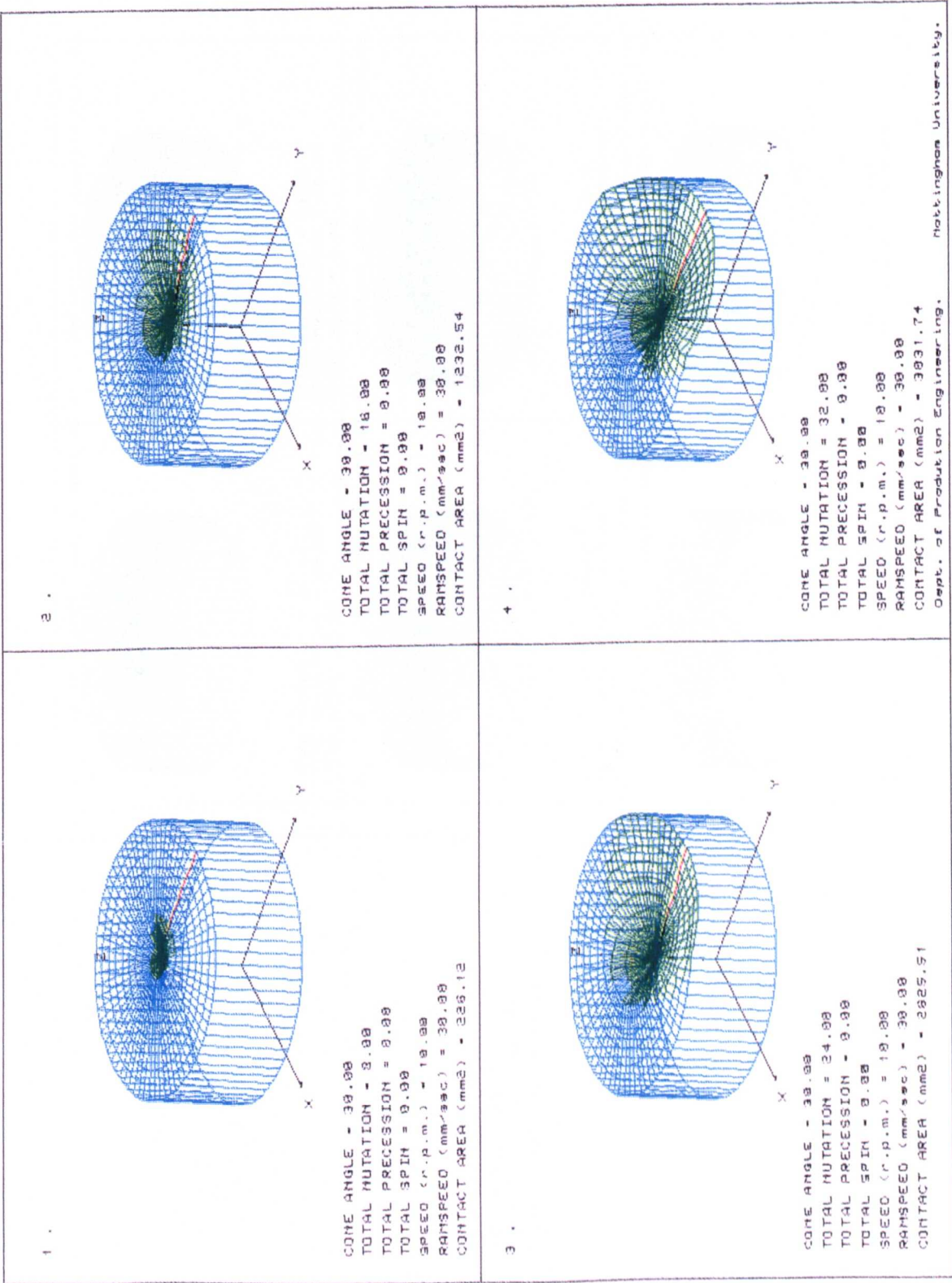
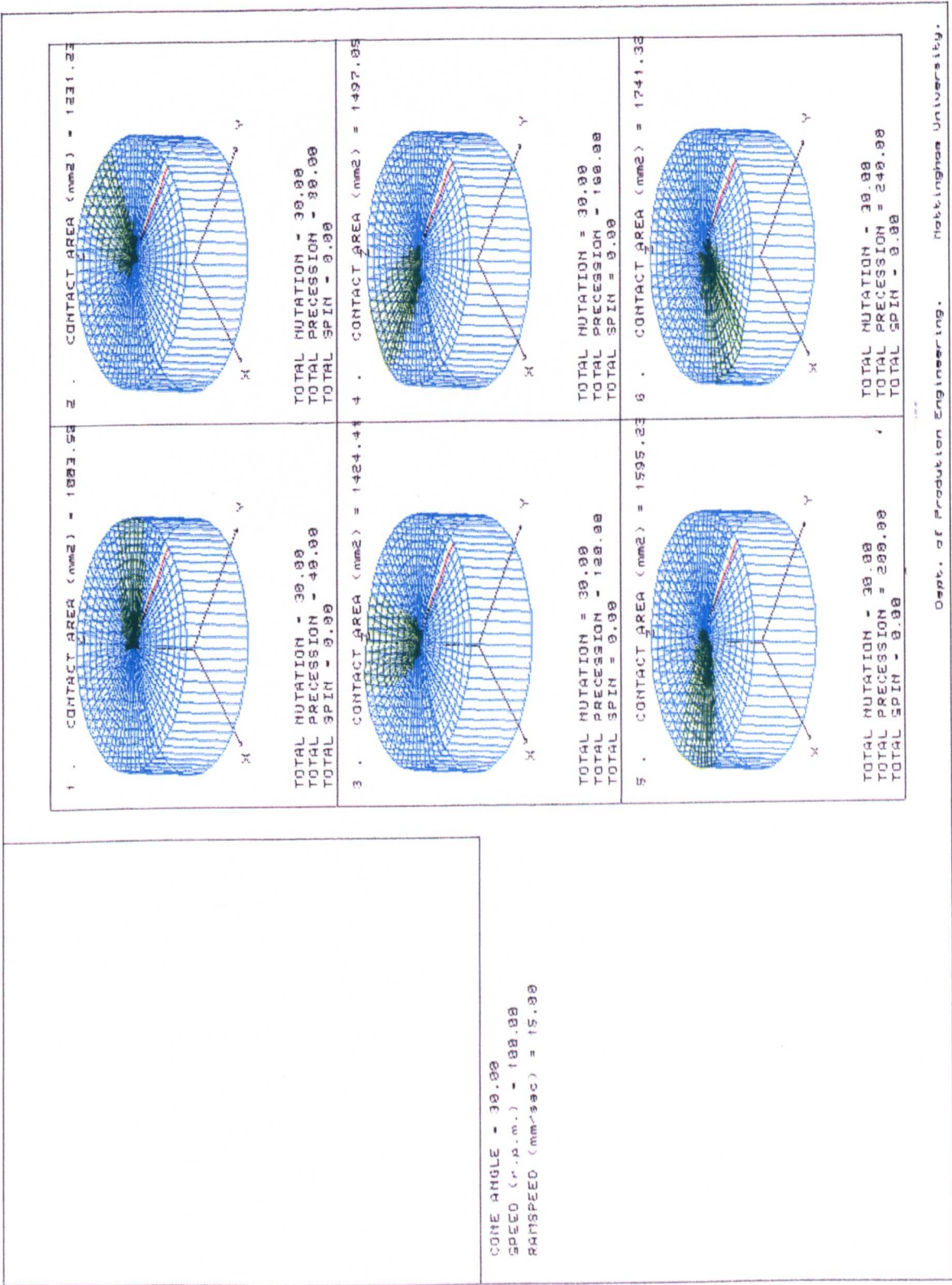


Figure 7.3 -a. The Precession Motion Using the Non - Constant Volume Model Workpiece.



CONC ANGLE = 30.00
SPEED (r.p.m.) = 100.00
RATSPED (mm/sec) = 15.00

Dept. of Production Engineering. Nottingham University.

Figure 7.3 -b. The Precession Motion Using the Non - Constant Volume Model Workpiece.

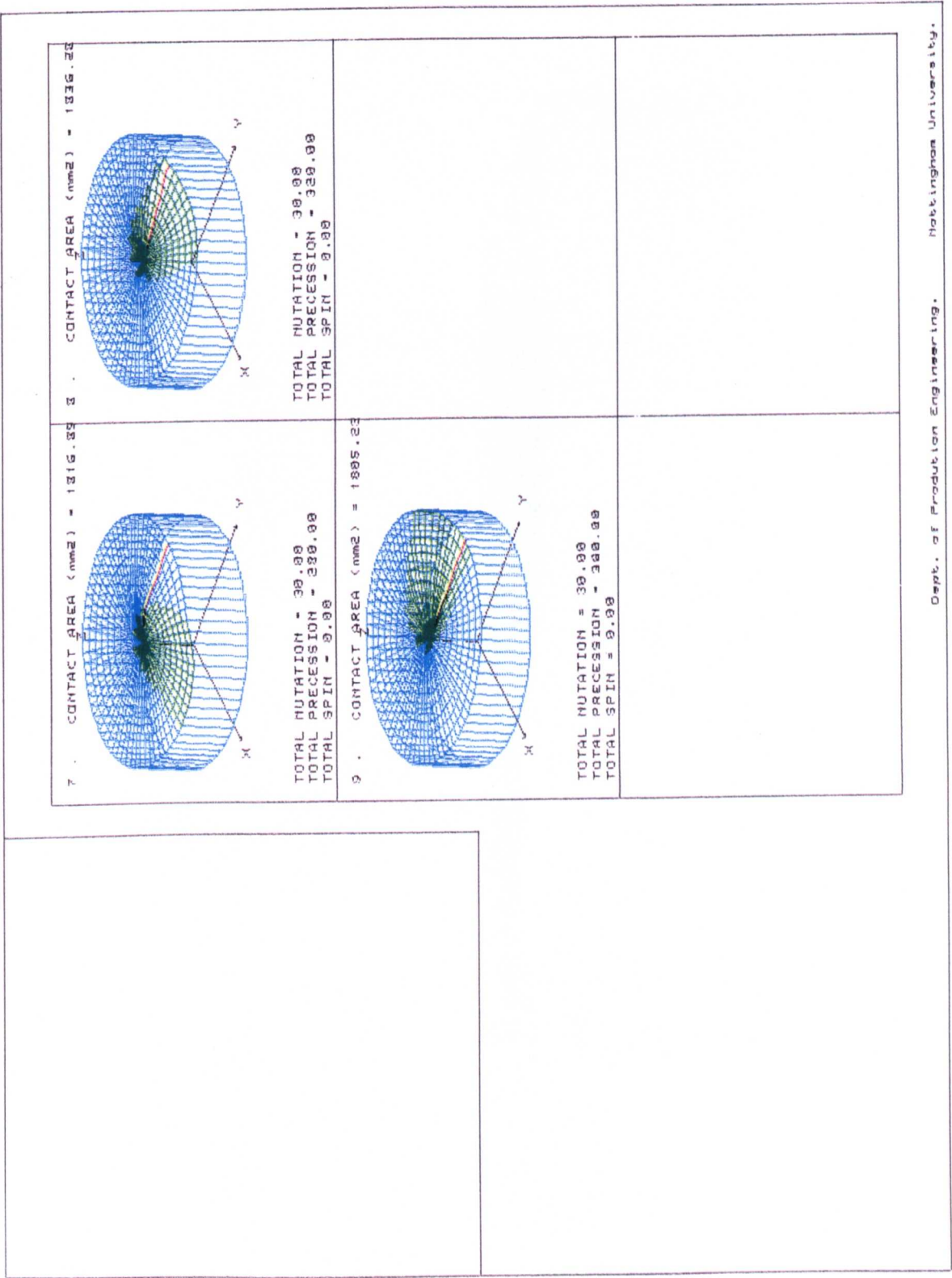


Figure 7.4 Showing the Helical Surface Developed On a Workpiece After the First Revolution of The Precession Motion.

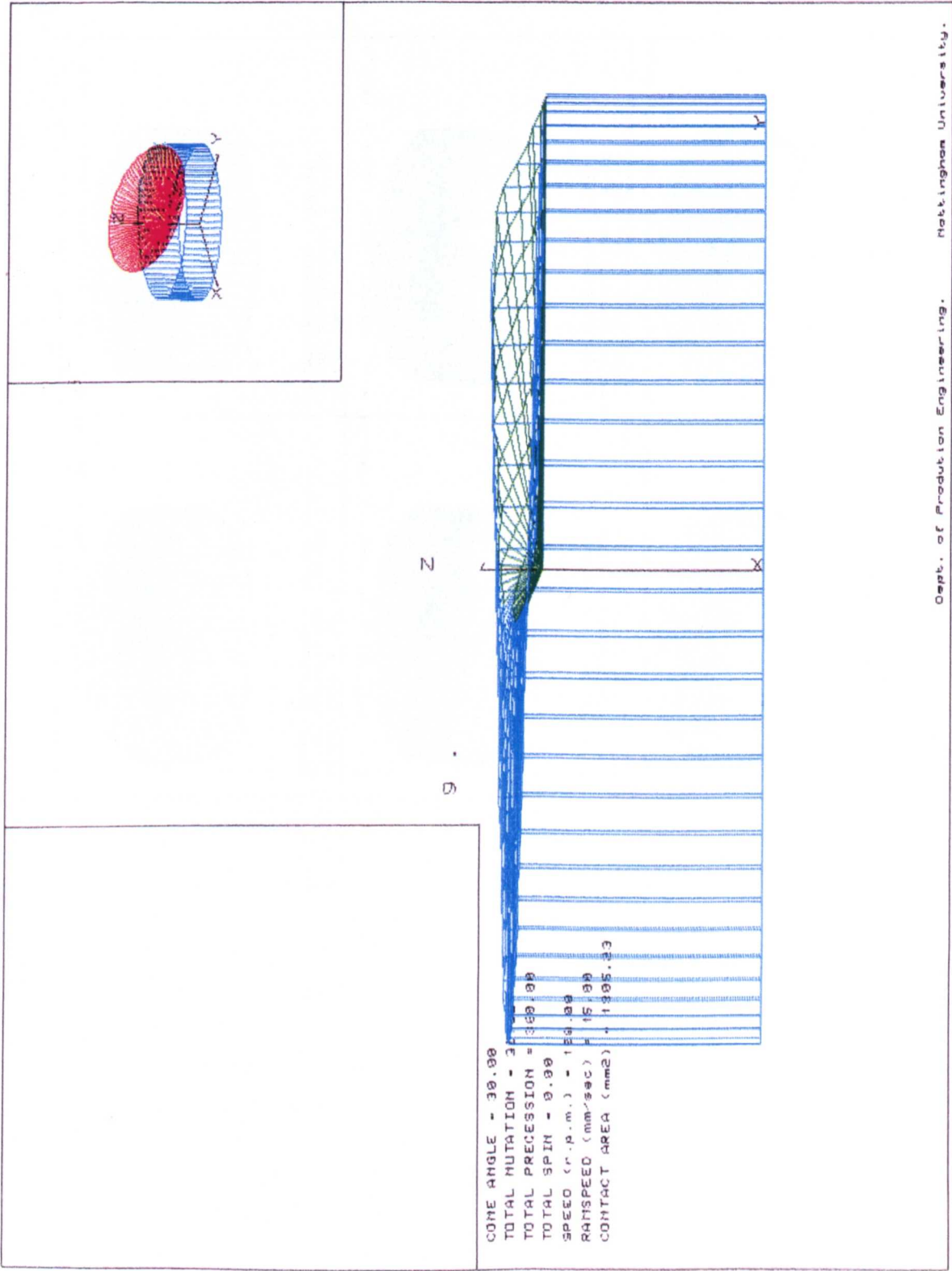
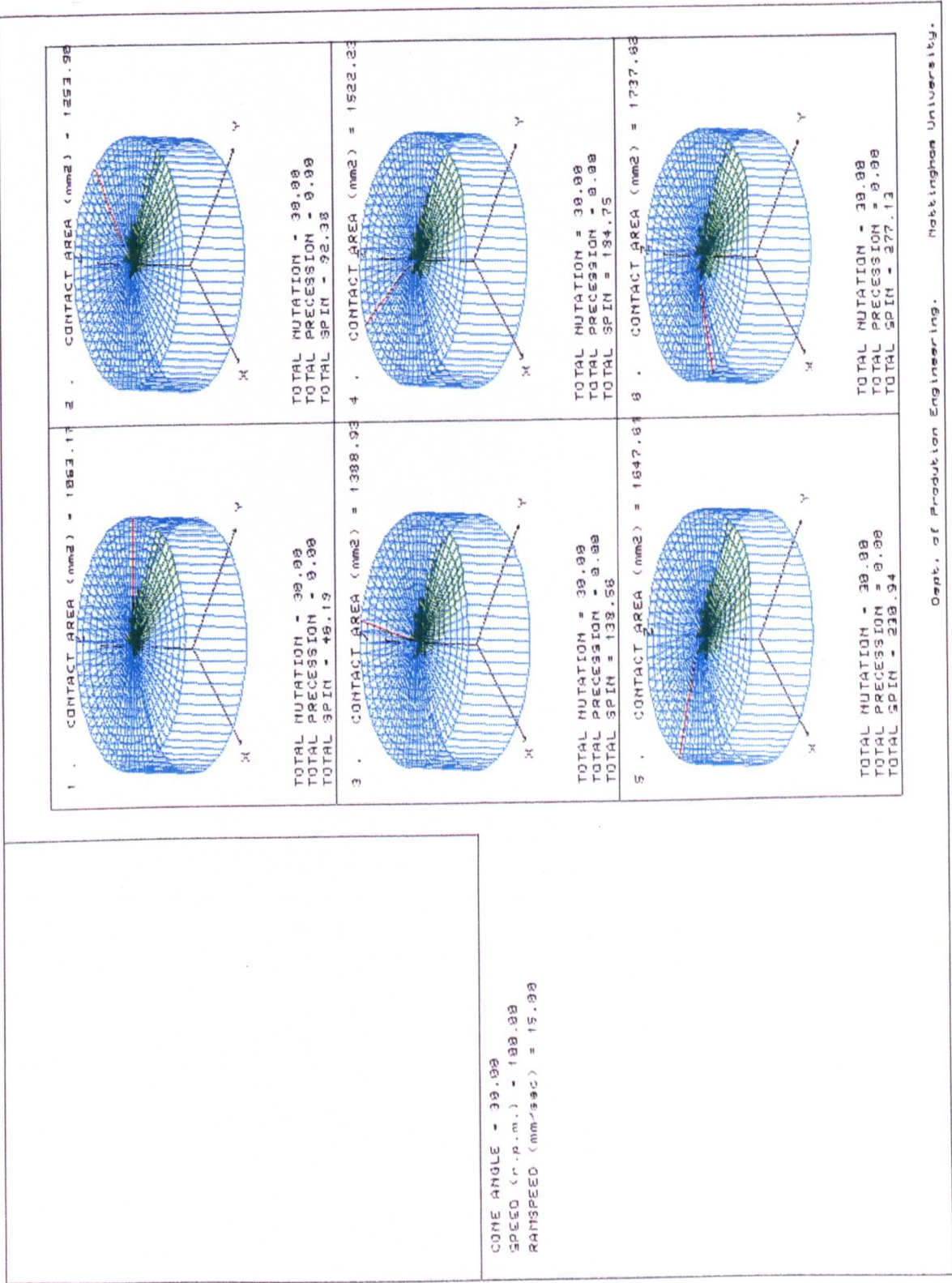


Figure 7.5 - a. The Spin Motion Developed on a Non - Constant Volume Model Workpiece.



COME ANGLE = 38.88
SPEED (r.p.m.) = 188.88
RAMP SPEED (mm/sec) = 15.88

Dept. of Production Engineering. Nottingham University.

Figure 7.5 - b. The Spin Motion Developed on a Non - Constant Volume Model Workpiece.

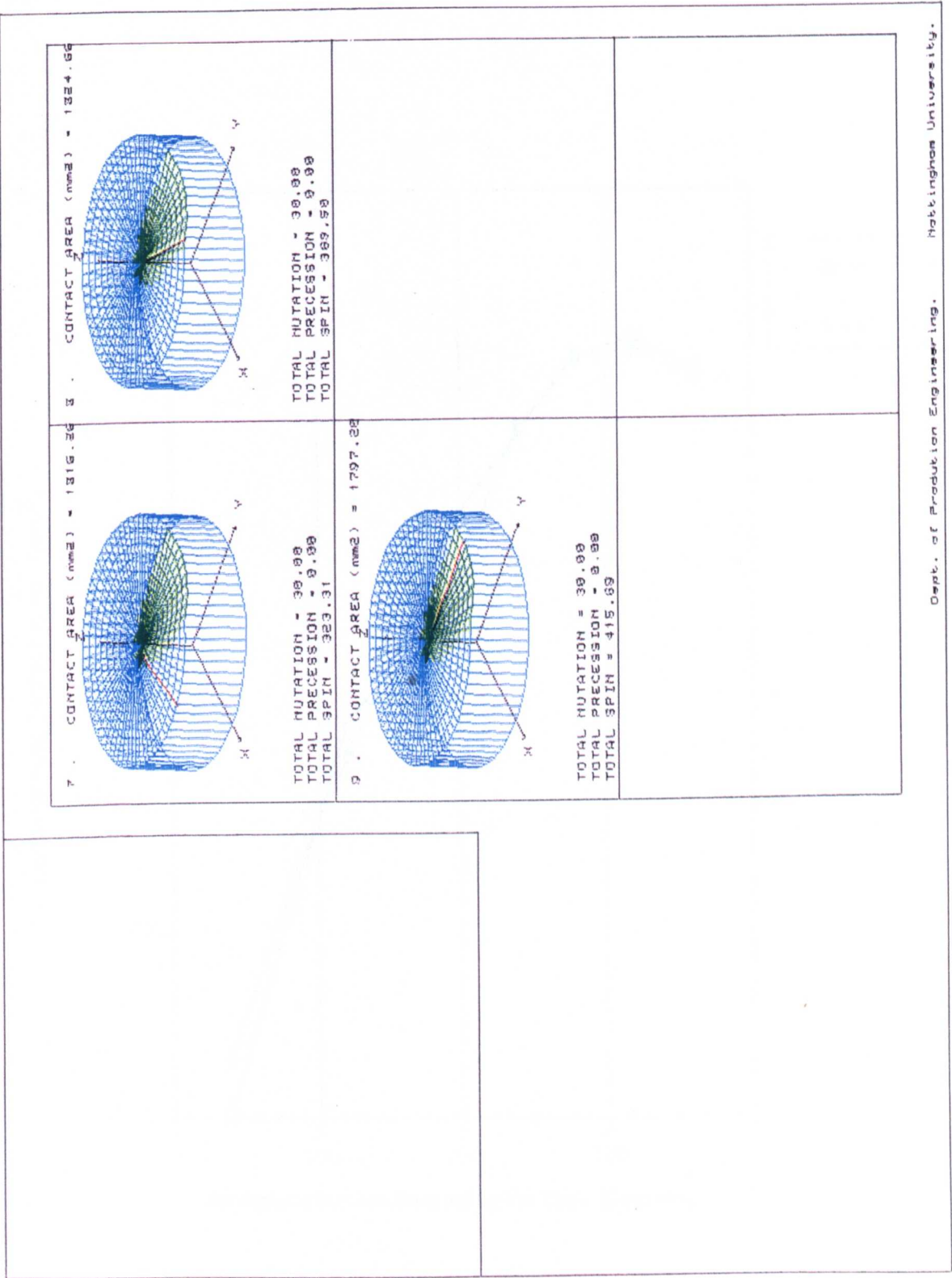


Figure 7.5 Showing the Contact Geometry on the Surface of a Workpiece

Figure 7.6 Showing the Similarity Between the Contact Areas Produced by the Precession and Spin Motions During the First Initial Revolution of Contact.

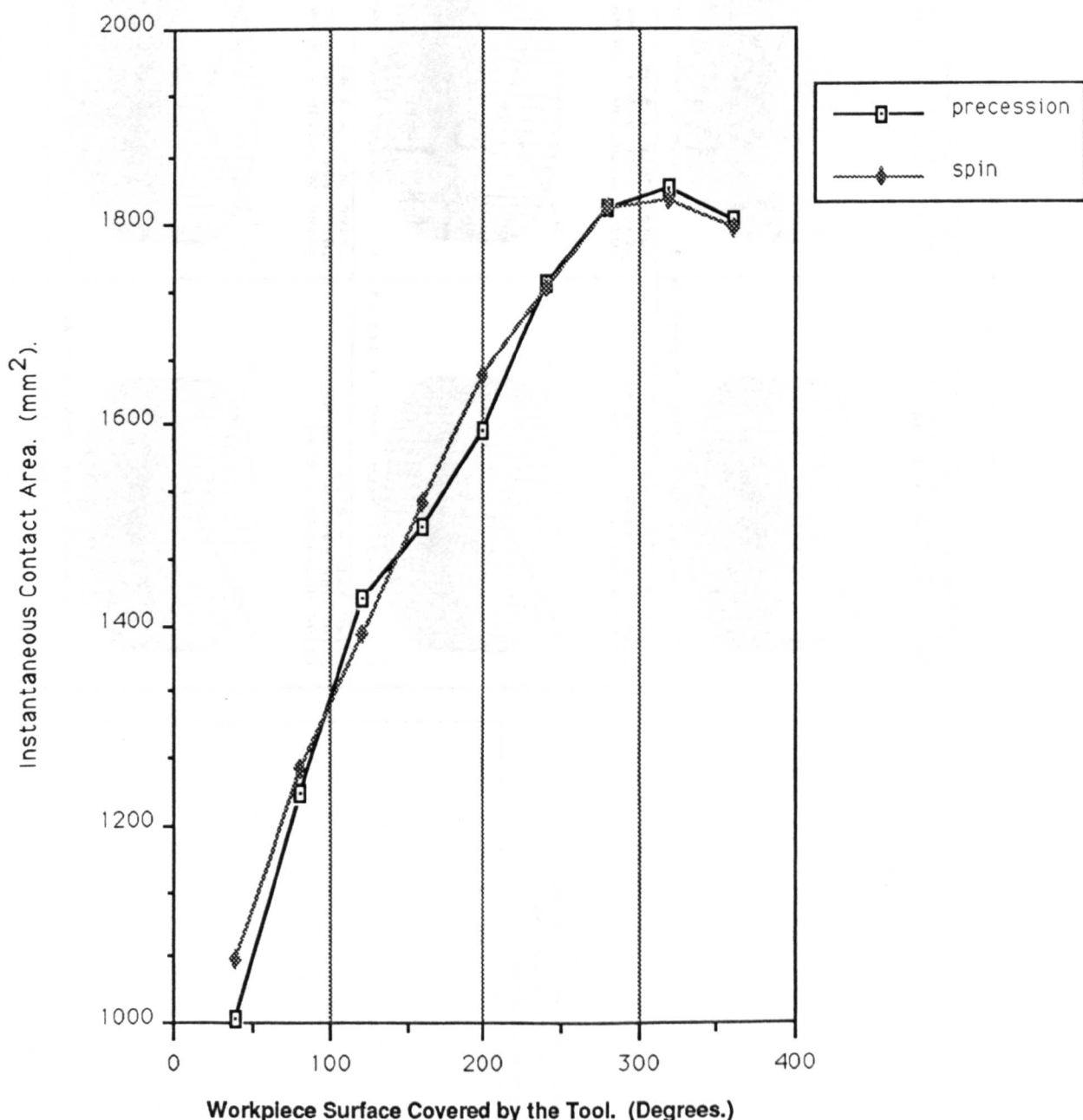


Figure 7.7 Shows the Contact Geometry on the Surface of a Workpiece During the First Revolution of a Nutation - Precession Motion.

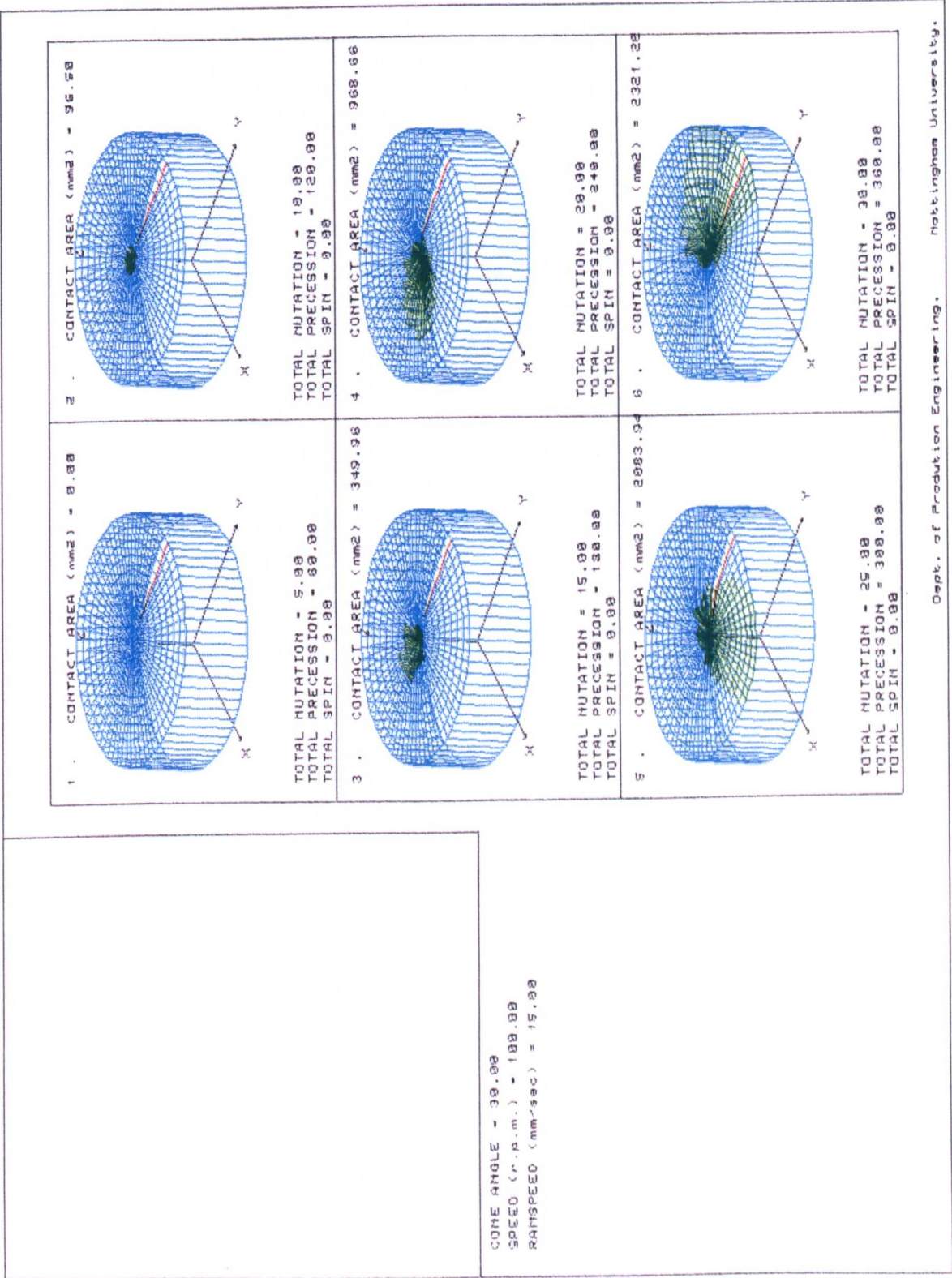


Figure 7.8 Shows the Contact Geometry on the Surface of a Workpiece During the First Revolution of a Non - Monotonic Nutation - Precession Motion. The Nutation Rate = 300 c.p.m. and the Precession Rate = 100 c.p.m. Producing a Three Petal Rosette Pattern of Tool Axis Movement as Shown in Figure 7.9.

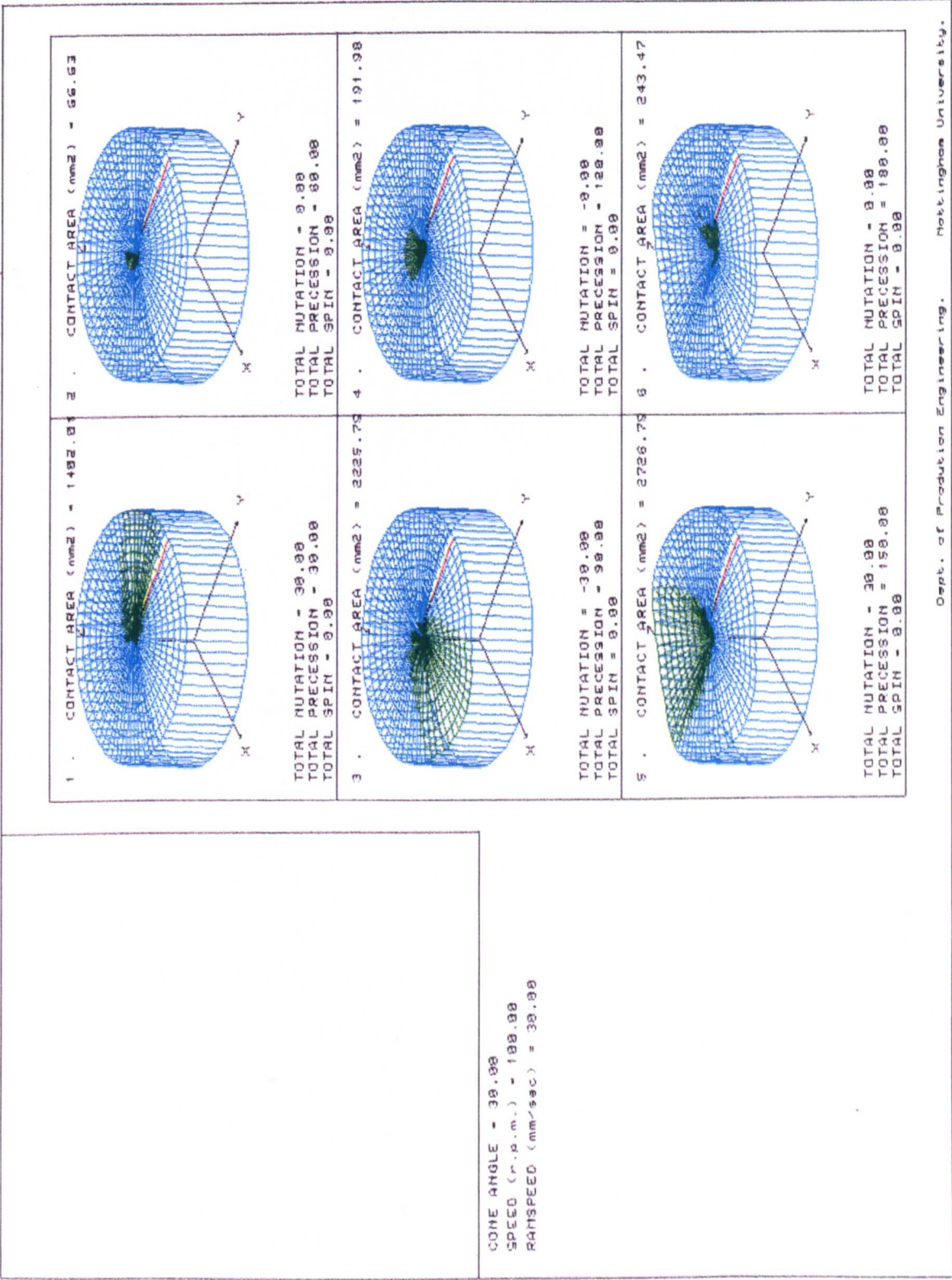
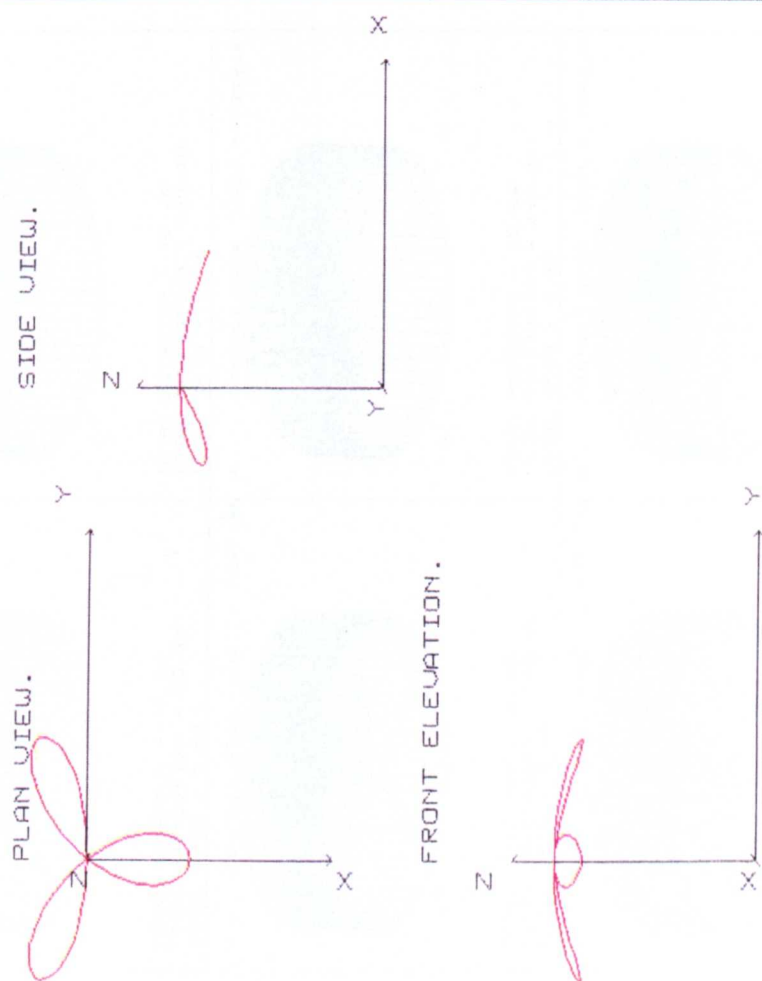


Figure 7.9 Shows a Three Petal Rosette Pattern of Tool Axis Movement Produced By the Non
 - Monotonic Nutation - Precession Motion. The Nutation Rate = 300 c.p.m. and the
 Precession Rate = 100 c.p.m.



MAX NUTATION = 39.00
 NUTATIONAL AMPLITUDE = 39.00
 PRECESSION = 360.00
 SPIN = 0.00
 NUTATION RATE (r.p.s.) = 300.00
 PRECESSION RATE (r.p.s.) = 100.00
 SPIN RATE (r.p.s.) = 0.00

Figure 7.10 - a. Shows the Contact Geometry on the Surface of a Workpiece During the First Revolution of a Non - Monotonic Nutation - Precession Motion. The Nutation Rate = 100 c.p.m. and the Precession Rate = 300 c.p.m., Producing a Spiral Pattern of Tool Axis Movement as Shown in Figure 7.11.

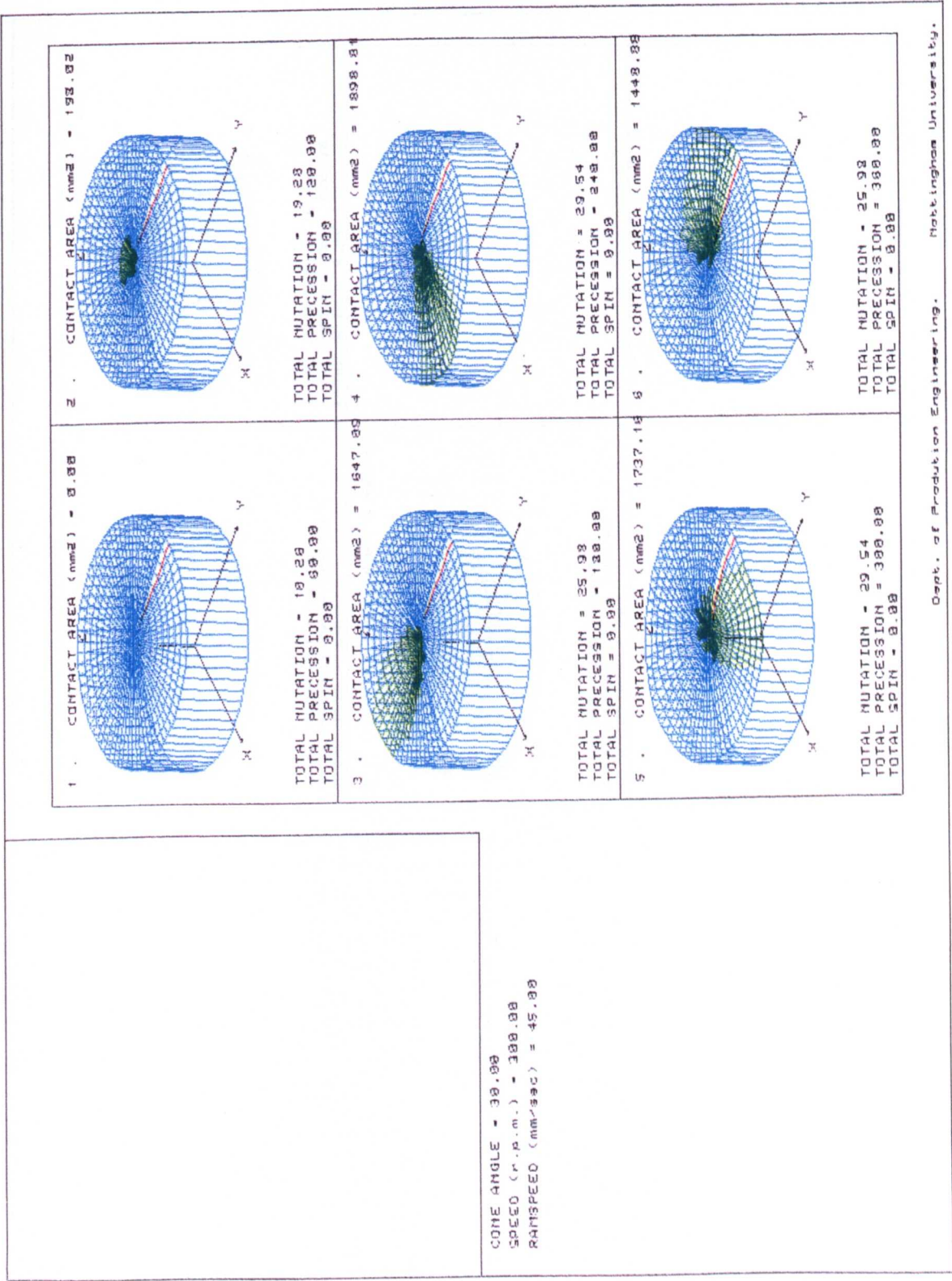


Figure 7.10 - b. Shows the Contact Geometry on the Surface of a Workpiece During the First Revolution of a Non - Monotonic Nutation - Precession Motion. The Nutation Rate = 100 c.p.m. and the Precession Rate = 300 c.p.m., Producing a Spiral Pattern of Tool Axis Movement as Shown in Figure 7.11.

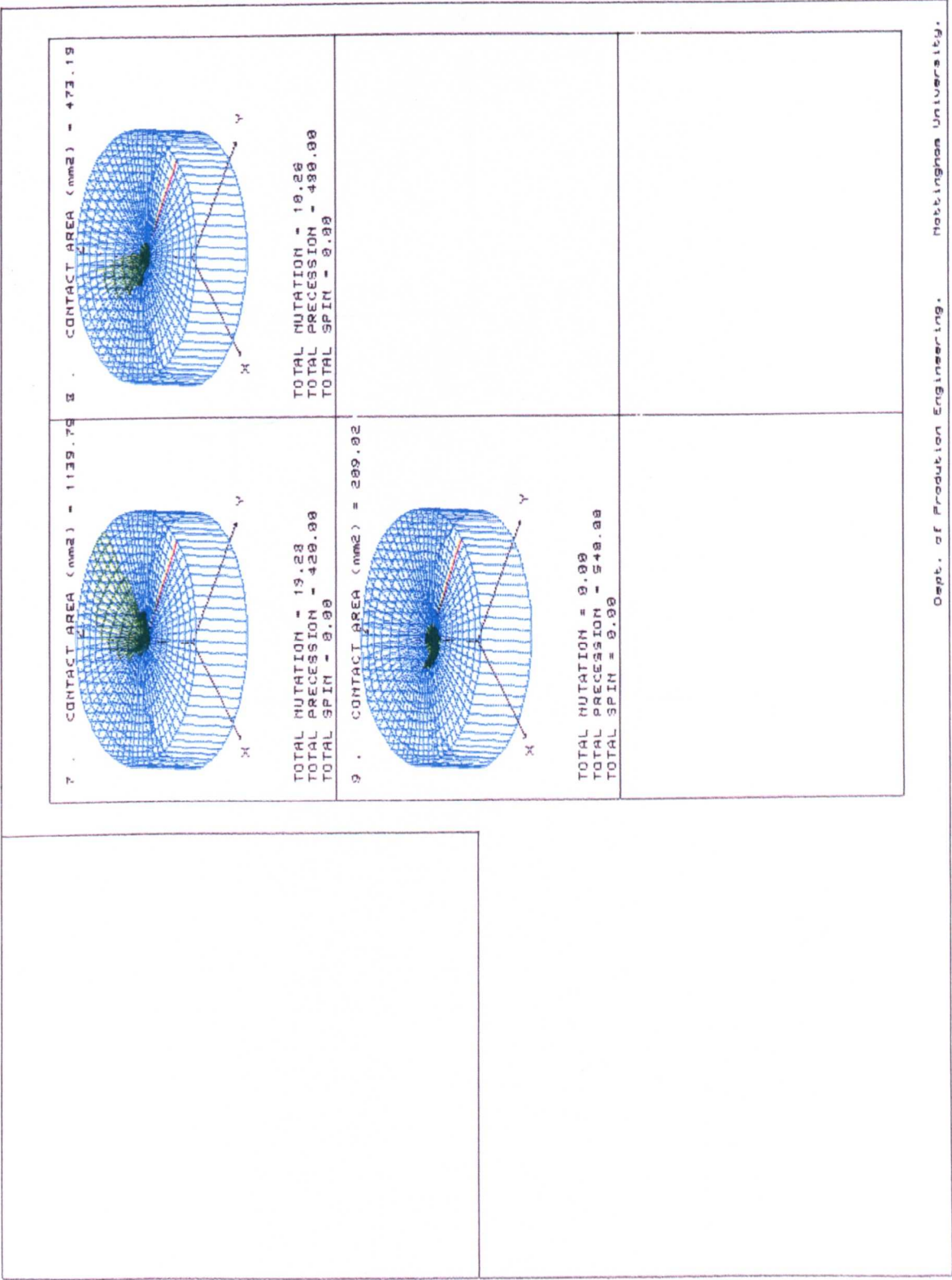


Figure 7.11 Shows a Spiral Pattern of Tool Axis Movement Produced By the Non - Monotonic Nutation - Precession Motion. The Nutation Rate = 100 c.p.m. and the Precession Rate = 300 c.p.m.

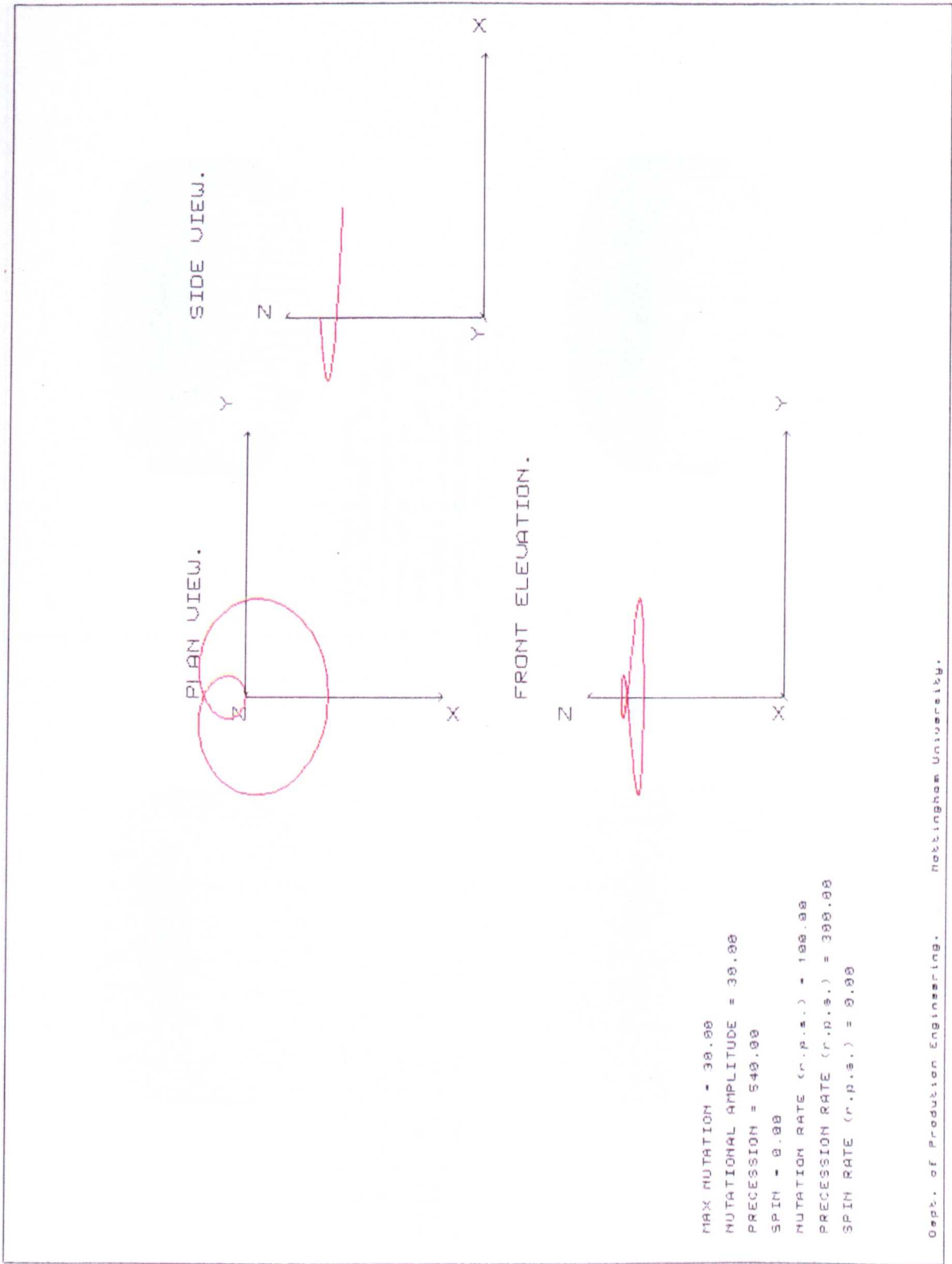


Figure 7.12 - a. Shows the Contact Geometry on the Surface of a Workpiece During the First Cycle of a Non - Monotonic Nutation Motion. The Nutation Rate = 33 c.p.m., Producing a Straight Line Pattern of Tool Axis Movement.

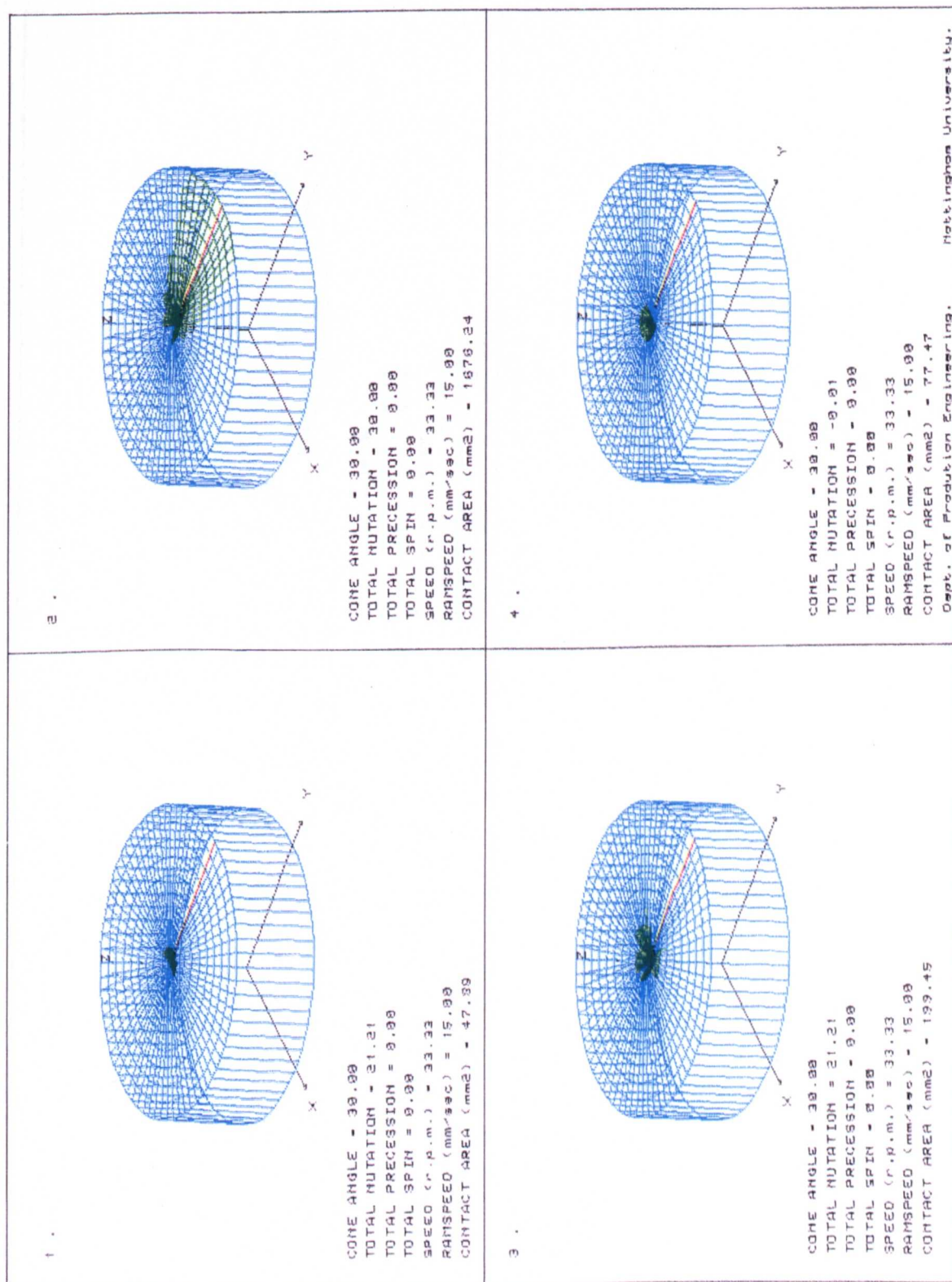


Figure 7.12 - b. Shows the Contact Geometry on the Surface of a Workpiece During the First Cycle of a Non - Monotonic Nutation Motion. The Nutation Rate = 33 c.p.m., Producing a Straight Line Pattern of Tool Axis Movement.

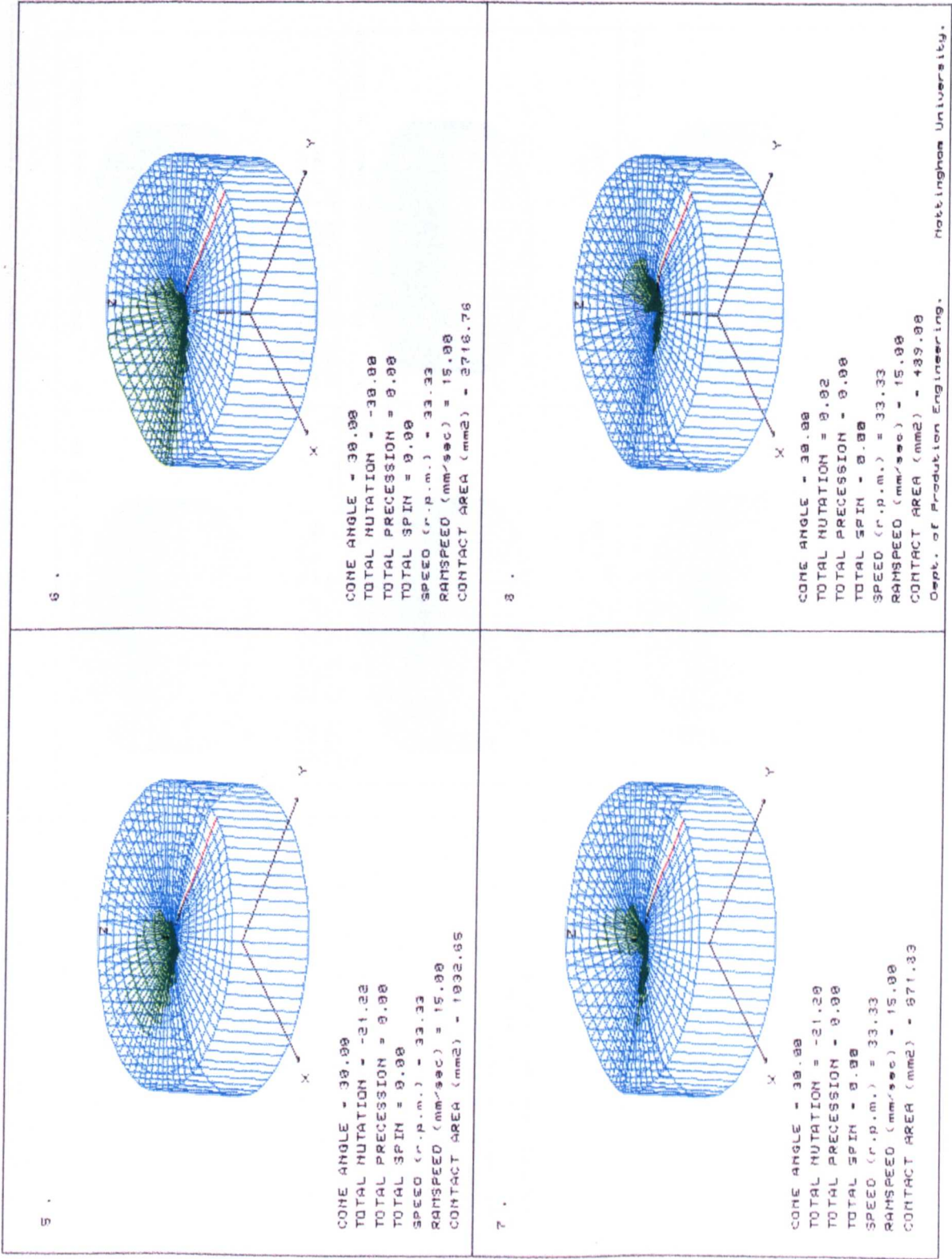


Figure 7.13. The Contact Geometries Produced During the Nutation - Spin Motion. The Upper Conic Die Speed = 100 c.p.m., and the Lower Die Speed = 86.8 c.p.m.

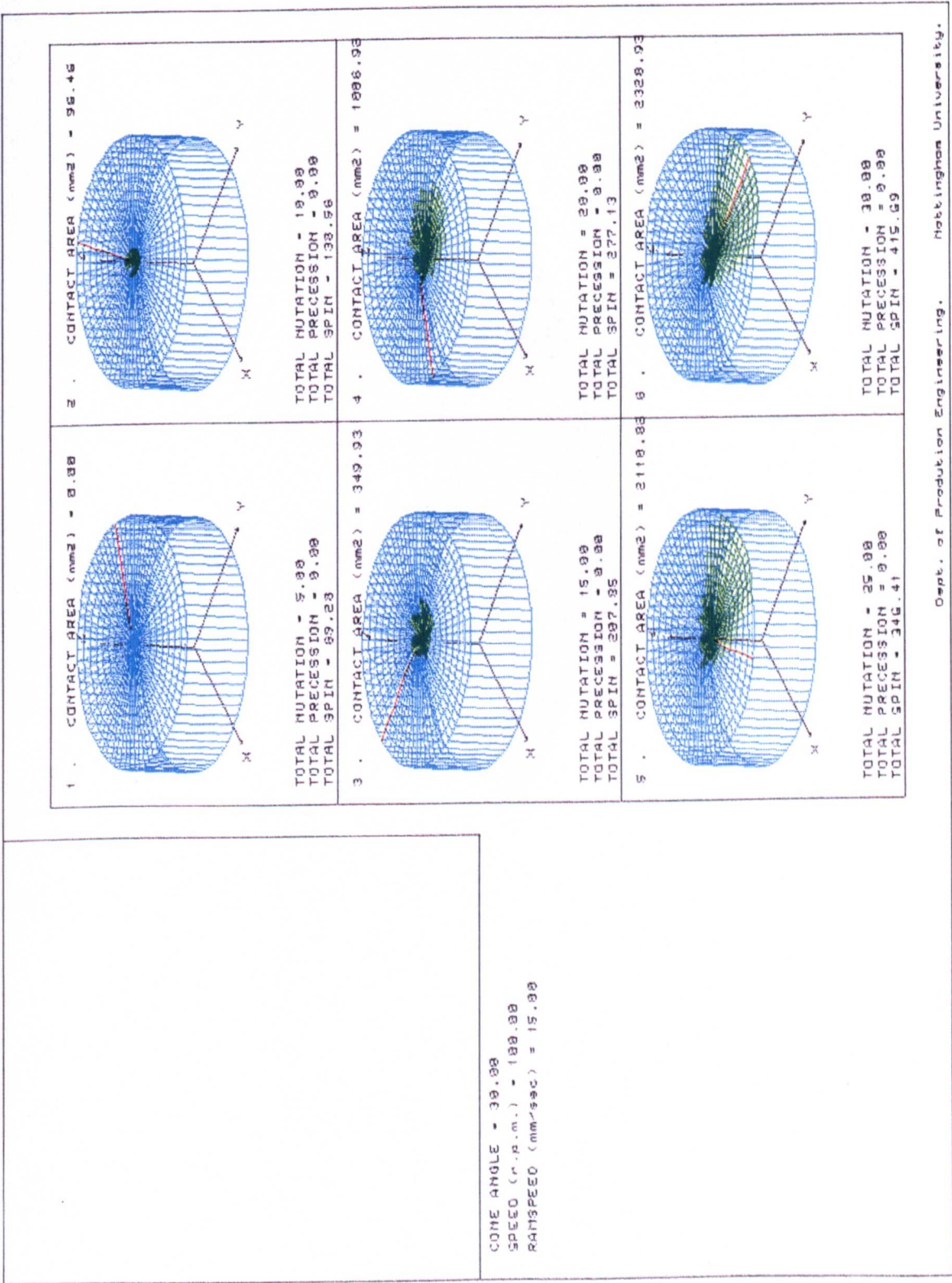


Figure 7.14 A Radially Profiled Tool Generated From Profile 4 of Figure 6.3, Incorporated into a Plain 30° Degree Cone.

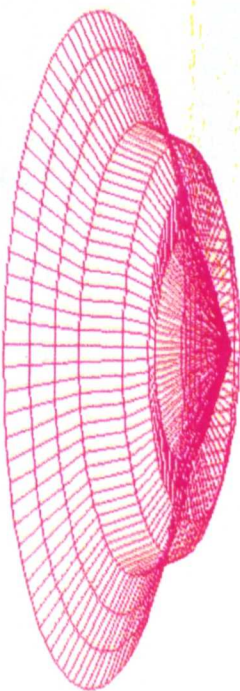


Figure 7.15 The Contact Geometries Produced By the Preprocessing Radially Profiled Tool, Shown in Figure 7.14.

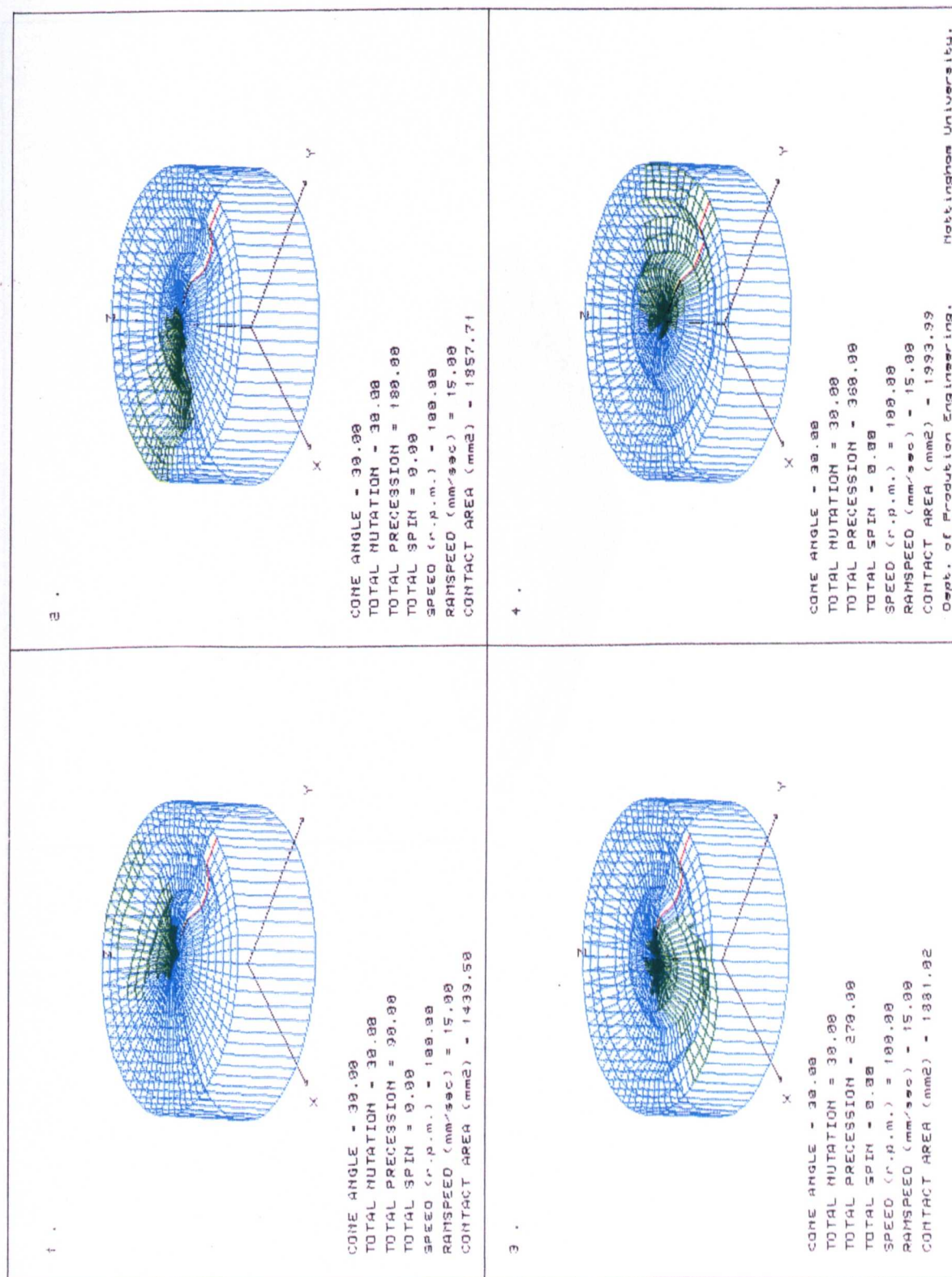


Figure 7.16 A Circumferentially Profiled Tool Generated From Profile 2 of Figure 6.5,
Incorporated into a Plain 30° Degree Cone.

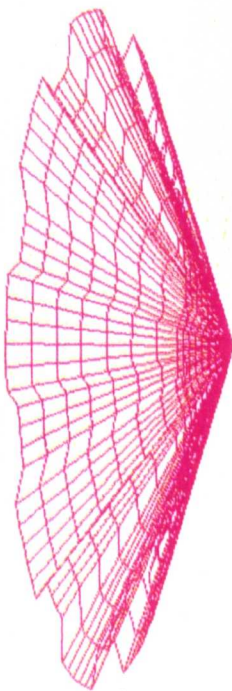


Figure 7.17 The Contact Geometries Produced By the Preprocessing Circumferentially Profiled Tool, Shown in Figure 7.16.

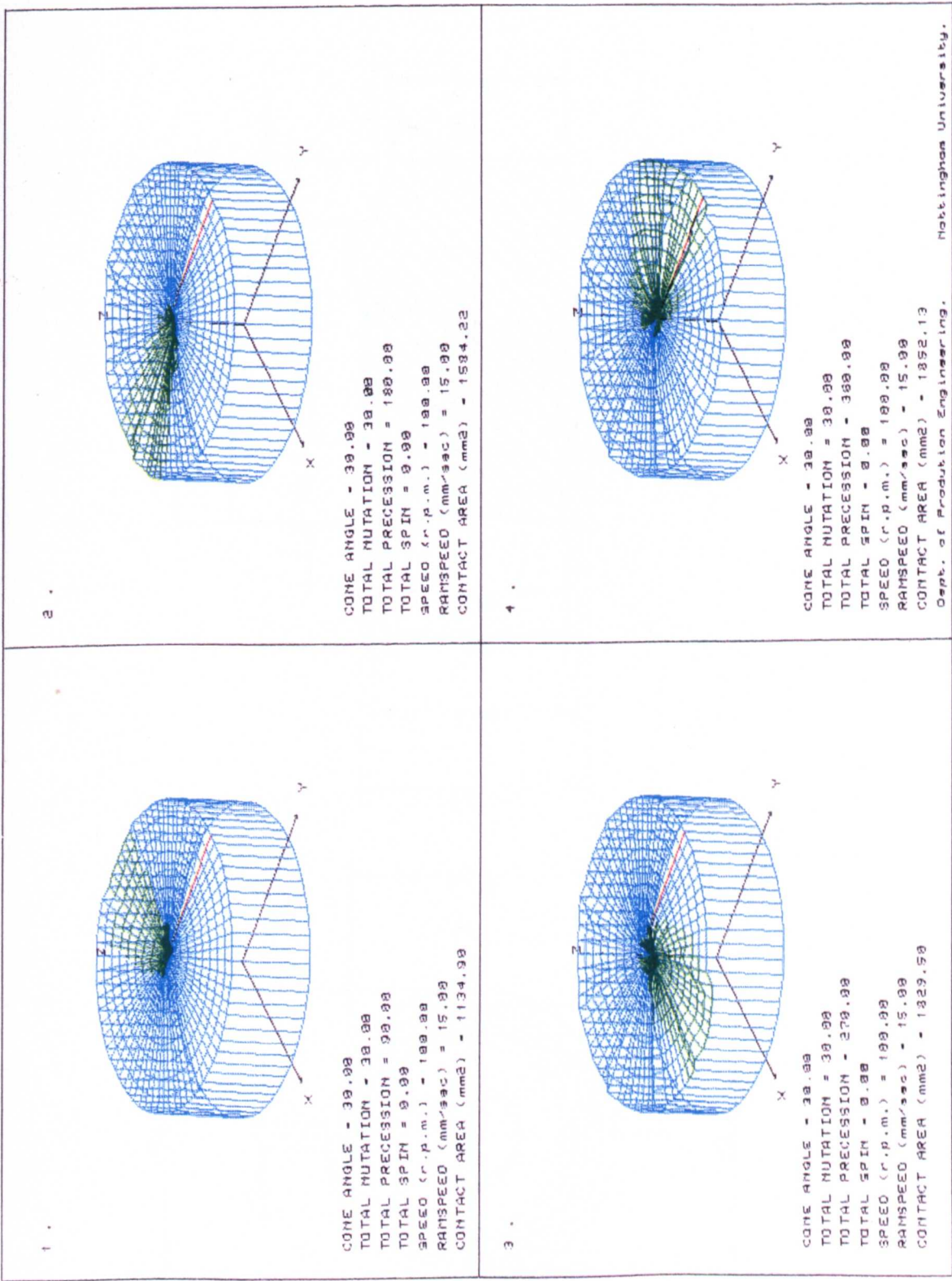


Figure 7.18 The Production Part Produced By a 200 Tonne Schmid Rotary Forging Machine.

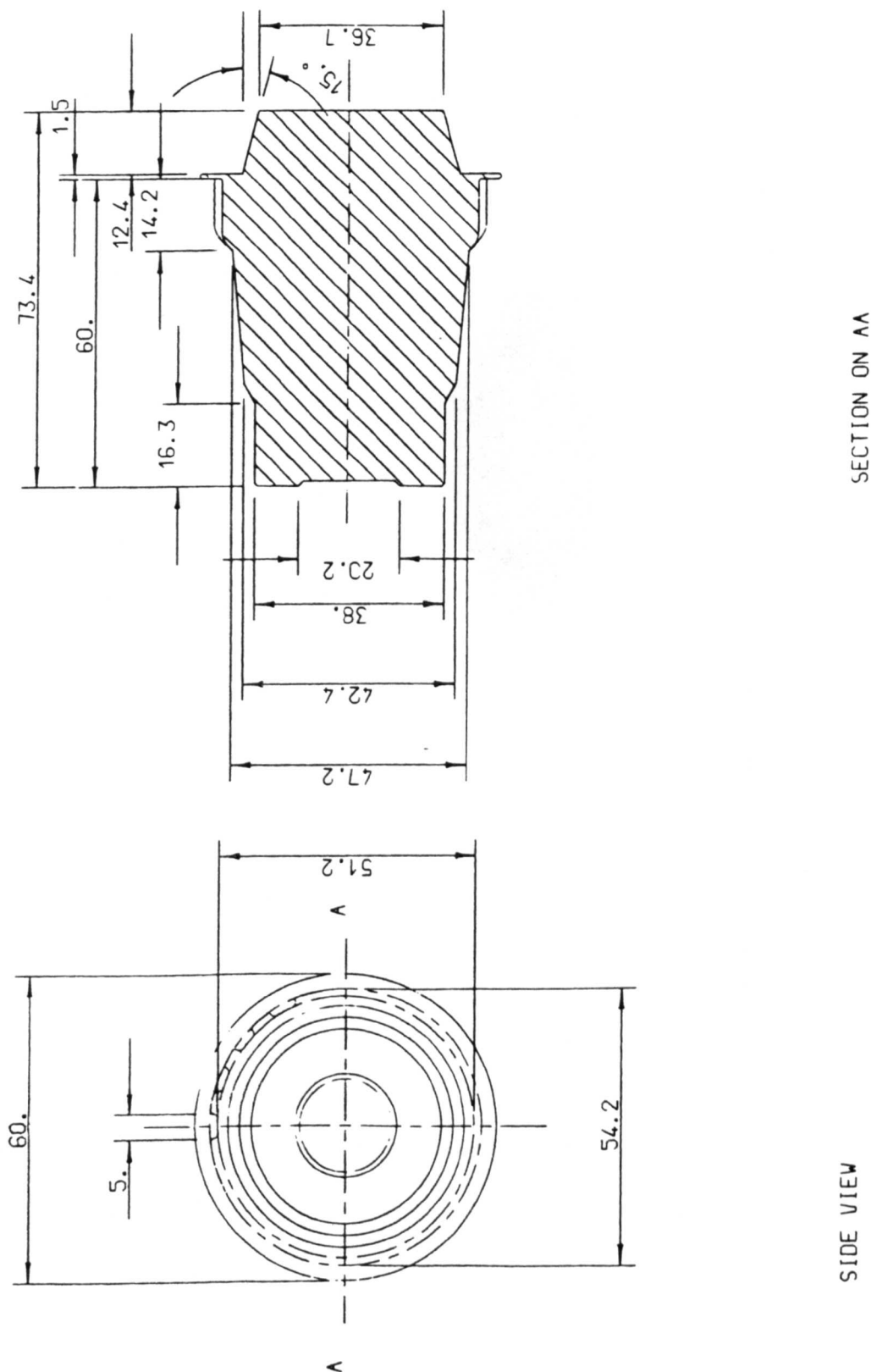


Figure 7.19. The Custom Made Upper Die Generated By the Pre - Processor PROFS, For the Simulation of the 200 Tonne Schmid Machine.

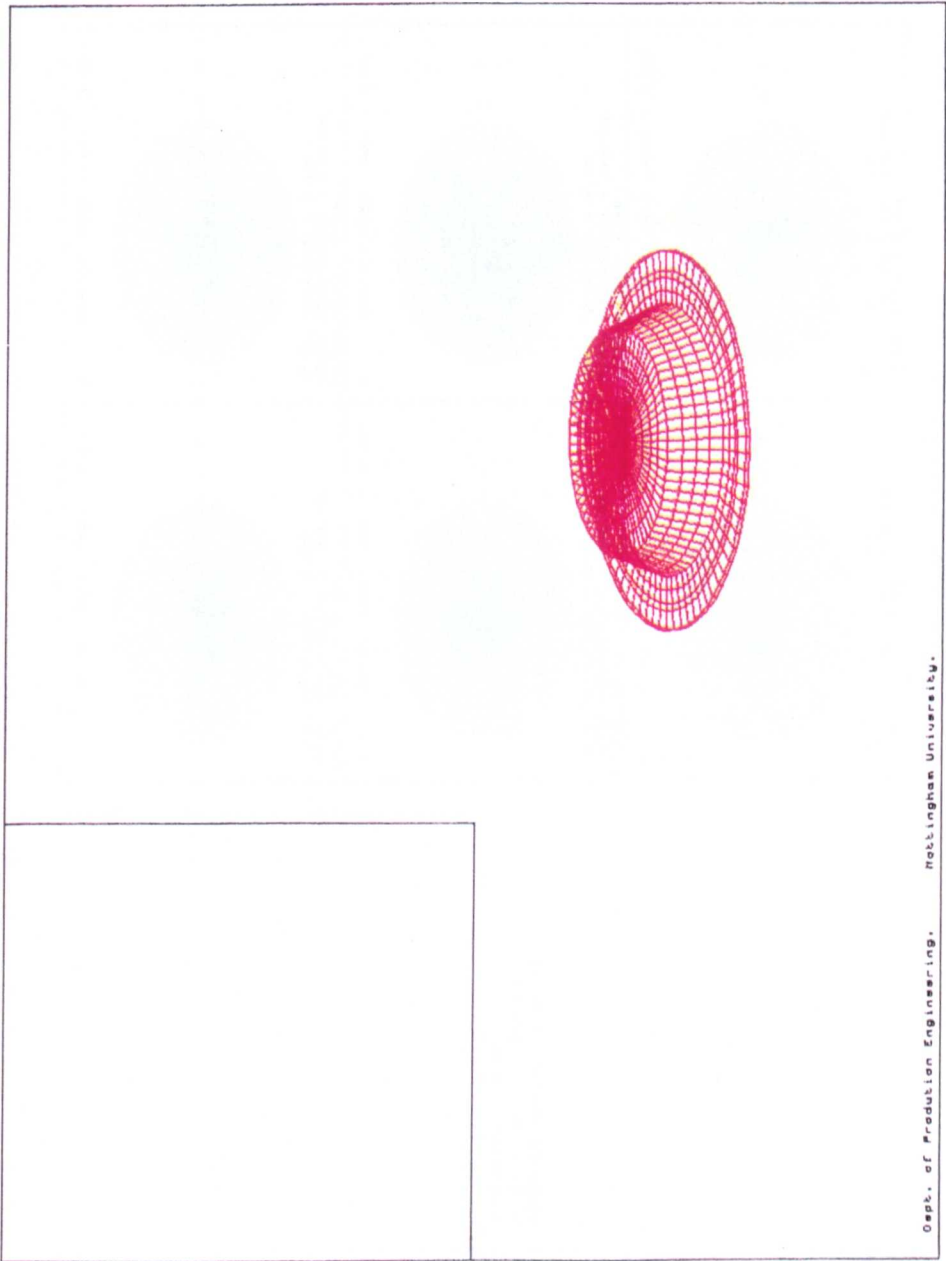


Figure 7.20 - a. The Contact Geometries Produced on a 37.8 mm Diameter Workpiece During the Stage i. of the Simulation of a Real Rotary Forging Process.

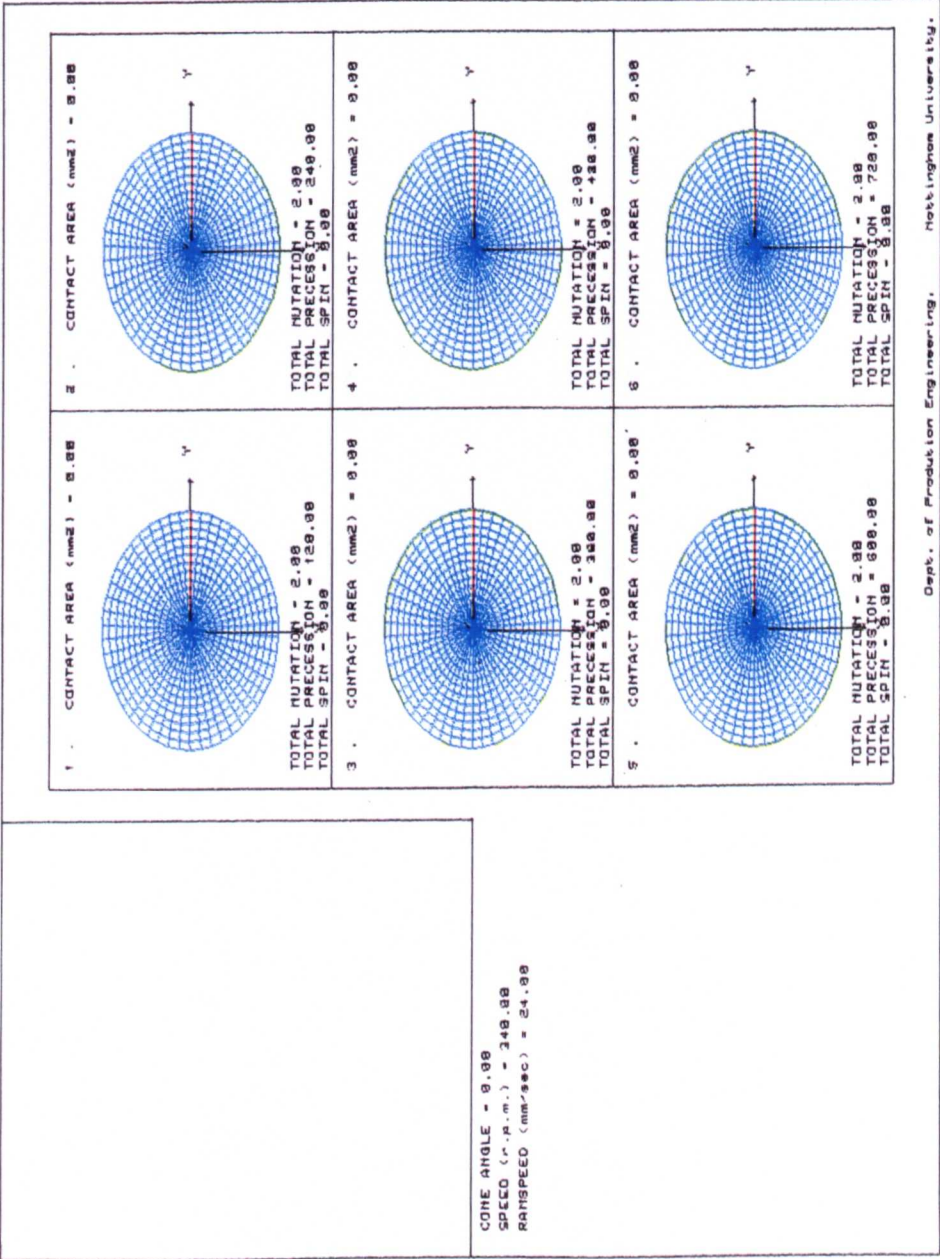


Figure 7.20 - b. The Contact Geometries Produced on a 37.8 mm Diameter Workpiece During the Stage i. of the Simulation of a Real Rotary Forging Process.

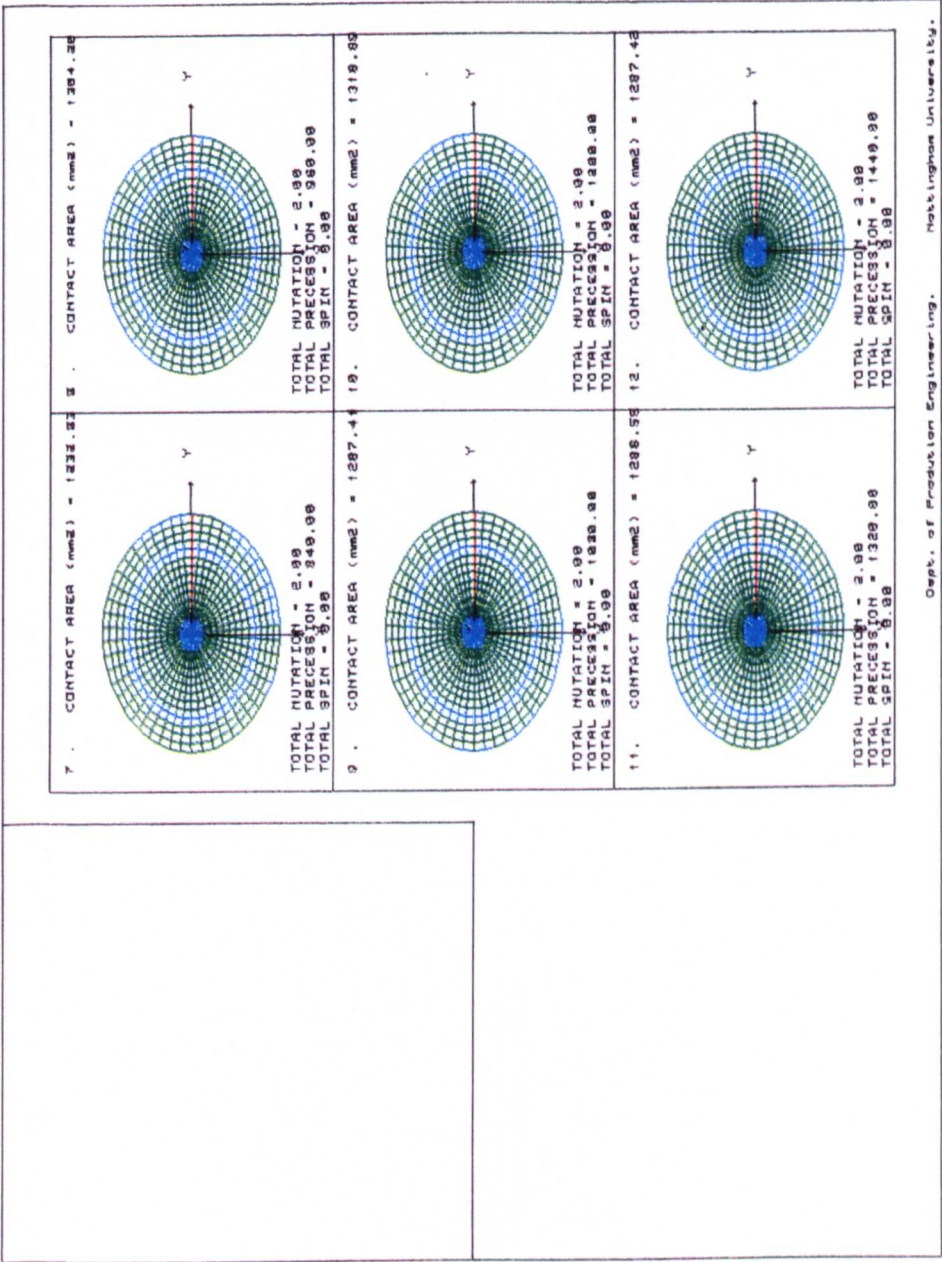


Figure 7.21 - a. The Contact Geometries Produced on a 46.0 mm Diameter Workpiece During the Stage ii. of the Simulation of a Real Rotary Forging Process.

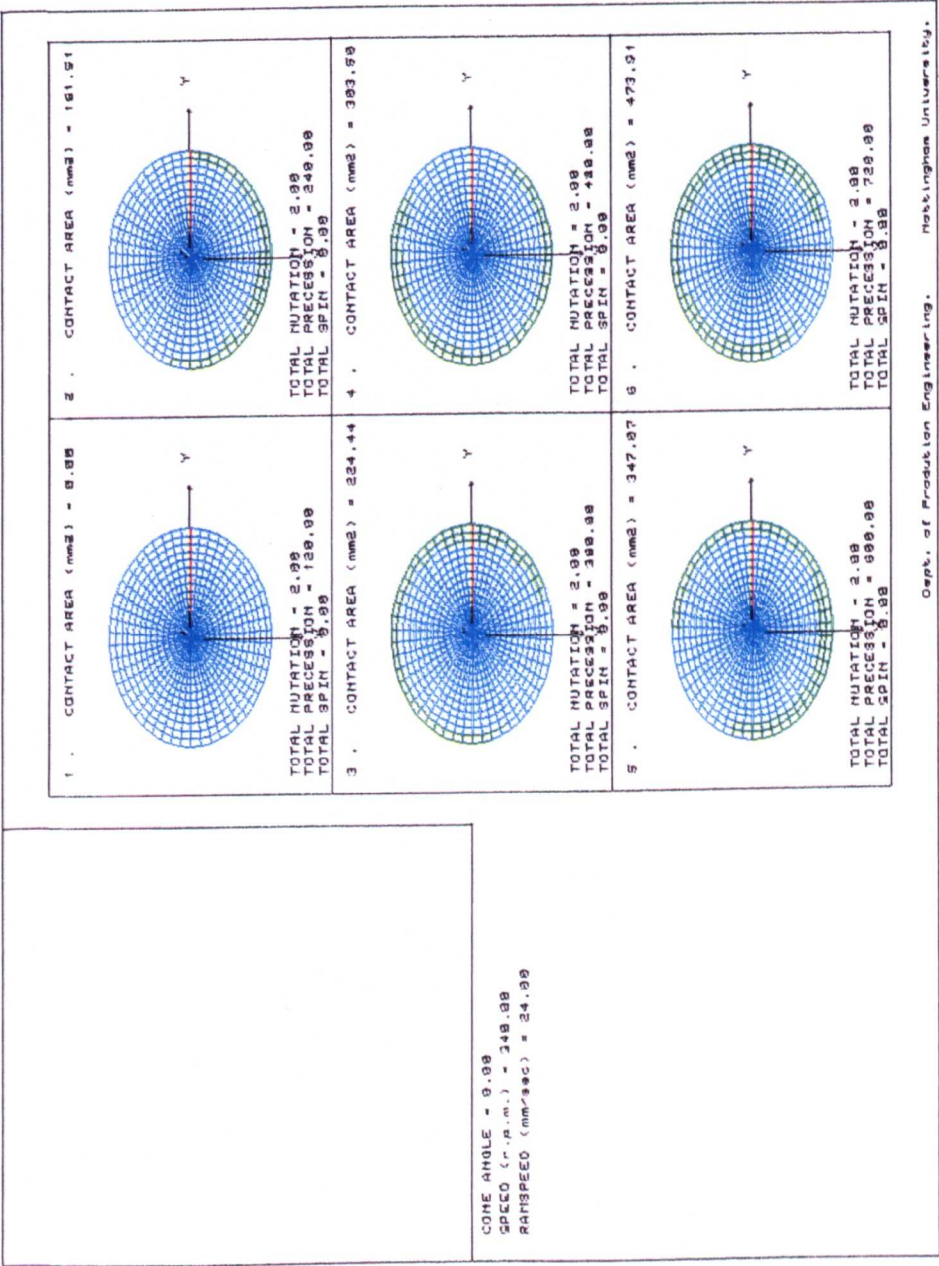


Figure 7.21 - b. The Contact Geometries Produced on a 46.0 mm Diameter Workpiece During the Stage ii. of the Simulation of a Real Rotary Forging Process.

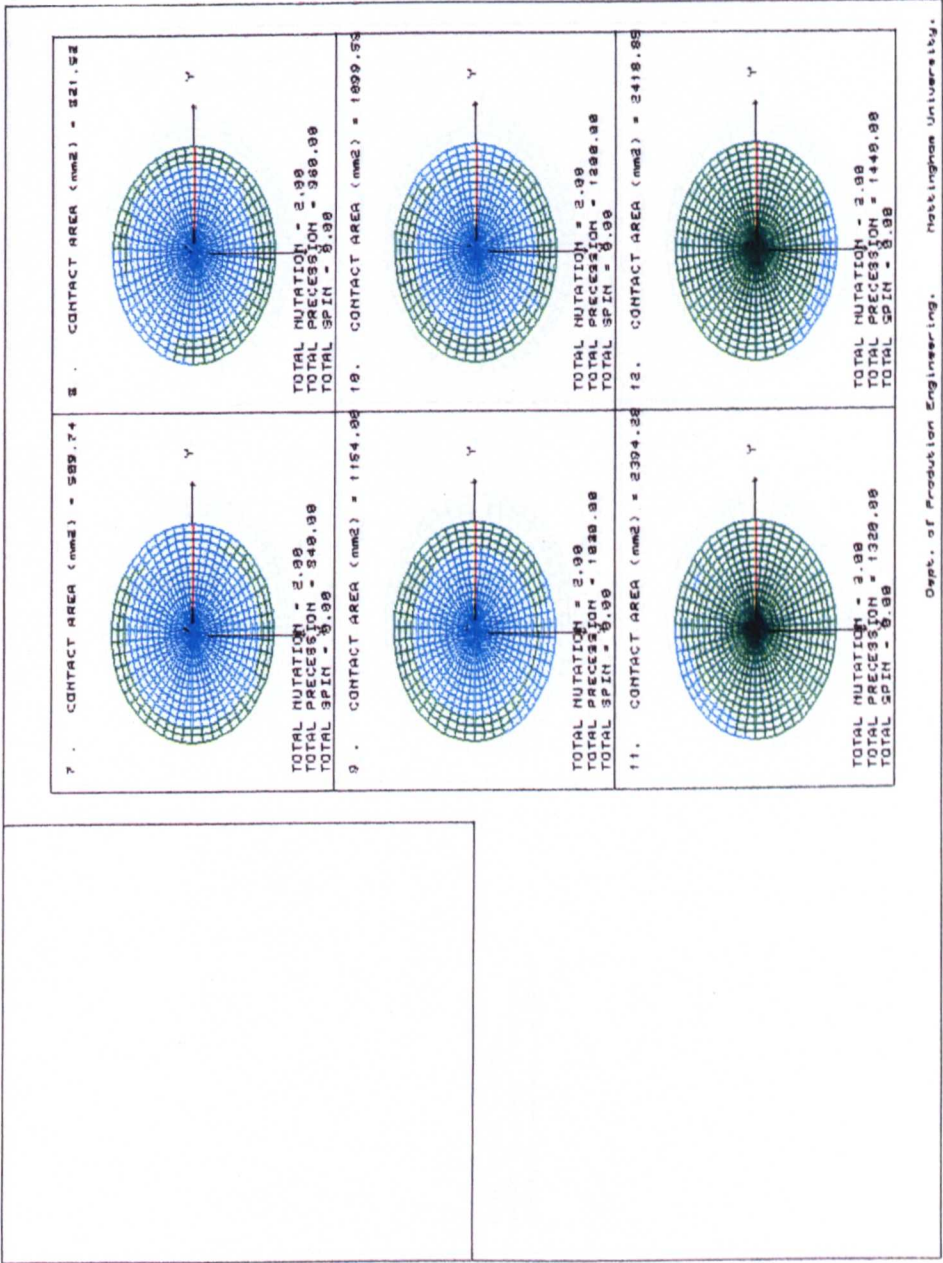
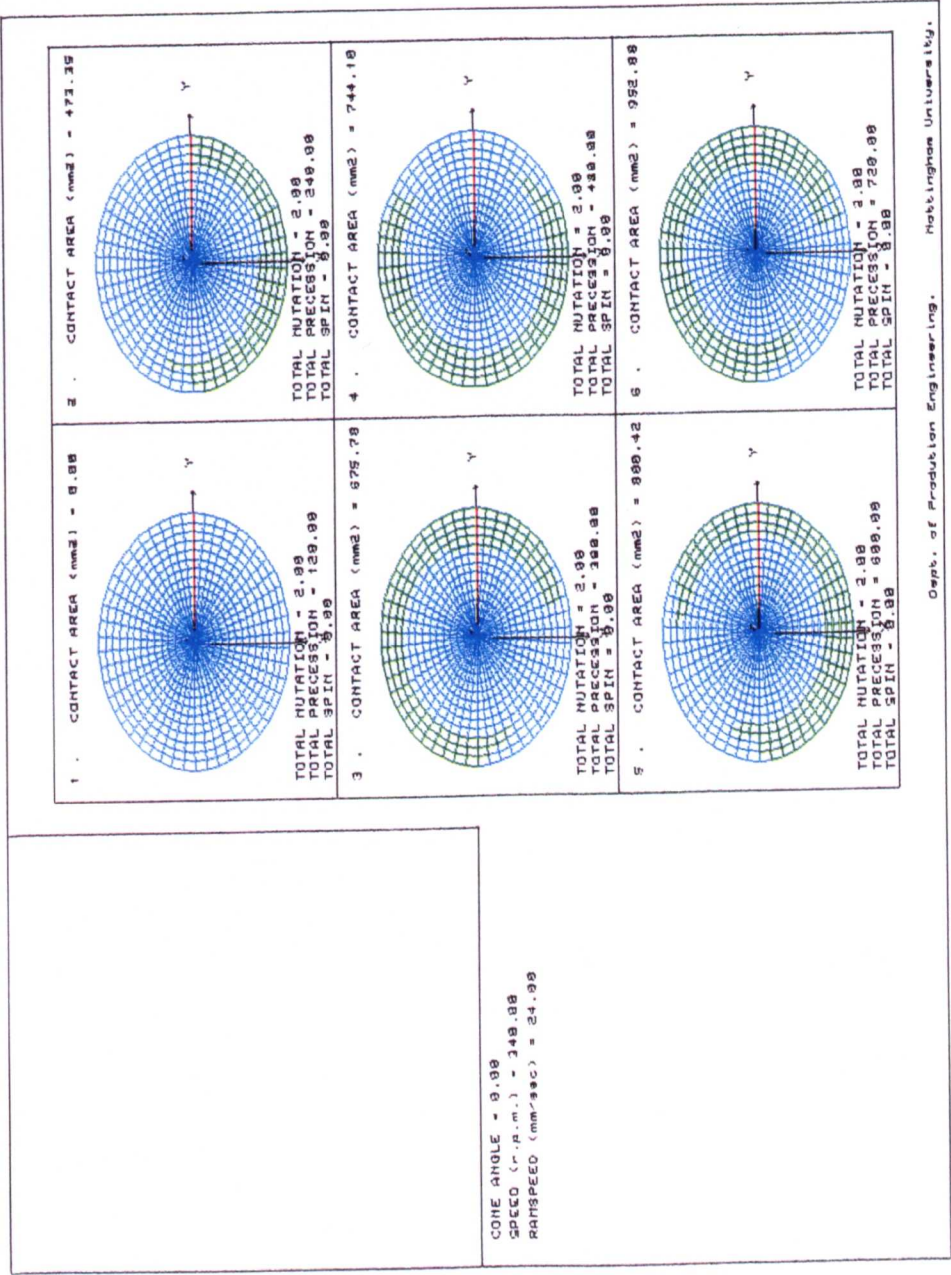


Figure 7.22 - a. The Contact Geometries Produced on a 54.2 mm Diameter Workpiece During the Stage iii. of the Simulation of a Real Rotary Forging Process.



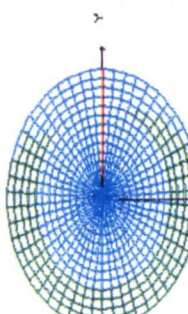

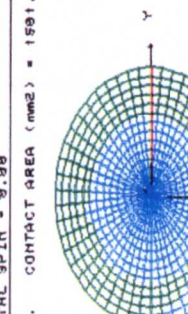
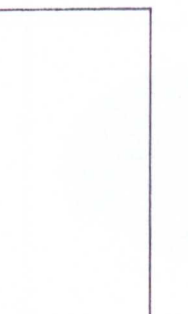
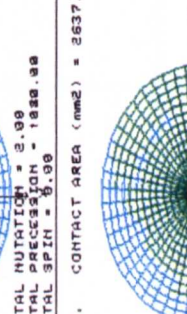

7. CONTACT AREA (mm2) = 272.44	 <p>TOTAL MUTATION = 2.98 TOTAL PRECESSION = 348.98 TOTAL SPIN = 8.98</p>	8. CONTACT AREA (mm2) = 1589.82	 <p>TOTAL MUTATION = 2.98 TOTAL PRECESSION = 988.98 TOTAL SPIN = 8.98</p>
9. CONTACT AREA (mm2) = 1591.96	 <p>TOTAL MUTATION = 2.98 TOTAL PRECESSION = 1888.98 TOTAL SPIN = 8.98</p>	10. CONTACT AREA (mm2) = 1516.89	 <p>TOTAL MUTATION = 2.98 TOTAL PRECESSION = 1888.98 TOTAL SPIN = 8.98</p>
11. CONTACT AREA (mm2) = 2637.93	 <p>TOTAL MUTATION = 2.98 TOTAL PRECESSION = 1328.98 TOTAL SPIN = 8.98</p>	12. CONTACT AREA (mm2) = 2598.33	 <p>TOTAL MUTATION = 2.98 TOTAL PRECESSION = 1448.98 TOTAL SPIN = 8.98</p>

Figure 7.23. Showing the Development of the Contact Geometries Throughout a Typical Rotary Forging Operation, using a Simulated Non - Constant Volume Model Workpiece.



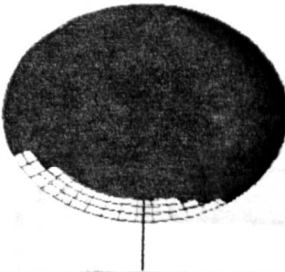
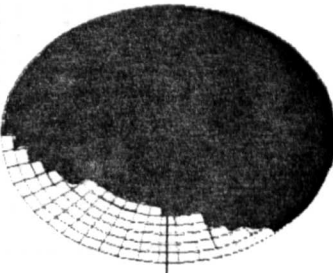
Workpiece Height (mm)	No. of Die Cycles	Stage	Contact Geometry	Contact Area (mm ²)	Volume Displaced (mm ³)
100.7	0.667	i		Line Contact	Line Contact
83.76	4.0	i		1287.42	3122.49
68.0	7.72	ii		2418.85	4236.96
49.0	12.2	iii		2598.33	8947.35

Figure 8.1 - a. Results For the 200 Tonne Precession Machine Simulations Showing the Progression of the Contact Geometry Throughout the Whole Simulation.

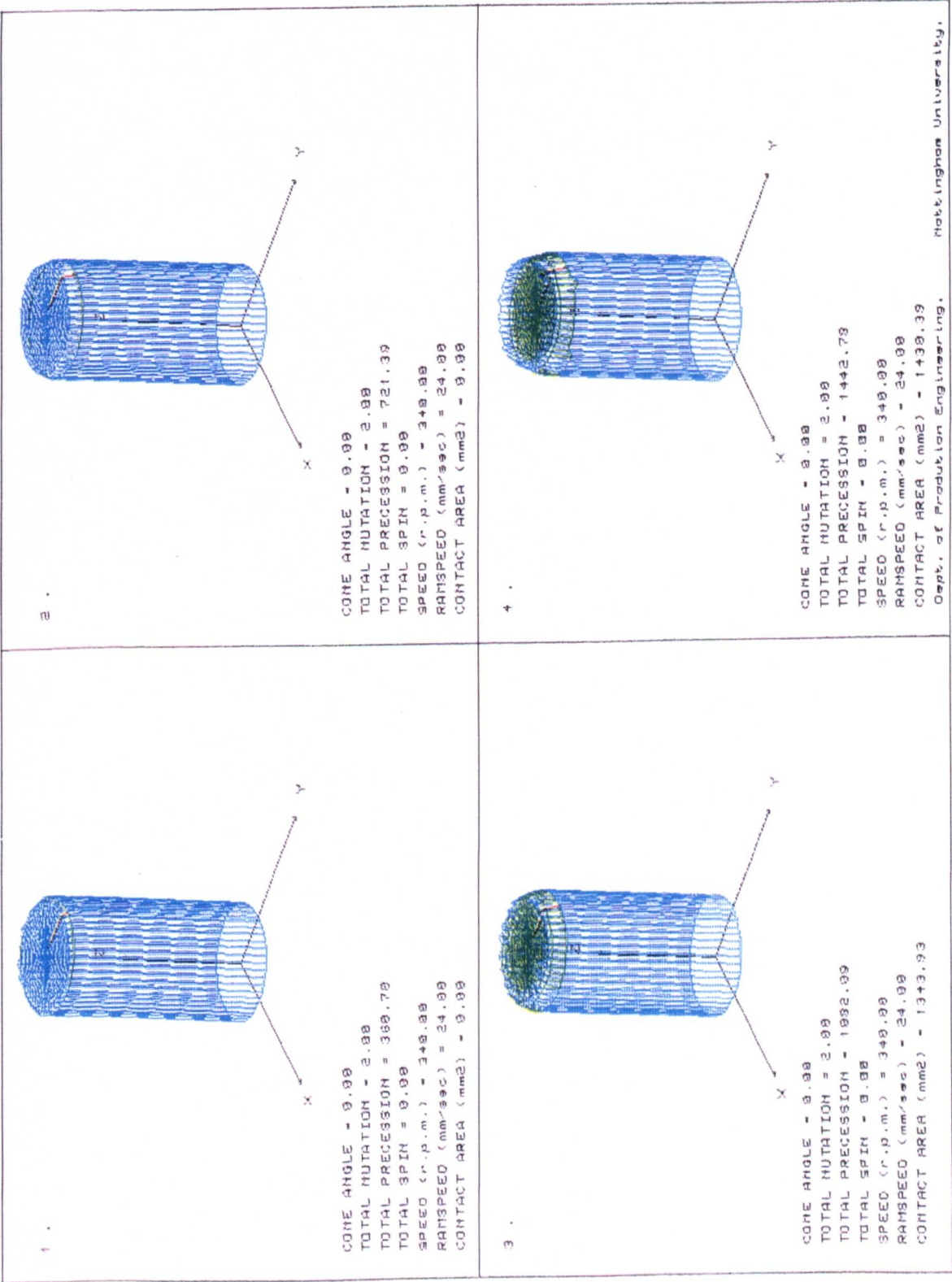


Figure 8.1 - b. Results For the 200 Tonne Precession Machine Simulations Showing the Progression of the Contact Geometry Throughout the Whole Simulation.

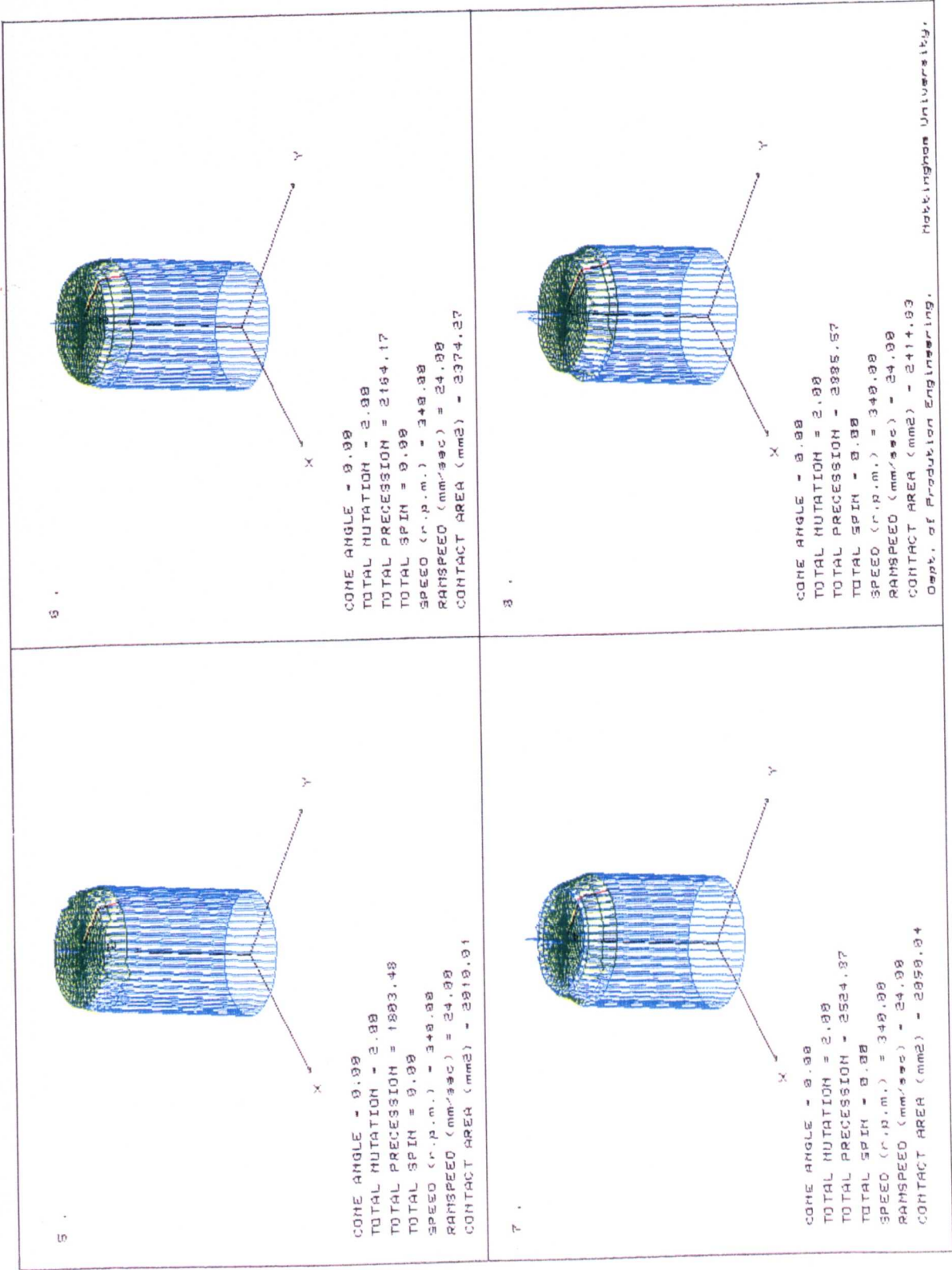


Figure 8.1 - c. Results For the 200 Tonne Precession Machine Simulations Showing the Progression of the Contact Geometry Throughout the Whole Simulation.

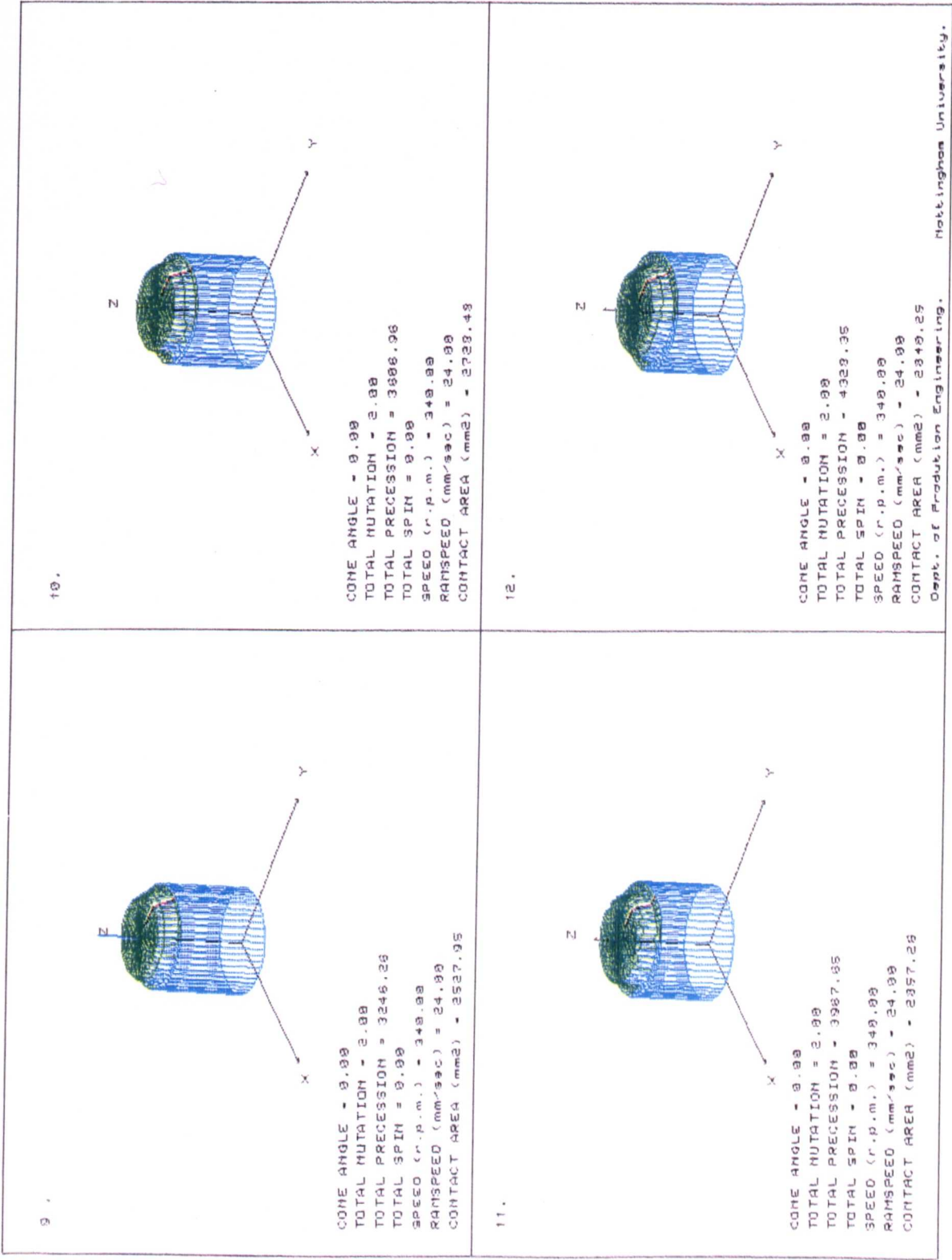


Figure 8.1 - d. Results For the 200 Tonne Precession Machine Simulations Showing the Progression of the Contact Geometry Throughout the Whole Simulation.

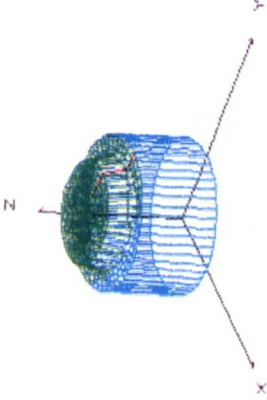
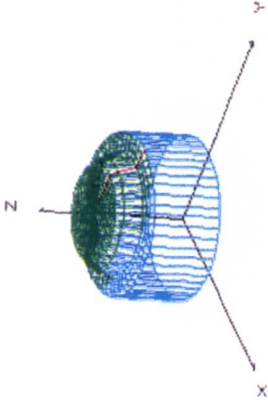
<div>13.</div> <div></div> <div><p>13.</p><p>CONE ANGLE = 9.00 TOTAL MUTATION = 2.00 TOTAL PRECESSION = 4689.84 TOTAL SPIN = 9.00 SPEED (r.p.m.) = 349.82 RAMSPEED (mm/sec) = 24.80 CONTACT AREA (mm2) = 3191.42</p></div>	<div>14.</div> <div></div> <div><p>14.</p><p>CONE ANGLE = 9.00 TOTAL MUTATION = 2.00 TOTAL PRECESSION = 5849.74 TOTAL SPIN = 9.00 SPEED (r.p.m.) = 349.82 RAMSPEED (mm/sec) = 24.80 CONTACT AREA (mm2) = 3125.94</p></div>
	<p>Dept. of Production Engineering. Nottingham University.</p>

Figure 8.1 - e. Results For the 200 Tonne Precession Machine Simulations Showing the Progression of the Contact Geometry Throughout the Whole Simulation.
(Plan View.)

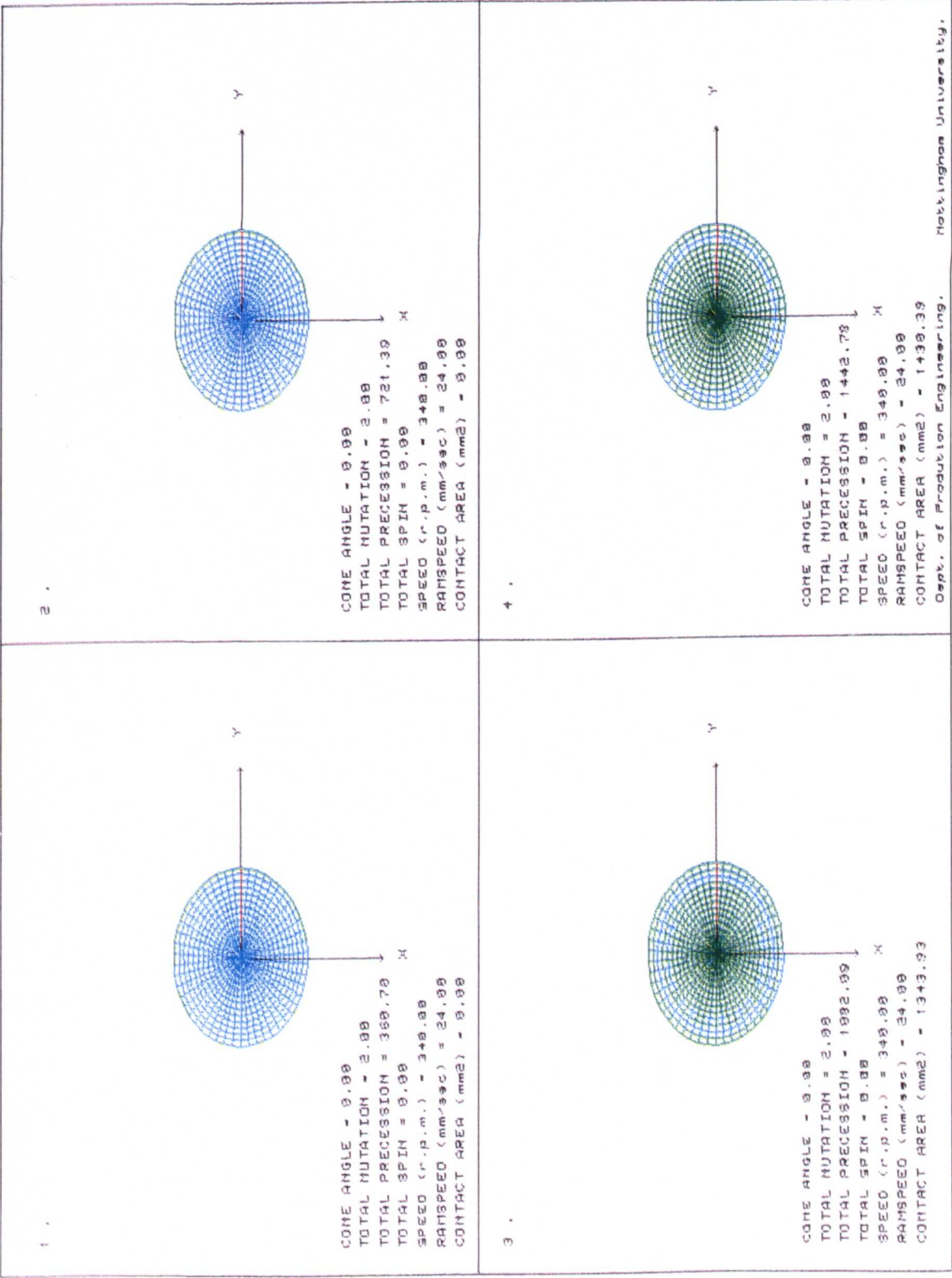


Figure 8.1 - f. Results For the 200 Tonne Precession Machine Simulations Showing the Progression of the Contact Geometry Throughout the Whole Simulation. (Plan View.)

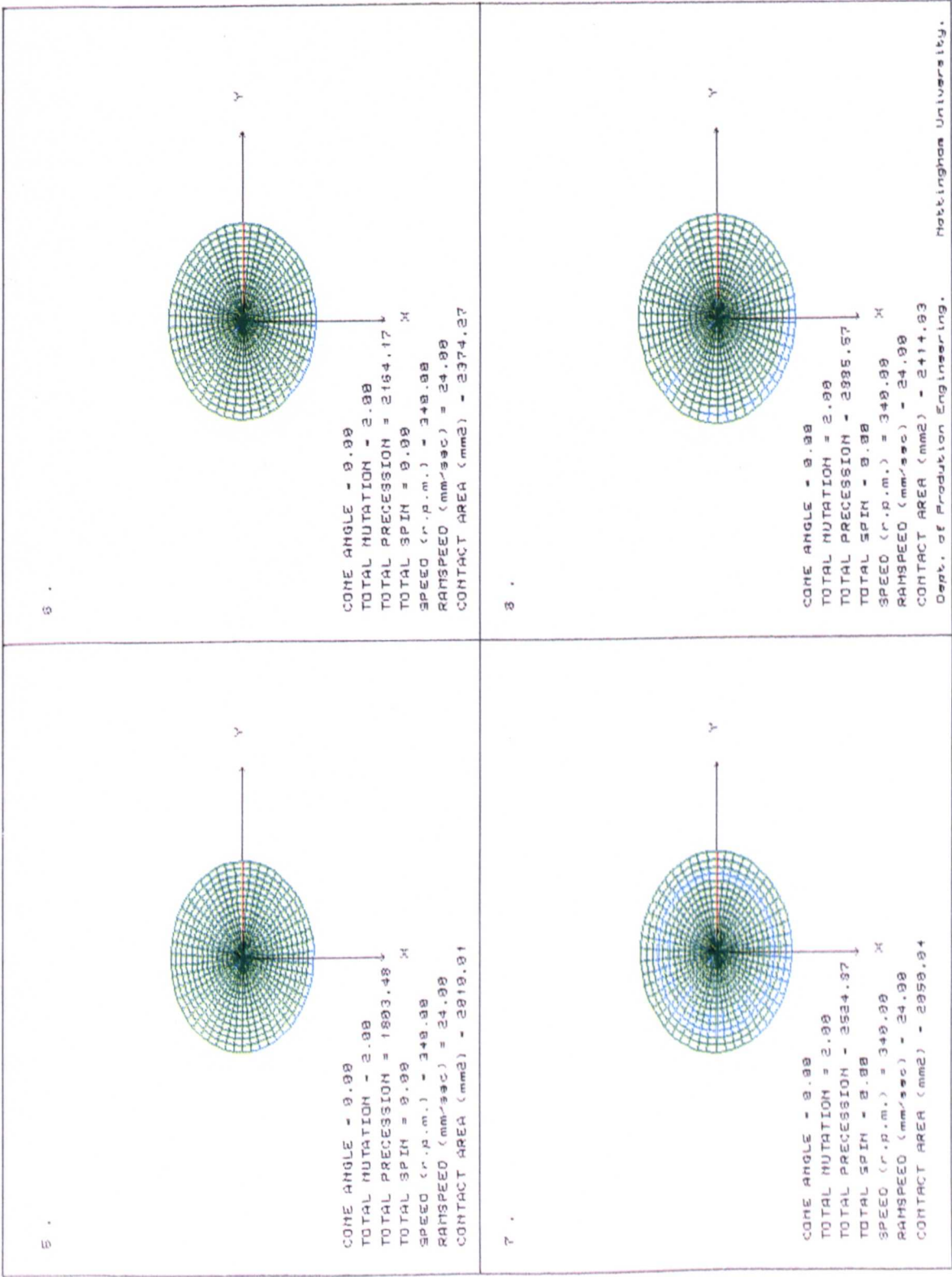


Figure 8.1 - g. Results For the 200 Tonne Precession Machine Simulations Showing the Progression of the Contact Geometry Throughout the Whole Simulation. (Plan View.)

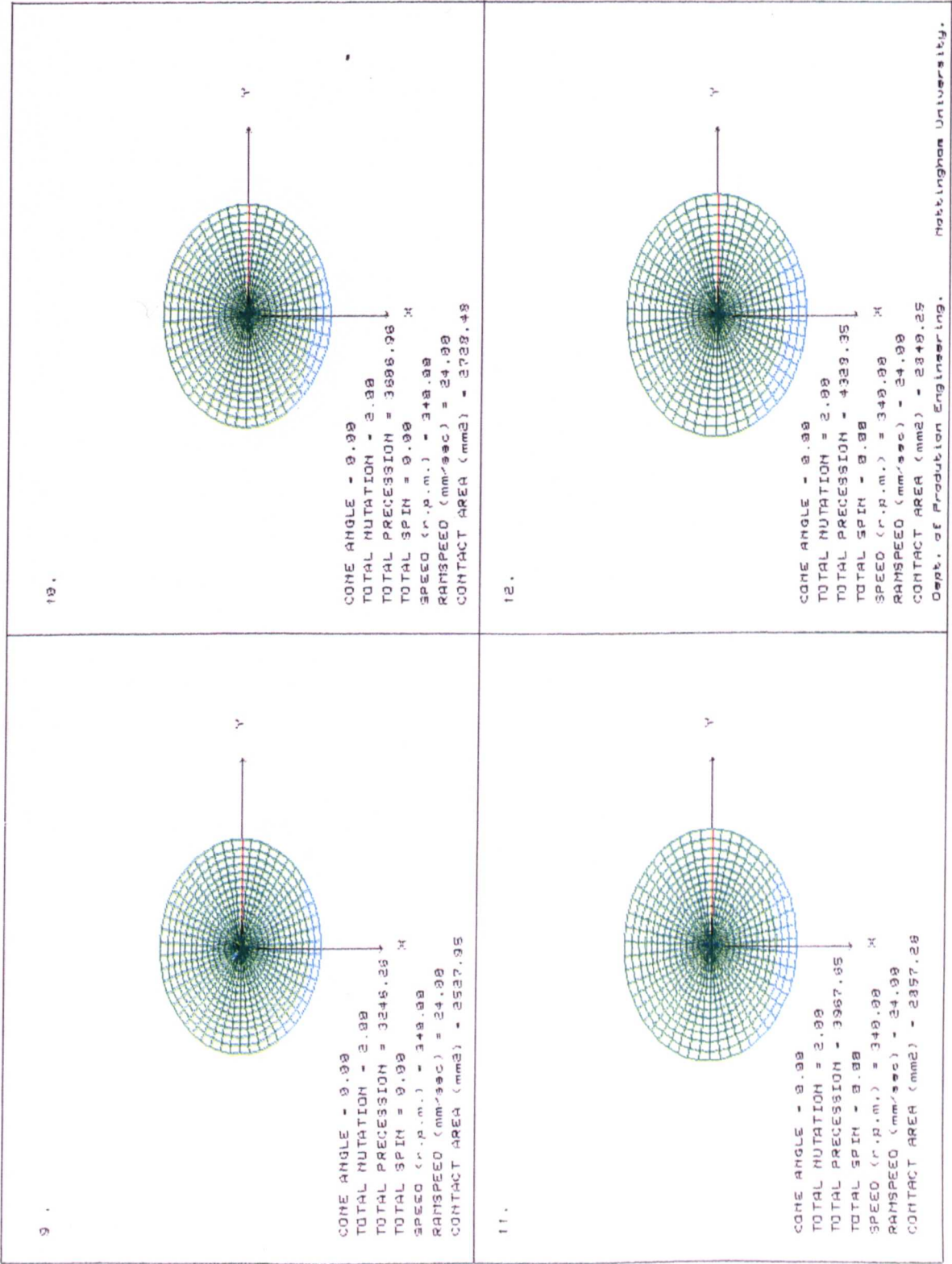


Figure 8.1 - h. Results For the 200 Tonne Precession Machine Simulations Showing the Progression of the Contact Geometry Throughout the Whole Simulation. (Plan View.)

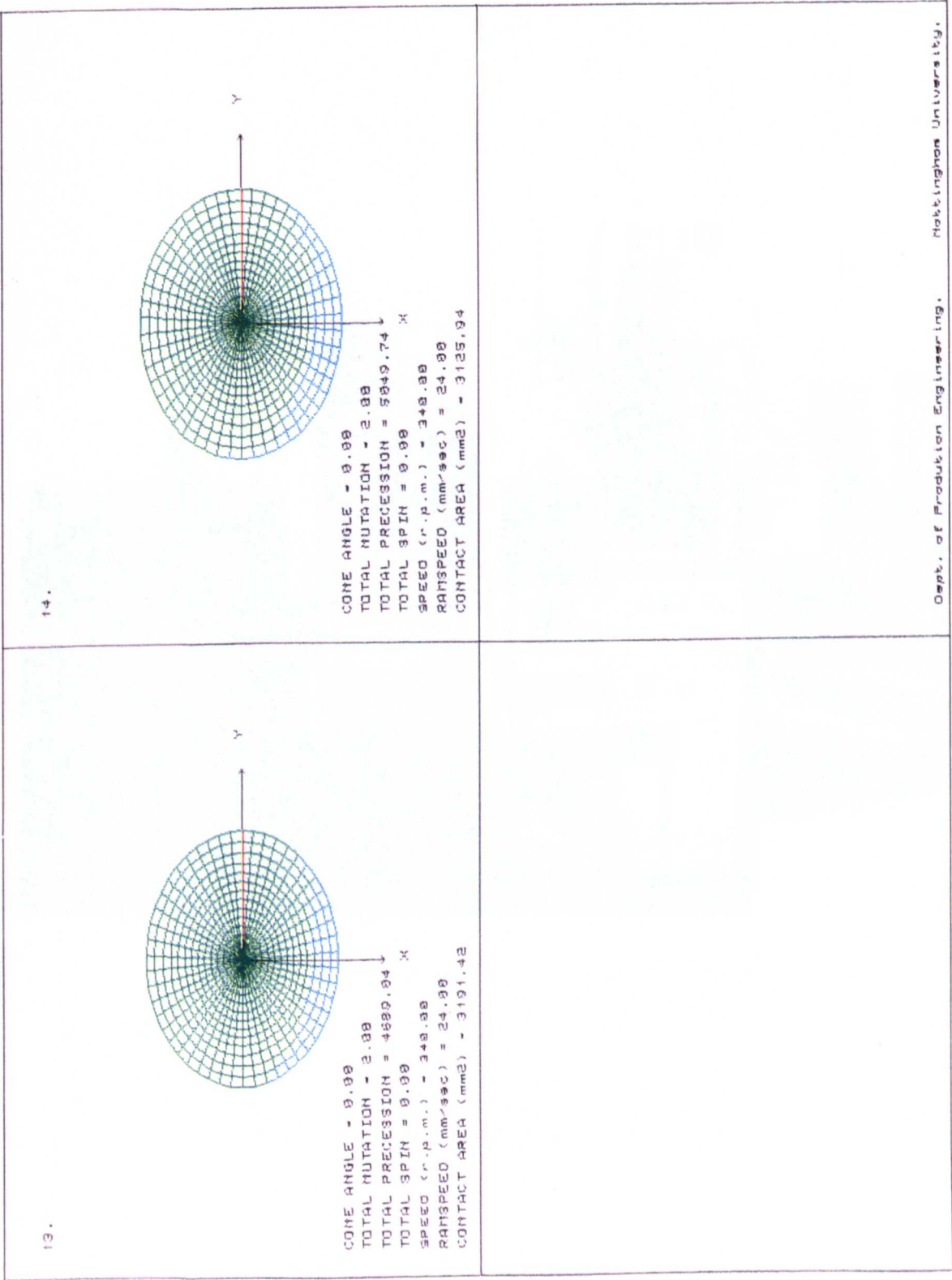


Figure 8.2 The 50 Tonne Nottingham University Rotary Forging Machine.

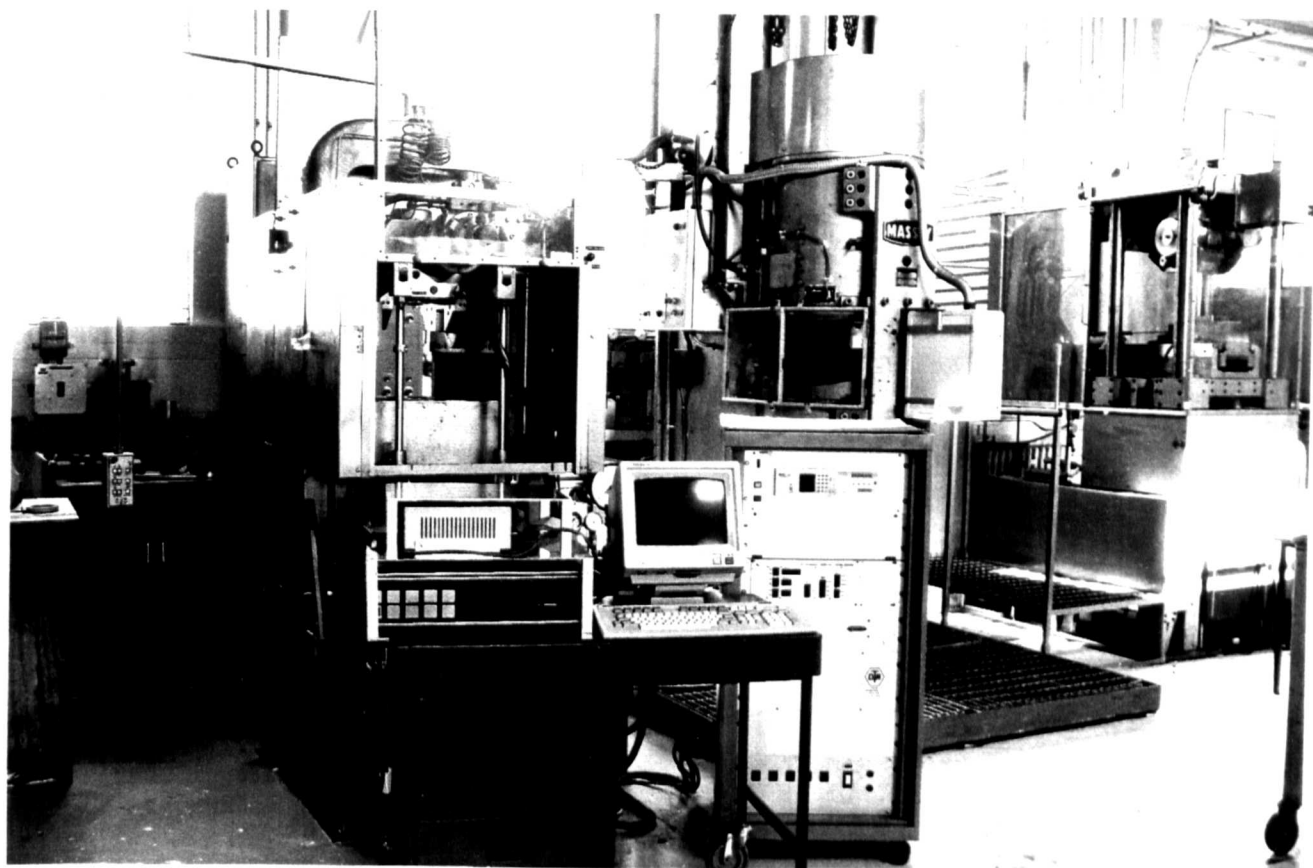


Figure 8.3 The Billet Used For the 50 Tonne Machine Experiments.

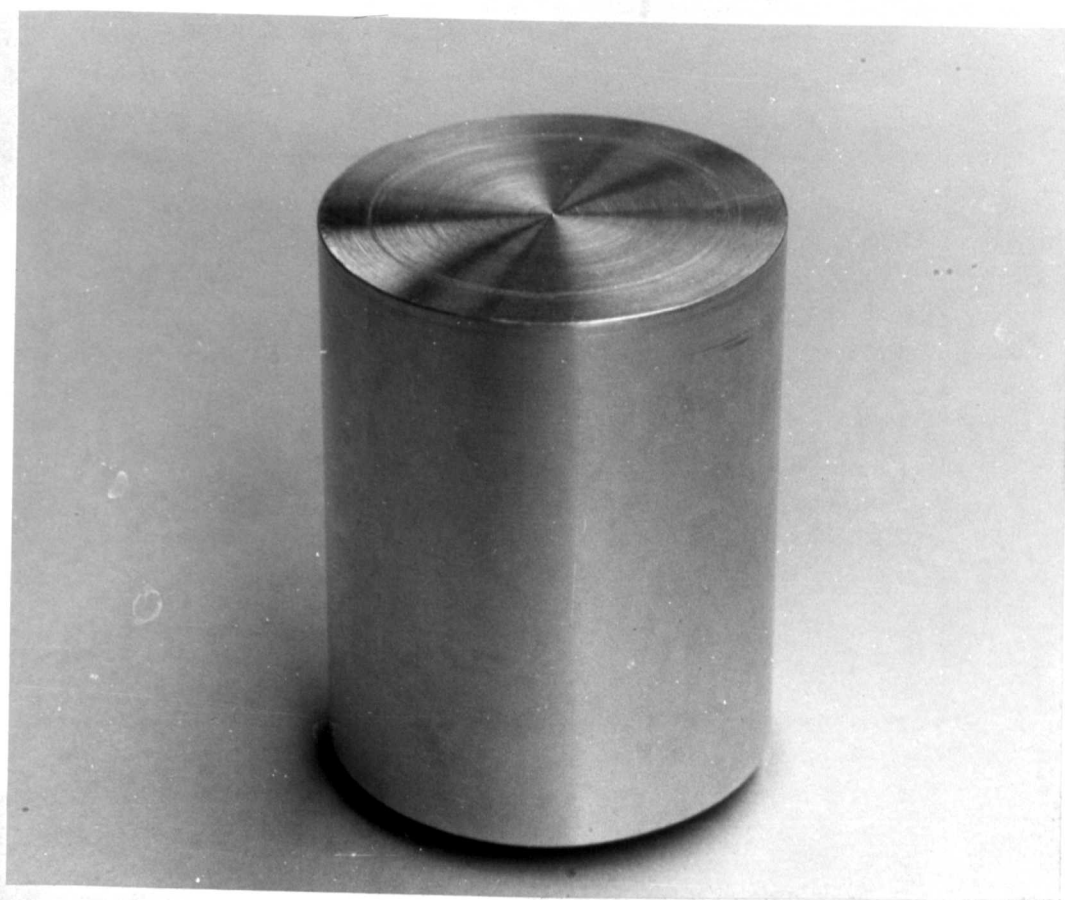


Figure 8.4 - a. The Results From the Simulation of the 50 Tonne Spin Machine Experiments
Showing the Radial Expansion of the Workpiece.

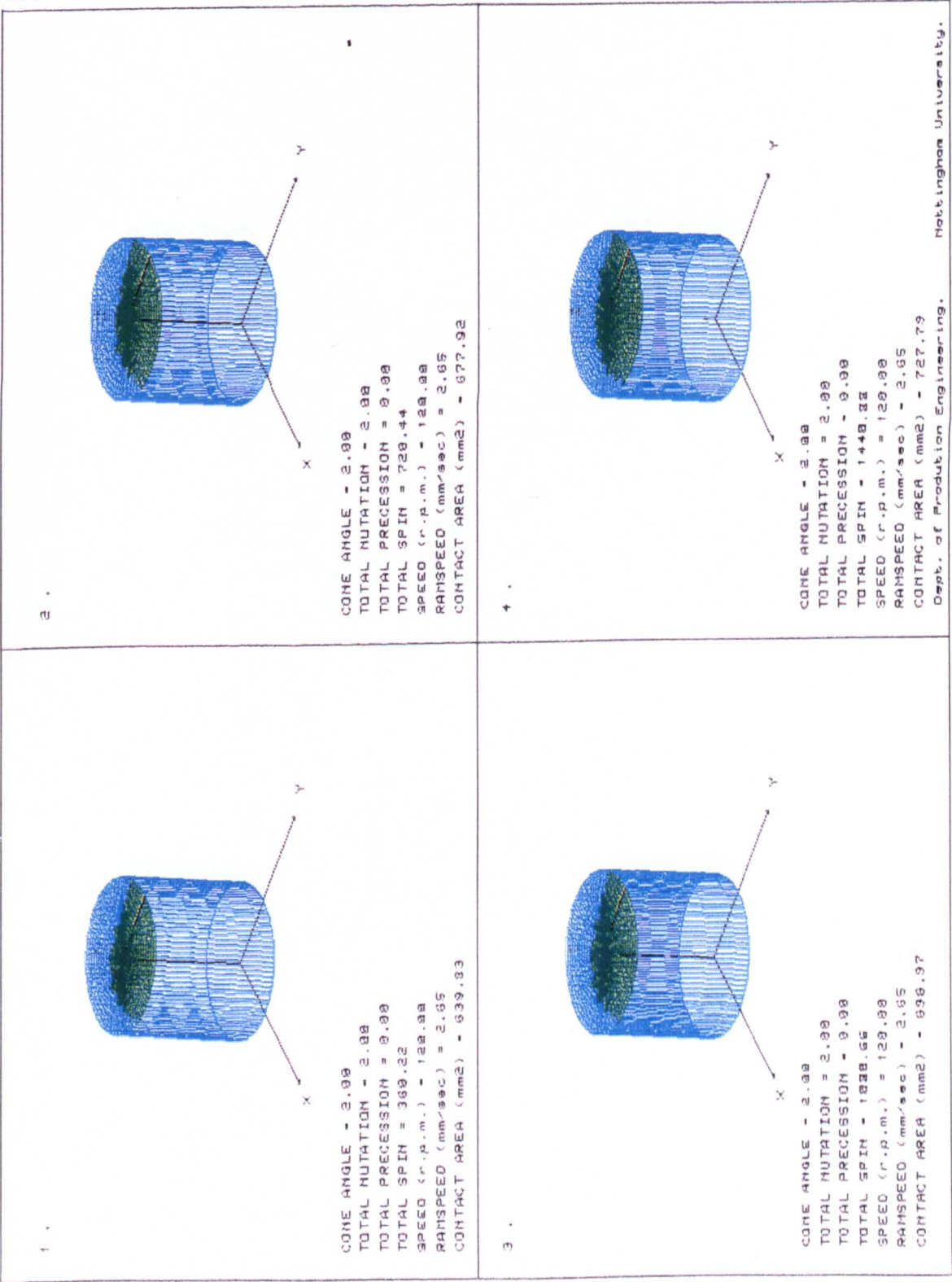


Figure 8.4 - b. The Results From the Simulation of the 50 Tonne Spin Machine Experiments
 Showing the Radial Expansion of the Workpiece.

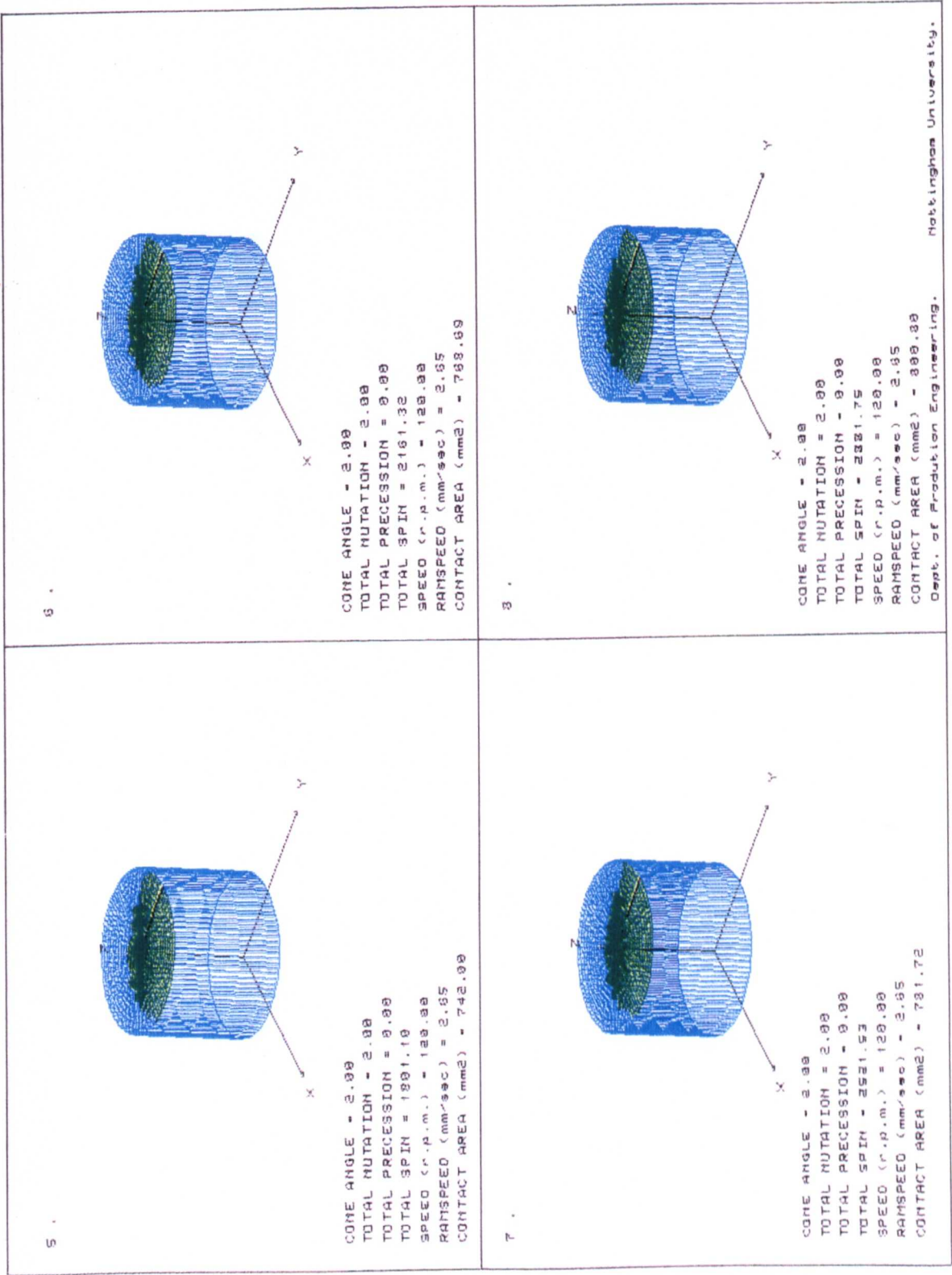


Figure 8.4 - c. The Results From the Simulation of the 50 Tonne Spin Machine Experiments
Showing the Radial Expansion of the Workpiece.

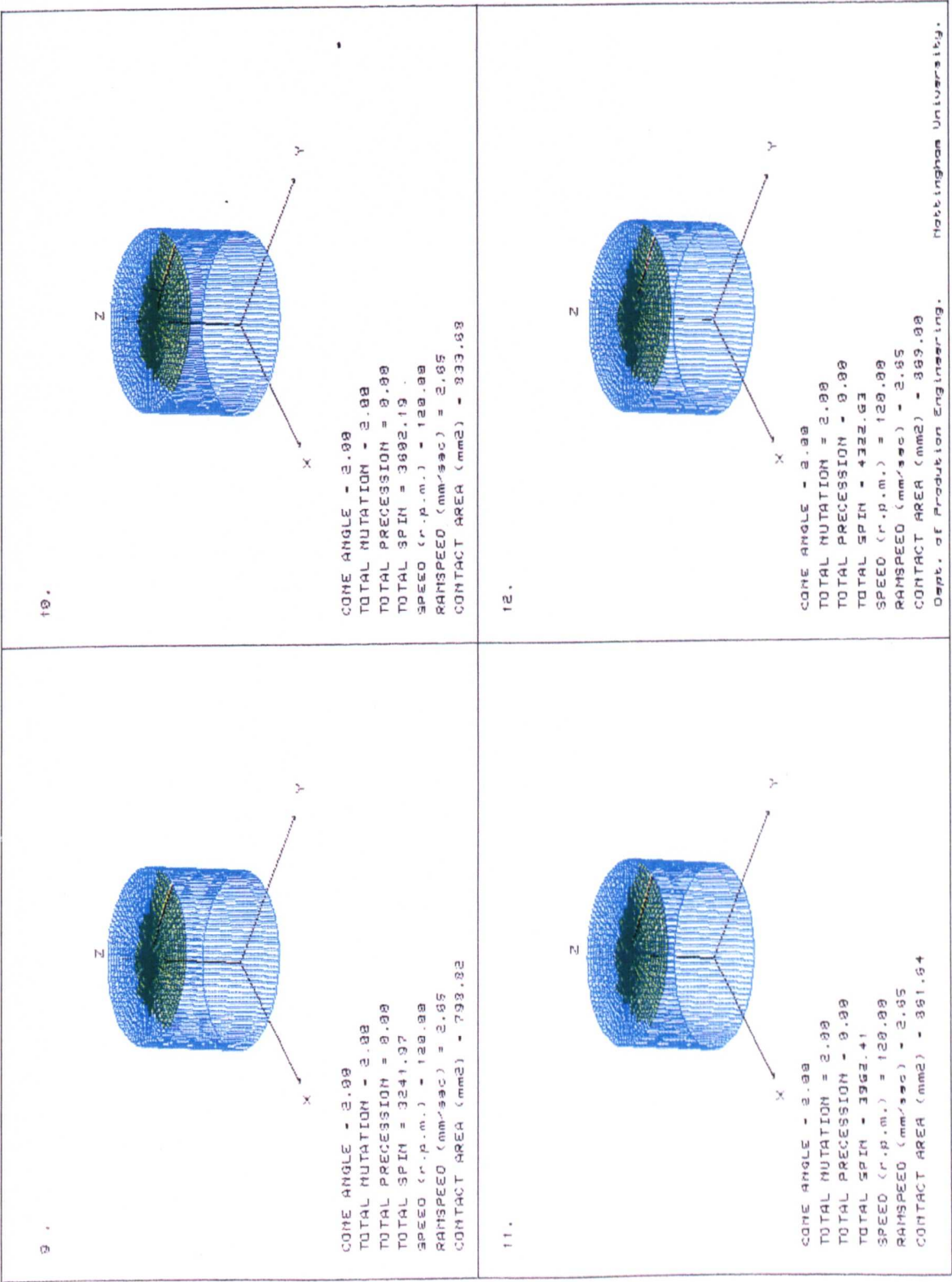


Figure 8.4 - d. The Results From the Simulation of the 50 Tonne Spin Machine Experiments
Showing the Radial Expansion of the Workpiece.

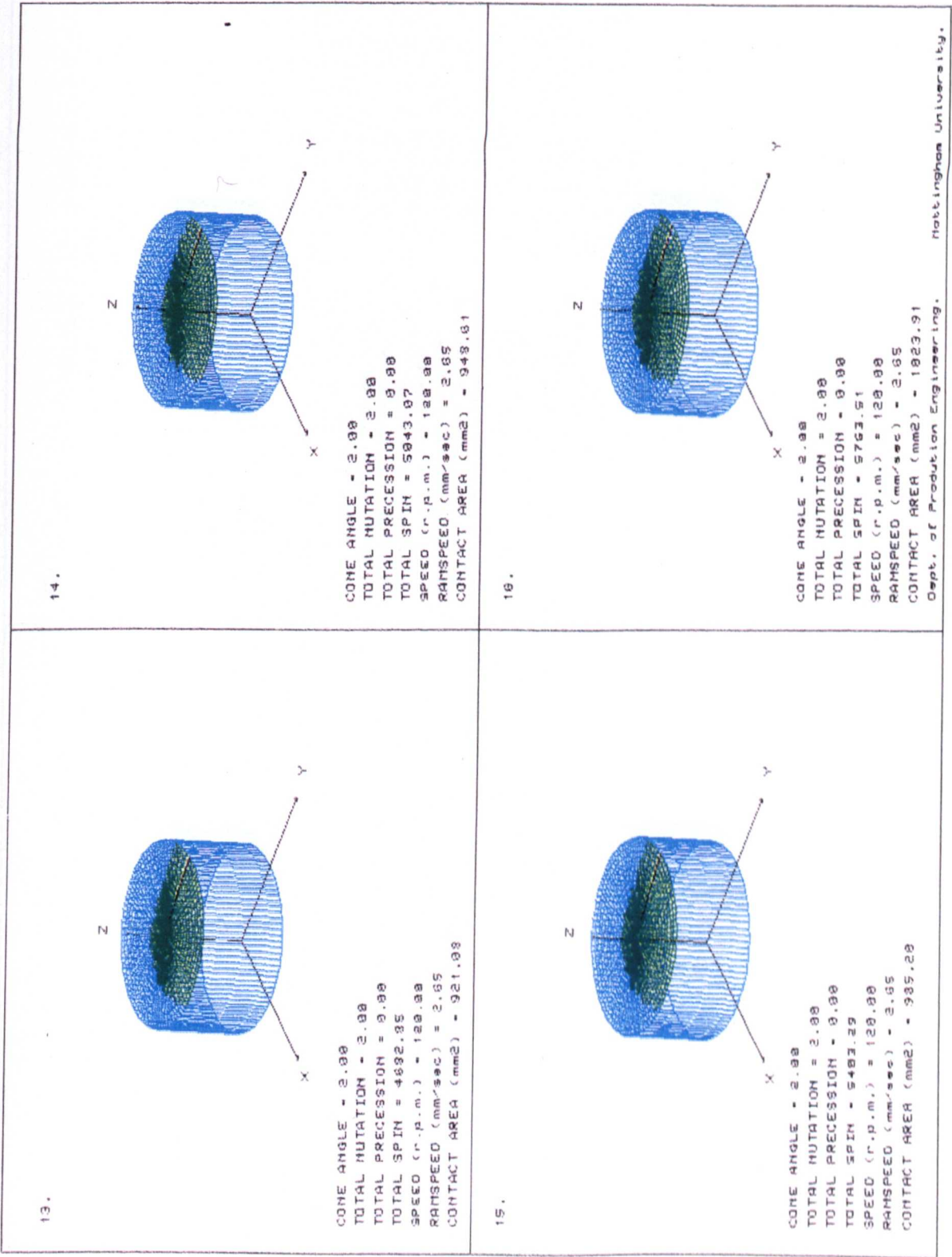


Figure 8.4 - f. The Results From the Simulation of the 50 Tonne Spin Machine Experiments
Showing the Radial Expansion of the Workpiece.

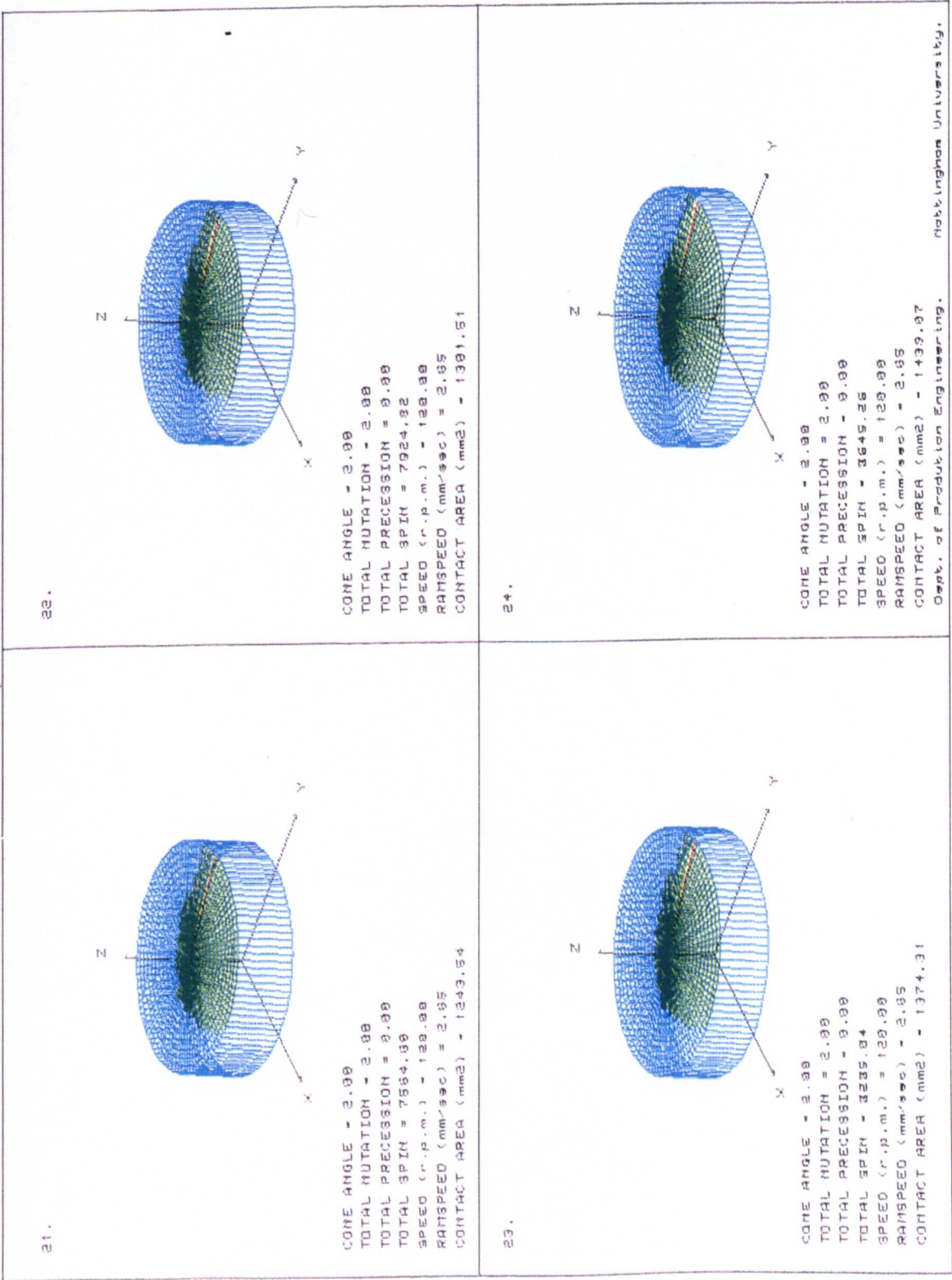


Figure 8.4 - g. The Results From the Simulation of the 50 Tonne Spin Machine Experiments
Showing the Radial Expansion of the Workpiece.

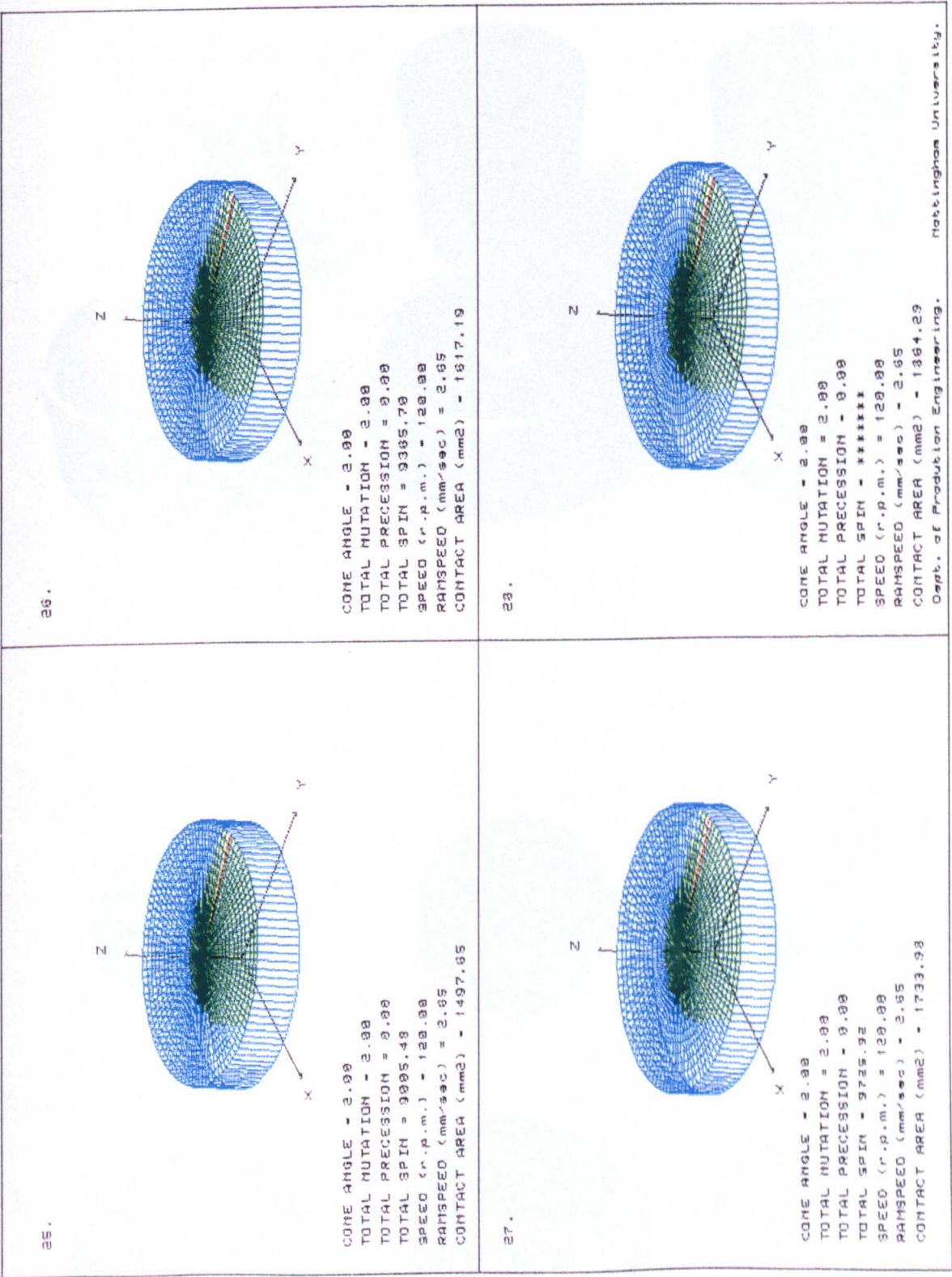


Figure 8.5 The Workpieces Produced During the 50 Tonne Machine Experiments.

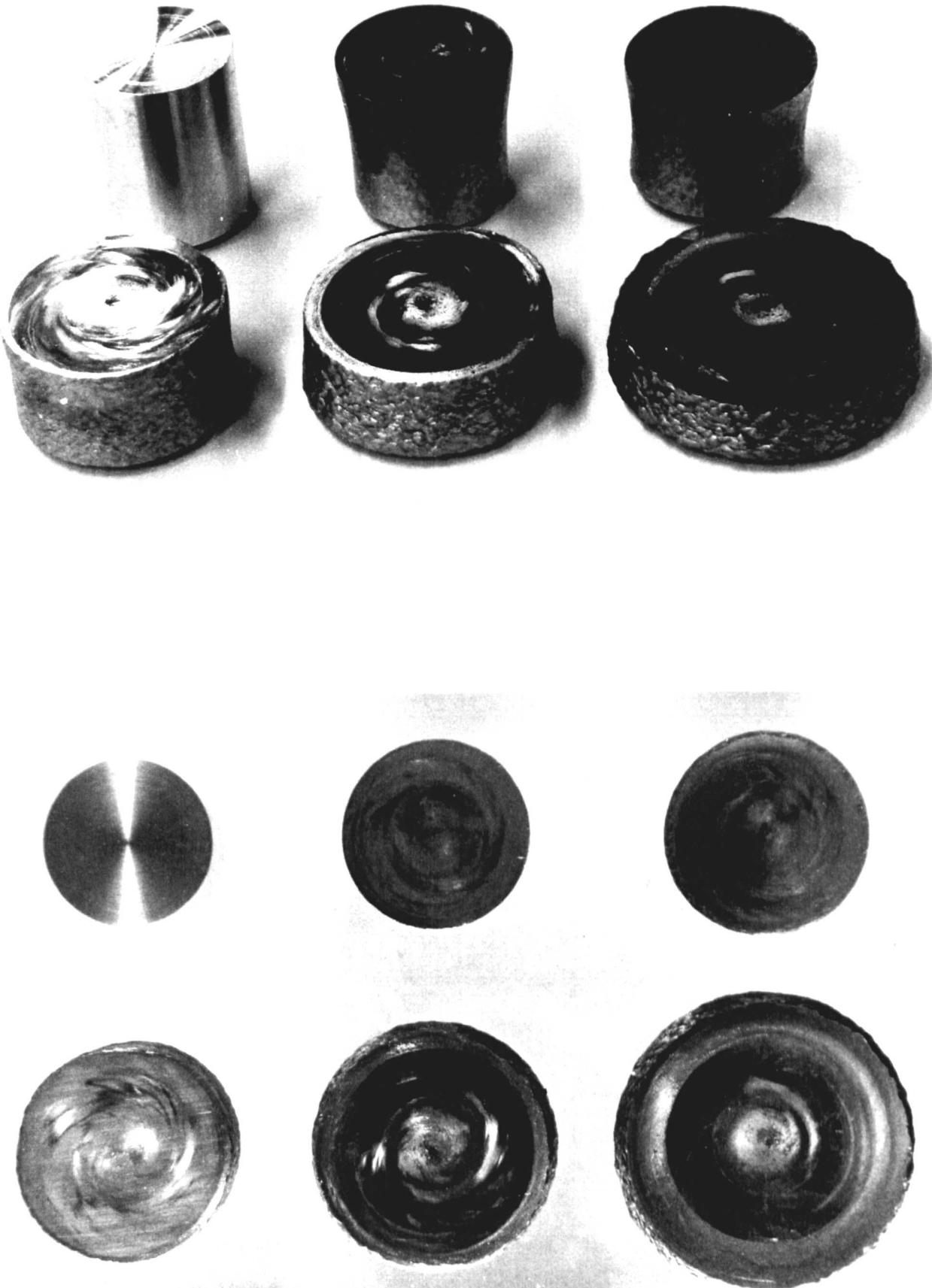


Figure 8.6 Showing the Radial Growth and Development of the Simulated Constant Volume Workpieces During the 50 Tonne Machine Experiments.

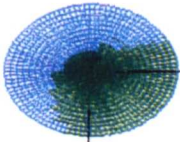
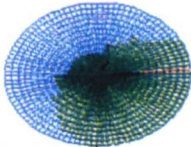
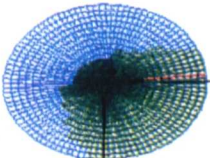
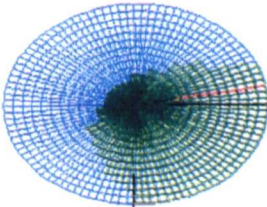
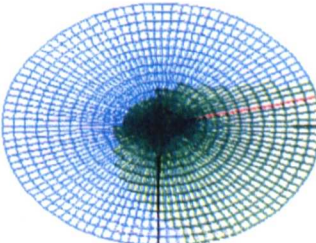
Cycles Forged / Simulated.	Workpiece Height.(mm)	Simulated Contact Area (mm2)	Simulated Workpieces.
1	42	639.83	
6	35	768.69	
11	28	861.64	
22	21	1301.51	
27	14	1733.98	

Figure 8.7 - a. Showing the Workpiece Diameters Vs. the Workpiece Heights.

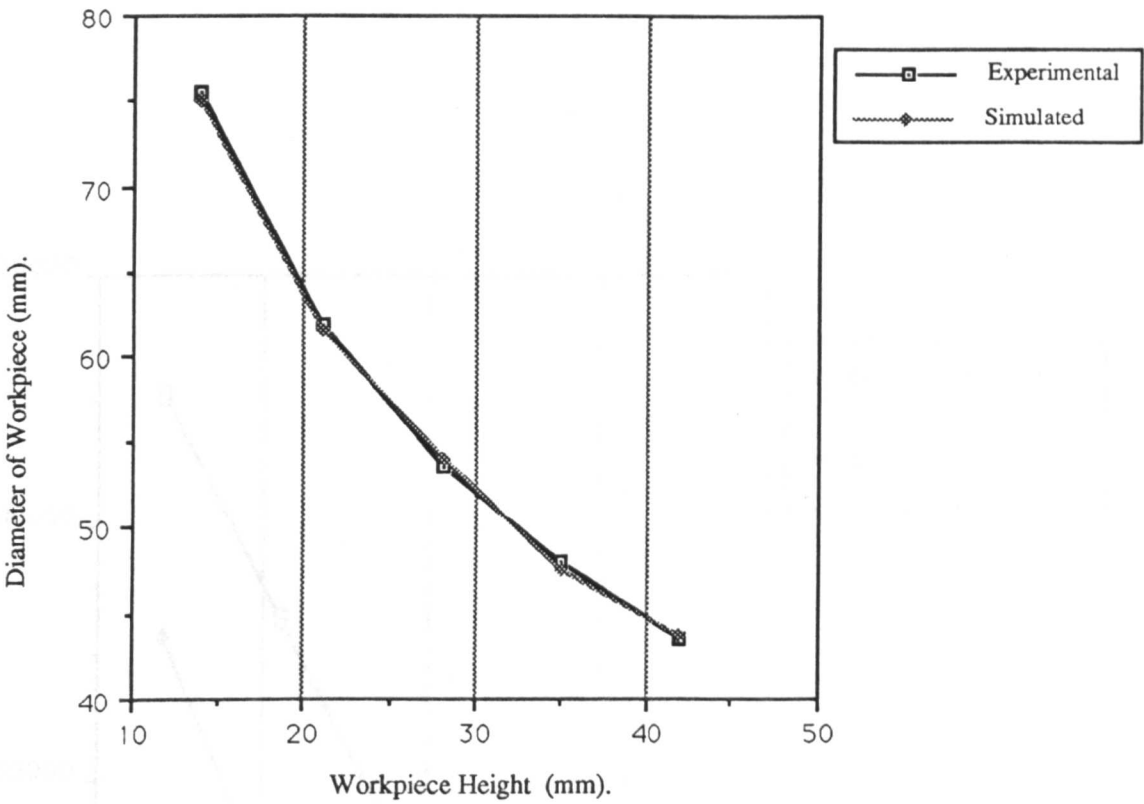


Figure 8.7 - b. Showing the Simulated Diameters Vs. the Experimental Diameters.

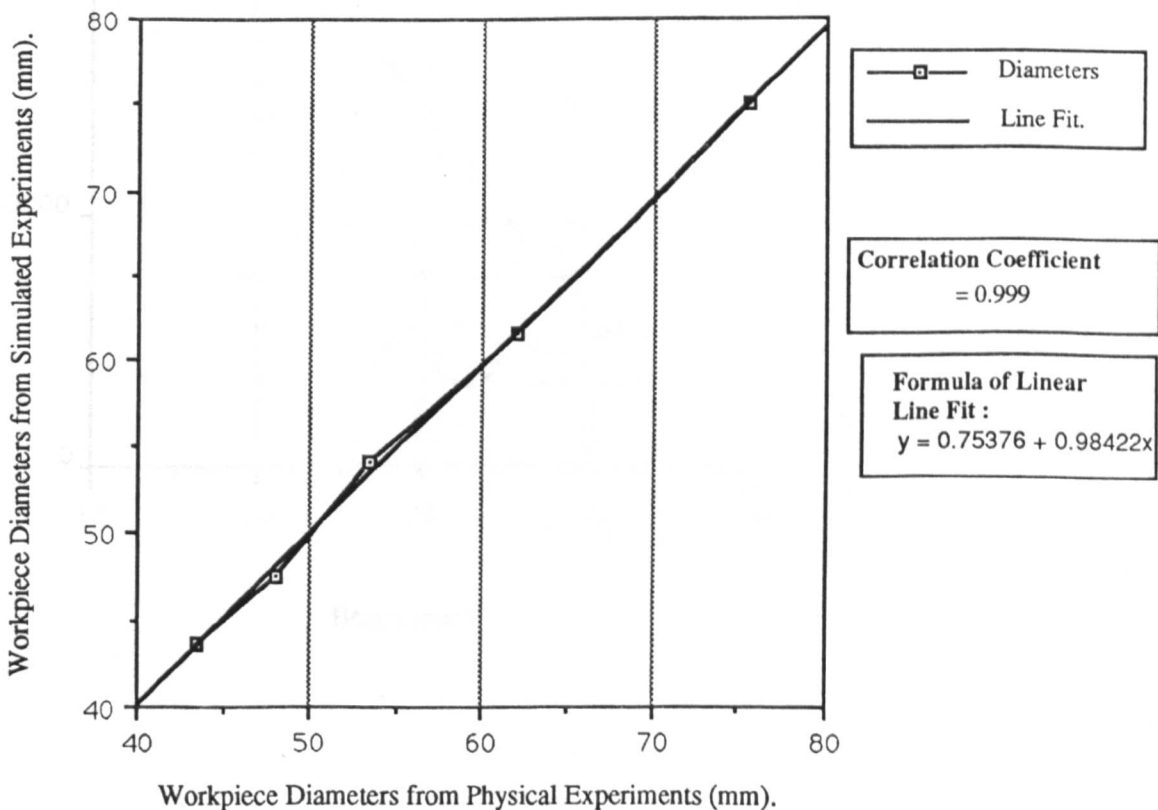


Figure 8.8 Showing the Experimentally and Simulated Displaced Volumes of Material Vs. the Height of the Workpiece at the Five Stages of the Forging.

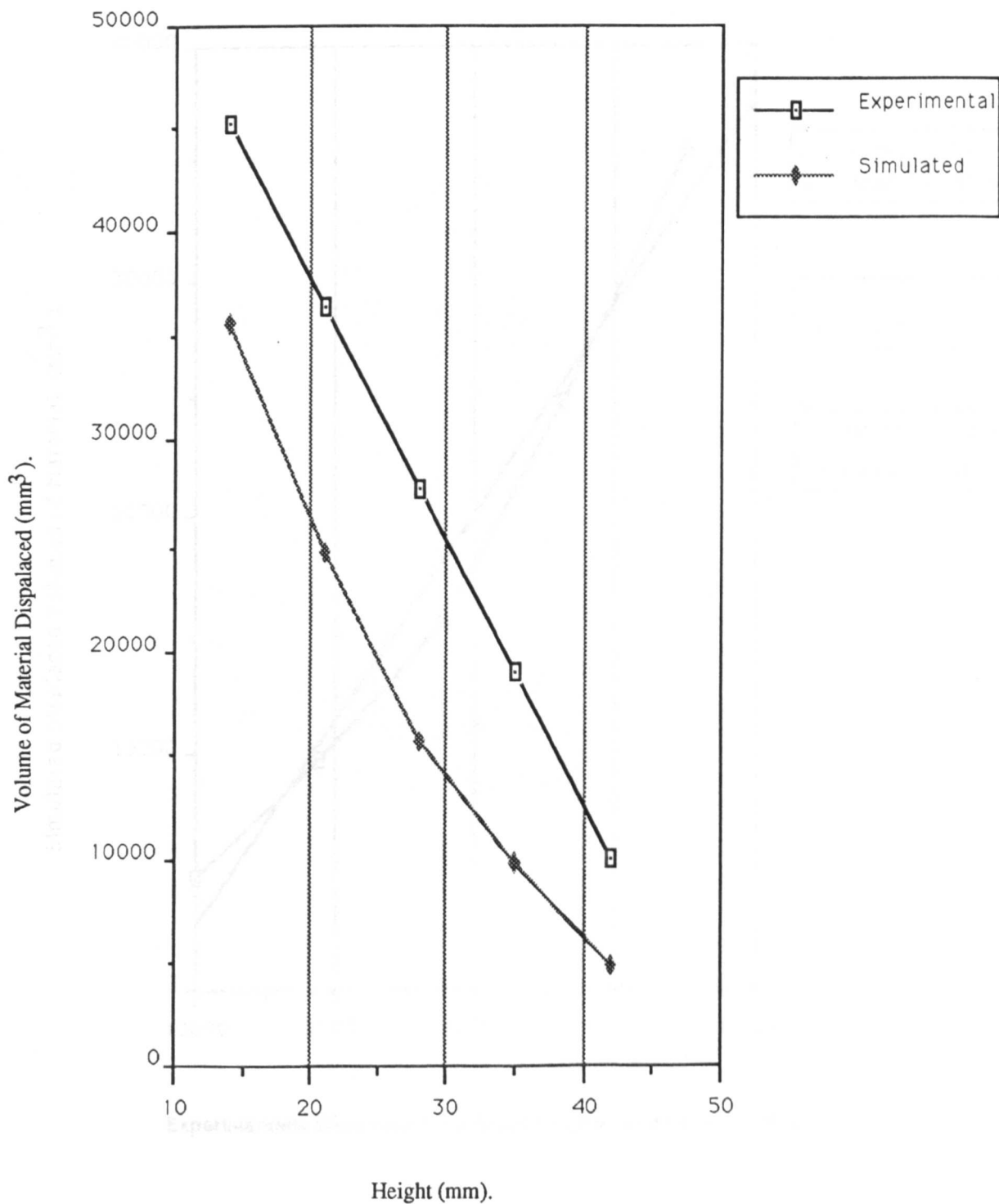


Figure 8.9 Showing the Simulated Displaced Volumes of Material Vs. the Experimentally Determined Values.

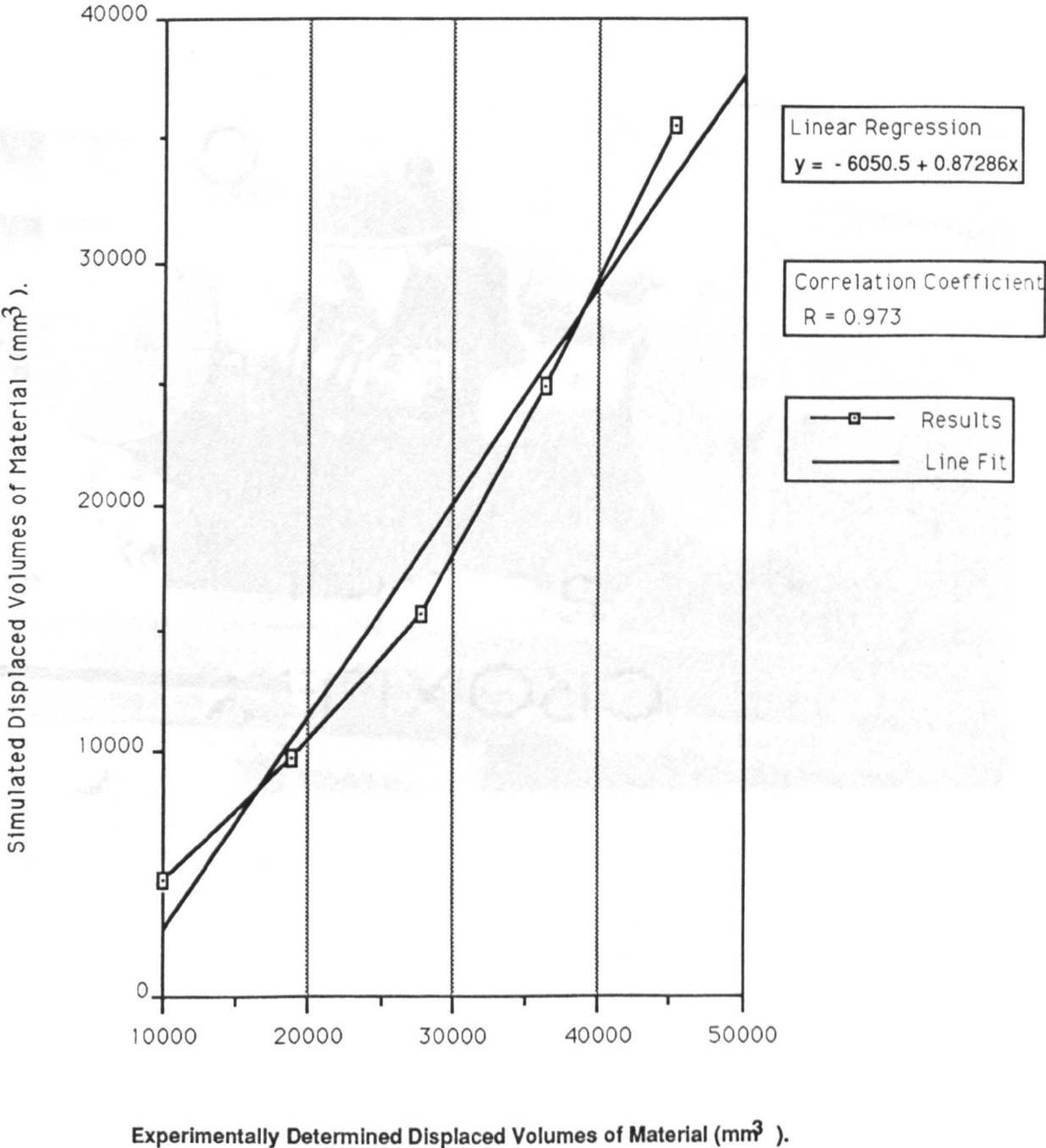


Figure 9.1 The Short Lead Milling Machine Setup For the Physical Simulation of the Rotary Forging Process.

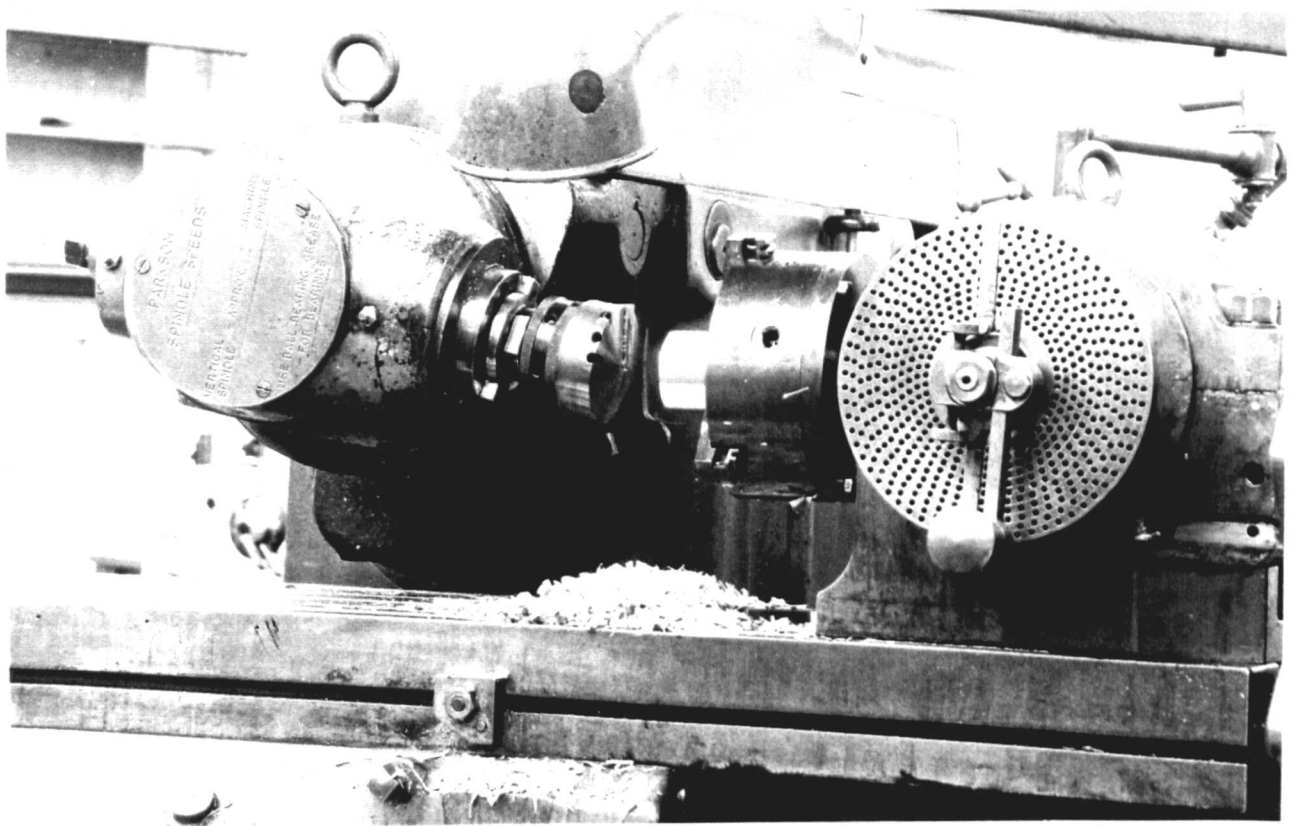


Figure 9.2 The Short Lead Milling Machine With Protractor, Handle and Pointer Attached to the Main Drive.

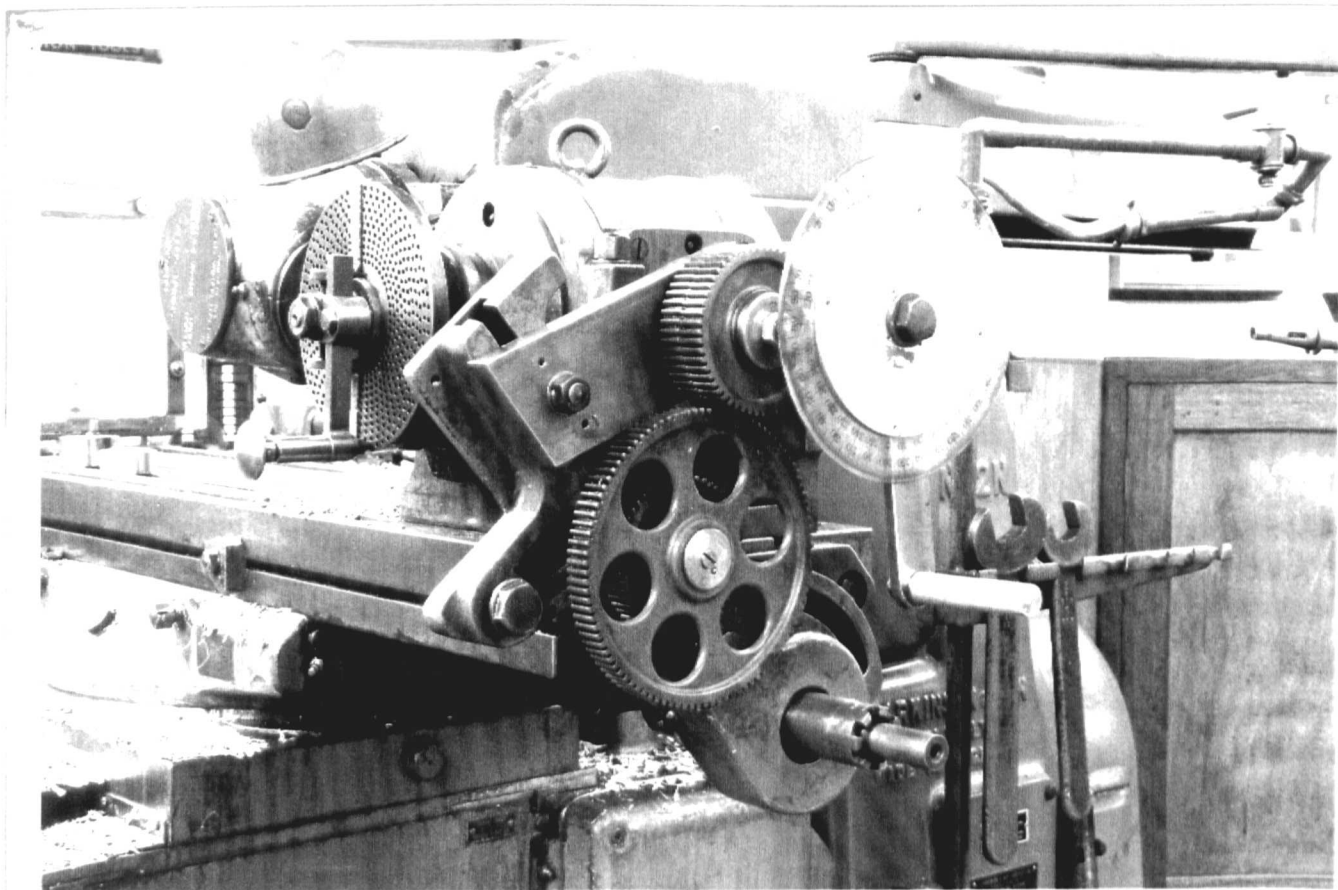


Figure 9.3 Showing the Simulated Contact Areas Vs the Milled Contact Areas in Perspex.

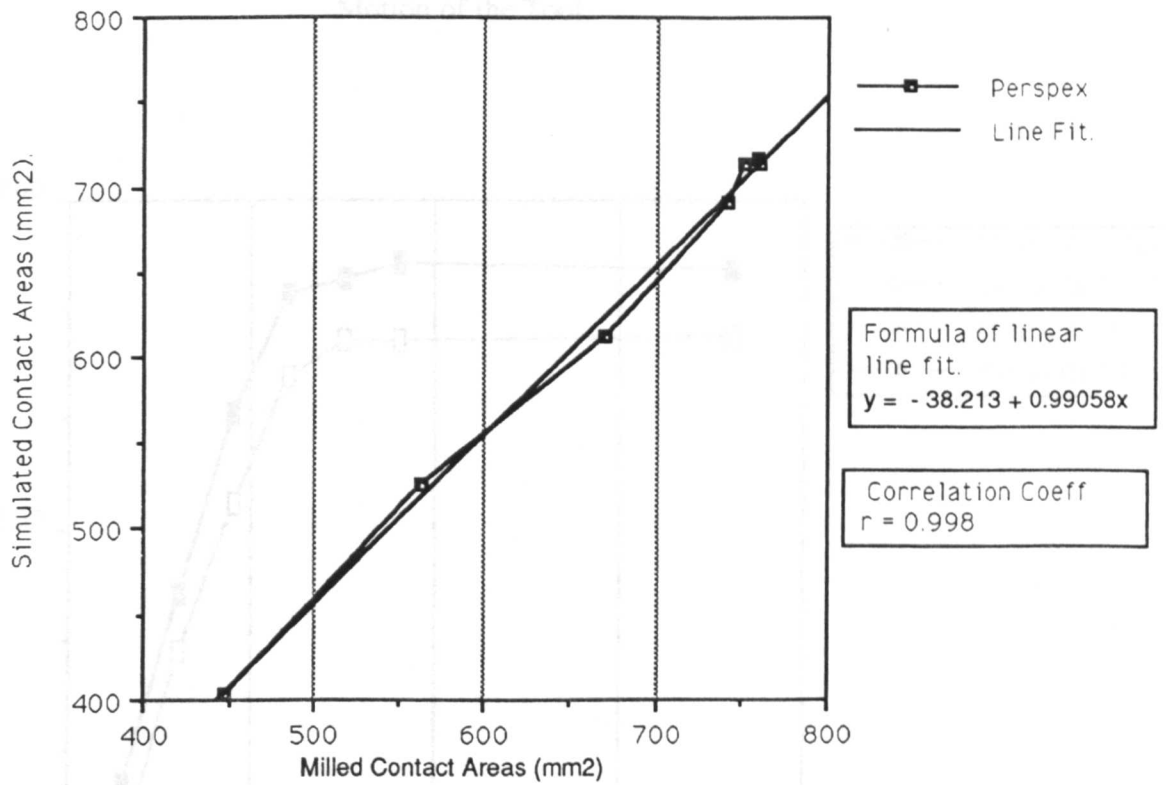


Figure 9.4 Showing the Simulated Contact Areas Vs the Milled Contact Areas in Aluminium.

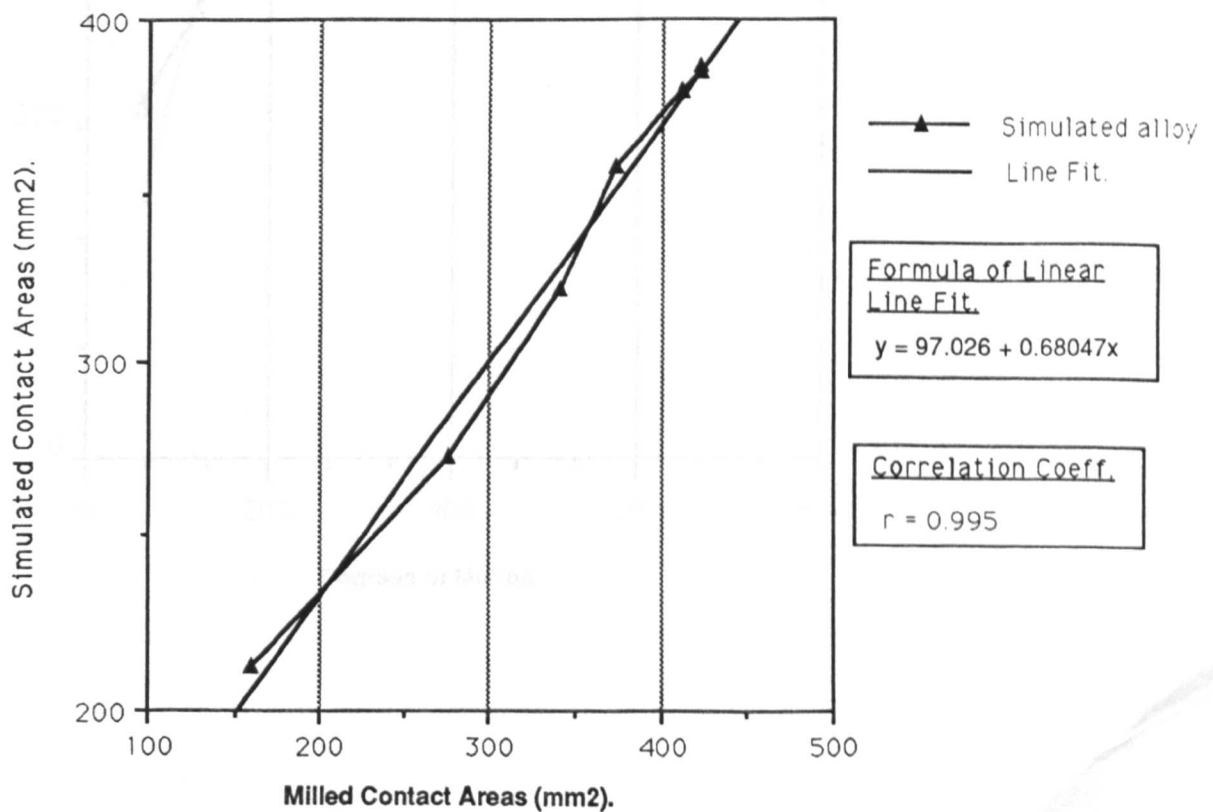


Figure 9.5 Showing the Contact Areas For Both the Simulated and the Milled Experiments Plotted Against the Degrees of Motion of the Tool.

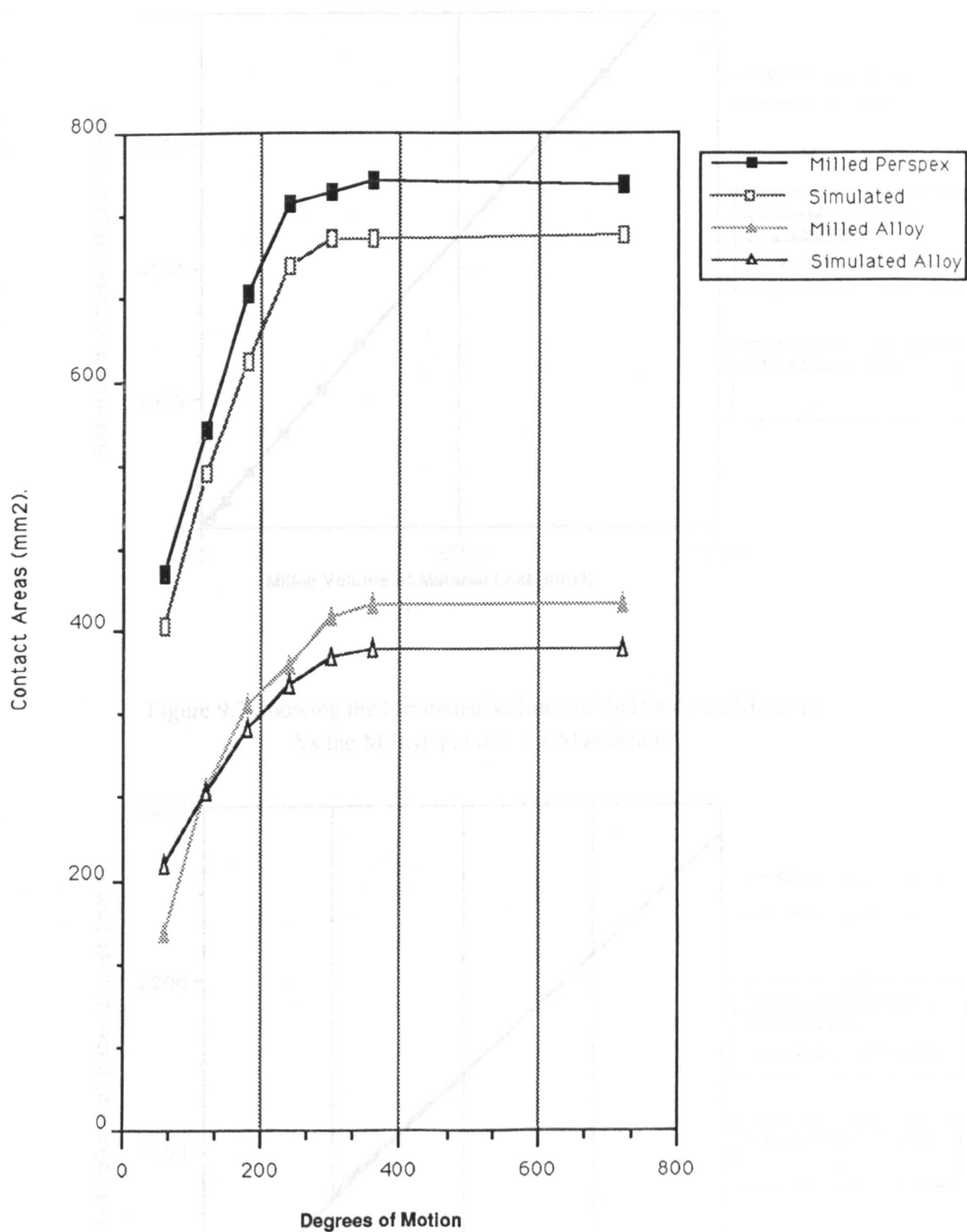


Figure 9.6 Showing the Simulated Volume of Displaced Material Vs the Milled Volume in Perspex.

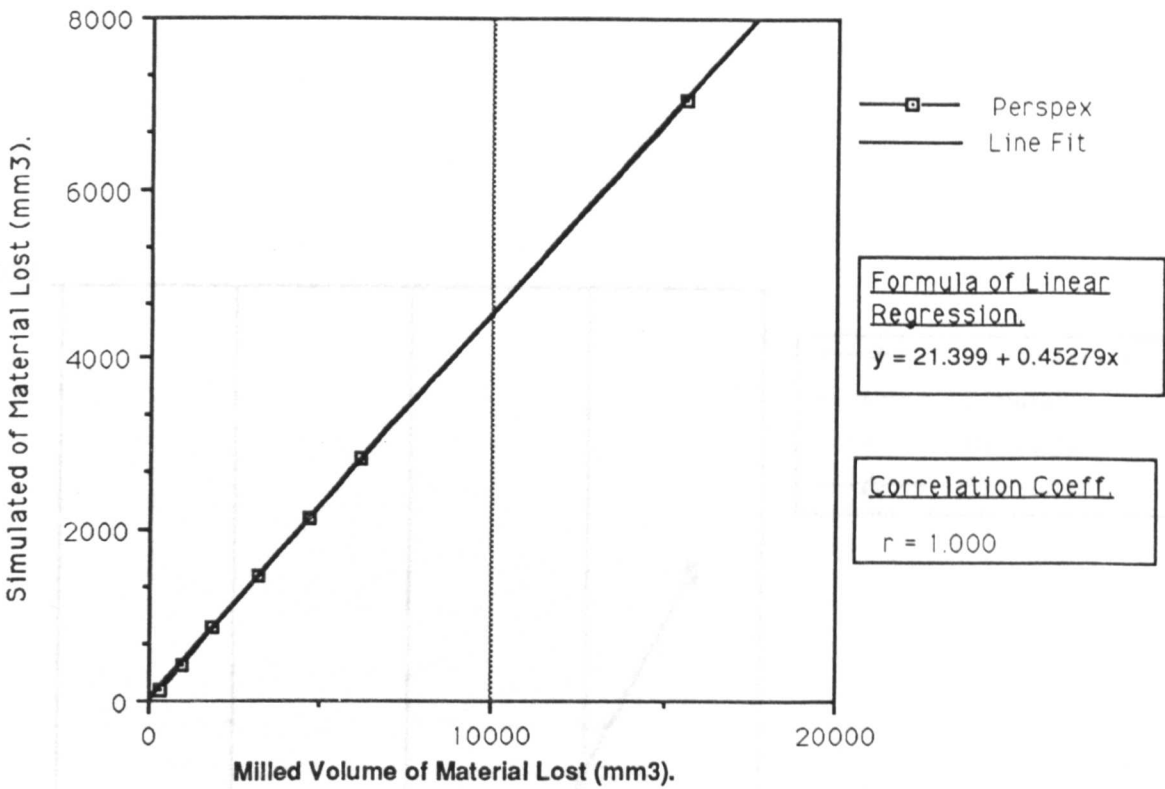


Figure 9.7 Showing the Simulated Volume of the Displaced Material Vs the Milled Volume in Aluminium.

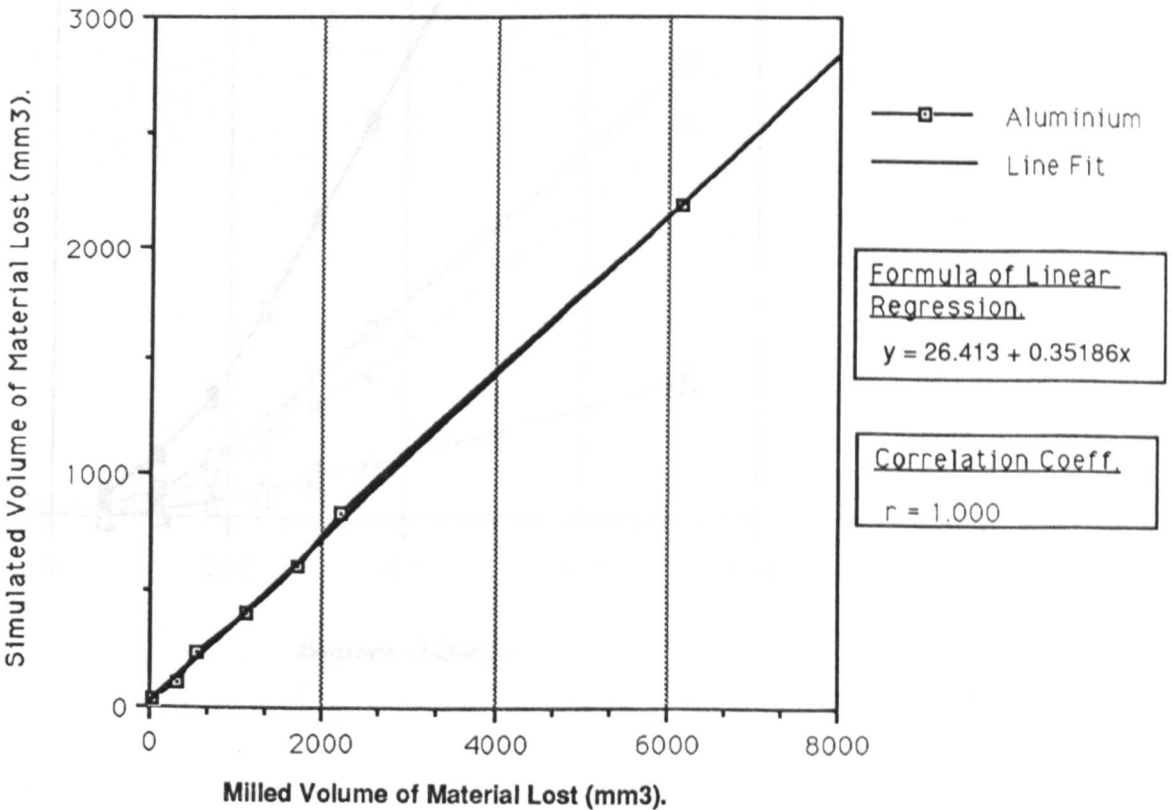


Figure 9.8 Showing The Displaced Volumes of Material for Both the Simulated and the Milled Experiments, Plotted Against the Degrees of Motion of the Tool.

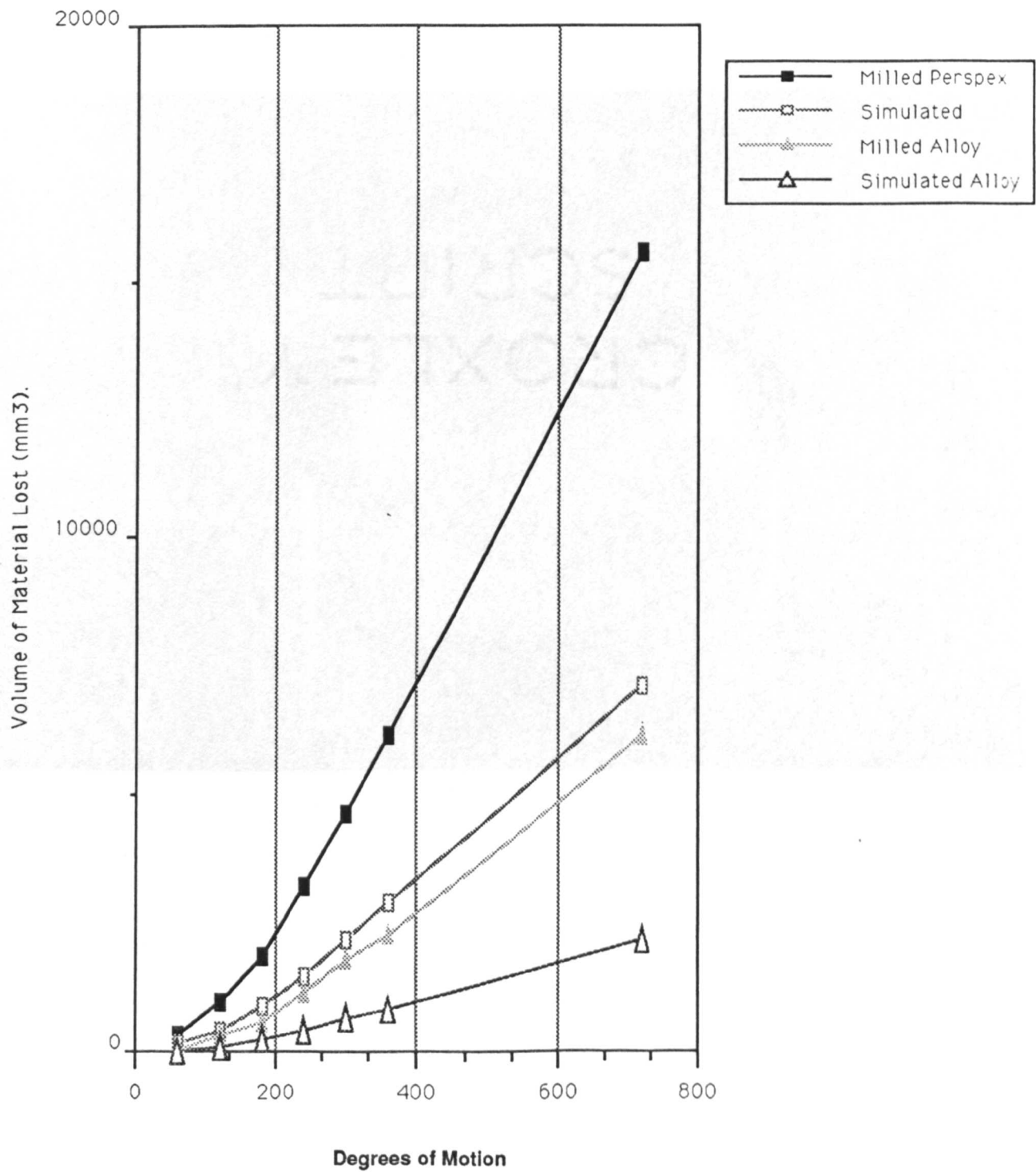


Figure 9.9 A Perspex Workpiece After 360 Degrees of Milling.

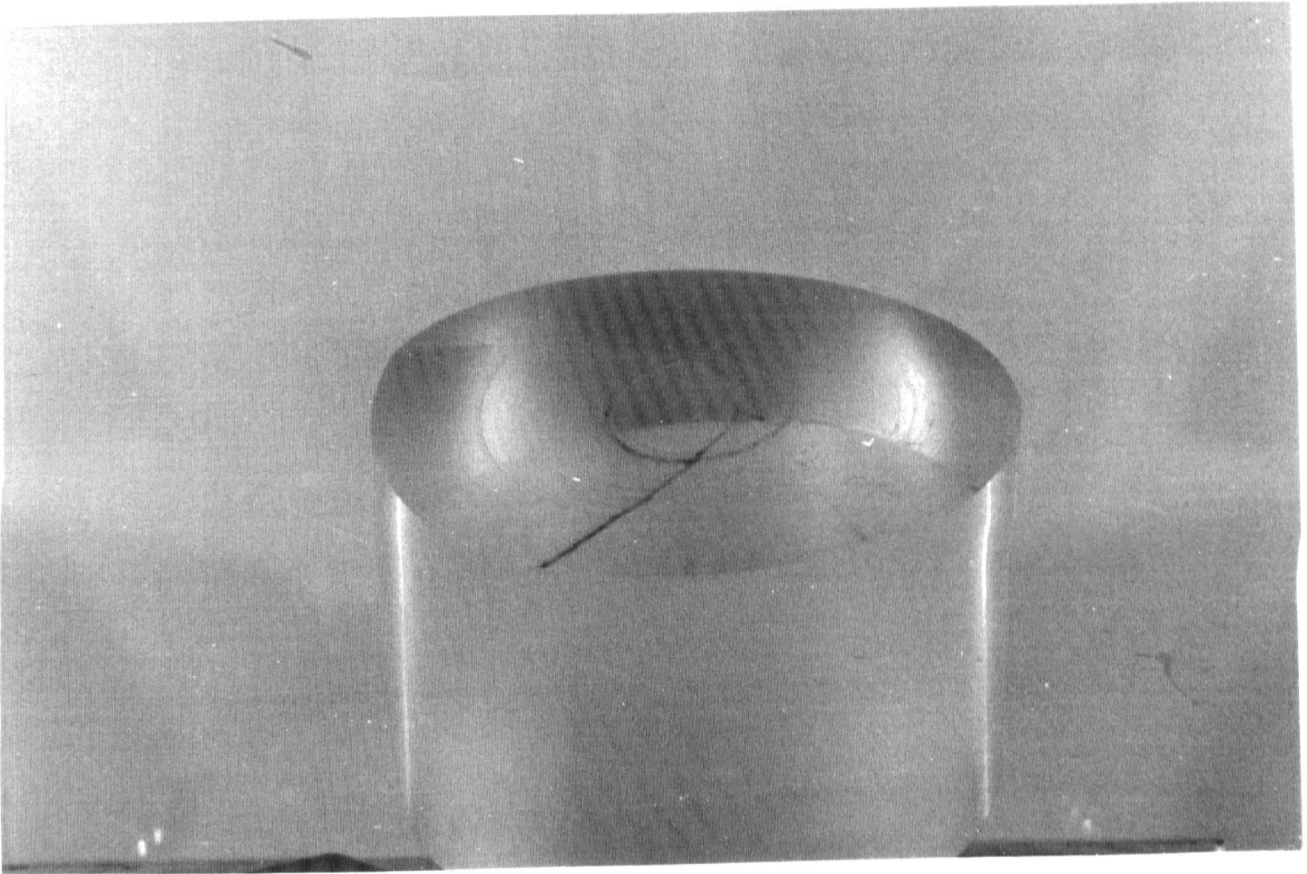


Figure 9.10 - a. The Simulation Using the Non - Constant Volume Model Workpiece of the Perspex Specimens Milled on the Short Lead Milling Machine.

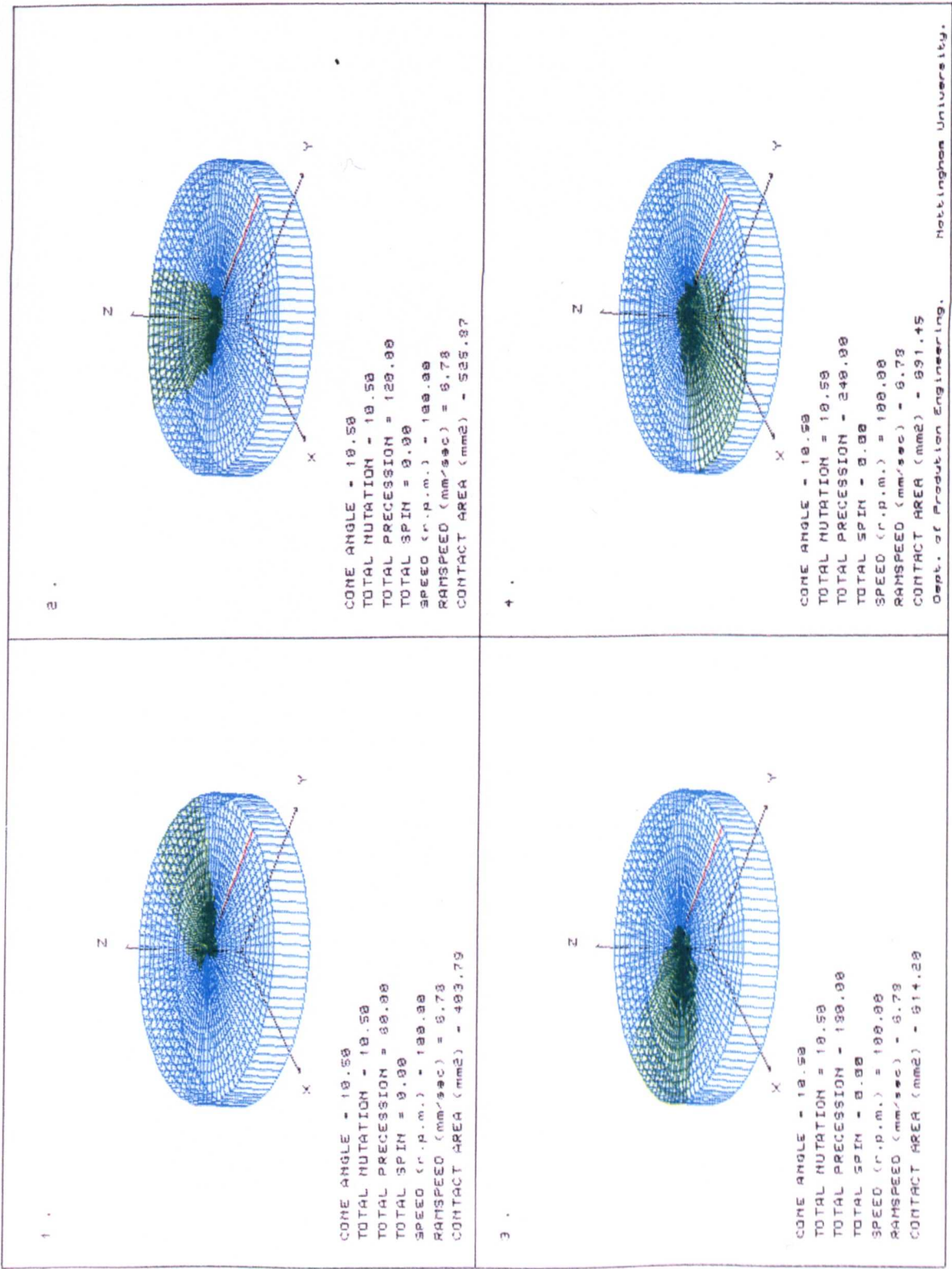


Figure 9.10 - b. The Simulation Using the Non - Constant Volume Model Workpiece of the Perspex Specimens Milled on the Short Lead Milling Machine.

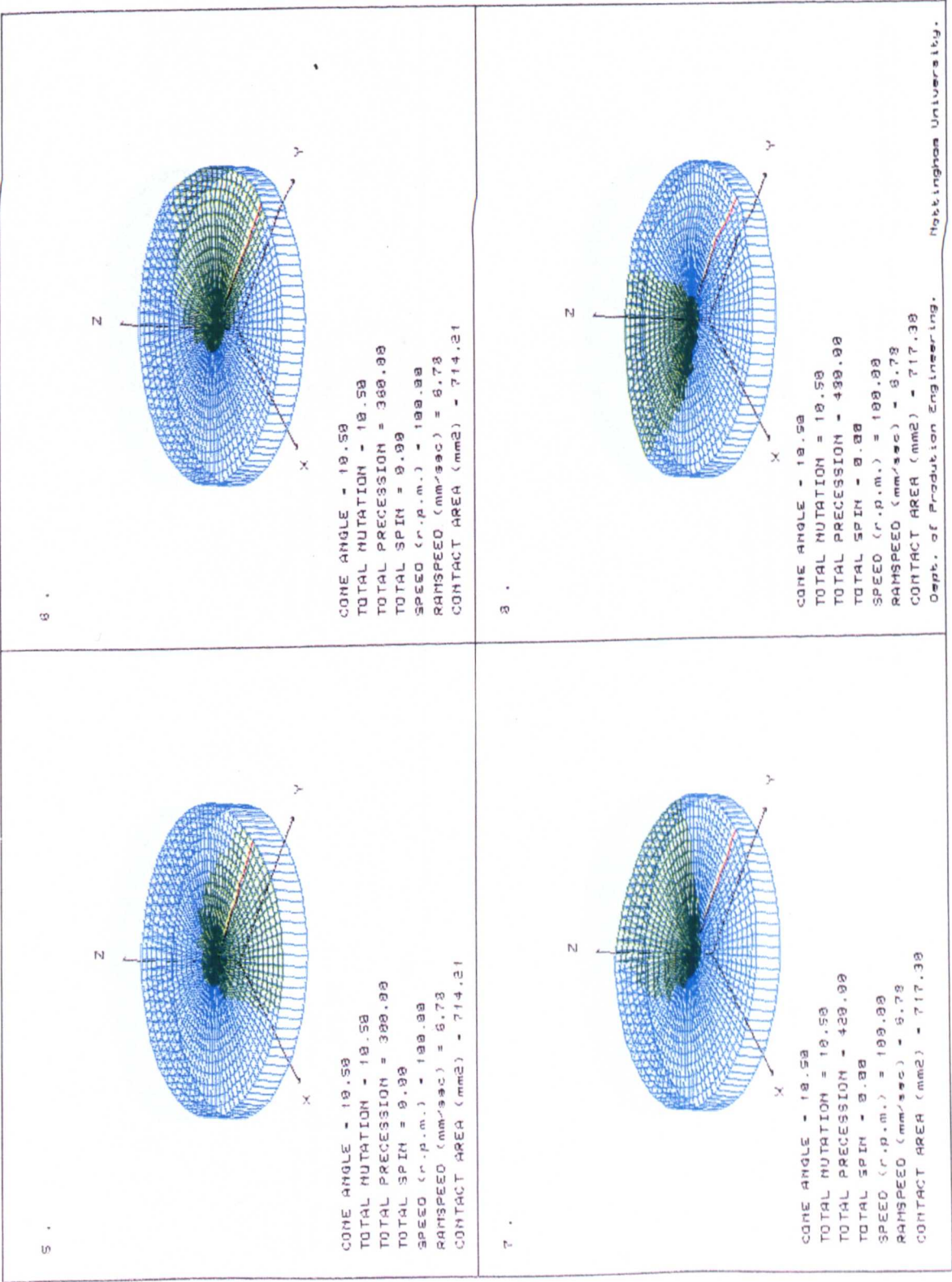


Figure 9.10 - c. The Simulation Using the Non - Constant Volume Model Workpiece of the Perspex Specimens Milled on the Short Lead Milling Machine.

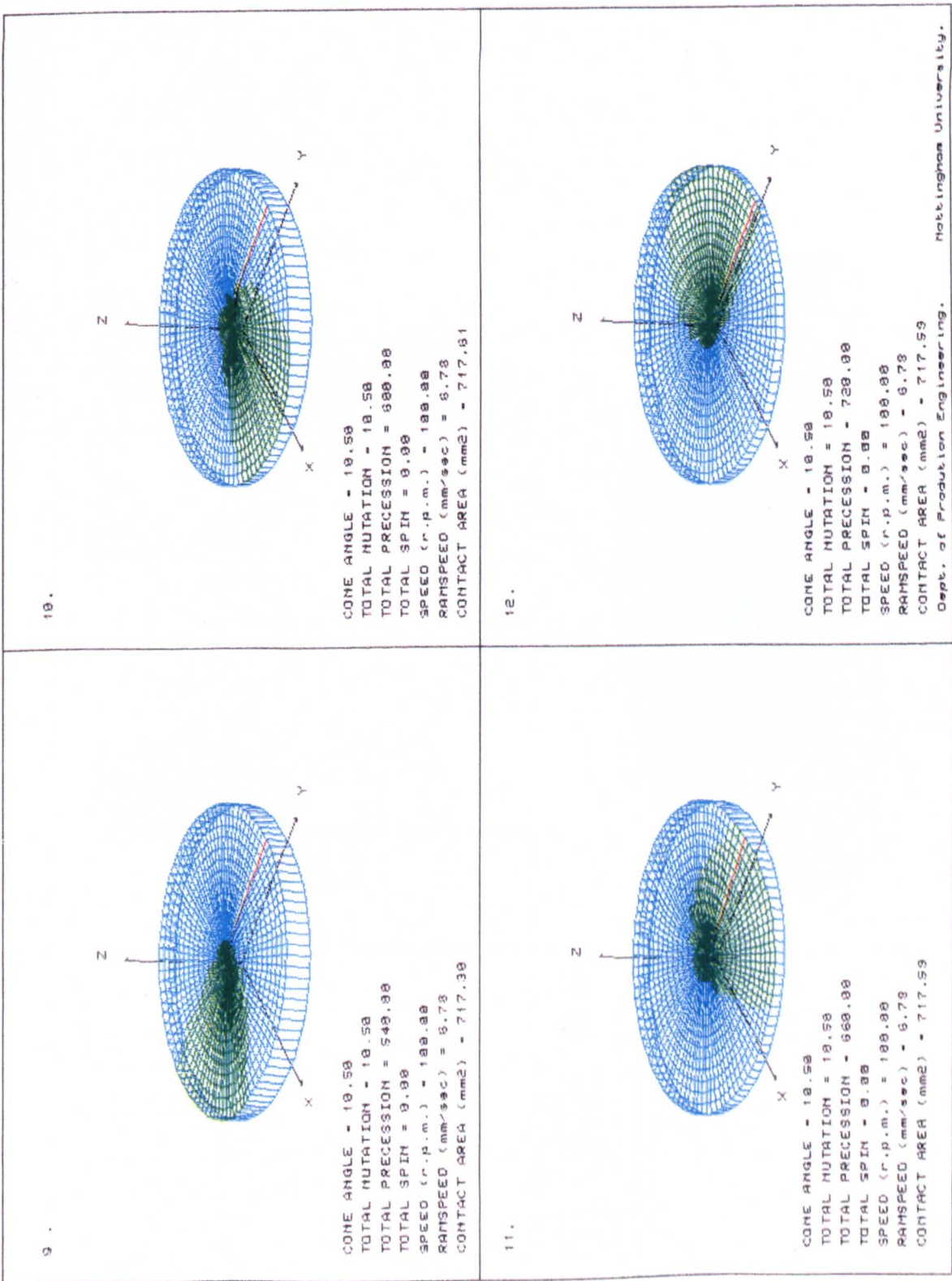


Figure 9.11 Showing the Simulation of the Perspex Workpiece after 360 Degrees of Rotary Milling / Forging.

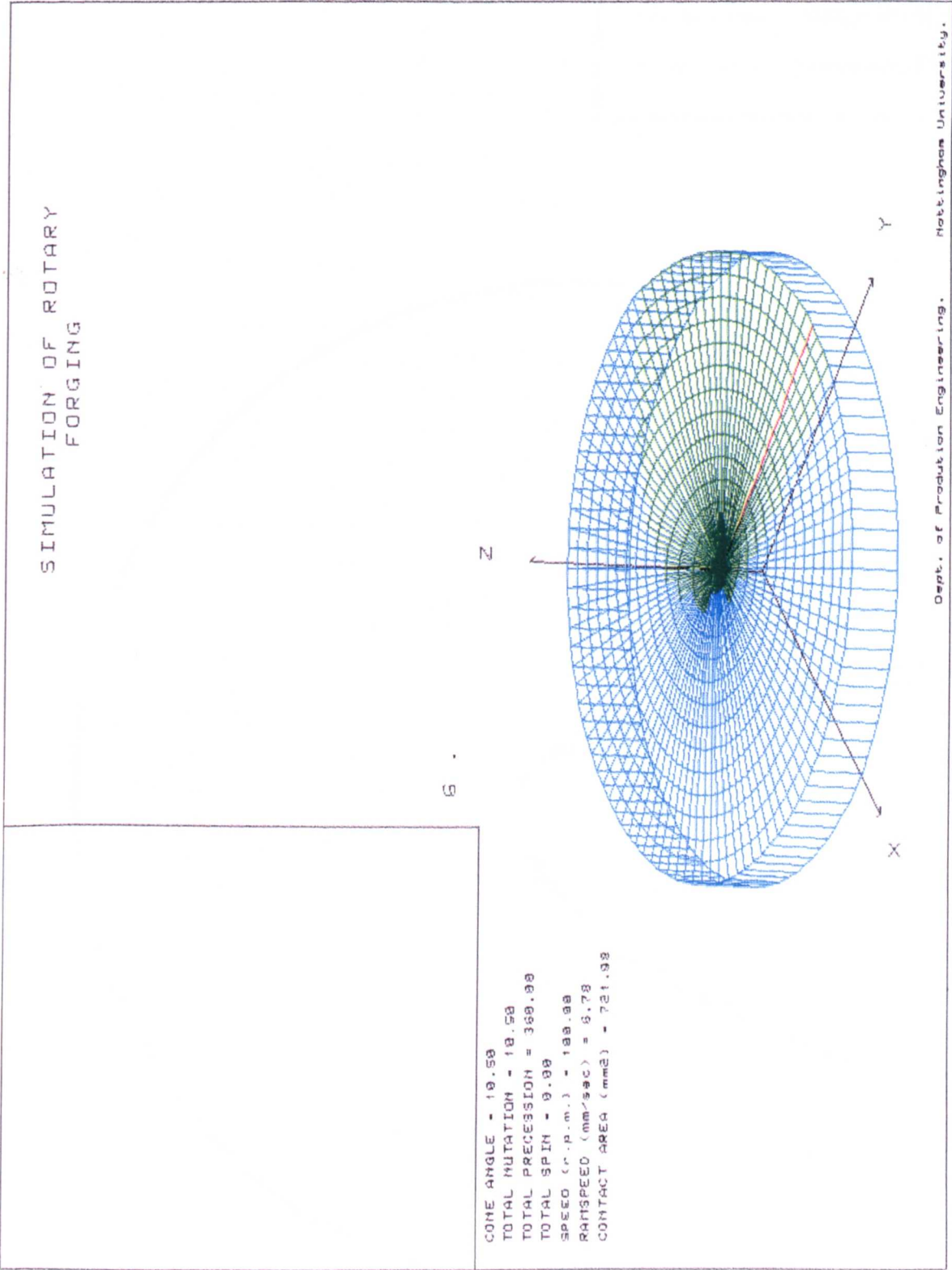


Figure 9.12 Showing the Comparison Between the Contact / Cutting Profiles Produced by the Milled and Simulated and Experiments in Perspex at 360° of Motion.

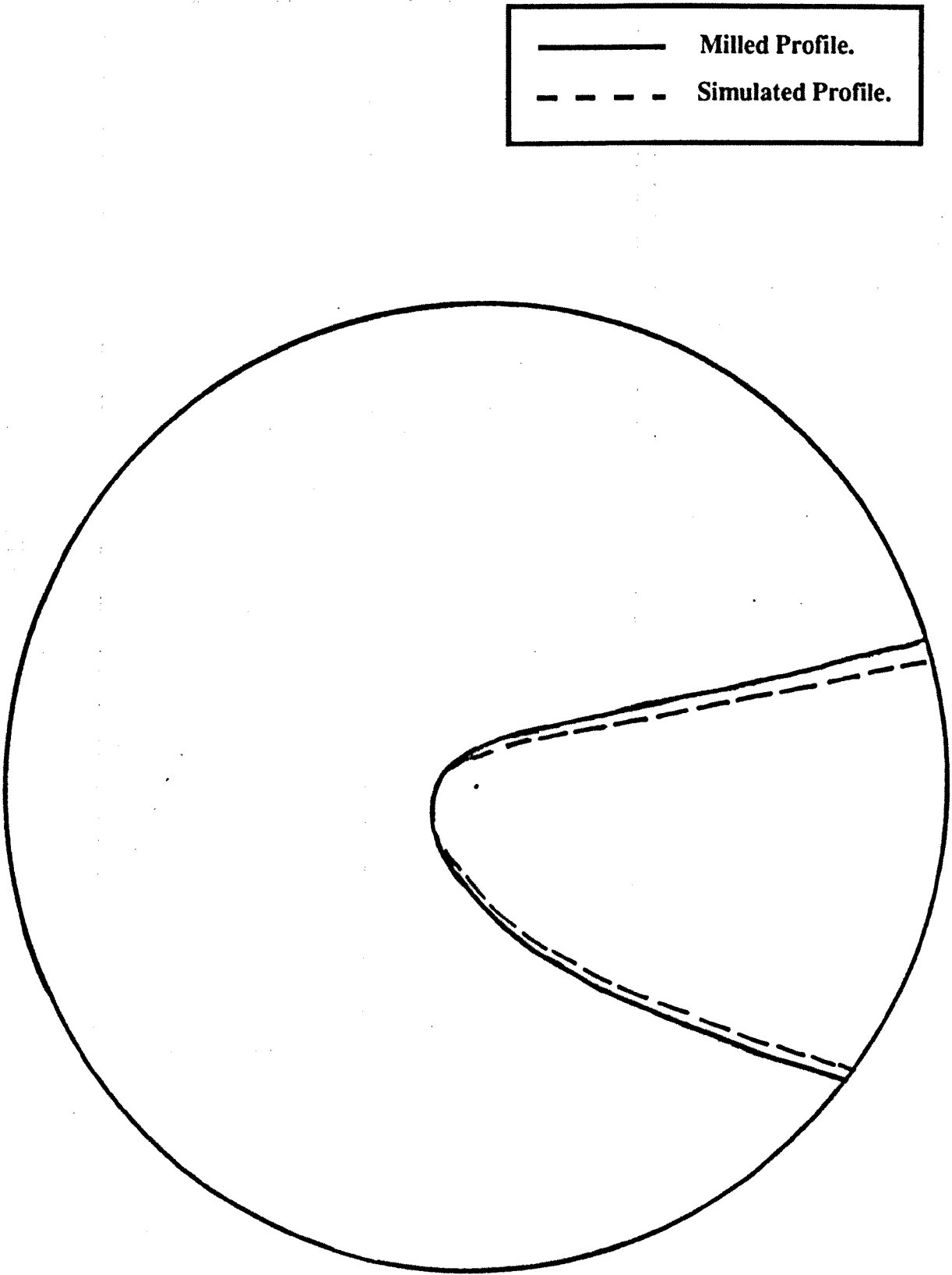
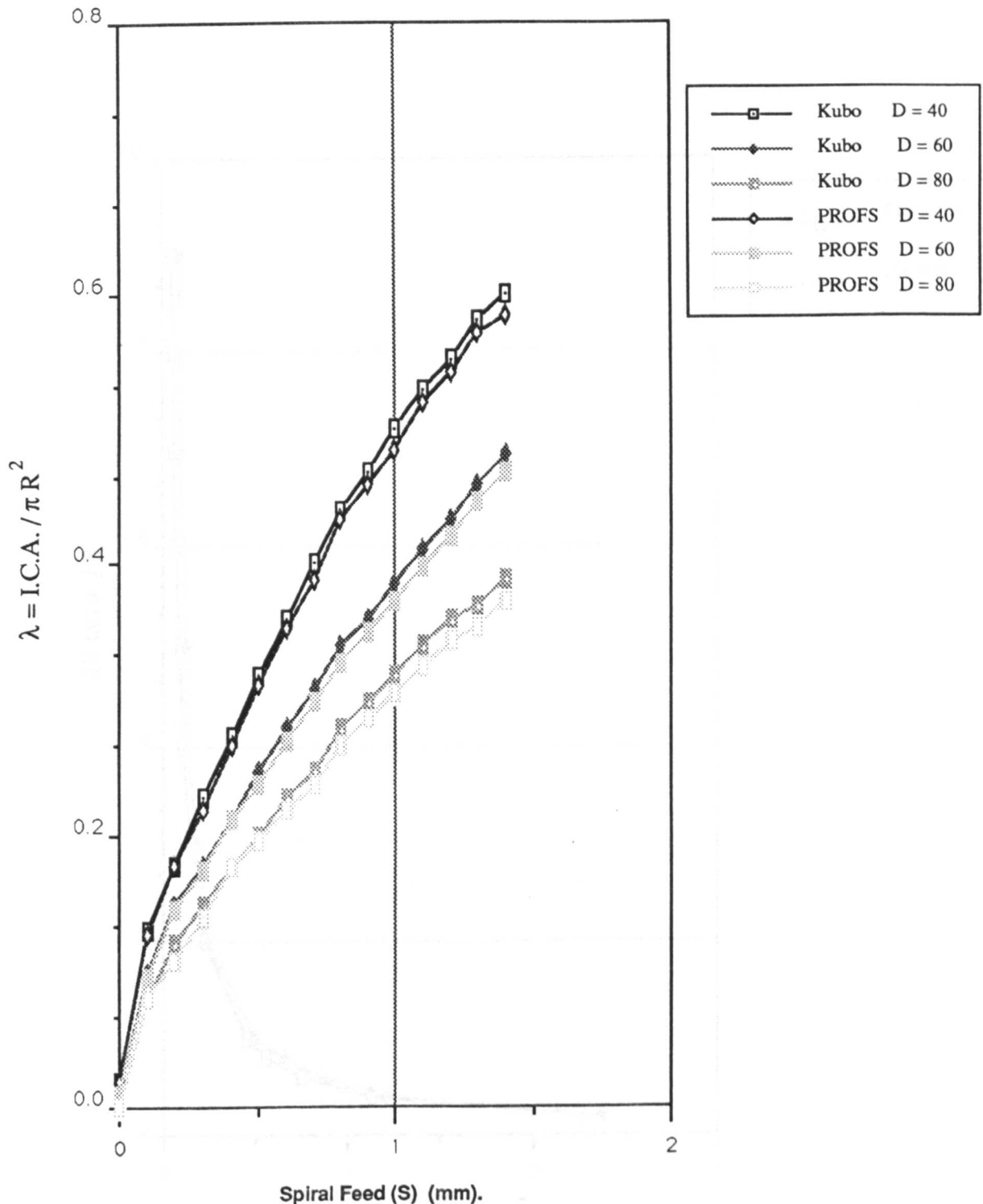


Figure 9.13 The Graph of the Coefficient λ vs Spiral Feed (S)
From Kubo and PROFS.



R = Radius of the Workpiece.
 I.C.A. = Instantaneous Contact Area.
 α = Die Angle.
 D = Diameter of the Workpiece

Figure 9.14 The Graph of the Coefficient λ vs $2R \tan \alpha / S$ from Marciniak and PROFS.

